VISOR

Visualisation of Real-Time System Dynamics using Enhanced Monitoring

TRANSITION INTO BUSINESS AS USUAL

Project start		GB WAMS live	Sandbox initiative	Project end
2014	2015	2016		2017

Installation Stage

- WAMS Infrastructure
- TO-SO Communications Links
- Application Specification

Operational Stage

- WAMS Application and Analysis
- System Modelling and Validation
- Demonstration of Benefits
- Study of Hybrid State Estimator
- 'Sandbox' testing facility
- Multi-platform visualisation tool

Our electricity networks are evolving to meet the needs of the changing energy landscape, and so must the technologies and practices we use to monitor and control them.

Foreword : Priyanka Mohapatra, VISOR Project Lead, SP Energy Networks

VISOR is a flagship innovative collaboration project between the three mainland GB Transmission Owners, SP Transmission, Scottish Hydro Electric Transmission, National Grid Electricity Transmission, and the Transmission System Operation, funded under Ofgem's Network Innovation Competition.

The project partners have come together to collectively establish a new type of monitoring system to give us a much better way of understand how the evolution in the way we generate and consume electricity affects the dynamic behaviour across the whole Electricity Network.

We have established the first unified GB "Wide Area Monitoring System" made available by modern technology, time-synchronisation and data-processing capabilities in order to develop and demonstrate the benefits and determine the most suitable future deployment strategy.

This information booklet combines the key technical papers produced by the VISOR team, documenting the ground-breaking research conducted by the University of Manchester and the market-leading technological developments by GE Grid Solutions (formerly Psymetrix).

The VISOR Team

		Project Team	Steering Group
SP ENERGY NETWORKS	SPEN:	Priyanka Mohapatra Jamie Campbell Finlay MacLeod	James Yu Colin Taylor
nationalgrid	NGET:	Mark Osborne Phil Ashton Nick Hird Sanjeev Gopalakrishnan	Duncan Burt John Haber Martin Bradley Ray Zhang
sse	SSE:	Chris Nendick David Wang	Stewart Reid
MANCHESTER 1824 The University of Manchester	UoM:	Vladimir Terzija Peter Wall Papiya Dattaray	Academic Partner
GE	GE: (formerly Pysmetrix)	Richard Davey Stuart Clark Douglas Wilson	WAMS Supplier

Contents

VISOR project: Opportunities for Enhanced Real Time Monitoring and Visualisation of System Dynamics in GB

Peter Wall (The University of Manchester), Papiya Dattaray (The University of Manchester), Priyanka Mohapatra (SP Energy Networks), James Yu (SP Energy Networks), Douglas Wilson (Alstom Grid – Psymetrix), Stuart Clark (Alstom Grid – Psymetrix), Mark Osborne (National Grid), Phil Ashton (National Grid), Vladimir Terzija (The University of Manchester)

peter.wall@manchester.ac.uk

United Kingdom

Abstract

This paper presents the scope and initial findings of the SP Energy Networks led "Visualisation of Real Time System Dynamics using Enhanced Monitoring" (VISOR) project that will showcase the role of an enhanced Wide Area Monitoring System (WAMS) in overcoming the challenges faced by the GB power system as it moves toward a low carbon future. VISOR is a collaborative UK innovation project that involves all three GB Transmission Owners (TOs) (SP Energy Networks, National Grid and SHE Transmission), the System Operator (SO) (National Grid), researchers (The University of Manchester) and suppliers (Alstom Grid – Psymetrix). VISOR received funding by successfully competing in the Network Innovation Competition (NIC) that was introduced by the GB regulator (Ofgem) as part of the RIIO-T1 price control mechanism to help ensure that the innovation necessary to deliver the reliable and secure operation of low carbon power systems is realised in a cost effective way for the consumer. VISOR will create the first WAMS to collate, store, visualise and analyse synchronised measurements in real-time from across all three of the GB TOs. The WAMS will incorporate wide area synchronised phasor measurements produced at a rate of 50 frames per second that will provide unparalleled monitoring and understanding of the dynamic behaviour of the GB system, when compared to unsynchronised SCADA data that is sampled at one frame per second. VISOR will also see the first deployment of new Waveform Measurement Units (WMUs) that generate 200 frames per second data for the detection of subsynchronous oscillations (SSO). VISOR's ambition is to show how this radical change in power system monitoring can be exploited to reduce both operational and capital expenditure through maximising asset utilisation and to increase resilience against high impact, low probability events that can cause network disruption, plant damage or even blackouts. This ambition can be realised through the innovative use of emerging monitoring, analysis and visualisation techniques to better understand the true capability of the power system and to determine in real-time how close the system is being operated to this maximum capability. Through this improved understanding, WAMS can provide operators/planners with greater confidence to fully exploit this capability when facing new challenges. Security can be enhanced by using real-time measurements to identify threats in advance, rather than during post-mortem analysis. Furthermore, creating the VISOR WAMS will generate valuable lessons learned for any future WAMS roll out in GB and elsewhere. Whilst WAMS can offer a wide variety of benefits to power system operators and planners, VISOR will focus upon the following key areas that are expected to be of the most benefit to the GB system in the short to medium term: 1) real-time monitoring and alarming of subsynchronous oscillations in the range 0.002 to 46 Hz, 2) dynamic model validation using post mortem analysis of WAMS data, 3) hybrid state estimation and 4) the potential use of angle based security limits to increase power flow on the B6 boundary between Scotland and England.

1   Introduction

The VISOR project [1] is funded by the GB regulator, Ofgem [2], and is a collaboration between the GB Transmission Owners (TOs) (SP Energy Networks, National Grid and SHE Transmission), System Operators (SOs) (National Grid), researchers (The University of Manchester) and suppliers (Alstom Grid – Psymetrix) that seeks to showcase the opportunities for Wide Area Monitoring Systems (WAMS) to address the challenges associated with a changing, increasingly complex and more heavily loaded GB power system as it moves toward a low-carbon future.

1.1   Background on Wide-Area Monitoring Systems (WAMS)

Wide Area Monitoring Systems (WAMS) are a rapidly developing practice in power systems that entail the use of system wide measurements that are time synchronised with errors of less than 1 micro second and then streamed in real time at high reporting rates (e.g. 50 frames per second (fps) in a 50 Hz system). WAMS data provides system operators and planners with significantly enhanced visibility

of power system dynamics, which is not possible with the data received by existing SCADA systems, which typically provides a complete set of system wide measurements every 4 to 10 seconds [3]. WAMS exploits the developments in time synchronisation, digital measurement, communication and computing technology to acquire, stream, collate and process time-aligned data from across the entire power system.

A generic overview of a WAMS is given in Figure 1. Data is acquired by PMUs synchronised with respect to a common time reference, usually provided by a Global Navigation Satellite System (GNSS) such as the Global Positioning System (GPS). Data is then streamed in real-time from multiple PMUs to one or more Phasor Data Concentrators (PDCs), where it is aggregated and time-aligned. The combined data can then be stored, analysed and visualised in real-time – as well as being forwarded to other PDCs as a real-time data stream. Regional or substation PDCs may form intermediate nodes receiving data streams from all PMUs in their region and re-packaging them into a single stream of time-aligned data.

The applications enabled by WAMS offer solutions during real-time operation and offline analysis, examples include real time visualisation of system dynamics, steady state condition monitoring (e.g. angular stress), advanced early warning systems, improved state estimation, real time stability analysis and enhanced model validation [4][5].The scope of possible WAMS applications means that WAMS is seen as a potential solution or solution enabler for many of the new problems faced by power systems as they move toward a low carbon future with radically different generation portfolios and system dynamics. Indeed, recent reports on major blackouts in the USA and India have concluded that WAMS could have helped to prevent them [6][7].
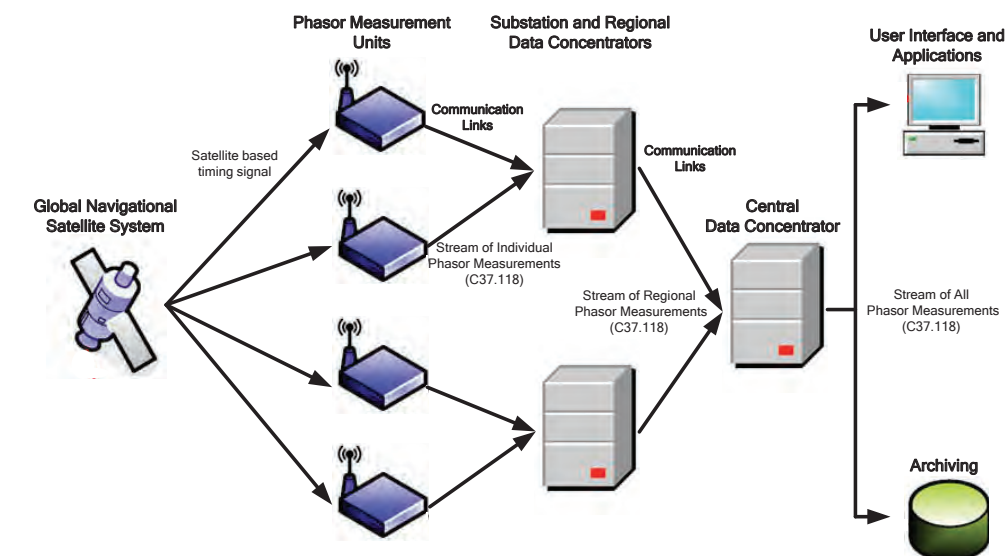
Figure 1: A generic example of a hierarchical WAMS. The substation and regional data concentrators will tend to fill a data aggregation, buffering and basic visualisation role by collecting data from PMUs in their local area, with more advanced analysis, user applications and long-term archiving carried out at PDCs that are further up the hierarchy. Other roles for PDCs lower in the hierarchy can include local, high performance PDCs with low-latency for control applications and TO-level PDCs with full visibility of their own transmission area and a high-level view of neighbouring regions provided by selected data streams from other TO PDCs or SO PDCs.

1.2   Applications of WAMS in VISOR

WAMS can offer a wide variety of benefits to both system operators and planners. However, the VISOR project will focus upon the following key areas:

- Improved monitoring of boundary flows and the interarea oscillations that currently limit the maximum power transfer between Scotland and England
- Extending the range of SSO monitoring to provide early warning of SSR
- Hybrid State Estimation
- Dynamic model validation

Through this, VISOR will seek to showcase the potential for WAMS to:

- Improve the management of risk and system contingencies.

- Maximise asset utilisation
- Reduce uncertainty

Improved monitoring of boundary transfers can allow operation closer to the physical limits of the system and thereby releases existing capacity. The VISOR project focuses on the B6 boundary (Figure 2), which sees significant power flow from Scotland to England and will soon be enhanced with series compensation and intra-network HVDC links. The power transfer on this boundary is a critical part of delivering a cost effective power supply to consumers in GB, as it allows the transfer of low cost and renewable generation from Scotland to the main load centres in England.

Figure 2: The B6 Boundary in the GB power System. The VISOR project is focused upon this boundary as it supports significant power flow between Scotland and England and will undergo significant reinforcement in the coming years.

VISOR complements these transmission enhancements by extending the capabilities of WAMS to observe sub-synchronous oscillations (SSO) in the range of 4 to 46 Hz. These extended capabilities will be realised through the installation of Waveform Measurement Units (WMUs), which are newly developed devices that will see their first demonstration under the VISOR project. Combined with suitable analysis algorithms, these devices should enable the real-time monitoring of SSO and may enable the creation of early warning systems that are capable of detecting incipient threats.

VISOR will introduce a risk management approach using dedicated SSO monitoring devices and support the creation of methods to alarm on pre-cursor indications of SSR. Sub-synchronous resonance (SSR) is a well-documented phenomenon that can cause severe damage to conventional and renewable generators [8]. However, the deployment of series compensation, combined with additional HVDC links and power electronic converters, will increase the potential for unwanted interactions with the AC network, this is becoming increasingly difficult to model and predict and so increased monitoring and analysis is required.

State estimation is one of the core tasks of energy management system (EMS) and underpins the vast majority of power system operation. VISOR will study the development of a hybrid state estimator (HSE) for the GB system that combines classical SCADA data with WAMS data to investigate the potential for improved accuracy, speed and convergence properties and the possible benefits for GB electricity stakeholders.

Dynamic models are the cornerstone of the operation and planning of modern power systems. The VISOR WAMS will provide a valuable source of comprehensive and accessible synchronised measurements for validating and improving GB system models, which will directly benefit both system planning and operation. This same data will also aid in accelerating the analysis of system events, both in the operational and post-mortem timescales, when compared to traditional methods for collating and processing event data.

Furthermore, the creation of the VISOR WAMS will provide the GB transmission industry with practical experience of the deployment of an integrated WAMS that incorporates multiple TO stakeholders, which should prove invaluable in guiding the further development and deployment of WAMS in both GB, Europe and internationally. Laboratory testing will verify the performance of the VISOR WAMS and will range from testing individual monitoring devices using Omicron amplifiers to testing visualisation tools using a real time digital simulator. This testing will provide a valuable platform for the future development of methods for the advanced wide area control of future power systems.

This collaboration between system designers, operators, developers and researchers seeks to not only deliver technical solutions for the targeted problems, but also to consider how best to visualise WAMS data for the end user and apply it to practical decision making during planning and operation.

The rest of this paper provides more details on each of the key areas that are being studied by the VISOR project and is structured as follows:

- Section 2 provides background on the nature of the B6 boundary between Scotland and England that is the focus of the VISOR project.
- Section 3 briefly describes the WAMS infrastructure and devices that will be installed as part of the VISOR project.
- Section 4 details the detection, monitoring, localisation and alarming of subsynchronous oscillations.
- Section 5 describes the application of WAMS in managing system disturbances.
- Section 6 provides an overview of state estimation in power systems and the potential benefits of including phasor measurements in this process as part of a hybrid state estimator.
- Section 7 outlines the approach of applying an angle-based stability constraint to the B6 boundary, a new concept that will be investigated by VISOR.
- Section 8 presents some results of the laboratory based testing of the monitoring devices that are the basis of any WAMS.
- Section 9 describes the benefits of WAMS based model validation and some of the validation techniques that will be used during VISOR.
- Section 10 summarises the existing progress of the VISOR project and describes the key next steps in the delivery of the project goals.

2   The B6 Boundary in the GB System

The Scottish Power Transmission (SPT) system is connected to the National Grid electricity transmission (NGET) system in the North of England via two double 400 kV AC circuits. These circuits, referred to as the East and West Interconnection, along with some neighbouring circuits at 132 kV, make up the Anglo-Scottish constraint boundary (B6).

The boundary is stability limited to around 2500 MW, requiring security under contingency of either the Eastern or Western interconnectors. The limit can be increased to approximately 3300 MW with the arming of an Operational Tripping Scheme (OTS). At day-ahead timescales the maximum capacity of the boundary is required to be planned such that the system does not experience any instability, unacceptable voltage condition, or overloading of any network assets for any credible system fault. The Security and Quality of Supply Standard (SQSS) defines the limits for these conditions [9], specifically it defines system instability in terms of pole slipping and poor damping
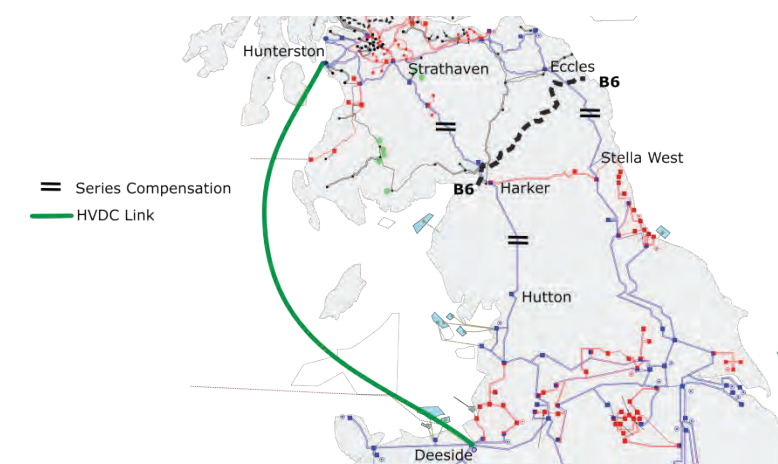
Figure 3: Locations of the series compensation, both fixed and thyristor controlled, and the intra-network HVDC link on the west coast that will be installed to enhance the B6 boundary.

In order to accommodate the increasing volumes of wind power connecting to the Scottish network, a program of upgrades to the capability of B6 is in progress. The connection of Thyrister Controlled Series Compensation (TCSC), Fixed Series Compensation (FSC) and intra-network HVDC links

should see the limit increase to 6600MW by 2017; these enhancements are marked in Figure 3. In line with National Grid's Gone Green 2014 scenario, the requirements of B6 could be greater than 11GW by 2035 [10].

With the continued schedule of changes to the GB transmission system from growing renewable deployment and increasing variability in power flows, a robust and ongoing system monitoring solution is required.

3 VISOR WAMS Deployment

Delivering the goals of the VISOR project requires a GB wide WAMS. Prior to the VISOR project, small, isolated WAMS were in place at National Grid and SPT. Therefore integrating, augmenting and extending these to create a WAMS capable of providing real time visibility across the entire GB power system was the first goal of the VISOR project. Figure 4 provides a schematic and geographical overview for this WAMS.

The VISOR WAMS, like any other WAMS, incorporates four main elements:

1) Time Synchronised Measurement Devices

2) Communication Networks

3) Data Concentration

4) Applications

The synchronised measurement devices in the VISOR WAMS will include PMUs, which are the most widely used synchronised measurement device [5], and Waveform Measurement Units (WMUs), a new device created to provide extended oscillation monitoring in the range of 4 – 46 Hz. Both devices are synchronised to a time reference provided by GPS. The key difference is that PMUs report phasor measurements at a rate of 50 fps, whilst WMUs report waveform samples at a rate of 200 fps. These devices can be stand-alone devices that use dedicated hardware or integrated devices that are implemented as part of substation relays or disturbance recorders. Most of the work in VISOR will utilise PMU data, whilst WMU data will be used solely for the monitoring of SSO. However, the WMU units are an essential component of the VISOR WAMS, as they can be used to capture oscillations that are above the 25 Hz Nyquist frequency of the PMUs, which defines the theoretical maximum frequency of oscillation that they can report.

The communication networks are the key infrastructure facilitating the transfer of measurements from the remote devices to data concentrators, designed to collate measurements into a single record for each time stamp. It is important that both the communications links to substations and those between the TO level data concentrators (Data Centres) and SO level data concentrator (Data Hub) function and perform correctly. Factors including bandwidth, traffic shaping / Quality of Service management, firewalls and network locations have been carefully considered.

In VISOR, as in many WAMS, the roles of 3) and 4) are both served by a WAMS server that provides PDC functionality, storage, analysis and visualisation of WAMS data. The WAMS applications can be considered, in many ways, to be the most important aspect of the WAMS, as they convert the WAMS data into useful information for operators and planners. Examples of WAMS applications are discussed in the later sections of this paper.

Figure 4 outlines the schematic and geographical overview of the integrated VISOR WAMS, which incorporates four new WAMS servers, in addition to the pre-existing SPT and NG systems. A new Data Centre at each of the three GB TOs will aggregate the data generated by the PMUs and WMUs connected within that TO's network. These Data Centres will provide storage, analysis and visualisation at the TO level. The Data Centres will also forward their data in a single re-packaged real time stream to the VISOR Data Hub server, installed at the SO, to provide GB-wide visibility, as required by VISOR. This architecture provides redundancy and reliability: in the event of communications failure between TOs, data is buffered locally and re-sent once links are restored. In the event of a disk failure at the Data Hub, copies of the data are available at the local server and vice versa.
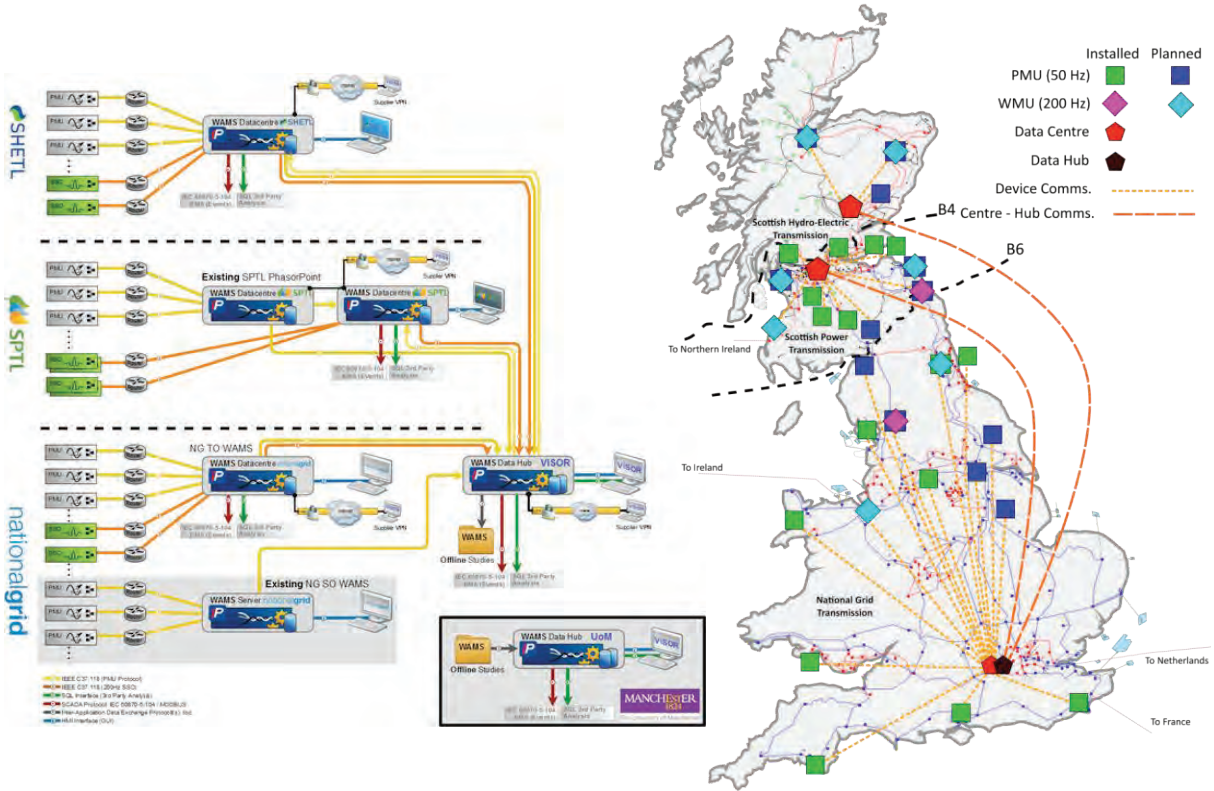
Figure 4: A schematic and geographical view of the VISOR WAMS. Data Centres will be installed in all three TOs to collect the measurements from their regions and a Data Hub has been installed in the system operator to provide a GB wide view in real-time. Furthermore, an offline Data Centre at The University of Manchester will be used for offline studies.

4 Detection, Monitoring and Alarming on Sub-Synchronous Oscillations

4.1 Background

The installation of Series Compensation, and the increasing penetration of Power Electronic converters associated with renewable generation and HVDC links, add vital flexibility and capacity to the power system and help in the move to a low-carbon grid. However, this plant also introduces new challenges, not only in protection when considering fault scenarios, but also in steady state and post-fault operation – with the potential for Sub-Synchronous Oscillations (SSO) [11][12]. These oscillations fall into three main categories [13]:

- **Sub-Synchronous Resonance** (SSR): probably the most well-documented form, this involves interaction between generator shaft torsional modes and electrical resonances created by series capacitors and network impedance.

- **Sub-Synchronous Control Interaction** (SSCI): interaction of power electronic converters, such as HVDC links and doubly-fed or fully-converted wind turbines, with electrical resonances created by series capacitors and network impedance.

- **Sub-Synchronous Torsional Interaction** (SSTI): interaction of power electronic converters with generator shaft torsional modes.

All of these oscillations entail some form of interaction between the torsional modes of oscillation of long shaft generators and some other part of the power system. These torsional modes exist because every mechanical system has a set of natural oscillatory frequencies A large generator rotor is composed of distinct turbine sections (e.g. high pressure, intermediate pressure and low pressure turbines) connected by solid shafts which can ideally be modelled as a set of masses interconnected by massless springs of finite stiffness, as shown in Figure 5 and Figure 6. Mode zero in Figure 5A represents the condition where the masses all move in phase and the entire shaft system behaves as a solid mass (Classical generator rotor model) with a common mode of oscillation, i.e. the whole system oscillates as one body at a given frequency. Figure 5B and Figure 6 are representative of turbine sections (masses M1,M2 and M3), connected by shafts (springs with stiffness K12 and K23)

that are experiencing the oscillatory modes in which they may interact. Any physical system composed of n masses produces (n-1) oscillatory modes as seen in Figure 5B and Figure 6, where a system of two masses produces one torsional frequency mode (Mode 1) while a system of three masses produces two torsional modes (Mode 1 and Mode 2, note Figure 6 shows only Mode 2). The dashed line represents the corresponding mode shape and demonstrates how individual sections contribute/participate in them. In contrast to mode zero, the torsional modes causes the masses to oscillate against each other exposing the shaft to cyclic stresses (torque) that might cause shaft fatigue and damage.
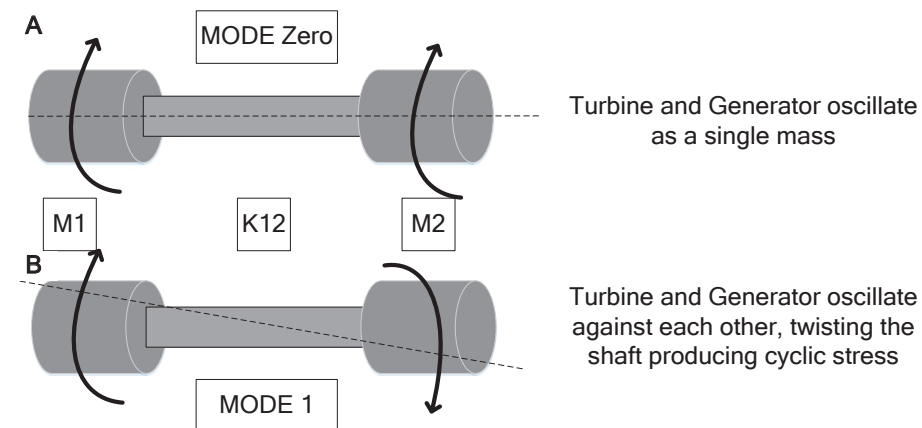

Figure 5: The mechanical system of a generator can be modelled as a set of *n* masses connected by springs, when these masses oscillate in phase the system can be viewed as a single mass with one speed (A). However, if the masses oscillate out of phase the shaft will experience cyclic stress from the torsional modes. The number of torsional modes in the system is equal to *n*-1 [38]
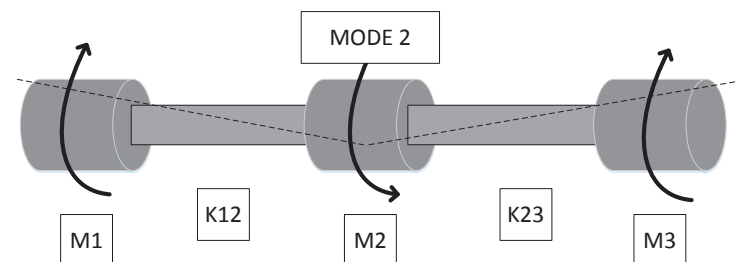

Figure 6: Dashed line represents the mode shape, Mode 1 and Mode 2represent torsional modes that cause shaft stress and fatigue [38]

In most cases, these torsional oscillations are well damped and the fatigue is negligible. However, interactions with other forms of oscillations (e.g. through SSR, SSTI and/ or SSCI) may excite one or more of these low frequency torsional modes and introduce negative damping, thereby exacerbating these oscillations to dangerously high amplitudes and causing severe damage to the generator shaft, which not only shortens its operational life but may also cause shaft failure or permanent damage. The first severe case of SSR occurred in 1970 in the Mohave desert when a generating unit became radially connected to the rest of the system through a single 70% series-compensated 500 kV line. The 30 Hz torsional oscillations experienced resonance over a period of several seconds and caused the generator shaft to heat up to such an extent that the electrical insulation failed. The subsequent arcing burned a hole in the shaft, as seen in **Figure 7**. A second failure occurred within a matter of months, as the analysis of the first event had failed to identify or correct the problem. Several other incidents have since occurred and severe shaft damage has been reported due to subsynchronous interactions, this has meant that System Operators and Transmission Owners have begun to take special care at the planning stage to avoid similar occurrences.

Figure 7: Shaft damage caused due to SSR at Mohave, 1970 [38]

These potential issues are carefully considered when new plant, such as Series Compensation or an HVDC link, is to be installed. The resulting mitigating actions often include careful network studies and design, the implementation of filters to prevent any predicted interaction, and the addition of protection systems to prevent damage should serious oscillations occur [12]. However, a key requirement remains for a monitoring approach that will:

- Characterise power system behaviour pre- and post-commissioning, serving to validate study conclusions and network and plant models

- Support the commissioning of the new plant and associated SSO protection

- Highlight underlying low-level oscillations that do not trigger protective action, but may cause undue plant wear, or may escalate to more serious levels following a system event.

- Provide early warning of emerging oscillation problems in operational timescales, prior to the triggering of protection equipment.

4.2   Monitoring solution

Traditional PMU based WAMS utilise synchronised phasor measurements transmitted via the IEEE C37.118 protocol at up to 50/60 frames per second (fps) – i.e. once per cycle in a 50/60 Hz system. The observable bandwidth from PMU measurements is influenced by two key factors:

- The need to ensure adequate attenuation of aliased components: this means filter roll-off must begin lower than the theoretical 25/30 Hz Nyquist limit.

- The window employed for phasor calculation: this is typically taken over multiple 50/60 Hz cycles, which provides greater accuracy at the cost of attenuating higher frequency content. Reducing the calculation window increases bandwidth but adds measurement noise and errors.

These factors lead to a practical observable range of up to about 10 Hz – the C37.118 standard defines a minimum performance bandwidth of 2-5 Hz [14]. This is sufficient to capture governor-mode and electromechanical oscillations accurately, along with some voltage control modes. With the proliferation of PMUs, wide-area monitoring of such oscillations has been implemented in many utilities across the world [15].

A further challenge emerges from the need to differentiate generator shaft torsional oscillations, which appear in grid electrical measurements as sidebands at fgrid ± fmechanical, from electrical-only oscillations, such as voltage control modes, that appear only at felectrical.

In order to extend this visibility up to the 4-46 Hz range required for observability of SSO in GB, a new approach was taken. A new Waveform Measurement Unit (WMU) was developed by the project supplier to provide time-synchronised voltage and current point-on-wave measurements, streamed in real-time via the C37.118 protocol as "analogue" type values. This approach serves to provide a true representation of oscillatory components in the 4-46 Hz range, whilst giving visibility of the 54-96 Hz range so as to differentiate generator torsional oscillations from electrical resonances. It should be noted that the use of a higher reporting rate of 200 frames per second is fully compliant with the C37.118 standard, and is in fact encouraged [16].

The WMU is implemented on a multifunction recorder that already incorporates PMU capability. Ten of these devices are being installed at key locations in the GB grid as part of the VISOR project; each device will monitor voltage and current and provide both a 50 fps PMU and 200 fps WMU stream to the VISOR WAMS servers. In addition to the PMU, WMU, and typical fault and disturbance recording capabilities the multifunction fault recorder also provides continuous local recording at 800 fps, which has already been useful in more detailed investigations of high frequency phenomena during the project.

The 200 fps voltage and current waveforms from each WMU stream are collated, processed and stored by the WAMS server. Real-time SSO analysis is then applied, extracting the amplitude, frequency and damping of SSO modes in the 4-46 Hz range. The analysis results are:

- Presented to users in a wide-area map view and live data charts – providing real-time SSO situational awareness, and identification of interacting plant.

- Monitored for alarming on high amplitude or poor damping – to give early warning of growing oscillations, and to highlight persistent mid-level oscillations that would not trigger protection but may cause plant damage. Alarms are based on user-configured thresholds and sorted into frequency bands of interest.

- Stored for historical review and wider analysis. Visibility of the 54-96 Hz range is also provided to enable users to differentiate between mechanical and electrical modes. Historical analysis is used to define suitable frequency bands of interest and alarm thresholds, as well as in study and plant / model validation work.

This solution represents a departure from previous approaches [11], where only severe resonance effects or those following a disturbance are captured, analysed or acted on. With this approach, users can gain understanding and experience from observation of low-level SSO behaviour, and can identify and respond early to significant oscillations, before automated protection is triggered and plant is tripped or bypassed.

4.3 Results so far

At this stage, WMUs have been installed on the Eastern and Western double-circuit interconnectors between Scotland and England, with further units to follow later in 2015. Analysis of data gathered thus far has highlighted the following:

- A number of low-level sub-synchronous modes that are fairly stationary in frequency and consistently observed over several hours – suggestive of generator torsional modes.

- Some oscillations with slow but widely-varying frequency – which is indicative of power electronic control behaviour.

- Distinct changes in oscillatory behaviour are observed corresponding to the arming and dis-arming of Series Compensation in the interconnection – this is to be expected.

It should be noted that these are initial observations that are pending further review with generator and series compensation engineering teams. Nevertheless they serve to demonstrate that such behaviour can be observed in real-time, and to reinforce the value of SSO visibility going forward. Further characterisation of system behaviour will be made as additional locations and longer periods of data become available, and as additional series compensation is commissioned.

5 Managing System Disturbances

5.1 Challenges

There are a number of challenges associated with the management of system disturbances, both in the operation control room domain and in post-event analysis and reporting:

- **Disturbance Characterisation: Information Overload**
  A single root-cause event can typically trigger multiple automated control and / or protection actions, which along with the original event can result in hundreds of detected deviations and reported control room alarms. Whilst any transmission generator or line trips may be quickly identified from these, the overall system impact can be difficult to digest – making the immediate risk to the system and appropriate restorative actions less obvious.
- **Cascading Disturbances: Increased System Risk**
  Experience has shown interdependence between power system events – which increases with

system stress. Many recent major blackouts have been the cumulative result of multiple cascading disturbances [6][7]. Managing these chains of events whilst maintaining a high-level view of system security can be difficult. It is important that occurrence and impact of such disturbances is highlighted to operators in real time, so that action can be taken where possible to prevent further cascade.
- **Post-Event Analysis**
  Post-event analysis of system disturbances can take several weeks or even months depending on the event; the power system in question; and fault recording equipment capabilities, time synchronism and communications [17]
- **Historical Review: Selection of Significant Events**
  Utilities will often conduct historical reviews of events, for example to extract statistical information on event severity, or to select a range of events to be used in model validation exercises. Such reviews require suitable event metrics to facilitate comparisons, such as MW loss. These metrics must be calculated and recorded, either during initial event logging or as part of the historical review.

5.2 WAMS Solutions

As part of the VISOR Project, a System Disturbance Monitoring (SDM) application module will be demonstrated. This WAMS application utilises time-synchronised voltage phasor and frequency measurements from PMUs across a power system in order to:

- **Detect** significant system disturbances including line trips, load or generation trips, and transient faults and establish an accurate time estimate.
- **Localise** the disturbance source, to the nearest monitored location.
- **Characterise** the disturbance as a frequency event (load / generation loss) or angle event (line trip or transient), whilst aiding operators in performing further diagnosis more quickly.
- **Quantify** the impact of the disturbance in terms of MW change
- **Highlight** chains of successive events

These functions are performed in real-time, as well as being available for retrospective historical analysis. Disturbances are detected and localised through analysis of Rate of Change of Angle (ROCOA) relative to a reference, using the principle that voltage angles will move earlier and faster closer to the trigger location. Events are then characterised based on observed Rate of Change of Frequency (ROCOF), from which the associated MW change is estimated based on the relationship between ROCOF, system inertia and MW change shown below [18]:

$$\Delta p = 2 \sum_{i=1}^{N} \Delta p_i = \frac{2}{f_n} \sum_{i=1}^{N} H_i \frac{df_c}{dt} = \xi \frac{df_c}{dt} \qquad (1)$$

$$\text{Where: } \xi = \frac{2}{f_n} \sum_{i=1}^{N} H_i \qquad (2)$$

For each detected event the trigger time, location, event type and estimated MW change are recorded. In addition, the trigger location is highlighted on a map display and successive events within a short time period are numbered in order of occurrence, so as to highlight cascading disturbances.

This serves to:

- **Provide a high-level view** of disturbance nature, location and impact to operators, giving them key information to help formulate a response
- **Highlight emerging cascades** so that they can be stemmed
- **Speed up post-event reporting** with immediate post-event high-level diagnosis and flexible access to underlying collated and time-synchronised WAMS data.
- **Supply summary information on historical system events** to enable faster review for statistical analysis and identification of significant events for study e.g. model validation.

5.3 Results so far

At this stage in the project, a historical review of WAMS data has been conducted in order to establish a behavioural baseline for ROCOA and ROCOF. This baseline allows optimal settings for event detection to be determined so that significant, abnormal events are logged but minor disturbances such as everyday network switching are ignored. In addition, a historical review of known load or generation-loss events has been performed to derive an appropriate value of ξ, which will be used to estimate MW change for future detected events.

The application is now being deployed on the VISOR WAMS servers, and will be demonstrated and evaluated over the coming months. Later in 2015, the application will be augmented to provide additional disturbance impact metrics to further characterise detected disturbances. The summary information provided by the SDM application will support work under the VISOR project to validate the GB system dynamic model. The disturbance analysis data will provide researchers with key metrics by which to extract a representative set of events to be compared with simulations from the system model.

6   Hybrid State Estimation

Hybrid State Estimation (HSE) is a method for creating an improved state estimator by including synchronised measurements of voltage and current phasors (magnitude and angle) in the state estimation procedure that has traditionally used unsynchronised measurements of voltage magnitude and active/reactive flows and injections. This has the potential to improve the accuracy of the state estimator output and the speed and reliability of its convergence to the optimal state estimate.

Static State Estimation (SE) in power systems is one of the core tasks of the Energy Management System (EMS) and is responsible for determining the optimal estimate of the complete state of the system based on measurements of voltage magnitude, power flows and power injections collected from unsynchronised measurement devices by the Supervisory Control And Data Acquisition (SCADA) system. This state is the voltage magnitude and phase angle at each node/bus and from this the line flows, load consumption and generator outputs are also estimated.

The SCADA measurement data that serves as an input to the State Estimator is not perfect; as it will contain random errors, or noise, and parts of it may even be unavailable or corrupted, referred to as bad data. Furthermore, measurements will not be available for every element, as measurement devices are not placed at every location in the system. Finally, the measurements are asynchronous and are reported at intervals of between 4 and 10 seconds. Therefore, they will most probably not have been recorded at the same times as one another, so will represent different system conditions. Whilst in most cases these differences will be small, they can cause a problem if a disturbance occurs during the time over which SCADA is collecting data.

Therefore, state estimation is a complex and challenging task that applies recursive estimation techniques to the available measurements to return a best estimate of the system state, whilst taking into account measurement errors, missing data and bad data.

6.1   Overview of Existing GB State Estimation
The method of state estimation (SE) employed in the GB control centre is based on asynchronously gathered data, collected by polling remote terminal units (RTUs) that provide information to the SCADA system. The RTUs measure data locally at a rate of one measurement per second, which is not time stamped at source. Due to the time taken to scan the entire network the data has an arrival rate of 1 complete set of samples every 4-10 seconds. The system is therefore at a slightly different state by the end of the scan allowing for potentially inconsistent results to be returned in the SCADA system, for instance, current can be indicated as flowing in a line with an open breaker.

A "snap-shot" of the SCADA data, based on the latest pole, is taken every time the SE is run; the process itself takes around 60 seconds, so considering the 10 seconds taken for the SACDA polling the corresponding estimate provided can be considered as about 70 seconds out of time, as shown in Figure 8.

The ability of the SE to provide a solution is becoming increasingly dependent on data quality and availability.
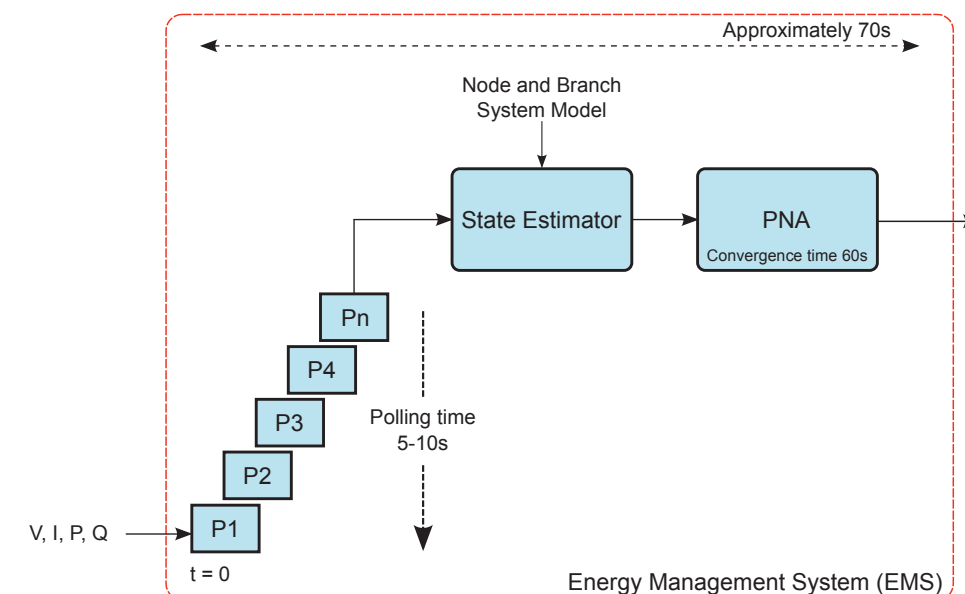

Figure 8: Overview of the execution of the existing state estimator in GB.

While the delayed estimate may not be considered a problem during normal operating conditions, it can be more problematic during system incidents, whereby the SE will not be capable of accurately representing the state of the network. The occurrence of any form of system event will eventually change the network to a new steady-state condition, so such an incident should act as a trigger for the SE to be re-run, so it is always providing the most accurate quasi-steady state approximation of the network [19].

The SE has been configured to calculate a load flow every 10-minutes with contingency analysis performed by the Power Network Analysis (PNA) system. A quasi-steady state solution for the network is then provided, with an assumption that the network is static during the 10-minute period. If lines or nodes are exceeding a limit then the operator will be notified, and may take corrective action.

6.2   Including Phasor Measurements as part of State Estimation

Phasor measurements from synchronised measurement devices are direct measurements of the power system state (Voltage magnitude and angle); therefore, from the advent of practical phasor measurements their potential application to state estimation has been an area of great interest [20].

If a sufficient number of PMUs are installed to allow complete observability of the power system then a Linear State Estimator (LSE) can be created. A LSE uses only synchronised measurements and can determine the state of the power system by solving only linear equations, as complete observability of the power system implies that the voltage phasor at any bus that is not directly measured by a PMU can be calculated based on the voltage phasor directly measured at neighbouring buses and the measured current flowing between the two buses. These linear equations do not require an iterative procedure to find the optimal solution; therefore, the execution time of a LSE is significantly shorter than a classical SE or HSE and convergence is not an issue.

However, complete observability of a power system requires the installation of a PMU at approximately a third or quarter of all buses [21][22] (depending on the topology and level of redundancy) and this is not a realistic expectation in contemporary power systems. Therefore, Hybrid State Estimators (HSEs) that use a combination of phasor measurements and SCADA data to estimate the power system state are viewed as an attractive opportunity to exploit the potential benefits of WAMS to state estimation in the short to medium term.

The main challenge faced when creating a HSE is determining how to combine the synchronous and asynchronous measurements during the state estimation procedure without a loss of accuracy or robustness. Various methods have been proposed for creating a HSE and the most common forms of centralised HSE are post processing HSEs [23] and integrated HSEs, Figure 9 provides a comparison of the execution of these forms of HSE.
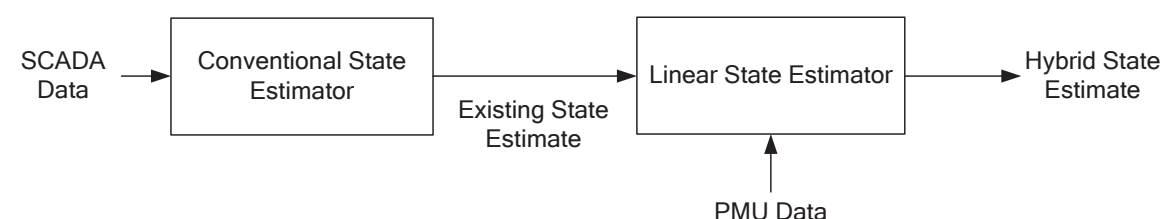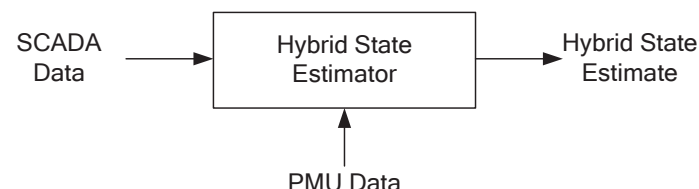
Post-Processing Hybrid State Estimator

Integrated Hybrid State Estimator

Figure 9: Execution of post-processing and integrated hybrid state estimators

A post processing HSE combines the output of the existing state estimator with phasor measurements to create an observable linear state estimator, the output of which is the final hybrid state estimate. The advantage of this is that it does not require the complete replacement of the existing state estimator with a new hybrid state estimator, which should reduce costs and improve reliability. However, if the traditional state estimator does not converge to a solution then the HSE cannot either; therefore, whilst the post-processing HSE can improve the accuracy of the state estimate it cannot improve its convergence properties.

An integrated HSE combines the asynchronous SCADA data and the synchronous PMU data into a single iterative estimation procedure. The challenge faced here is including the measurements of current from PMUs, which are naturally in polar form, into the estimation procedure that uses polar form to represent the voltages and rectangular form for the MW/MVar injections and flows, without loss of precision or the propagation of uncertainty. Four methods have been proposed to overcome this in the literature: Rectangular Currents [24], Pseudo Voltages [25], Pseudo Flows [26] and a Constrained Formulation [27].

VISOR will focus on studying the improvements in the reliability of convergence that may be achieved by using different forms of integrated hybrid state estimator. Whilst HSE can also improve the accuracy of the state estimate and the speed of the convergence, it was felt that reducing the number of cases in which no state estimate was available would offer the most significant benefit to the system operator. This work will also include the development of algorithms for determining the optimal placement of PMUs for supporting HSE, in contrast to existing opimal placement algorithms that determine the best placement for delivering the complete observability required for a LSE [22].

7   Application of a Combined Power – Angle Boundary Constraint to B6

7.1   Background

The B6 boundary can be considered as a corridor connecting the two main inertia centres of Scotland and northern England. Due to the line length and impedance, and the large power flow predominantly southwards, the boundary stability constraint mainly relates to a fault and loss of lines in the corridor causing acceleration of central-north Scotland relative to the north of England.

In the present practice, the B6 boundary transfer and limits are defined in terms of the MW transfer through the cut-set of lines crossing the Scotland-England border. Historically, when the Scottish generation mix was primarily of the synchronous thermal type, this provided a reasonable measure of the stability limit, as the corridor consisted of mainly passive lines, and the Anglo-Scottish generator rotor angles were closely related to power flow across the boundary. However, recent years have seen the connection of significant volumes of wind generation (>1.5 GW) at various points in the corridor. This wind generation may contribute to voltage support and will affect the pre-fault angle separation between the centres of inertia, but provides little or no direct contribution to the inertia or

angular stability. This, together with a reduction in thermal synchronous generation in Scotland, changes significantly the Power-Angle characteristics of B6.

7.2   Concept

The concept to be demonstrated and evaluated under VISOR is that a new boundary constraint expression incorporating both B6 MW flow and the angular separation between the Scottish and English centres of inertia will better represent the B6 stability limit. An approach combining the existing MW limit with a new corresponding critical angle separation limit is expected to permit a significant number of additional stable operating scenarios, where the MW limit is exceeded but the Anglo-Scottish angular separation remains lower than a corresponding threshold.

This concept has been tested through some initial simulation study work on a simplified 11-bus system similar to the B6 boundary [28]. The applicability of these results to the real B6 boundary has since been tested on a reduced equivalent of the GB system model. Whilst further detailed study, demonstration and evaluation is required, these studies support the suggestion that additional capacity can be released through the use of a combined power-angle constraint.

7.3   Work Under VISOR

Under the VISOR project, this concept will be demonstrated in the form of a new WAMS display driven by PMU power and angle measurements on and around the B6 boundary, including the key influential generators in Scotland and Northern England. This demonstration will serve to evaluate:

- **The potential for capacity release**, through a combination of reduced security margin due to improved monitoring of the constraint and allowing a wider range of operating scenarios, which may breach the MW limit but respect the angle limit.
- **The reliability and robustness** of the approach against system dynamic behaviour and limited loss of observability due to infrastructure failure.

8   Laboratory Testing of WAMS Devices

The performance of the measurement devices in a WAMS is a critical factor in determining how useful any applications based on the data from the WAMS will be. Therefore, an ongoing aspect of VISOR will be the assessment of the performance of these measurement devices in a laboratory environment. This assessment will be tasked with identifying a baseline for the performance of these devices and to attempt to identify the source of any anomalous behaviour observed in data recorded by the VISOR WAMS.

8.1   Laboratory Test Setup

An overview of the laboratory setup is presented in Figure 10 and this setup is described in more detail in [29]; some results from the initial testing of PMUs and the WMU are discussed below.

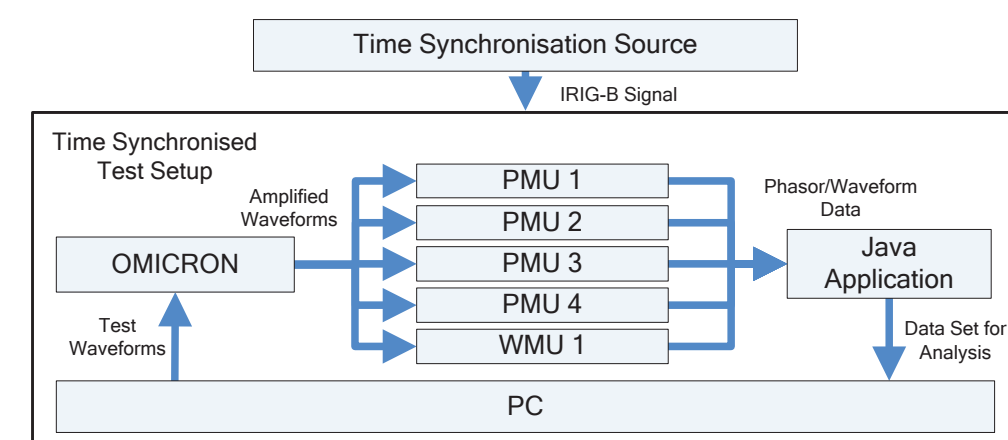**Figure 10: Overview of the time synchronised test setup at The University of Manchester. Simulated signals are replayed using an OMICRON amplifier and the device response is captured using a Java Application based on Open PDC**

Three types of sinusoidal voltage test signals are considered in these examples, these are described below and Figure 11 provides a comparison of their properties in the frequency domain:

1) Additive sinusoidal oscillation in voltage magnitude:

This additive signal consists of a fixed oscillation, $v_f(t)$, at fundamental frequency, f_f, and magnitude, V_f, to which a second oscillation, $v_a(t)$, with frequency, f_a, and magnitude, V_a, is added. This can be represented as follows:

$$v_{add}(t) = v_f(t) + v_a(t) = V_f \sin(2\pi f_f t) + V_a \sin(2\pi f_a t) \qquad (3)$$

This signal is of interest as electrical modes of oscillation, e.g. oscillations from series compensation or controllers, will be observed as additive oscillations with a single frequency.

2) Amplitude modulation of the voltage magnitude

This signal consists of modulating the fixed fundamental oscillation, $v_f(t)$, with a second oscillation, $v_M(t)$, with frequency, f_m, and magnitude, M:

$$v_{AM}(t) = \left[1 + v_M(t)\right] v_f(t) = \left[1 + M\cos(2\pi f_m t)\right] V_f \sin(2\pi f_f t) \qquad (4)$$

This multiplication of the fundamental oscillation by the modulating oscillation creates two sidebands in the frequency domain, which can be viewed as two additive oscillations in the time domain at frequencies of $f_f + f_m$ and $f_f - f_m$:

$$v_{AM}(t) = V_f \sin(2\pi f_f t) + \frac{V_f M}{2}\left[\sin\left(2\pi\left(f_f + f_m\right)t\right) + \sin\left(2\pi\left(f_f - f_m\right)t\right)\right] \qquad (5)$$

This form of test signal is useful as the torsional modes of generators create sidebands in the electrical signals observed in a power system.

3) Frequency Modulation of the fundamental signal

This test signal does not modify the magnitude of the fundamental oscillation, as is the case with the other test signals. Instead, the frequency of the fundamental oscillation is varied as a function of time:

$$v_F(t) = V_f \sin\left(2\pi f_f(t) t\right) \qquad (6)$$

Where, in this case, the function that describes the variation in the system frequency is a sinusoidal oscillation with frequency of f_{osc} and amplitude A_{osc} of:

$$f_f(t) = A_{osc} \sin(2\pi f_{osc} t) \qquad (7)$$

This form of test signal is useful for observing the behaviour of measurement devices when exposed to oscillations that are best observed in the system frequency, e.g. common mode oscillations. The frequency content of this signal, as observed in the voltage magnitude, is made up of side bands that can be described using a Bessel function of the first kind.
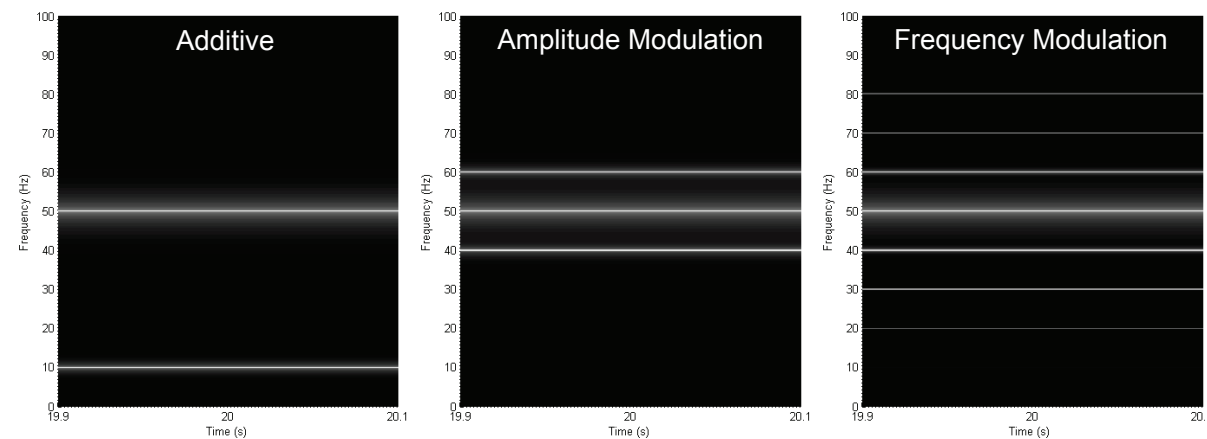

Figure 11: Spectrograms comparing the true frequency content of the instantaneous voltage of the three test signals used here for f_a, f_m and f_{osc} values of 10 Hz.

8.2 Selected Test Results

Comparison of Additive Oscillations and Amplitude Modulation

The example presented here compares the response of the devices when exposed to a 10 Hz additive oscillation and a 40 Hz amplitude modulation, which creates side bands at 10 Hz and 90 Hz. Both of these signals were sustained for sixty seconds to provide an extended period over which to evaluate the device response.

Figure 12 shows the FFT output for the voltage magnitude reported by PMU 1 and 3 and the instantaneous voltage reported by the WMU for the 10 Hz additive signal and Figure 13 shows these same outputs for the case of the 40 Hz amplitude modulation. Note that the different scaling of the x-axis is due to the Nyquist frequency of the different reporting rates of the devices, i.e. the PMU data is reported at 50 fps so provides visibility up to a theoretical maximum of 25 Hz, whilst the 200 fps WMU data has a theoretical maximum of 100 Hz.

These limited results are sufficient to demonstrate that the PMUs, whilst capable of accurately reporting the 10 Hz additive signal, are incapable of distinguishing between the 10 Hz additive signal and the 40 Hz amplitude modulation, as their nyquist frequency prevents the upper side band from being captured accurately.

Indeed, the amplitude modulation is simply reported as a larger 10Hz oscillation, possibly due to aliasing of the 90 Hz side band. It is important to note that the y axis of the sub plots in Figure 12 and Figure 13 are not on the same scale. Whilst this does limit the direct comparison of these plots, it is necessary due to the significant variation in the energy of the oscillations reported by each device. In future work this significant variation in the size of the oscillation reported by each device will be an area of study, as it may compromise the correct reporting of the true oscillation magnitude.

The output of PMU 1 contains a 2.5 Hz oscillation for both cases, the source of which is unclear. Finally, the waveforms for the voltage magnitude, angle and frequency reported by the PMUs are not shown here, for the sake of brevity, but for all of the PMUs, apart from PMU 3, an oscillation was also observed in the frequency estimate returned by the PMUs. In contrast, the WMU output can be used to distinguish between the additive oscillation and the amplitude modulation, albeit with the upper side band at 90 Hz attenuated somewhat by the roll off of the WMUs anti-aliasing filters.
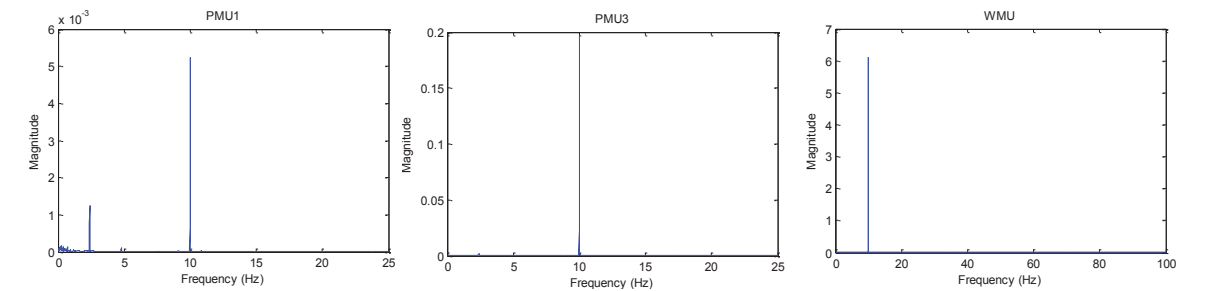
Figure 12: FFT of the Voltage Magnitude for PMUs 1 and 3 and the Instantaneous Voltage for the WMU when exposed to a 10 Hz additive oscillation with magnitude of 0.01. The limits of the x axis are set by the Nyquist frequency of the devices 25 (PMU) or 100 (WMU) Hz. The y axis limits are different for each device; this is due to the marked differences in the energy of the oscillations reported by each device, e.g. the oscillation seen for PMU 1 is approximately 40 times weaker than the oscillation seen for PMU 3.
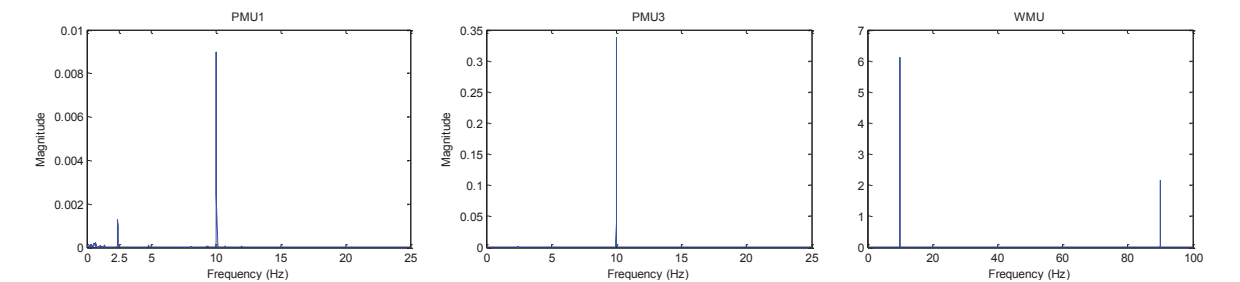
Figure 13: FFT of the Voltage Magnitude for PMUs 1 and 3 and the WMU when exposed to a 40 Hz Amplitude Modulation with M=2. The limits of the x axis are set by the Nyquist frequency of the devices 25 (PMU) or 100 (WMU) Hz. The y axis limits are different for each device; this is due to the marked differences in the energy of the oscillations reported by each device. As in the additive case the oscillation seen for PMU 1 is approximately 40 times weaker than the oscillation seen for PMU 3.

Frequency Modulation

In this example the devices were exposed to a 0.5 Hz oscillation in the frequency of the fundamental waveform. Figure 14 shows the frequency output of PMUs 1, 3 and 4 and Figure 15 shows the FFT of the frequency output for PMUs 1 and 4 and the WMU when exposed to this signal. These figures show that: As in Figure 12 and Figure 13, the y axis of the sub plots in Figure 14 and Figure 15 are given on different scales due to the markedly different energy of the oscillation reported by each device.

- PMU 4 is capable of accurately tracking the frequency oscillation throughout the test with the correct magnitude.
- PMU 1 reports a frequency oscillation of 0.5 Hz in the FFT results, but it can be seen in the time domain that the fixed oscillation is distorted by other low frequency oscillations that should not be present and the magnitude is attenuated by a factor of approximately five.
- PMU 3 does not reflect any change in its frequency output, this is surprising given the large amplitude of the frequency oscillation and suggests that the lack of an erroneous oscillation in frequency during the previous tests may be due issues in its frequency estimation algorithm.
- The WMU output contains a 0.5Hz oscillation of the proper magnitude.

It should be noted that, whilst not shown here, the voltage magnitude of all the PMUs was distorted slightly by the frequency modulation although the exact nature of this distortion is unclear, whilst the FFT of the WMU voltage was a Bessel function when the 50 Hz component was removed by a notch filter, as would be expected (see the frequency modulation case in Figure 11).
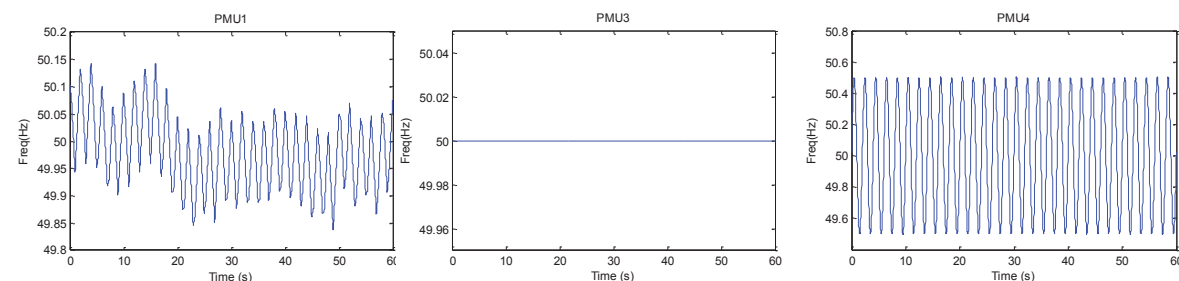

Figure 14: Frequency output of PMUs 1, 3 and 4. The y axis scales are different for each plot as the range of frequency variation is quite different, e.g. PMU 3 shows no variation, PMU4 has a steady 10 Hz oscillation with a 1 Hz peak to peak magnitude and PMU1 has a 10 Hz oscillation with 0.15 Hz peak to peak amplitude superimposed onto other, unexpected low frequency behaviour.
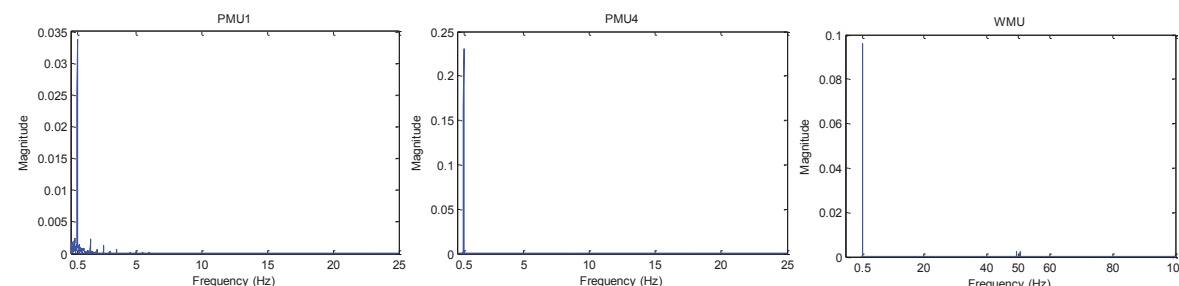

Figure 15: FFT of Frequency for PMUs 1 and 4 and the WMU. The limits of the x axis are set by the Nyquist frequency of the devices 25 (PMU) or 100 (WMU) Hz. The y axis limits are different for each device; this is due to the marked differences in the energy of the oscillations reported by each device.

These results are not comprehensive, but do demonstrate the fact that measurement device performance must be a key consideration when deploying WAMS and when developing WAMS applications, in order to prevent measurement artefacts being interpreted as power system behaviour, and when developing WAMS applications.

9   Model Validation using WAMS data

The growing complexities of the power system are placing increasing reliance on the accuracy of system models. Poor system modelling may result in poor, or even dangerous, planning/operational decisions. At the planning stage this may lead to underutilization of assets leading to wasted resources (money). At the operational stage, this may prompt System operators to take faulty decisions as the system behaviour or component interactions cannot be judged properly. Generally,

instances of instability are avoided through system model simulation studies performed as part of system planning and in recent years as part of on-line stability assessment. However, it is important that these model simulation results correctly reflect well the dynamic behavior of the real system. Validation and improvement of the accuracy of the system models using monitoring data is therefore becoming vital.

Power engineers rely heavily on simulation models in order to carry out planning tasks like determining transmission line operational capacities, network expansion planning and renewable integration. Any new controller design before field deployment has to be tested extensively over a simulation platform to ensure adequate and desired performance. Absence of validated and accurate system models will expose the system to greater risk during operation, as seen in the severe impact of the infamous 1996 WSCC (now WECC) system separation in North Amercia, where simulations failed to emulate the real system behavior (see Figure 16) and caused the operators to take erroneous actions in real time [30].
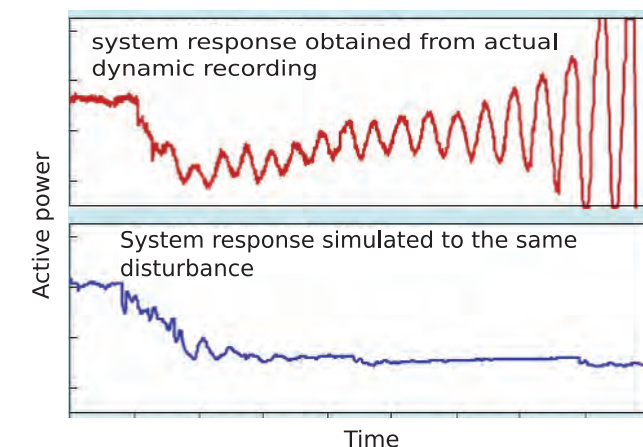
Figure 16: Comparison of the recorded system response to the 1996 disturbance in the USA with simulation results [37]

With increasing demands for reliable electricity supply coupled with increasingly meshed interconnections, FACTS and other non-conventional plant, the dynamic behavior of the system has become ever more complex to monitor. Most existing renewable plants, which are known to introduce uncertainties, do not have disturbance monitoring at present. For example, in the case of wind generation average hour-ahead forecasts have been reported to introduce errors as significant as 7%, which translates into hour-ahead MW forecast errors as high as 1000 MW [36]. In response to this threat, the Bonneville Power Administration (BPA) and the PJM interconnection require all new generators to install a PMU at the point of interconnection for this purpose [36]. Furthermore, with market economy forcing the system to operate closer to its stability limits, operational decisions are required to be based on accurate, online system information and simulations. Therefore, the importance of validation and improved accuracy of system models has never been of greater importance than it is today. It is however a massive challenge to find erroneous components in a complex and huge power system model that is composed of thousands of components and parameters.

Synchronized system-wide phasor measurements of system disturbances can be very helpful in model validation applications. Unlike event/fault recorders, PMUs are designed to make data available on a continuous basis and can capture a wide variety of disturbances, from major contingencies to switching transients that would be sufficiently severe to trigger an event recorder. Simulation output results can be compared against these recorded dynamics to identify any discrepancies that help reveal model inadequacies. Using synchrophasor data to perform the recalculation of voltage stability limits and reactive power management to stabilize the grid during disturbances has the ability to increase generation and transmission throughput that can yield a reduction in operation costs in the order of millions of pounds over decades of use without incurring additional capital investments. However, as with offline studies, these online assessments will require accurate system models.

Open-loop simulations cannot guarantee model validity; however, when complemented with distributed WAMS measurements, discrepancies can be identified. After establishing a correct baseline model structure, like the one shown in Figure 17, and an initial data set, it is imperative to validate and update the model periodically to ensure that it remains accurate over time with various changes or enhancements. Model validation can be based on 'Ambient data analysis' where simulation results are compared with measurements and any changes in the spectral signature can be regarded to be indicative of system changes. Model validation can also be based on 'Response to Major disturbances' which is a good source of information concerning behavior of oscillatory dynamics and the control systems affecting them.
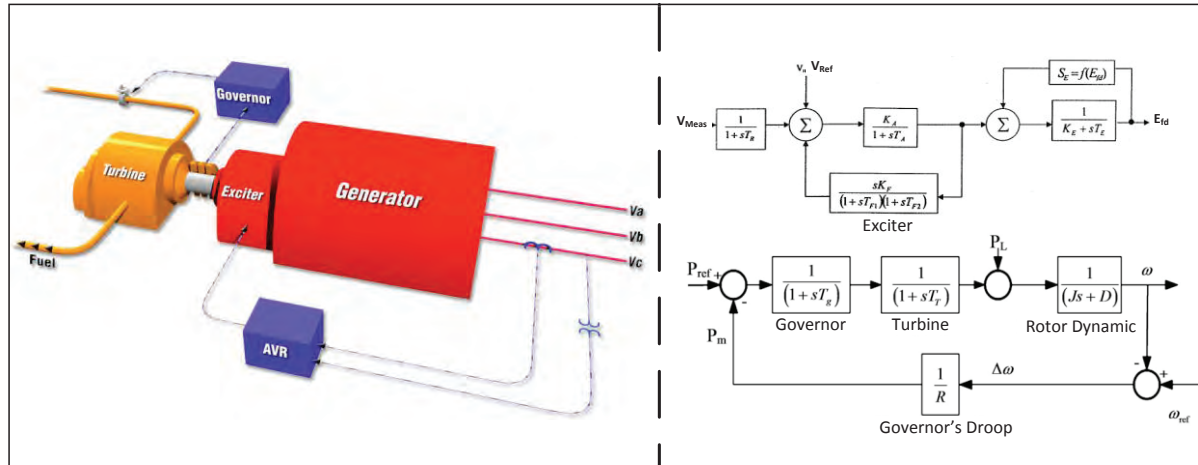

Figure 17: Example of Model Base lining for real turbine, governor, exciter, generator system

In order to ensure a valid comparison, certain requirements need to be fulfilled. Firstly, measurement data should have sufficient dynamic content (e.g. large disturbances) for validation. Moreover, pre-event power flow conditions in the simulation should closely conform to the recorded measurements. Also, the dynamic simulation should mimic the sequence of events reported by system monitoring devices as closely as possible

Two broad model validation approaches have been discussed in literature [31] - [35];

a) System-wide Model Validation
b) Subsystem Model Validation

System-wide Model validation carries out the dynamic simulation of the whole system and benchmarks model quality by comparing results against recorded dynamics at selected locations (e.g. Aug. 10, 1996 WSCC system break-up event [30]). However this approach suffers from certain key limitations that hinder its widespread applicability. For instance, setting up of the pre-event power flow conditions requires the collection of large amounts of measurements (depending upon the number of nodes under consideration for the whole grid) which may take up a long time. Also, under certain scenarios, it gets particularly difficult to gather information regarding the sequence of events from across the whole system (e.g. large number of relay actions, control actions and other adjustments that may occur simultaneously, many of which may not have been recorded or be available for duplication in simulations). Most of all, it requires significant technical expertise to identify any problems, as there are numerous models involved.

The Subsystem Model Validation on the other hand simulates the response of a small sub-system to an actual disturbance. The disturbance is applied to the subsystem model through playback of actual measurements at the point of connection. This is called Hybrid dynamic simulation where the set of variables used for solution of system differential equations is split into two separate vectors, one derived from simulations, the other from real time PMU measurements [33], [34], [35]. The objective of the playback is to ensure the boundary conditions are correctly represented in the simulation when compared to the actual events. It offers distinctive advantages over the System-wide approach in making the 'power flow case setup' easier (smaller system). Also, the sequence of events is no longer required, as the recorded signals are played back at the point of connection to excite the subsystem model, guaranteeing valid comparison. The method can be further illustrated through Figure 18 which shows how a meshed network composed of three areas can be reduced to a single subsystem with

the neighboring areas replaced at their boundaries by measurements that effectively capture its dynamics.
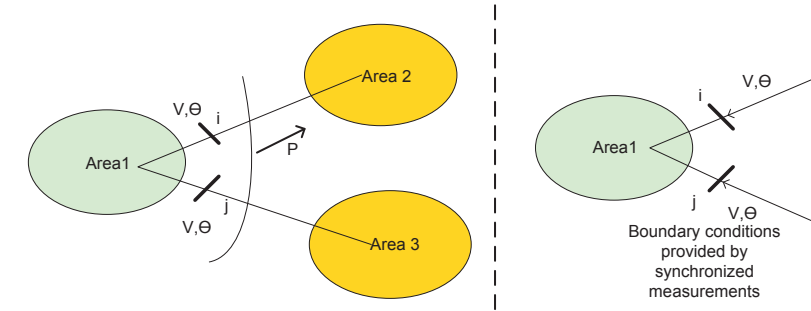
Figure 18: Subsystem Model validation using Hybrid dynamic simulation [32]

Common techniques for playback that have been reported in the literature include

a) Ideal phase shifter – adds an ideal phase shifting transformer and a large synchronous generator at the boundary bus. The large synchronous generator acts as a constant voltage source, the complex ratio of the ideal phase shifter is adjusted at every simulation step to match the voltage and angle measurements at the boundary bus as shown in Figure 19.
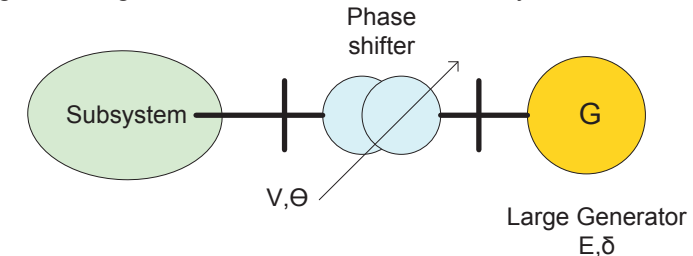
Figure 19: Schematic for Ideal Phase shifter technique of indirect method for hybrid simulations [31]

b) Fast responding generator method –involves application of a large synchronous generator with a fast acting exciter and governor as shown in Figure 20. Measurements are input as references to the exciter-governor system so as to force the generator output to follow them closely.
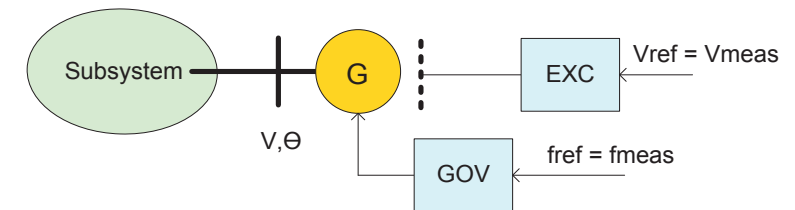
Figure 20: Schematic for Fast responding generator technique for indirect method of hybrid simulation [32], [35]

c) Variable impedance method – measurements at the boundary buses are replaced by equivalent impedances given by (8) as further shown in Figure 21(a).

$$Z(k) = \frac{U^2(k)}{P(k) - jQ(k)} \qquad (8)$$

Where, k denotes the kth step of simulation, $U(k)$ denotes the measured voltage; while $P(k)$ and $Q(k)$ denote the active and reactive power flows measured through PMUs. The method is named variable impedance as the impedance changes at each simulation step based on synchronous measurements. Forced power injection technique is another very similar technique to the variable impedance method, shown in Figure 21(b), the only difference being that here instead of imposing the voltage and frequency measurements, real and reactive power is injected to a load so that ideal responses can be attained for bus voltage and angle.
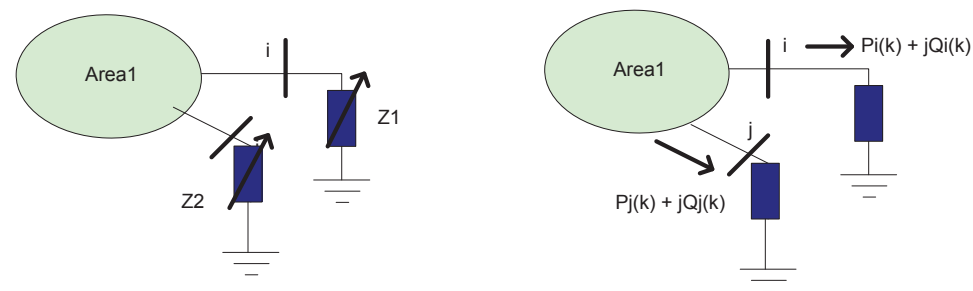
Figure 21 : (a) Variable Impedance Technique (B) Power Injection Technique of indirect method of hybrid simulations [35].

d) Non-linear least squares Optimization technique has also been used to achieve best fit between simulation results and measurements, where one of the measured quantities (e.g. voltage for a given SVC/ STATCOM model) is regarded as a model input while other measured quantities (e.g. reactive power and current for the same device models) could be used as system output. The measured input is played into the simulation model and simulation parameters (e.g. controller gains) are tuned in order to achieve best fit between measurement and simulated output results [39].

10 Conclusions and Next Steps

The VISOR WAMS will provide real-time monitoring from across the GB power system, which will allow VISOR to begin to showcase the potential benefits of WAMS by deploying new WAMS applications. The first new application to be deployed will be for the monitoring of SSOin the range of 4 to 46 Hz. A particular benefit of the SSO monitoring application is that it will provide observability of electrical control modes and their behaviour as throughout 2015-16 new, more complex controllers are introduced into the power system as part of the installation of HVDC, TCSC and PE connected generation (e.g. wind turbines and PV).

This new SSO monitoring will also complement the existing applications for monitoring oscillations in the range of 0.1 to 4 Hz (e.g. local and inter area oscillations). Furthermore, in the long term VISOR will deploy an application for monitoring very low frequency oscillations below 0.1 Hz, e.g. common mode oscillations.

These oscillation monitoring tools will include source location capabilities that will aid in the development of new algorithms that will guide the placement and future deployments of monitoring devices. In this way monitoring can be deployed to better identify oscillation sources, and better monitor sources of particular oscillatory threats or areas of the system that are vulnerable to oscillations. Through better understanding and monitoring of oscillatory behaviour, oscillation based system constraints could be relieved, helping to maximise asset utilisation.

Offline studies will be performed to validate the dynamic behaviour of the full GB system model in terms of both small-signal oscillatory behaviour and post-disturbance transient behaviour, based on synchronised data from the VISOR WAMS. This will include data recorded during normal system operation and where available during significant system disturbances. This study should enhance the quality of the GB system model and provide a baseline for the alarming of power system oscillations observed in the real time data.

The VISOR project will also include an assessment of the impact of uncertainty in dynamic models, as well as generation dispatch and transmission line parameters, on security margins calculations and model based studies.

A new tool will be demonstrated that will use WAMS data to provide detection, localisation and characterisation of system disturbances in real time. This could support real-time operation, post-event analysis, and long-term historical review and will aid in the model validation work by helping to identify disturbances that may be suitable for simulation comparison.

VISOR will also perform an offline trial of the application of an angle and power-based stability constraint on the B6 boundary, evaluating the potential benefits, reliability and robustness.

The VISOR team has identified that the research into the application of HSE to the GB system should focus upon the improvement of the convergence of the state estimator, rather than its accuracy, as failure to converge is a growing threat to GB system operation. Furthermore, it has been identified that

the development of placement methodologies that determine the best placement of a fixed number of PMUs to support HSE and not for determining the placement of PMUs to provide a completely observable linear state estimator should be an area of interest.

VISOR has nearly completed the WAMS deployment stage of the project and will soon have created the first WAMS to provide real time visualisation of the power system dynamics across the entire GB system.

References

[1] VISOR project online portal: http://visor-project.org.uk/
[2] Office of Gas and Electricity Markets (Ofgem), regulator of GB electricity markets: https://www.ofgem.gov.uk/
[3] V. Terzija; G. Valverde; Deyu Cai; P. Regulski; V. Madani, J. Fitch; S. Skok; M.M. Begovic, A. Phadke, "Wide-Area Monitoring, Protection, and Control of Future Electric Power Networks," *Proceedings of the IEEE*, vol.99, no.1, pp.80,93, Jan. 2011
[4] S. Chakrabarti, E. Kyriakides; Bi Tianshu; Deyu Cai; V. Terzija, "Measurements get together," *Power and Energy Magazine, IEEE*, vol.7, no.1, pp.41,49, January-February 2009
[5] Phadke, A. G.; Thorp, J.S., Synchronized Phasor Measurements and their Applications. 1 ed. 2008, New York: Springer Science+Business Media.
[6] U.S.-Canada Power System Outage Task Force "Final Report on the August 14, 2003 Blackout in the United States and Canada: Causes and Recommendations [Online], Available: http://energy.gov/sites/prod/files/oeprod/DocumentsandMedia/BlackoutFinal-Web.pdf [Accessed: April 27, 2015]
[7] Central Electricity Regulatory Commission "Report on the Grid Disturbance on 30th July 2012 and Grid Disturbance on 31st July 2012", [Online], Available: http://www.cercind.gov.in/2012/orders/Final_Report_Grid_Disturbance.pdf [Accessed: April 27, 2015]
[8] K.R. Padiyar, "Analysis of Subsynchronous Resonance in Power Systems", 1 ed, 1998, New York, Springer Science & Business Media.
[9] NETS Security and Quality of Supply Standard - Issue 2.3. National Grid, UK, December, 2014.
[10] Electricity Ten Year Statement. National Grid, UK, 2014. Available online: http://www2.nationalgrid.com/UK/Industry-information/Future-of-Energy/Electricity-Ten-Year-Statement
[11] A. Mulawarman; P. Mysore "Detection of Undamped Sub-Synchronous Oscillations of Wind Generators with Series Compensated Lines" (Minnesota Power Systems Conference, 2011)
[12] North American Electric Reliability Council "Lesson Learned - Sub-Synchronous Interaction between Series-Compensated Transmission Lines and Generation" (2011)
[13] T. Ackerman, R Kuwahata "Lessons Learned from International Wind Integration Studies" (AEMO Wind Integration WP4(A), 2011)
[14] IEEE C37.118.1-2011 - IEEE Standard for Synchrophasor Measurements for Power Systems (as amended in IEEE C37.118.1a-2014)
[15] "Identification of Electromechanical Modes in Power Systems" (IEEE Task Force Report, Special Publication TP462, IEEE Power and Energy Society, 2012)
[16] IEEE C37.118.2-2011 - IEEE Standard for Synchrophasor Data Trasfer for Power Systems
[17] D. Novosel, "Phasor Measurement Application Study – Final Project Report", June 2007, uc-ciee.org/downloads/PMTA_Final_Report.pdf
[18] V.Terzija, "Adaptive Underfrequency Load shedding based on the Magnitude of the Disturbance Estimation", IEEE Trans. Power Sys, vol. 21, no. 3, pp 1260-1266, 2006
[19] P. M. Ashton, G. A. Taylor, M. R. Irving, I. Pisica, A. Carter, and M. E. Bradley. Novel application of detrended fluctuation analysis for state estimation using synchrophasor measurements. IEEE Transactions on Power Systems, 28(2): 1930 - 1938, May 2013.
[20] A.G. Phadke; J.S. Thorp; K.J. Karimi., "State Estimation with Phasor Measurements," *Power Engineering Review, IEEE*, vol.PER-6, no.2, pp.48,48, Feb. 1986
[21] T.L. Baldwin; L. Mili; M.B. Boisen, Jr.; Adapa, R., "Power system observability with minimal phasor measurement placement," *Power Systems, IEEE Transactions on*, vol.8, no.2, pp.707,715, May 1993
[22] N.M. Manousakis; G.N. Korres; P.S. Georgilakis. "Taxonomy of PMU Placement Methodologies," *Power Systems, IEEE Transactions on*, vol.27, no.2, pp.1070,1077, May 2012

[23] Z. Ming, V. A. Centeno, J. S. Thorp, and A. G. Phadke, "An alternativefor including phasor measurements in state estimators," IEEE Trans. Power Syst., vol. 21, no. 4, pp. 1930–1937, Nov. 2006.

[24] T. S. Bi, X. H. Qin, and Q. X. Yang, "A novel hybrid state estimator for including synchronized phasor measurements," Elect. Power Syst. Res., vol. 78, pp. 1343–1352, 2008.

[25] C. Yunzhi, H. Xiao, and G. Bei, "A new state estimation using synchronized phasor measurements," in Proc. IEEE Int. Symp. Circuits and Systems (ISCAS 2008), May 2008, pp. 2817–2820.

[26] M. Asprou and E. Kyriakides, "Enhancement of hybrid state estimation using pseudo flow measurements," presented at the Power and Energy Society General Meeting, San Diego, CA, 2011.

[27] G. Valverde; S. Chakrabarti; E. Kyriakides; V. Terzija, "A Constrained Formulation for Hybrid State Estimation," *Power Systems, IEEE Transactions on* , vol.26, no.3, pp.1102,1109, Aug. 2011

[28] D. Wang, D. H. Wilson and S. Clark, "Defining Constraint Thresholds by Angles in a Stability Constrained Corridor with High Wind", IEEE T&D, Chicago, April 2014

[29] Nechifor, A; Albu, M; Hair, R; Terzija, V. "A flexible platform for synchronised measurements, data aggregations and information retrieval". Electric Power Systems Research, Vol. 120, March 2015, Pages 20 -31.

[30] D. N. Kosterev, C. W. Taylor, and W. Mittlestadt, "Model Validation for the August 10 , 1996 WSCC System Outage," *IEEE Transactions on Power Systems*, Vol. 14, no. 3, pp. 967–979, August, 1999.

[31] Z. Huang, Bo Yang and D. Kosterev, "Benchmarking of Planning Models Using Recorded Dynamics", *IEEE Power and Energy Society Power Systems Conference and Exposition*, 2009

[32] J. Ma, D. Han et. al, "Wide area measurements-based model validation and its application", *IET Generation, Transmission & Distribution*, July, 2008

[33] Z. Huang, R. T. Guttromson and J. F. Hauer, "Large-Scale Hybrid Dynamic Simulation Employing Field Measurements", IEEE Power Engineering Society General Meeting, 2004

[34] Z. Huang, D.N. Kosterev, R. Guttromson and T. Ngyuyen, " Model validation with hybrid dynamic simulation", IEEE Power Engineering Society General Meeting, 2006

[35] J.E. Gomez, I. C. Decker and R. A. Leon, "Hybrid Simulations, a smart way to perform parameter validation in power systems", IEEE Innovative Smart Grid Technologies (ISGT), 2011

[36] John Adam, "ERCOT Operational concerns with Wind Energy", Electrical Reliability Council of Texas, June 7, 2012 as part of NASPI Technical Workshop, "Synchrophasor Technology and Renewable Integration", Tech Rep, June, 2012

[37] E. Allen, S. Member, D. Kosterev, and P. Pourbeik, "Validation of Power System Models," *IEEE PES General Meeting*, pp. 1–7, 2010.

[38] Bruce English, "Reactive Power Solutions, Subsynchronous Oscillations (SSO): Risk Analysis, Protection, and Mitigation Techniques", GE Digital Energy. Available: http://www.slideshare.net/GEEnergyConsulting/v5-ssr-ssciwebinar

[39] P. Pourbeik and G. Stefopoulos, "Validation of Generic Models for Stability Analysis of two Large Static Var Systems in New York using PMU Data", *T&D Conference and Exposition, IEEE PES*, 2014

Addressing Emerging Network Management Needs with Enhanced WAMS in the GB VISOR Project

S. Clark, D. Wilson,
N. Al-Ashwal
GE's Grid Solutions
Edinburgh, UK
stuart.clark2@ge.com

F. Macleod,
P. Mohapatra, J. Yu
SP Energy Networks
Blantyre, UK

P. Wall, P. Dattaray,
V. Terzija
University of Manchester
Manchester, UK

P. Ashton, M. Osborne
National Grid UK
Wokingham, UK

Abstract—This paper describes a number of novel Wide-Area Monitoring System (WAMS) capabilities and analysis tools, including a new monitoring solution that covers the 4-46Hz sub-synchronous oscillation range, and the deployment of a new oscillation source location algorithm. These are being demonstrated under VISOR – an innovation project that has created the first integrated GB WAMS in order to demonstrate the capabilities and tangible business benefits of WAMS to the GB system. Other work from the project is discussed including hybrid state estimation, dynamic model validation, line parameter estimation and a new boundary constraint approach that uses angle difference in addition to power. Finally, selected learning from a review of existing GB WAMS performance is presented, along with details of next steps in the project.

Index Terms--governor mode, hybrid state estimation, line parameter estimation, sub-synchronous oscillation, wide-area monitoring system (WAMS).

I. INTRODUCTION

The GB (Great Britain) power system is undergoing a period of major change – with the addition of series compensation and intra-network HVDC transmission, the increasing penetration of renewable generation, and the closure of large synchronous generation plant. These changes alter existing dynamic behavior and introduce new issues – raising the need for improved monitoring and understanding of system behavior to support reliable and efficient operation of the GB grid. The VISOR project [1] was instigated to address this need – involving all three GB Transmission Owners, the GB System Operator, academia and vendors.

The objective of VISOR is to demonstrate, using the first integrated GB Wide-Area Monitoring System (WAMS), a suite of new wide-area monitoring capabilities and analysis tools including novel algorithms – with a focus on management and early warning of system risks, and on relieving transmission constraints through increased situational awareness and operator confidence. There is strong emphasis on clear and concise presentation of real time decision-making information to operators, and on valuable long-term analysis. VISOR will showcase the tangible benefits from these tools, taking account of the operational processes that will also be required, and will generate learning on infrastructure requirements, issues and implementation. This learning will feed future work as wide area monitoring, protection and control play a bigger role in GB grid operation [2].

The VISOR applications include:

- Wideband Oscillation Monitoring and Source Location (0.002–46Hz)
- Area-Angle Based Constraint Definition for the Scotland-England Transmission Boundary
- Validation of Dynamic Models
- Real-time and off-line disturbance reporting
- Line Parameter Estimation
- Hybrid State Estimation

Related study work is also being undertaken as part of VISOR. This includes annual System Performance Reports covering dynamic behavior of the GB power system and performance of the WAMS itself, laboratory performance testing of WAMS infrastructure and applications, and assessment of the impact of uncertainty on system security margins.

II. OSCILLATION MONITORING AND SOURCE LOCATION

Monitoring of "low frequency" (LF) electromechanical oscillations, typically 0.1–2Hz, using synchronized measurements from Phasor Measurement Units (PMUs) is already established in GB and elsewhere [3]. The reducing and variable inertia of the GB system, together with the recent and imminent closure of large synchronous generation units with a power system stabilizing role, the deployment of series compensation and the proliferation of Power Electronic systems, necessitate extended and enhanced monitoring of power system oscillations in GB. In particular, there is need for:

- New tools to aid in identifying the sources of oscillations – in both real time and study domains.
- Renewed focus on oscillations in the 0.002-0.1Hz governor or "Very Low Frequency" (VLF) range, driven by changing system inertia.

- New monitoring of the 4-46Hz range, commonly termed "sub-synchronous oscillations" (SSO) – though to be correct the VLF and LF ranges are also sub-synchronous. This is motivated by the risk of interaction between new series compensation, power electronic controls, and generator shafts.

VISOR is demonstrating new WAMS analyses, applications and infrastructure to meet these needs. A number of common principles are applied, in line with the VISOR goal of providing clear and actionable information to operators, and valuable and usable data for long-term study:

- **Analyses are performed in real-time**, with results stored for later study e.g. model validation, baselining or operational review. Live and historical values can be accessed within the application, and can be exported for further analysis in third party tools as comma separated value (CSV) files or via a database driver.
- Results are grouped into **configurable frequency bands** for independent alarming and visualization, enabling focus on modes of interest such as generator torsional frequencies. The analysis and results stored are unaffected, so as not to influence historical review.
- **Mode selector tabs** allow users to switch between bands in charts and map views, and display the present dominant frequency and alarm state of each band.
- **Alarm and source location information is shown in map views** through simple "traffic light" or color gradients respectively. Charts below display mode frequency, damping and amplitude for the user-selected location, alongside the worst-case system-wide value.

A. Oscillation Source Location (0. 002-4Hz)

Whilst monitoring of electromechanical oscillations in using WAMS is well-established, identification of which generator(s) are contributing to an oscillation is less so. Currently, operational response to an oscillation will either require prior study of the mode, or else apply general guidance such as reducing power flow between participating regions. Both will usually impact the economic and efficient operation of the grid. Targeting action directly at the source ensures effectiveness whilst minimizing the impact on grid operation.

The capability to identify oscillation sources is thus of significant benefit in targeting both real-time response and offline investigation to a contributing region or plant. Once the source(s) and cause have been identified, procedures can be developed, models validated and controller tuning instigated.

1) Previous Work

Some previous work has been undertaken on oscillation source location, however existing methodologies are of limited effectiveness for real-time application in a typical power system.

One existing approach involves the use of power and frequency measurements to trace oscillation energy to its source [4]. However, this relies on PMU observability of plant / regional boundaries, and on sustained oscillations. Thus it is impractical on typical WAMS or less poorly damped modes.

Other methods [5] use statistical analyses to find correlation between oscillation behavior and system conditions e.g. generator output. However this is most effective when applied over multiple events rather than in real-time. There is also a risk of highlighting correlative but noncausal links.

2) New VISOR Source Location Approach

A new approach has been developed which uses PMU voltage angle measurements to locate an oscillation source to the nearest monitored bus(es) - allowing useful location information to be derived from sparse measurements. This is particularly valuable in large interconnected systems, since only a few voltage and frequency measurements, considered commercially nonsensitive, need be shared between operators.

Contributions are identified through the relative phase of oscillations in voltage angle. A location with leading mode phase indicates a "source" contributing to poorer damping, whilst a lagging phase indicates a "sink" providing a more positive damping contribution.

In the case of opposing-phase oscillations e.g. an inter-area mode, the participants must be first split into two opposing groups. The average phase of each group is determined, and individual phase differences or "contributions" derived for each signal relative to its group average. If one group leads the other by <180º, its most leading constituent is considered to be the oscillation source. If neither group has a notable lead, then the leaders of each group are candidate sources.

The method has been applied to a number of off-line study cases - [6] gives one, along with a more detailed description of the algorithm. VISOR is demonstrating this approach offline as part of historical reviews, and as a real-time application.

3) Example VISOR Offline Demonstration Case

As part of the first VISOR System Performance Report, the source location approach was applied offline to a governor mode oscillation from the GB system. The results, shown in Fig. 1, indicate that the oscillation source is in the region of Sites A and B (the most leading locations) – which both have local thermal and wind generation. Site C, which lags A and B, sits nearby on a different voltage level.
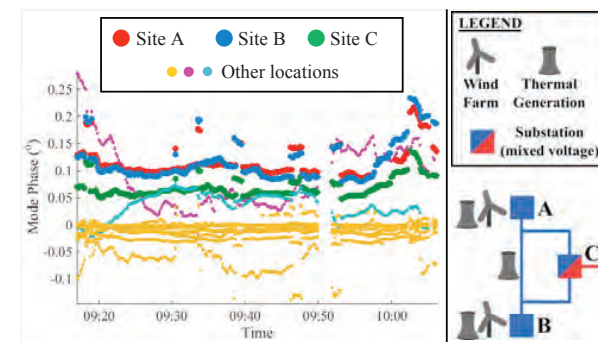

Figure 1. Mode phase analysis of common mode oscillation at locations across GB (left) and topological arrangement of leading sites (right)

This suggests two, equally feasible, possibilities – either that generation at both A and B is contributing to the oscillation to a similar degree, or that a third generator between the

two locations is the actual source. Whilst not definitive, this information allows real-time response and offline investigation to be targeted and thus more effective and efficient.

4) New Real-Time Source Location Display

For demonstration under VISOR, the new source location approach has been implemented as an enhancement to an existing application module. The algorithm is executed in real time on oscillation analysis results reported by the software, with the derived individual and group phase information stored alongside the original oscillation data for later analysis.

In order for source location information to be useful in a real-time operational context, significant focus has been placed on presenting it to users in a clear, comprehensible and actionable form. Fig. 2 shows the updated application display.
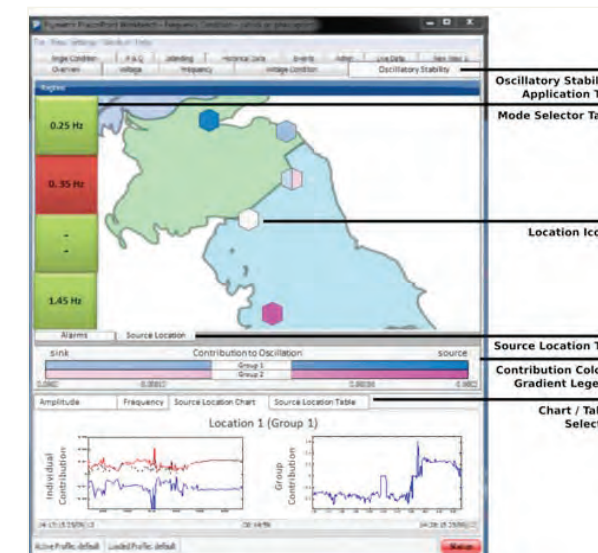

Figure 2. Real-time oscillation source location display

A map view highlights the relative contribution of each monitored location to the dominant mode in the selected band through a simple color gradient, allowing users to quickly identify oscillation sources and sinks. A different gradient is used for each group (pink and blue in Fig. 2). Where a location is split between different groups, such as in a split bus scenario, the icon coloring is also split, as shown.

New charts plot the individual contribution of the user-selected location, the minimum / maximum contributions in the system, and the phase difference between groups.

B. New Very Low Frequency Monitoring (0.002-0.1Hz)

Though real-time analysis of very low frequency oscillations is certainly feasible with present technology, monitoring of oscillations below 0.1Hz is limited. This is due to the focus of existing real-time oscillation analysis tools on the 0.1-4Hz electromechanical range, which has been the foremost oscillatory concern of transmission system operators. Inclusion of 0.002-0.1Hz modes in the range covered by these tools would require either a) a longer analysis window, reducing detection

performance for electromechanical modes; or b) a separate algorithm, requiring development and extra processing power.

Driven by increasing concern around governor mode oscillations and changing inertia, a new algorithm and application module targeted at this range have now been developed and will be demonstrated under VISOR. This algorithm operates on system frequency, and extracts the frequency, amplitude and phase of oscillations in the 0.002-0.1Hz range. It should be noted that accurate derivation of mode phase, used in source location (see section A), is challenging at these frequencies as all generators will oscillate in near-unison.

The new very low frequency software module executes this algorithm in real-time, stores the results for historical review, and provides alarming and visualization. The module incorporates similar features to the display for low frequency modes shown in Fig. 2, with some notable differences:

- **Only one oscillation group exists**, since oscillations in this range are common mode. Correspondingly only one color gradient is used to present mode contributions, and there is no "group contribution" concept.
- **Damping is not monitored**, as it is of questionable practicality given the long wave periods in this frequency range – amplitude is considered to be a sufficient real-time measure.
- Single frequency / amplitude values are used, as these should be identical across the system for a given band.

C. Monitoring of Sub-Synchronous Oscillations (4-46Hz)

1) Background and Motivation

The installation of transmission line Series Compensation, and the increasing penetration of Power Electronic converters associated with renewable generation and HVDC links, add vital flexibility and capacity to the power system and help in the move to a low-carbon grid. However, this plant introduces new challenges not only in protection and fault management, but also in steady state and post-fault operation – with the potential for SSO interaction in the 4-46Hz range. Three primary categories of oscillation occur in this range and are of concern:

- **Grid RLC** (resistor-inductor-capacitor) **modes:** resonant frequencies established by the combination of transmission network inductance with the capacitance of series compensation. These frequencies will change with the effective impedance of the network, e.g. when faulted lines trip.
- Potential **control modes** introduced by power electronic converters, such as at wind farms and HVDC links. These may vary significantly in frequency according to the operating conditions of the converter.
- **Generator shaft torsional modes:** a shaft linking n masses (generator + turbines) will have $n-1$ torsional modes. These are fixed in frequency, determined by the physical characteristics of the plant. It should be noted that a torsional oscillation of frequency f_{shaft} will appear in voltage and current as a modulation: $f_{synchronous} \pm f_{shaft}$. Similarly, an electrical oscillation at f_{grid} will appear as a shaft torque at $f_{synchronous} - f_{grid}$.

Under normal conditions these modes will be well-damped and low in amplitude. However there is potential for severe adverse consequences should two modes coincide and interact – for example following a network fault and line trip:

- **Sub-Synchronous Resonance** (SSR): this involves interaction between generator torsional and grid RLC modes. Consequences range from increased shaft fatigue due to sustained low-level interaction, to shaft failure as observed at the Mohave plant in 1970 [8].

- **Sub-Synchronous Control Interaction** (SSCI): interaction of a control and grid RLC mode – see [7].

- **Sub-Synchronous Torsional Interaction** (SSTI): interaction of control and generator torsional modes [9].

In addition, sub-synchronous oscillations in the electrical network can be amplified by generators through the "Induction Generator Effect" [9]. This occurs because the machines will exhibit negative slip relative to grid sub-synchronous frequencies, and consequently present a negative rotor resistance. Amplification will occur if this resistance exceeds the generator and network resistance as seen at the generator terminals.

The GB transmission owners have implemented a number of measures to mitigate the risk of SSO in the GB system. These include studies to check for potential interactions, the use of filters or thyristor controls on series compensation to avoid interaction, and generator protection systems which bypass capacitors should significant oscillations occur. There remains a need however for real-time wide-area monitoring to:

- **Provide visibility and alarming** of low-level modes that may escalate or cause cumulative plant fatigue.

- **Assess the true behavior of the system** so as to support plant and protection commissioning, validate models and studies, and to identify unexpected modes.

2) New SSO Monitoring Solution
a) Real-Time Data Acquisition

Typical WAMS utilize synchronized phasor measurements transmitted via the IEEE C37.118 protocol at up to 50/60 frames per second (fps) – though some devices offer higher rates. Two key factors influence observable bandwidth:

- The need to ensure adequate attenuation of aliased components: this means filter roll-off must begin lower than the theoretical 25/30Hz Nyquist limit.

- The phasor calculation window: typically multiple 50/60Hz cycles, this gives greater accuracy at the cost of attenuating higher frequencies. Reducing the window increases bandwidth but adds noise and errors.

These factors lead to a practical observable range of up to about 10Hz – the C37.118 standard defines a minimum performance bandwidth of 2-5Hz [8]. This is sufficient to capture governor, electromechanical and some voltage control modes, but is not suitable for monitoring of the full SSO range.

In order to extend visibility to the 4-46Hz SSO range, a new approach was taken. A new Waveform Measurement Unit (WMU) was developed to provide synchronized voltage

and current point-on-wave measurements at 200 samples / second, streamed in real-time via the C37.118 protocol as "analogue" type values. Speed measurements from turbine shaft transducers can also be sent. This approach accurately represents oscillatory components in the 4-46Hz range, and also gives visibility of the 54-96Hz range so as to differentiate modulations such as torsional modes from added components such as grid RLC modes. It should be noted that the use of a higher reporting rate of 200fps is fully compliant with the C37.118 standard, and is in fact encouraged [11].

The WMU is implemented on a multifunction recorder that already incorporates PMU capability. Ten of these devices are being installed in GB as part of the VISOR project, each monitoring voltage and current and providing both a 50fps PMU and 200fps WMU stream to the VISOR WAMS servers.

b) SSO Management Application

The 200fps voltage, current and speed waveforms are collated and stored by central WAMS servers. They are then processed by a new SSO management application module, applying the features and principles discussed at the start of section II and using a dedicated algorithm to extract the amplitude, frequency and damping of modes in the 4-46 Hz range. Visibility is extended up to 96Hz through a spectrogram, to enable users to differentiate between added components and modulations of the 50Hz waveform.

The system-wide SSO map view, shown in Fig. 3, presents mode amplitude and alarm state across the system. A particular challenge was to rationalize oscillation information from multiple signal types for clear and useful presentation to users.
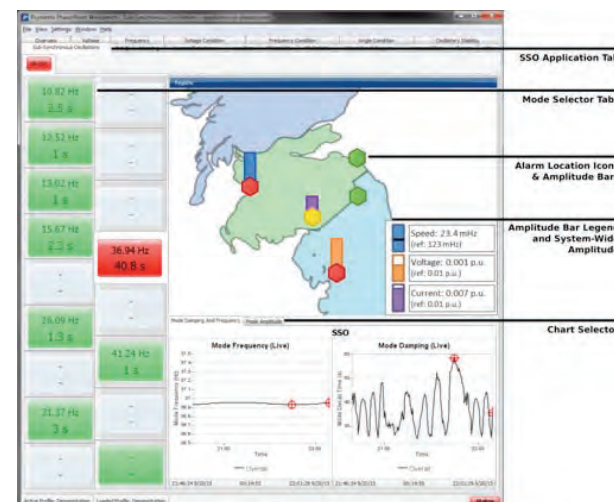
Figure 3. SSO management application display (patent pending)

To enable unified presentation of SSO modes across electrical and mechanical domains, users are able to switch between "perspectives" to account for the frequency translation from mechanical shaft speed to electrical grid waveform. In electrical perspective mode frequencies detected in shaft speed are complemented to grid frequency (i.e. $50 - f_{shaft\_mode}$), whilst mechanical perspective does the same for voltage and current oscillations. This remains valuable when only one signal type

is present, e.g. avoiding human error in comparing observed electrical oscillations with documented torsional modes.

As with the VLF and LF modules, displays are split into mode bands. For each band, mode amplitude values are normalized per signal type (voltage/current/speed) to the largest in the system. The largest normalized amplitude across all measurement types and signals for each location is then displayed on the map as a bar, color coded to its type. In this way, users can quickly identify key participants as the larger bars of each type – e.g. a large generator speed oscillation and current oscillation on a wind farm output, indicating SSTI.

3) Initial SSO Observations from the GB System

The SSO monitoring solution is now in place, with some months of data collected from a number of WMU devices. This will feed a long-term review of observed GB SSO behavior, including recommendations for further investigation. Fig. 4 shows some initial analysis, depicting frequencies detected over a one month period on a GB transmission circuit adjacent to a generator. Expected torsional modes at the generator are shown - frequency values have been omitted for reasons of confidentiality. The following may be noted:

- All 4 expected torsional modes are observed, though modes 1 and 3 are most prevalent. At another monitored generator, only mode 1 is regularly visible.

- A mode with variable frequency, suggestive of control behavior, (5% peak, far left) is regularly observed at this and other locations. Its occasional proximity to torsional mode 4 warrants further investigation.

- Mode detection varies between current and voltage, highlighting the need to monitor both types of signal.
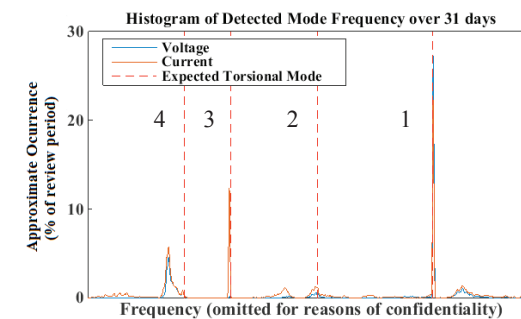
Figure 4. Detected SSO frequencies at one location in the GB system

The detected oscillations are generally considered to be small and well-damped, with the majority in the region of 2V and 0.1A at the 400kV level. There are some instances of non-torsional modes with higher amplitudes and poorer damping that may warrant further investigation. Such behavior is to be expected, and demonstrates well the benefits and need for online SSO visibility and alarming.

4) Future Deployment: Optimal WMU Placement

There are no barriers beyond implementation effort to the adoption of WMU functionality within other PMUs. In the short term however, WMUs will likely remain specialized units deployed for SSO monitoring, and so a placement meth-

odology is needed. A number of mathematical PMU placement methods exist [20], however the wide SSO frequency range and lack of a simple mathematical model for observability means that approaches are likely to incorporate some heuristic aspects, or otherwise be focused on a narrow range.

Careful placement remains important, however. Whilst generator and capacitor sites are obvious candidates for WMU placement, investigations for the IEEE First Benchmark Model shown in Fig. 5 highlight that the specific point of measurement can have a significant impact on observations.
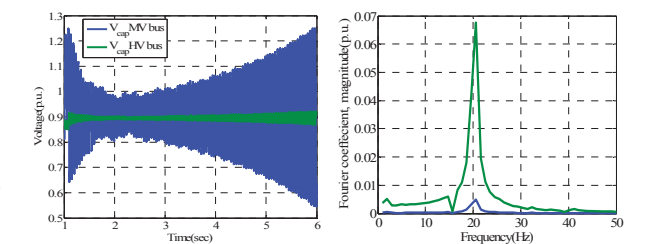
Figure 5. Difference in subsynchronous frequency observations in terminal voltages on two ends of the series capacitor in the IEEE FBM

III. HYBRID STATE ESTIMATION

A. Background

A state estimator (SE) is a critical component of any modern power system control room. Its role is to estimate the system state, i.e. voltage phasor at every bus, based on a limited but observable set of unsynchronized voltage magnitudes and active and reactive power flow measurements. A broad range of control room functions depend directly on the availability and the accuracy of the SE solution – e.g. stability assessment.

Synchronized phasor measurements are direct measurements of the power system state. Thus, the potential for application of PMUs to state estimation has long been an area of great interest [12]. The use of Linear State Estimation (LSE), where the system state is derived from a fully-observable set of synchrophasors using linear equations and a non-iterative procedure [13], requires a level of PMU coverage that is unrealistic in the medium term for GB. However, Hybrid State Estimation (HSE) methods have been proposed that combine a limited set of synchrophasors with the traditional full observability of nonsynchronized data [14]. In this way the potential for phasors to improve SE performance (convergence speed and reliability, and solution accuracy) can be leveraged with a more realistic level of PMU deployment.

B. VISOR Work

The focus of the VISOR HSE work is on improving the reliability of convergence, highlighted by the system operator to be of most immediate value. A literature review identified four main types of HSE: Post Processing, Integrated, Fusion and Distributed. Post-Processing HSE depends on the output of the existing state estimator and thus cannot improve convergence; Fusion requires full PMU observability; and Distributed HSE uses local estimates rather than directly improving the central SE. Thus it was decided that VISOR would focus on the integrated HSE, which offers improved convergence by combin-

ing PMU data and SCADA data directly into a single, iterative estimation procedure. A post processing HSE will also be used as a means of comparison when assessing the accuracy improvement offered by the integrated HSE – which despite the focus on convergence should not be ignored.

The next stage of work will use offline simulations of IEEE benchmark systems and parts of the GB system to assess the improvements in convergence offered by the different types of integrated HSE: rectangular current, pseudo flows, pseudo voltage, and constrained formulation. A key aspect of this assessment will be the development of an index combining multiple relevant metrics to quantify SE performance across different scenarios.

IV. MODEL VALIDATION

Model based simulation of dynamic behavior is critical to the proper planning and operation of a power system, being used for both steady state and post-fault contingency analyses to determine if the system is operating within security margins and quality of supply standards. Model inadequacies can thus have real and significant consequences for the power system. Overly conservative limits can lead to costly inefficient operation, whilst misleading stability assessment results can lead to separation or blackout as in [19]. Validation and improvement of system models is therefore vital, and is likely to only become more challenging and resource intensive with the increasing complexity of power system plant, protection and control schemes and the range of possible operating conditions as we move toward a low carbon future.

WAMS data is ideally suited to model validation, being a continuous time-aligned record of steady-state and disturbed power system behavior - albeit without full observability. It removes much of the effort and risk of error associated with collating other forms of data such as triggered fault records (which may be accurately time-stamped but have different start/end times). Two main model validation approaches are raised in literature [15]-[19]: system-wide and subsystem.

The system-wide approach uses simulations of the complete power system, and attempts to replicate the scenario under study by recreating it as a sequence of events (e.g. a line loss), validating the simulation results against WAMS data. This relies on accurate event reconstruction from records – in order to be sure that any observed discrepancies are due to the model rather than an unrepresentative simulation.

Subsystem model validation uses PMU measurements at the boundaries between a subsystem (e.g. generator) and the rest of the system to excite only the subsystem model. This effectively mimics the conditions the subsystem was exposed to during the scenario and validates the subsystem model using the PMU measurements recorded within it. A disadvantage of this approach, which has been encountered during VISOR, is that it is limited in application to subsystems that are fully bound by PMU measurements.

VISOR will assess the potential for validation of the GB system models using both of these approaches, with data from the VISOR WAMS. Furthermore, the extent to which SSO small and large-signal behavior observed by VISOR is replicated in the system model will be assessed.

V. LINE PARAMETER ESTIMATION

Line Parameter Estimation (LPE) is one of the obvious applications of phasor measurements at both ends of a transmission line, with potential benefits to State Estimation, fault level calculation and voltage stability assessment to name a few. The key challenge to LPE lies in addressing measurement noise and systematic error so as to calculate consistent and reliable results. For example, over a typical transmission line with an X/R ratio of 10, a 0.57° error in angle alone – equivalent to the 1% Total Vector Error limit set in IEEE C37.118 [8] – results in a resistance error of 10%. Prior work carried out [21]-[24] does not always consider realistic systematic errors and noise, and/or assumes that parameters do not vary.

A correlation-based Robust LPE (RLPE) approach has been developed and will be demonstrated under VISOR. Initial application to GB WAMS data highlighted the impact of PMU data quality on LPE, with issues such as periodic angle drift and poor anti-aliasing filtering impairing performance. However RLPE still showed significant improvement over direct calculation averaged over the RLPE analysis window, with ~90% reduction in standard deviation (to 15% and 2% in R and X respectively). Further work can be done during the project to address the identified issues, including upgrade of older PMUs, and to improve the algorithm error correction as more data is collected. RLPE performance can then be re-evaluated.

Fig. 6 shows the application of the VISOR Robust LPE algorithm to "good" quality PMU data from another power system. The data reports better performance with ~5% and 0.5% standard deviation in R and X respectively – which are comparable to the daily variations that are evident. It should be noted that factors such as line voltage, length and load variation will also have influenced the algorithm performance.
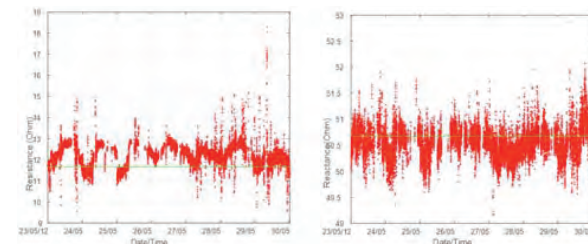

Figure 6. Results of VISOR Robust Line Parameter Estimation on "good" data from another power system.

VI. AREA-ANGLE BASED CONSTRAINT DEFINITION FOR THE SCOTLAND-ENGLAND TRANSMISSION BOUNDARY (B6)

B6 is primarily constrained by small and large-signal angle stability. The significant levels of Scottish wind generation change the constraint characteristics from its present MW flow definition: wind adds to the B6 MW flow, but does not contribute the inertia which impacts post-fault stability. VISOR will trial a new representation of the boundary state that incorporates a derived voltage angle difference between the Scottish and English centers of inertia, which is more closely related to the physical stability limit and should release capacity if deployed. This concept is discussed in greater detail in [25].

The representative Scottish and English "centers of angle" are derived as weighted averages of chosen bus angles in each area. A confidence measure for each highlights the impact of any measurement loss. The new display will be demonstrated and evaluated for operational readiness during 2016.

VII. ASSESSMENT OF GB WAMS PERFORMANCE

An early task of VISOR was to assess the performance of the existing GB WAMS infrastructure, which was not used or maintained at a real-time production level. A report was produced evaluating PMU data quality and availability. Some site-specific problems were highlighted, e.g. GPS reception and CT/VT wiring, as well as widespread issues e.g. communications performance. Such issues were not unexpected given the non-production nature of the system – they are now being addressed, and performance will be re-evaluated at the close of VISOR. Two general issues should be noted – these are less relevant to the newest PMUs but may affect many others:

- **Reported frequency resolution** was limited to 1mHz or more, due to the choice of 16-bit integer format and/or the calculation process in many PMUs. Whilst within the 5mHz standard [8], this significantly impairs the analysis of ambient level oscillations. Identified firmware and/or hardware upgrades are required for some devices to enable 32-bit floating point format and to improve the frequency calculation resolution.

- **Quantization in integer-format current phasors**. Integer format reduces phasor data bandwidth and storage requirements and so is generally recommended, provided that polar form is used in conjunction with a reasonable full-scale value – not fault level. As with frequency, reported values may meet standard requirements but impair ambient oscillation analysis.

VIII. CONCLUSIONS AND NEXT STEPS

This paper has presented some of the work to date on the VISOR project, notably in the areas of oscillation source location, sub-synchronous oscillation monitoring and robust line parameter estimation. An introduction to the VISOR work on Hybrid State Estimation, dynamic model validation and a new power-angle constraint approach has also been covered, along with discussion of GB WAMS infrastructure performance.

During 2016 VISOR will demonstrate further real-time software applications – namely the very low frequency and source location interfaces presented here – as well as line parameter estimation; enhanced disturbance detection, location and characterization; and the new power-angle display discussed in VI. Additional reports will also be delivered: assessing the dynamic behavior of the GB power system and performance of WAMS infrastructure over 2016, and evaluating the operational feasibility & effectiveness of the proposed power-angle boundary constraint.

ACKNOWLEDGMENT

REFERENCES

[1] *Visualisation of Real-Time System Dynamics Using Enhanced Monitoring*, http://visor-project.org.uk, http://spenergynetworks.co.uk/visor

[2] V.Terzija, G.Valverde, D.Cai, P.Regulski, V.Madani, J.Fitch, et al., "Wide area monitoring, protection and control of future electric power networks", *Proc. IEEE*, vol. 99, pp. 80-93, Jan. 2011.

[3] "Identification of electromechanical modes in power systems" *IEEE Task Force Report*, Special Publication TP462, IEEE PES, 2012.

[4] L. Chen, Y. Min, W. Hu "An energy-based method for location of power system oscillation source", *IEEE Trans. Power Syst*, vol. 28, pp. 828- 836, May 2013.

[5] P. McNabb, D. Wilson, J. Bialek: "Classification of mode damping and amplitude in power systems using synchrophasor measurements and classification trees", *IEEE Trans. Power Syst*, vol 28 pp. 1988-1996, May 2013.

[6] N. Al-Ashwal, D. Wilson, and M. Parashar, "Identifying sources of oscillations using wide area measurements", unpublished, *Grid of the Future Symposium*, CIGRE US National Committee, 2014.

[7] NERC, "Lesson learned - sub-synchronous interaction between series-compensated transmission lines and generation", 2011, [Online]. Available: http://www.nerc.com/pa/rrm/ea/Pages/Lessons-Learned.aspx

[8] D. N. Walker, C. E. J. Bowler, R. L. Jackson, D. A. Hodges, "Results of subsynchronous resonance test at Mohave," in *IEEE Trans. Power App. Sys*, vol.94, pp.1878-1889, Sept. 1975.

[9] L. C. Gross "Sub-Synchronous Grid Conditions: New Event, New Problem, and New Solutions" [online], *Western Protective Relay Conf.*, Washington, 2010. Available: http://relayapplication.com/docs/WPRC_2010_SSF_Detection_Paper.pdf

[10] *IEEE Standard for Synchrophasor Measurements for Power Systems*, IEEE Std. C37.118.1a-2014

[11] *IEEE Standard for Synchrophasor Data Transfer for Power Systems*, IEEE Std. C37.118.2-2011

[12] A.G. Phadke; J.S. Thorp; K.J. Karimi,, "State estimation with phasor measurements", *IEEE Power Eng. Rev.*, vol. 6, p.48, Feb. 1986.

[13] S. G. Ghiocel, J. H. Chow, G. Stefopoulos, B. Fardanesh, et al., "Phasor-measurement-based state estimation for synchrophasor data quality improvement and power transfer interface monitoring," *IEEE Transactions on Power Systems*, vol. 29, pp. 881-888, Sept. 2014.

[14] G. Valverde, S. Chakrabarti, E. Kyriakides, and V. Terzija, "A constrained formulation for hybrid state estimation," *IEEE Transactions on Power Systems*, vol. 26, Aug. 2011.

[15] Z. Huang, Bo Yang and D. Kosterev, "Benchmarking of planning models using recorded dynamics", *IEEE/PES Power Systems Conf. and Expo.*, 2009

[16] J. Ma, D. Han et al, "Wide area measurements-based model validation and its application", *IET Gener. Transm. Dis.*, vol. 2, July 2008.

[17] Z. Huang, D.N. Kosterev, R. Guttromson and T. Ngyuyen, "Model validation with hybrid dynamic simulation", *IEEE PES GM*, 2006.

[18] J.E. Gomez, I. C. Decker and R. A. Leon, "Hybrid Simulations, a smart way to perform parameter validation in power systems", *IEEE Innovative Smart Grid Technologies*, 2011.

[19] E. Allen, S. Member, D. Kosterev, and P. Pourbeik, "Validation of power system models," *IEEE PES General Meeting*, 2010.

[20] N. M. Manousakis, G. N. Korres, P. S. Georgilakis, "Taxonomy of PMU placement methodologies", *IEEE Transactions on Power Systems*, vol. 27, no. 2, pp.1070-1077, May 2012.

[21] R. E. Wilson, G. A. Zevenberger, D. L. Mah, et al. "Calculation of transmission line parameters from synchronized measurements". *Electric Machines and Power Systems*, vol. 27, no. 12 pp. 1269-1278, 1999.

[22] Y. Liao and M. Kezunovic, "Online optimal transmission line parameter estimation for relaying applications", *IEEE Trans. on Power Del.*, vol. 24, pp. 96-102, Jan. 2009.

[23] D. Shi, D. J. Tylavsky, N. Logic and K. M. Koellner, "Identification of short transmission-line parameters from synchrophasor measurements", unpublished, *North Amer. Power Symp.*, 2008.

[24] A. Abur and A. Exposito, *Power System State Estimation, Theory and Implementation*, Marcel Dekker INC., New York, 2004.

[25] D. Wang, D. H. Wilson, S. Clark, "Defining constraint thresholds by angles in a stability constrained corridor with high wind," *T&D Conference and Exposition, 2014 IEEE PES*, 2014.

VISOR Project: Initial learning from Enhanced Real Time Monitoring and Visualisation of System Dynamics in Great Britain

Stuart Clark, Douglas Wilson, Karine Hay, Oleg Bagleybter (GE's Grid Solutions)
Priyanka Mohapatra, Finlay Macleod, James Yu (SP Energy Networks)
Phil Ashton, Mark Osborne (National Grid)
Peter Wall, Papiya Dattaray, Vladimir Terzija (The University of Manchester)

stuart.clark2@ge.com

United Kingdom

Abstract

This paper presents some of the learning from the first stages of VISOR – an innovation project that has created the first integrated GB (Great Britain) Wide-Area Monitoring System (WAMS), aiming to demonstrate the capabilities and tangible business benefits to the GB power system. The WAMS capabilities being demonstrated under VISOR include management of system disturbances and oscillations across the 0.002-46Hz range; reducing uncertainty in system models, state estimation and transmission line parameters; and the use of a representative inter-area angle as a transmission constraint.

Experience from the deployment and performance evaluation of the VISOR WAMS is discussed. The architecture incorporates a regional WAMS server at each of the 3 GB Transmission Owners, a central WAMS "Data Hub" server at the GB System Operator, and 70+ Phasor Measurement Units (PMUs) deployed across the GB system. In addition 10 Waveform Measurement Units (WMUs – a new device) have been deployed in a world-first, for the purposes of providing visibility of the 4-46Hz Sub-Synchronous Oscillation (SSO) range.

In addition, key observations are presented from long-term reviews of GB oscillatory behaviour and the demonstration of new oscillation management tools. These cover very low frequency governor behaviour, low frequency electromechanical oscillations, and sub-synchronous oscillations involving generator torsional modes, power electronic converters and series compensation. The results presented include the application of a new oscillation source location technique to an inter-area mode and a governor frequency mode.

1 Introduction

The GB power system, as many others, is undergoing a period of major change as it moves toward a low carbon future. The increasing penetration of renewable generation and the closure of large synchronous generation plant are have, among other effects, a significant impact on inter-region power flows. In particular the Scotland-England boundary ("B6") has become a major bottleneck, limiting the export of renewable power from Scotland. Additional network capacity to accommodate these increased flows is being provided through the addition of both Thyristor-Controlled and Fixed Series Compensation (TCSC, FSC) on B6, and the deployment of an intra-network HVDC transmission link.

All of these changes alter the existing dynamic behaviour of the GB system and introduce new issues – raising the need for improved monitoring and understanding of system behaviour to support reliable and efficient operation of the GB grid. The VISOR project [1] was instigated to address this need.

The potential of WAMS as a solution for many of the challenges faced in power systems is often cited [2], both in its benefits to system operation [3], [4] and as the future monitoring and control platform necessary for secure, reliable and efficient operation of a low carbon power system. Much of this potential however has yet to be realised as part of an operational system, and the consequential benefits quantified. This is the goal of VISOR – to demonstrate the concepts and applications, as well as tangible benefits of WAMS to the GB power system.

This paper presents an introduction to the VISOR project, its aims and components (Section 2); the infrastructure deployed under VISOR, experience from its implementation and review of its performance (Section 3); and learning to date from the project in the area of power system oscillations (Sections 4 & 5).

2 The VISOR Project

VISOR (VISualisation Of Real-time system dynamics using enhanced monitoring) is a GB innovation project that brings together the three GB transmission owners (TOs): SP Energy Networks (SPEN), National Grid (NG) and Scottish Hydro Electric (SHE), the GB system operator (also NG), researchers (The University of Manchester) and vendors (GE's Grid Solutions). The project is funded through the Network Innovation Competition mechanism, awarded by Ofgem – the GB regulator.

VISOR has created the first integrated GB WAMS for the purpose of demonstrating the concepts and tangible benefits of WAMS capabilities to business-as-usual electricity transmission operations. The project focuses on three key areas, each incorporating the planning, real-time and event/trend analysis domains:

- **Management of system risks and events**: early warning, response and analysis
- **Reducing uncertainty**: improved situational awareness, confidence in system models & limits
- **Maximising assets**: efficient and effective use of WAMS and transmission infrastructure

It may be noted that the application of WAMS in the future control of the GB system is being explored in a related Network Innovation Competition project – Smart Frequency Control (formerly known as Enhanced Frequency Control Capability) [5].

2.1 Project Components

The critical first stage of the project was the deployment of the 3 regional WAMS "Datacentre" servers, a central WAMS "Data Hub" server, the deployment of 10 Waveform Measurement Units (WMUs – a new device, detailed in Section 4.2), and the incorporation of existing WAMS at SPEN and NG. Further details of the VISOR WAMS, lessons learned from its deployment, and review of its performance are described in Section 3.

Enabled by the VISOR WAMS, the core components of the project consist of demonstration and evaluation of the following capabilities:

- Real-time monitoring, analysis and visualisation applications:
  - Monitoring & source location of oscillations from 0.002Hz governor modes, through 0.1-4Hz electromechanical behaviour to 4-46Hz sub-synchronous interaction.
  - A novel hybrid power-angle boundary constraint
  - Rapid detection, location & characterisation of system disturbances
  - Line parameter estimation
- Offline demonstration & study
  - Hybrid state estimation
  - Dynamic model validation
  - The influence of uncertainty in managing transmission constraints

Alongside this demonstration and evaluation work, annual reviews of WAMS infrastructure performance and power system dynamic behaviour are being conducted. These provide insight into project progress, guide subsequent project work such as model validation and monitoring deployment, and deliver suitable case studies that illustrate the benefits of the WAMS capabilities being demonstrated under VISOR.

A final and essential aspect of VISOR, as a GB Network Innovation Competition project, is the dissemination across the GB electricity industry of knowledge gained from the project and recommendations for future deployment of the technologies, applications and concepts demonstrated.

2.2 Power System Oscillations in VISOR

Firstly a note on terminology: various labels are applied to power system oscillations across the industry and academia. For the purpose of this paper, the following classifications are used:

- **0.002-0.1Hz : Very Low Frequency (VLF)**
  This range covers generator governor behaviour

- **0.1-4Hz : Low Frequency (LF)**
  This range features generator electromechanical behaviour such as inter-area, local and plant modes (typically 0.1-2Hz); as well as other phenomena such as forced oscillations and some voltage control modes.

- **4-46Hz : Sub-Synchronous Oscillations (SSO)**
This range incorporates generator torsional frequencies, power electronic control modes and the network natural frequencies created by series capacitors with transmission line inductance. Interactions in this range include sub-synchronous resonance, sub-synchronous torsional interaction and sub-synchronous control interaction. Section 4.1 provides further detail on SSO.

Monitoring of "Low Frequency" (LF) 0.1–4Hz oscillations, typically electromechanical modes, using synchronized measurements from PMUs is already established in GB and elsewhere [6]. The reducing and variable inertia of the GB system, together with the recent closure of large synchronous generation units with a power system stabilizing role, the deployment of series compensation and the proliferation of Power Electronic systems, necessitate extended and enhanced monitoring of power system oscillations in GB. In particular, there is need for:

- New tools to aid in identifying the sources of oscillations – in both real time and study domains.
- Renewed focus on oscillations in the 0.002-0.1Hz governor or "Very Low Frequency" (VLF) range, driven by changing system inertia.
- New monitoring of the 4-46Hz range, termed "sub-synchronous oscillations" (SSO). This is motivated by the risk of interaction between new series compensation, power electronic controls, and generator shaft torsional modes.

VISOR is demonstrating new WAMS analyses, applications and infrastructure to meet these needs. The tools being demonstrated provide real-time wide-area monitoring of oscillations across the entire 0.002-46Hz range. The results are presented in real-time geographic displays for operator situational awareness, feed alarms to warn of emerging issues, and are stored for historical trend and event review. Source location analysis is also performed in real-time, presented to users on a geographical display and stored for historical review.

These tools have recently been deployed, and have already provided valuable insight into grid behaviour. This initial learning is outlined in Section 4 and Section 5.

3   VISOR WAMS Infrastructure

The VISOR WAMS infrastructure, illustrated in Figure 1, incorporates a regional WAMS "Datacentre" server installed at each TO, 1 central WAMS "Data Hub" server installed at the SO (National Grid). The Datacentres and Data Hub provide data aggregation as Phasor Data Concentrators (PDCs), in addition to providing storage, analysis and visualisation of WAMS data over their respective areas of coverage. The WAMS includes 70+ Phasor Measurement Units (PMUs) deployed across the GB system. In addition, 10 new Waveform Measurement Units (WMUs) have been deployed in a world-first, for the purposes of extending the real-time observable range of oscillations.

WMUs are similar to PMUs (Phasor Measurement Units) in that they also provide synchronised measurements of voltages and currents and utilise the same IEEE C37.118-2 communications mechanism. Unlike PMUs however, WMUs report point-on-wave measurements of the voltage or current waveform at a 200Hz sampling and reporting rate. This provides extended visibility from the present PMU capability of around 10Hz, up to 46Hz to fully cover sub-synchronous oscillation (SSO) behaviour involving series capacitors, generator torsional behaviour and power electronic systems.
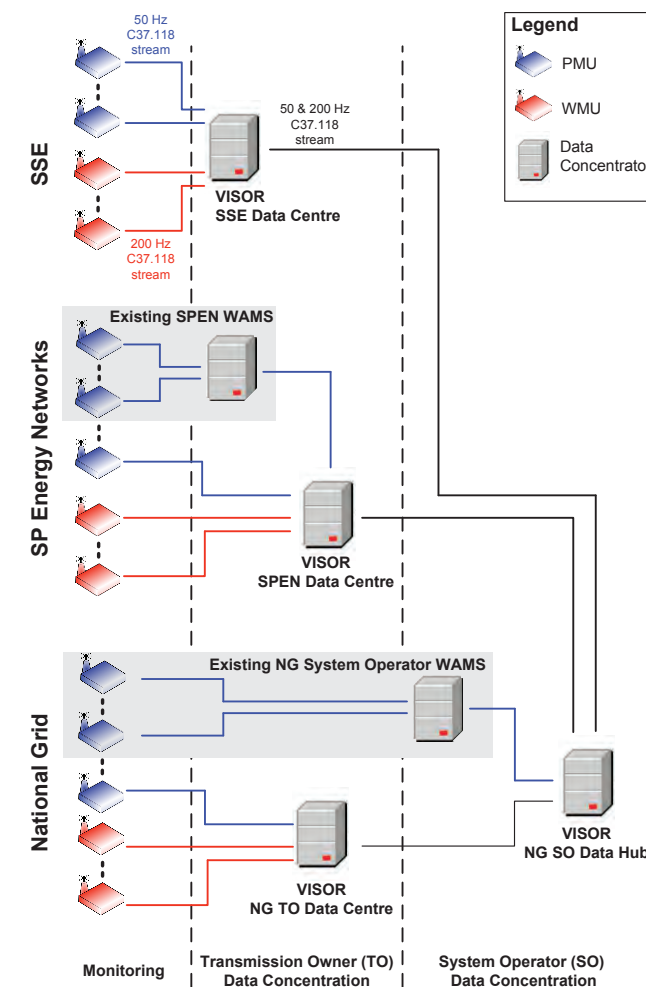
Figure 1 : The VISOR WAMS infrastructure: monitoring equipment, communications links and servers

3.1   Key Learning from Deployment of the VISOR WAMS

Implementation of the VISOR WAMS was an ambitious undertaking, involving in particular:

- Deployment of new data acquisition devices at substations (PMUs and WMUs).
- Installation of new WAMS servers at each TO and at the SO.
- Incorporation of the existing WAMS at SPEN and National Grid.
- The implementation / accommodation of communications links:
  - From substation to WAMS Datacentre server in each TO (ranging from 56kbit/s for a simple 1-circuit PMU, to 500kbit/s for PMU and WMU data from a 6-circuit substation)
  - From each TO WAMS Datacentre server to the SO WAMS "Data Hub" server (up to 2.5Mbit/s for SPEN, with 50 PMUs and 10 WMUs)

The need to carry out each of these tasks across all three GB TOs added further complexity, with each TO having differing rules, procedures, infrastructures and architectures across the substation, telecommunications and IT domains.

Some key experience from this process includes:

- The need for careful architecture design. Plans need to be comprehensive and clear from the outset (though this can be difficult on innovation projects). Information should include data flow details including direction, ports and protocols; and should cover both data streams and the support interfaces required – e.g. for remote configuration, debugging, and software / firmware upgrade. Access to control room and substation networks in particular is strictly controlled, for obvious reasons.
- The need for flexibility and redundant approaches on inter-TO communications links: original plans for a dedicated MPLS link between TOs – the technical and logistical option – were

delayed by external contractors for 6 months. Escalation options were limited due to the multi-layered contractual relationships in place. The use of an IPsec link – initially rejected in favour of MPLS – was adopted as a short-term stopgap.

- Export of large quantities of data for analysis – such as undertaken for model validation work and data reviews under VISOR – needs careful planning. The set-up of an external link for real-time or part-time streaming to a third party may turn out to be more efficient and straightforward than the regular connection of an external hard drive to a server located in a secure server farm. Similar consideration needs to be given to any backup philosophy.

3.2   Considerations for Communications Infrastructure

One particular topic that has been raised in the context of VISOR and the related Smart Frequency Control project [5] – which is exploring wide-area triggered frequency response using phasors – is the choice of communication infrastructure for carrying measurement data: i.e. PMU and WMU streams.

3.2.1   Monitoring and Control: Different Requirements

Monitoring and Control applications have different latency requirements. One way this can be expressed is the "wait time" employed by PDCs. This is the length of time a PDC will wait for measurement data to arrive from all devices for a given time sample, before sending on and/or processing what data it already has – forgetting about the rest. This is essentially the maximum "age" of data for it to be considered useful.

In the monitoring domain of VISOR, it is more important that data arrives eventually (e.g. within 2-5 seconds) than that it arrives quickly. Since the data is time-synchronized at source, it is easily aligned at the receiving PDC; and any control room alarms or user observations will not be significantly impacted by a few seconds of delay.

For wide-area protection and control applications, such as within the Smart Frequency Control project, it is most important that the relevant information about power grid events is received and processed quickly. Data frames therefore must arrive within a very short time (e.g. 50-100ms) in order to be useful, while any measurements that fail to arrive within the given timeframe would have to be discarded if they eventually arrive. Timing requirements might also vary significantly for specific wide-area protection and control schemes, depending on the power system phenomena targeted (e.g. first-swing transient stability, frequency stability) and on the power system itself (e.g. higher or lower inertia).

3.2.2   TCP and UDP

TCP is connection-oriented protocol featuring reliable delivery (missed packets are detected and re-sent), albeit with an associated cost in larger packet size. In addition, as a connection-oriented protocol, traffic is always initiated by one party. In the typical WAMS scenario, the receiver (e.g. a PDC) will initiate the connection, requesting that the PMU start sending data. This has advantages for cybersecurity – only allowing traffic into the control room network that has been requested by a server within it.

The alternative, UDP, is by comparison a connectionless "fire and forget" protocol with no guarantee of delivery. Furthermore, because there is no concept of a connection or an initiating party, firewalls must allow traffic to flow freely in both directions between the PMU and receiver. This can be a major problem for cybersecurity, particularly for strictly controlled environments such as a utility control network. However, the reduced complexity of UDP generally leads to smaller packets, less network traffic (no acknowledgement or resend requests) and faster send/receive processing relative to TCP.

It should be pointed out that both TCP and UDP are used in WAMS across the world [7]. UDP PMU streams will often undergo intermediate aggregation to a single stream and conversion to TCP at one or more PDCs situated outside of the secure operations network – for the cybersecurity reasons highlighted, as well as for bandwidth efficiency and buffering of data. This aggregation and conversion can be performed at a central, regional or substation level.

3.2.3   Specific Experience from VISOR

In the context of VISOR and Smart Frequency Control the following particular points have been raised:

- **Cybersecurity:** as discussed above, the use of UDP to transmit PMU data to a WAMS server inside an operational environment (e.g. control room network) can present cybersecurity issues. This arrangement is not acceptable for operational deployment in GB – connections must use TCP.

- **Traffic congestion:** In VISOR, some isolated issues were encountered at certain PMU sites (resolved quickly), involving frequent TCP packet and connection drops. In such scenarios the resulting increase in traffic due to reconnect and packet resend requests might exacerbate any underlying congestion problem leading to increased packet loss and connection drops. In these (albeit rare) cases, data stream availability may be worse under TCP than if using UDP.

Experience to date suggests that for the roll-out of WAMS as an operational tool in GB, data must be received at the control centre via TCP. However in situations where network performance is concern and/or PMU-based control is employed, UDP will likely form the first stage of the PMU data route. Aggregation for monitoring purposes and bandwidth reduction can then be carried out at a regional or central level, followed by conversion to TCP for reliable and security-compliant delivery into the control room environment.

Generally, it remains to be determined whether a single measurement and communication infrastructure can be utilised both for monitoring and control applications of synchrophasor technology. The Smart Frequency Control project should provide valuable learning in this respect, which will then be coupled with VISOR experience to shape a unified view on the infrastructure requirements for wide-area monitoring, protection and control applications.

3.3   Performance Analysis of the VISOR WAMS

Equally challenging as the deployment of new assets and functionality, has been the integration of pre-existing "legacy" WAMS at SPEN and National Grid. This was an essential aspect of the VISOR deployment, providing the breadth of monitoring necessary for an effective and meaningful demonstration and evaluation of WAMS capabilities, delivered at an acceptable cost. These legacy WAMS were installed as "pilot" systems primarily for analysis, and were not used or maintained as production-level systems critical to everyday operation of the power system.

In particular, much of the pre-existing PMU install base consisted of legacy Digital Fault Recorder (DFR) devices that had not been originally designed for synchronised phasor measurement but had been firmware-upgraded to add PMU functionality.

Therefore, a key component of VISOR has been to assess the compliance, capabilities and performance of the WAMS infrastructure – across measurement acquisition, processing and communications. This is an on-going task covering both legacy and new infrastructure, with reviews conducted annually to identify new issues and highlight improvements or degradation in performance.

These performance reviews have highlighted many issues – this was to be expected given the non-production nature of the pre-existing WAMS infrastructure, and the PMU install base of legacy DFRs. Some problems identified were unremarkable e.g. poor GPS reception, incorrect CT/VT phase rotation or polarity, and communication link congestion. However a number of more fundamental issues were highlighted – some of these are described in the following subsections.

3.3.1   Resolution of Frequency Measurements

Figure 2 presents a comparison of reported power system frequency across 4 different PMU models within the GB WAMS. It can immediately be seen that the output from PMUs 4 and 2 are limited to a reporting resolution of 1.25mHz and 1mHz respectively.

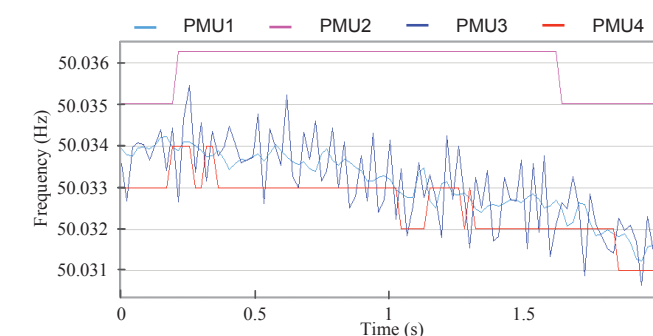**Figure 2 : Comparison of reported frequency across 4 different models of PMU from the VISOR WAMS**

In both cases, the reporting resolution is within the 5mHz accuracy required by the IEEE C37.118.1 standard [8], and is sufficient for analysis of disturbances or large oscillations in system frequency. However this limited resolution inhibits the detection and analysis of normal ambient power system

oscillations, often <5mHz in amplitude. It is analysis of these that enables the long-term normal behaviour of modes such as inter-area oscillations to be characterised and source location analysis to be applied.

With resolution limited in this way, oscillations can only be detected when they have already become a problem. The consequence of this is that key benefits of oscillation management – the ability for long-term characterisation of ambient oscillation behaviour and contributors so as to inform models, form operational procedures, or target pre-emptive correction action – are not fully realised.

The 1mHz resolution seen in the output from PMU 4 is a limitation of the 16-bit integer format used when reporting the frequency measurement [9]. A firmware upgrade has been identified that will enable the PMU model in question to report frequency in the higher-resolution floating-point format. The increase in bandwidth and storage requirements associated with using floating-point frequency is negligible relative to overall size of the PMU data frame.

The 1.25mHz quantisation seen from PMU 2 was found to be a result of the underlying PMU hardware and frequency derivation process, requiring a hardware upgrade to achieve improved resolution.

Although PMU models 2 and 4 make up a significant portion of the GB PMU install base, the new installations under VISOR and improved communications to sites with other PMU models have reduced the impact of this issue. Nevertheless, the firmware and hardware upgrades mentioned above are being instigated, to provide vital wide-area, high-precision frequency visibility.

3.3.2 Format of Current Measurements

Figure 3 shows some strange movement in current magnitude and angle reported by one PMU in the GB WAMS. This behaviour, which could easily cause confusion to users, is again due to the measurement reporting format selected at the PMU. In this case phasors are reported in rectangular format as 16-bit scaled integers – with a full scale value equal to maximum fault current, due to the device's primary role as a Digital Fault Recorder (DFR).
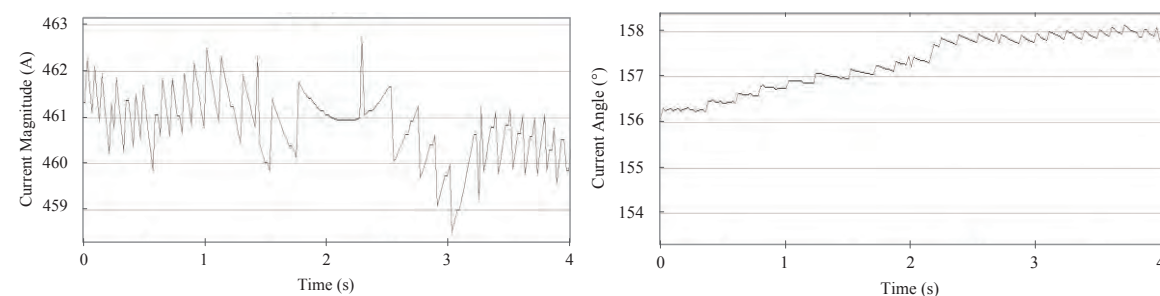

Figure 3 : Rectangular quantisation of current phasors, seen in magnitude and angle reported by a PMU

In the case of phasor measurements, unlike frequency, 16-bit integer format can provide sufficient resolution for monitoring and analysis – provided that polar format is used (see below) and a suitable full-scale value is applied for scaling, e.g. 4x line rated current. This configuration is often recommended due to the associated saving in bandwidth and storage requirements over 32-bit floating point format.

In the case of the PMU shown, the full scale value is fixed by the analog-to-digital acquisition channels used. Normally, where practical, a second channel with a lower full scale value would be fed with the same signal, to provide higher precision measurements for PMU purposes without impacting the DFR function.

Even in isolation, the use of polar format phasors, where supported by the PMU, can reduce the maximum step size observed and also transfers the quantisation to the polar space. This makes the observed behaviour more immediately obvious as quantisation rather than some other measurement or real power system phenomenon, such as an oscillation.

3.3.3 Anti-Aliasing Filtering

Normally, in order to ensure adequate attenuation of frequency components greater than the Nyquist limit of 25Hz (for a 50fps reporting rate), PMUs would be expected to employ low-pass filtering with a roll-off beginning well below this frequency. Without adequate filtering higher frequency content such as harmonics and sub-synchronous oscillations in the 25-50Hz range can be aliased – introducing measurement error or causing confusion about the frequency of any oscillations observed.

It has been observed that some older models of PMU present in the GB system do not appear to employ anti-aliasing filtering for 50fps reporting. Figure 4 shows a comparison of frequency content of voltage phasor magnitude, taken from two different PMU models monitoring the same voltage bus. The filter roll-off is apparent in the measurements from PMU 2 (a newer model) – however there appears to be no filtering taking place in PMU 1 (an older, legacy model).
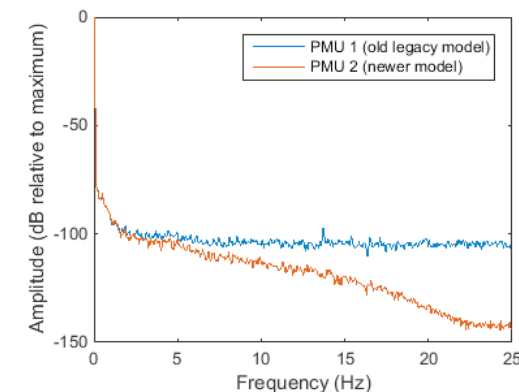

Figure 4 : Comparison of frequency content of voltage phasor magnitude, taken from two different PMU models monitoring the same voltage bus

Again, this highlights the importance of performance testing, particularly when deploying WAMS using legacy hardware.

3.3.4 Internal Clock Drift

Figure 5 shows the difference in voltage angle from two PMUs at opposite ends of a transmission line in the GB system. A 1s sawtooth component is evident – this is due to drift of the internal clock of one PMU.

The PMU receives a one pulse per second (PPS) signal from a GPS-locked time source. This is used as the basis for microsecond-level measurement synchronization and is particularly important as a reference for phase angle measurements. However, between these pulses the internal PMU clock relies on a crystal oscillator to maintain time, re-synchronising when the next pulse is received. In this case, the oscillator is not able to keep time correctly. Therefore the PMU clock time, and consequently the angle measured by the PMU, drifts in the time between PPS pulses – jumping back to the correct value each second. This problem is overcome by replacing the crystal oscillator in the PMU – a maintenance program to upgrade the affected PMUs is now almost complete.
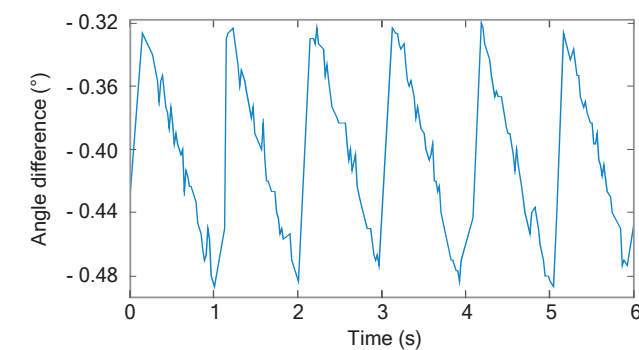
Figure 5 : Angle difference across a transmission line - the sawtooth variation is due to internal clock drift in the PMU at one end of the line

3.3.5 Reporting Loss of Time Synchronisation

The IEEE C37.118 standard [9] requires that PMUs report loss of time synchronism. For this purpose, a number of time quality status indicators are incorporated in the C37.118 protocol for synchrophasor data transmission – these include a binary SYNC flag and an "unlock time" value.

In some legacy devices using older firmware versions, it has been observed that unlock is highlighted through one unlock indicator but not another, perhaps assuming that both will be checked by any receiving application. It has also been observed on rare occasions that a device will exhibit clear

synchronisation loss in its measurements whilst continuing to be marked as "Locked" at the C37.118 protocol level – such a situation is shown in Figure 6.

These two issues, though easily corrected through firmware and software changes, highlight the necessity of careful protocol compliance testing when deploying WAMS in an operational environment. Unreported losses of synchronism will at a basic level translate to misleading angle measurements (see 3.3.4) which may be incorrectly interpreted as power system behaviour, and to delays in signal traces that would impact event analysis. At a more critical level, loss of time precision will impact on high-precision analyses such as disturbance management, oscillation source location and line parameter estimation.

Figure 6 An example of a clearly unsynchronised PMU (delayed trace) that was not flagged at the C37.118 protocol level

3.3.6 Performance Under Heavy Processing Load

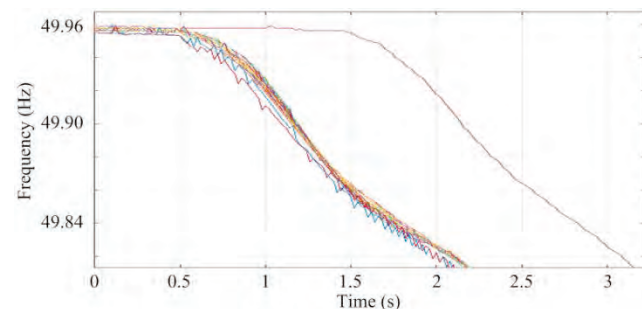It has been observed that some PMUs provide intermittent data following a system disturbance - an example of this is shown in Figure 7. Note the red trace jumping intermittently to 50Hz. These are frames where the PMU has sent blank packets (correctly flagged as invalid) or dropped them altogether.
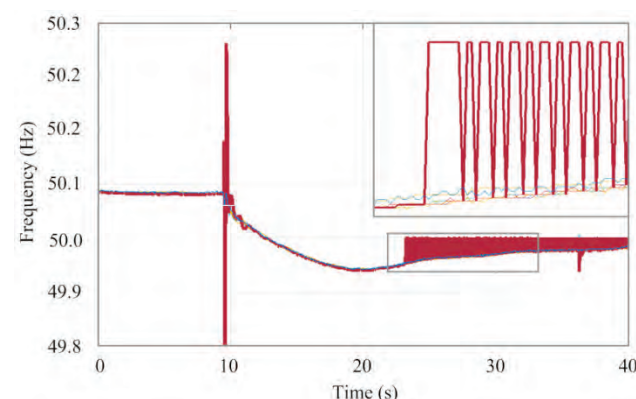

Figure 7 : Frequency reported by GB PMUs during a power system disturbance. The red trace jumping intermittently to 50Hz corresponds to the PMU has sent blank packets (correctly flagged as invalid) or none at all.

This is believed to be a result of additional computing load associated with processing and storing a transient fault record of the preceding event. Whilst these PMUs are not reporting incorrect data, and the invalid packets would be ignored by any WAMS applications, the loss of measurements is regrettable since captures of system disturbances are of particular value. Such data is ideal for model validation work, and for analysing system oscillatory behaviour and any cascading disturbances. This highlights the importance of load testing of WAMS infrastructure.

4 Sub-Synchronous Oscillations (4-46Hz)

4.1 Background

The installation of transmission line Series Compensation, and the increasing penetration of power electronic converters associated with renewable generation and HVDC links, add vital flexibility and capacity to the power system and help in the move to a low-carbon grid. However, this plant introduces new challenges not only in protection and fault management, but also in steady state and

post-fault operation – with the potential for SSO interaction in the 4-46Hz range. Three primary categories of oscillation occur in this range and are of concern:

- **Grid RLC** (resistor-inductor-capacitor) **modes:** resonant frequencies established by the combination of transmission network inductance with the capacitance of series compensation. These frequencies will change with the effective impedance of the network, e.g. when faulted lines trip.
- Potential **control modes** introduced by power electronic converters, such as at wind farms and HVDC links. These may vary significantly in frequency according to the operating conditions of the converter.
- **Generator shaft torsional modes:** a shaft linking n masses (generator + turbines) will have n-1 torsional modes. These are fixed in frequency, determined by the physical characteristics of the plant. It should be noted that a torsional oscillation of frequency f_{shaft} will appear in voltage and current as a modulation: $f_{synchronous} \pm f_{shaft}$. Similarly, an electrical oscillation at f_{grid} will appear as a shaft torque at $f_{synchronous} - f_{grid}$.

Under normal conditions these modes will be well-damped and low in amplitude. However there is potential for severe adverse consequences should two modes coincide and interact – for example following a network fault and line trip:

- **Sub-Synchronous Resonance** (SSR): this involves interaction between generator torsional and grid RLC modes. Consequences range from increased shaft fatigue due to sustained low-level interaction, to shaft failure as observed at the Mohave plant in 1970 [10].
- **Sub-Synchronous Control Interaction** (SSCI): interaction of a control and grid RLC mode – see [11].
- **Sub-Synchronous Torsional Interaction** (SSTI): interaction of control and generator torsional modes [12].

The GB transmission owners have implemented a number of measures to robustly mitigate the risk of SSO in the GB system. These include extensive model and site monitoring studies to check for potential interactions, the use of filters or thyristor controls on series compensation to avoid interaction, and generator protection systems which bypass capacitors should significant oscillations occur. There remains a need however for real-time wide-area monitoring to:

- **Provide visibility and alarming** of low-level modes that may escalate or cause cumulative plant fatigue.
- **Assess the true behaviour of the system** so as to support plant and protection commissioning, validate models and studies, and to identify unexpected modes.

4.2 VISOR Demonstration

VISOR has deployed a new solution to provide continuous real-time wide-area visibility of SSO in GB, incorporating the world's first deployment of a new substation data acquisition function – the Waveform Measurement Unit (WMU) – and a new central WAMS server SSO application module.

Typical WAMS utilize synchronized phasor measurements transmitted via the IEEE C37.118 protocol at up to 50/60 frames per second (fps) – though some devices offer higher rates. The practical observable range in these WAMS extends to about 10Hz – limited by the requirement for sufficient anti-aliasing filtering of components above the 25/30Hz Nyquist limit, and by the length of window used for phasor calculation which is a compromise between accuracy and attenuation of higher frequencies. Whilst sufficient to capture governor, electromechanical and some voltage control modes, this is not suitable for monitoring of the full SSO range.

To provide visibility of SSO in GB, 10 WMUs are being installed as part of VISOR. These provide synchronized voltage and current point-on-wave measurements at 200 samples / second, streamed in real-time via the C37.118 protocol as "analogue" type values. Speed measurements from turbine shaft transducers can also be sent. This approach accurately represents oscillatory components in the 4-46Hz range, and also gives visibility of the 54-96Hz range so as to differentiate modulations such as torsional modes from added components such as grid RLC modes. It should be noted that the use of a higher reporting rate of 200fps is fully compliant with the C37.118 standard, and is in fact encouraged [9].

The 200fps voltage, current and speed waveforms from each WMU are received and stored at each of the VISOR WAMS servers. They are then analysed in real-time by a new SSO application module which extracts the amplitude, frequency and damping of modes in the 4-46Hz range present in each

signal. As with the other oscillation applications in VISOR, results are presented in real-time geographical displays, feed alarms and are available for historical trend and event analysis. For diagnostic purposes, a spectrogram provides visibility up to 96Hz, to enable users to differentiate between added components and modulations of the 50Hz waveform.

4.3 Learning to Date on SSO

The SSO monitoring solution has been in place for a number of months, and long term review of the data has provided valuable insight to SSO behaviour in GB.

Numerous modes have been detected - these are generally considered to be small and well-damped, with the majority in the region of 2V and 0.1A at the 400kV level. The detected modes include expected generator torsional frequencies, as well as a number of other modes – some are relatively fixed in frequency whilst others are more mobile.

The observations made emphasise the benefit in two key aspects of the VISOR SSO monitoring approach. The first aspect is that measurements are collected in a synchronised manner over a wide area and presented from a system-wide perspective. This means that behaviour detected at each site is put in the proper context – oscillations that are normally separate (either geographically or in frequency) but that might interact in some scenarios are highlighted. It also means that the shape of an oscillation across the system is visible – making the key participants more obvious. The second aspect is that monitoring is continuous. This means that all behaviour is captured – including modes that might only appear occasionally – and importantly that the times of any changes are captured, which makes diagnosis of any issues much more straightforward.

Some specific observations are discussed in the rest of this section.

4.3.1 Generator Torsional Modes

One question asked in the early stages of VISOR was whether generator torsional modes would be visible in grid-side electrical signals under normal conditions – this has now been answered. Figure 8 shows SSO frequencies detected over a 1 month period at a location in the GB system adjacent to a generator. Expected torsional modes at the generator are shown - frequency values have been omitted for reasons of confidentiality. It can be seen that the four expected torsional modes are visible, though some (modes 1 & 3 here) are more prevalent than others.

This demonstrates that torsional oscillations can be observed in the grid under normal conditions, and thus grid-side measurements could be effective in detecting early signs of interaction, and in confirming the torsional frequencies predicted by a generator physical model. This is valuable learning, since grid-side monitoring can be easier to deploy than direct generator measurements.

It should be noted however that the visibility of modes in electrical measurements will be influenced by a number of factors including the shape of the mode along the turbine shaft - i.e. whether the generator section of the shaft falls near a null of the mode or a point of maximum deflection. For example, measurements taken near to another generator showed only the 1st expected torsional mode.
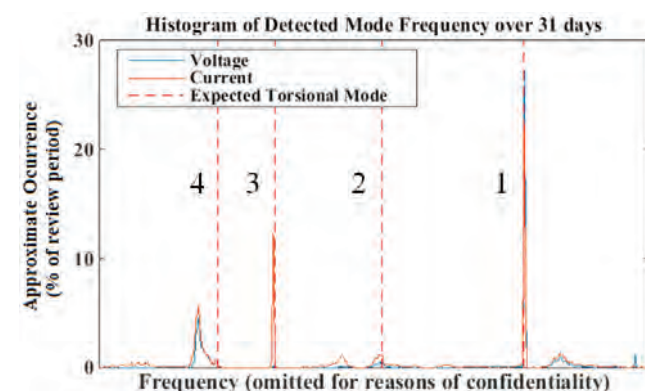

Figure 8 : Detected SSO frequencies over a 1 month period, at a location in the GB system, adjacent to a generator

The occasional proximity of some variable-frequency modes to generator torsional modes (for example the peak at 5%, lower-left of Figure 8) has warranted further investigation as a matter of prudence. However there have been no signs to date of adverse interaction.

4.3.2 Support of Series Compensation Commissioning

Together with the SPEN Series Compensation project, the SSO monitoring solution has now been used to support the commissioning of series compensation onto the GB power system, providing additional reassurance during live tests and post-event review for any sign of low-level interaction. No adverse impact associated with the series compensation has been observed.

The data gathered has also enabled alarm levels to be configured around a baseline of normal observed SSO behaviour, so that any excursions of behaviour with raised amplitude and/or poor damping can be flagged in real-time and for post-event analysis.

4.3.3 Modes That Appear and Disappear

A number of modes have been detected in the GB power system in addition to the expected generator torsional modes. Many of these oscillations tend to appear consistently for sustained periods of hours, days or weeks and then disappear for equally as long, only to reappear again. The presence of such oscillations was to be expected – and none showed signs of concerning behaviour.

This aptly highlights a key benefit of the continuous monitoring being demonstrated, which complements other SSO mitigation measures such as model studies and special investigations. Model studies will explore a range of system operating conditions that would not normally be observed, and special investigations will provide detailed analysis of specific plant or events. Continuous, long-term observation of SSO can reveal behaviour not presented in the scenarios modelled or in "black box" models of wind farms and HVDC links; and can highlight behaviour that did not occur during time- or site-restricted investigations.

4.3.4 A significant mode

Whilst most of the modes observed in the GB system are relatively local, one mode suspected to be power electronic in origin has been observed over a 100-mile area. The mode varies in frequency and occasionally moves close to an expected generator torsional frequency. Some occurrences of reduced damping and raised amplitude have been observed - although the amplitudes involved remain small-scale.

Review of the appearance and disappearance of this mode in the gathered data has provided vital information that has allowed engineers to target further investigation, as a matter of prudence.

This again highlights the benefit of the monitoring being demonstrated – to provide validation and additional assurance against unexpected behaviour, to flag potential issues and provide information to target investigation where appropriate.

5 Very Low Frequency and Low Frequency Oscillations (0.002-0.1Hz, 0.1-4Hz)

5.1 Background

The GB system was the first to implement real-time oscillation monitoring in the 1990s – this system fed operational alarms and guidelines to manage a 0.5Hz inter-area oscillation between Scotland and England. Whilst this mode is now almost always well-damped, there are other modes present in the GB system that are less well understood. Furthermore, the frequencies and patterns of GB oscillations are likely to change as the power system evolves in the coming years with changing inertia, generation profile, and transmission topology and plant. This highlights the need for closer and more extensive monitoring of oscillatory behaviour in GB.

Whilst real-time monitoring of electromechanical oscillations in the 0.1-4Hz range is well-established, monitoring of the 0.002-0.1Hz governor frequency range is limited. Although perfectly feasible with existing WAMS technology, this lower frequency range requires separate analysis algorithms and processing to that of the electromechanical range, which till recently there has not been demand for in real-time WAMS software. However the trend of changing power systems inertia has driven increased concern around governor oscillations, leading to the demonstration under VISOR of a new dedicated VLF monitoring application.

Furthermore, whilst solutions for oscillation monitoring are relatively straightforward, there are limited means of identifying which generators are contributing to an oscillation. Without this information, response to an oscillation relies on either detailed study of a mode, or the application of general

guidance such as reducing power flow on a heavily loaded interconnection. Source location analysis is therefore of significant value both in real-time operational response, and in post-event and trend analysis to direct follow-up action such as generator control tuning. Previous source location approaches have relied on pattern identification in system operating conditions, or on oscillation power flow tracing. VISOR is demonstrating a new source location approach that avoids the need for high penetration of power flow measurements or statistical review of multiple events, through analysis of oscillation phase [13]. This approach can produce useful results from only a sparse distribution of voltage and frequency measurements.

5.2   VISOR Demonstration

Under VISOR, complementing existing applications for the monitoring of electromechanical oscillations, a new application module dedicated to the management of very low frequency oscillations is being demonstrated. Also being trialled is new source location approach, for both VLF and L F ranges, based on analysis of voltage angles. The resultant suite of oscillation management tools being evaluated is of relevance both to real-time operation, incorporating geographical displays and alarming; and to post-event and long term trend analysis, with all analysis results stored for later retrieval.

This work serves to improve understanding of GB system dynamics – supporting the model validation work of VISOR and demonstrating the benefits of these tools to GB system operation. These benefits include confidence in system models and the security limits that are derived from them; more effective management of system oscillations, with the potential for constraint relief; and awareness of local behaviours that may indicate plant malfunction or grid code non-compliance.

Further details of the learning delivered to date in VISOR, and the consequential benefits, are set out in the rest of this section.

5.3   Learning to Date on VLF and LF oscillations

5.3.1   Characterisation of System Modes

Long-term baselining of the behaviour of GB system modes has produced useful information that can be applied to a number of areas:

- **Model Validation:**
  - Confirming that observed system modes are correctly represented in system models
  - Confirming that observed occurrences of poor damping are replicated in model simulations.
- **Management of Oscillations** (source location information is particularly crucial here)**:**
  - Forming operational procedures to deal with specific oscillations if they become an issue in the system.
  - Targeting investigative or maintenance action such as generator model validation or control tuning.

Some specific modes that have featured in the VISOR reviews are described here.

0.04-0.05Hz Governor Mode

There have been some historical occurrences of large amplitude, very low frequency oscillations in the GB network, related to governor frequency dynamics - however no major recurrences have been observed so far during the VISOR project. Oscillations in this frequency range tend to be more common and larger in amplitude on low-inertia systems. Hence, although the governor mode oscillations seen in the GB system are not a problem at present, it is important to monitor and characterise their behaviour as the inertia landscape and frequency response mechanisms continue to change.

In addition, because of their low oscillation frequency and uniform presence in system frequency measurements across the GB system, these modes are very obvious to control room users when they appear. A better understanding and awareness of their normal behaviour enables operators to judge more comfortably whether a "wobble" observed on their screens should be a concern or not.

The new source location approach was applied offline to one of the few occurrences of raised amplitude on this mode. The results, shown in Figure 9, indicate that the oscillation source is in the region of Sites A and B (the most leading locations) – which both have local thermal and wind generation. Site C, which lags A and B, sits nearby on a different voltage level.
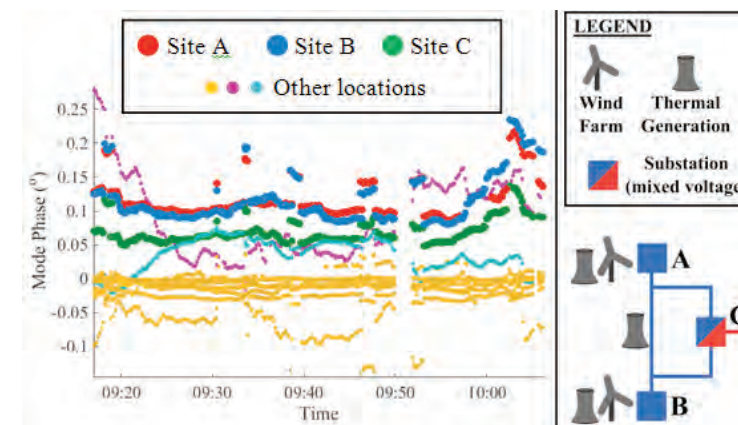

Figure 9 : Mode phase analysis of common mode oscillation at locations across GB (left) and topological arrangement of leading sites (right). Locations with leading phase are considered to have larger contributions to an oscillation.

This suggests two, equally feasible, possibilities – either that generation at both A and B is contributing to the oscillation to a similar degree, or that a third generator between the two locations is the actual source. Analysis of future events will confirm whether this is a consistent scenario, or whether different generators exert influence on different occasions.

0.5Hz Scotland-England Mode

The 0.5Hz inter-area mode between Scotland and England, the original reason for deployment of oscillation monitoring in GB 20 years ago, has for some time been well-behaved following the installation of power system stabilisers [14]. Over the monitoring period of VISOR, this mode has been observed as generally well-damped. A few events in 2014 reported raised amplitude and poorer damping, with the largest event showing oscillations of 55 MW observed on one of the four Scotland-England "B6" interconnector circuits (Figure 10). Investigation by National Grid confirmed that these events coincided with scheduled circuit outages in the B6 region, and that the reduced damping observed was in line with expectations. Capturing system behaviour during these events will help network planners and system design teams to better validate their system models.
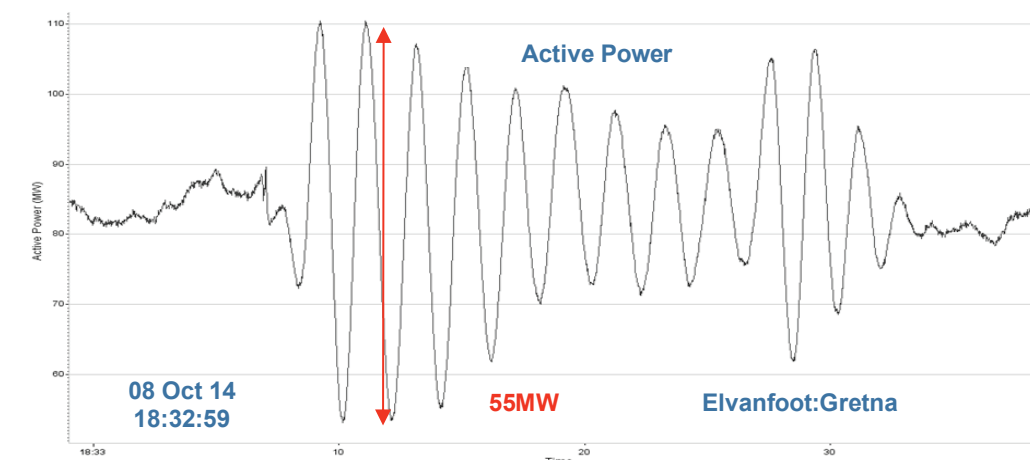
Figure 10 : Large 0.54Hz oscillations observed on 1 of the 4 B6 interconnector circuits following a system disturbance

0.7Hz Mode

There has been a mode at 0.7-0.8Hz observed over several years in GB, with occasional incidences of poorer damping – though these oscillations have never grown to be an issue. The mode has been observed over a wide area from Scotland to England but in the past there was insufficient information to identify the main contributing regions. Application of the new source location analysis under VISOR across three events showing poor damping has produced consistent results pointing to a large contribution from the generation-rich region around the Humber estuary in North England (Figure 11).
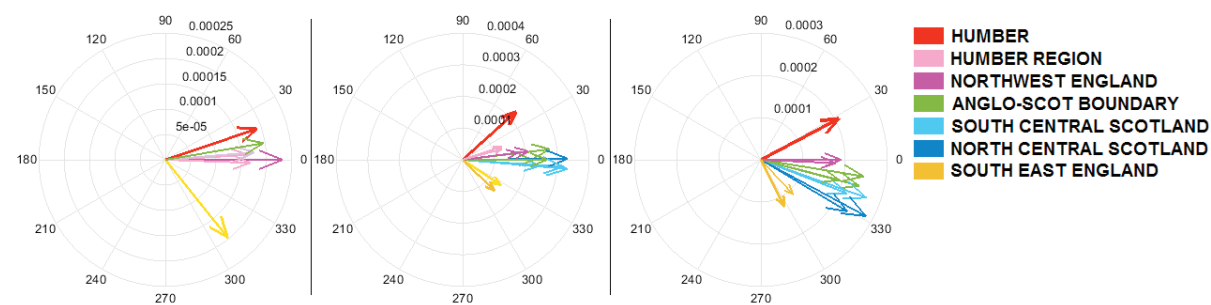
Figure 11 : Mode shape of 0.79Hz oscillation across 3 separate events, showing the Humber PMU leading the group, indicating a significant source near the monitored point

This is a particularly good example of the benefit of this source location approach – highlighting the perhaps counter-intuitive fact that the location of largest contribution (red arrow – Humber) is not always the location of largest amplitude (pink: northwest England / blue: central Scotland). This information on the oscillation source, when confirmed by the restoration of visibility to two temporarily unmonitored regions (South-West England and Northern Scotland), will help to inform operational procedures on how to respond to this mode if it becomes an issue in the future.

**5.3.2   Flagging of Oscillation Events and Local Behaviours for Awareness and Investigation**

In addition to improving knowledge of those modes that are consistently present across the GB system, the VISOR reviews have highlighted a number of limited-occurrence events and local behaviours. These tend to be small, but can be poorly damped. Not all are electromechanical modes, and some oscillations vary in frequency, or appear as non-sinusoidal periodic forcing (potentially power electronic controls). Some issues appear to be related to dynamics of wind farms.

Whilst not necessarily relevant to day-to-day operation of the power system, it is important to flag this information to the relevant parties, as it is beneficial for:

- Asset owners (both at Transmission Owners and generators), for highlighting potential plant malfunction – or validating expected behaviour.
- Highlighting potential grid code non-compliance.
- Raising awareness of behaviours that may become relevant in future – for example to teams involved in transmission network development, managing new connections to the grid, or investigating the behaviour if it later becomes a problem.

It is for these types of issues that regular, concise reporting and effective record-keeping are important.

6   Conclusions

This paper has presented some of the initial learning from the VISOR project, notably experience from the deployment of the VISOR WAMS and insight from the first reviews of GB oscillatory behaviour across the governor, electromechanical and sub-synchronous oscillation range.

Implementation of the VISOR WAMS has provided useful learning that together with learning from the Smart Frequency Control project will inform the future roll-out of WAMS in GB. In particular, it has been highlighted that the design of the future GB WAMS architecture will need to carefully accommodate:

- Differing requirements for monitoring and control applications: monitoring data is "better (a few seconds) late than never", whilst control data is only useful if it arrives quickly (e.g. 50-100ms).
- Challenges around streaming data from substation to control centre, and between control centres, in a cyber-secure manner – whilst maintaining sufficient flexibility in implementation to accommodate other considerations.
- Bulk transport of WAMS data, such as for backup or external analysis.

Review of WAMS performance has highlighted a number of important aspects that must be considered in the future specification and testing of the GB WAMS:

- The data formats applied to phasor and frequency measurements (integer / floating-point and cartesian / polar), as well as the precision of underlying signal acquisition and processing, and the impact that these have on subsequent analysis such as the monitoring of ambient oscillations.
- Performance and reporting of time synchronisation: extensive end-to-end testing of this is important if synchronisation is to be relied upon for precision WAMS applications such as disturbance analysis and oscillation source location.
- Performance under heavy load: many PMU models perform other functions such as disturbance recording and power quality monitoring. It should be ensured that all functions continue to perform to requirements under heavy load such as following a system disturbance.

Deployment of SSO monitoring in the GB system and review of observations over several months has delivered valuable insight and experience. In particular:

- VISOR has demonstrated that grid-side measurements can provide visibility of generator torsional modes under normal conditions.
- SSO monitoring and behaviour review has supported the deployment of series compensation on the GB system.
- A number of oscillations have been observed in addition to the expected generator torsional modes, displaying a variety of characteristics. No concerning behaviour has been observed, but the continuous, wide-area visibility of these modes has been valuable in instigating and guiding further investigation in some cases, as a matter of prudence.

Finally, review of very low and low frequency oscillatory behaviour in GB using new WAMS oscillation management tools, including the application of a new source location approach, has provided the following learning:

- Application of source location analysis to a low-amplitude governor frequency mode has suggested a source, and analysis of future occurrences will confirm whether this location is a consistent contributor.
- Observation of the 0.5Hz Scotland-England interarea oscillation has highlighted some events that will help in the validation of system models.
- Application of source location analysis to the 0.7-0.8Hz mode occasionally observed in GB has shown a consistent pattern over multiple events pointing to a particular source. This information will inform future operational procedures for managing this mode if it becomes a problem in the future.
- Numerous localised or limited-occurrence oscillations have been observed, with a variety of characteristic behaviours observed, such as forced oscillations and wind farm dynamics. These are not of operational concern, but the information is useful for other purposes such as asset management, compliance and to inform future planning, studies and investigations.

During the final year of VISOR, further reviews will be conducted and applications now deployed will be evaluated in the field. The project will conclude with a set of recommendations on the benefits of and next steps for roll-out of WAMS to the operation of the GB power system.

References

[1] VISOR project online portals: http://spenergynetworks.co.uk/visor , http://visor-project.org.uk/

[2] V. Terzija, et al. "Wide-Area Monitoring, Protection, and Control of Future Electric Power Networks," Proceedings of the IEEE , vol.99, no.1, pp.80,93, Jan. 2011

[3] U.S.-Canada Power System Outage Task Force "Final Report on the August 14, 2003 Blackout in the United States and Canada: Causes and Recommendations, http://energy.gov/sites/prod/files/oeprod/DocumentsandMedia/BlackoutFinal-Web.pdf ,

[4] Report of the Enquiry Committee on Grid Disturbance in Northern Region on 30th July and in Northern, Easter and North-Eastern Region on 31st July 2012, August 2012, http://www.powermin.nic.in/pdf/GRID_ENQ_REP_16_8_12.pdf, retrieved: 10/11/15

[5] National Grid UK "Enhanced Frequency Control Capability (EFCC)" (now known as "Smart Frequency Control") Electricity Network Innovation Competition Full Submission, October 2014, http://www.smarternetworks.org/

[6] "Identification of electromechanical modes in power systems" IEEE Task Force Report, Special Publication TP462, IEEE PES, 2012.

[7] NASPI 2014 Survey of Synchrophasor System Networks – Results and Findings, July 201,5 https://www.naspi.org/File.aspx?fileID=1541,

[8] IEEE Standard for Synchrophasor Measurements for Power Systems, IEEE Std. C37.118.1a-2014

[9] IEEE Standard for Synchrophasor Data Transfer for Power Systems, IEEE Std. C37.118.2-2011

[10] D. N. Walker, C. E. J. Bowler, R. L. Jackson, D. A. Hodges, "Results of subsynchronous resonance test at Mohave," in IEEE Trans. Power App. Sys, vol.94, pp.1878-1889, Sept. 1975.

[11] NERC, "Lesson learned - sub-synchronous interaction between series-compensated transmission lines and generation", 2011, [Online]. Available: http://www.nerc.com/pa/rrm/ea/Pages/Lessons-Learned.aspx

[12] L. C. Gross "Sub-Synchronous Grid Conditions: New Event, New Problem, and New Solutions" [online], Western Protective Relay Conf., Washington, 2010. Available: http://relayapplication.com/docs/WPRC_2010_SSF_Detection_Paper.pdf

[13] N. Al-Ashwal, D. Wilson, and M. Parashar, "Identifying sources of oscillations using wide area measurements", unpublished, Grid of the Future Symposium, CIGRE US National Committee, 2014.

[14] D.Cai, P.Regulski, M.Osborne, V.Terzija, "Wide Area Inter-area Oscillation Monitoring Using Fast Nonlinear Estimation Algorithm", IEEE Trans. on Smart Grid, Volume: 4, Issue: 3, 2013, pp. 1721-1731

Advances in Wide Area Monitoring and Control to address Emerging Requirements related to Inertia, Stability and Power Transfer in the GB Power System

**D. H. WILSON, S. CLARK, S. NORRIS[1]; J. YU, P. MOHAPATRA[2];
C. GRANT, P. ASHTON[3]; P. WALL, V. TERZIJA[4]
[1] GE Grid Solutions; [2] SP Energy Networks; [3] National Grid; [4] The University of Manchester
United Kingdom**

SUMMARY

This paper describes recent innovations in wide area monitoring and control in the GB power system to address challenges as the penetration of renewable energy and power electronic conversion increases. The shift away from large synchronous generation sources with inertia towards power sources such as wind and solar energy, and HVDC interconnectors, which do not contribute to the system inertia, changes the dynamic characteristics of the grid as well as the pattern of network loading. With limited opportunities to establish new onshore transmission routes, technologies such as series compensation and parallel AC and DC paths are being used to extend the power transfer capability of the network, however these also introduce certain new risks to be managed. Given these risks, it is important for the GB transmission owners and system operator to have greater clarity of the dynamic behaviour and physical capability of the system, and through this create novel active control methods where appropriate for network use and efficient provision of ancillary services.

There is therefore a need for more detailed monitoring of the power system performance to identify and interpret changing risks. In response to these needs, the GB transmission system owners and system operator are collaborating to apply a suite of new system monitoring applications based on synchronised wide area monitoring, using established phasor measurements as well as the first deployment of a new monitoring approach for higher frequency phenomena. The applications address a wide range of dynamic phenomena from very low frequency governor/frequency control oscillation (0.002-0.1Hz), through electromechanical oscillations (0.1-4Hz) to higher frequency sub-synchronous oscillations (4-46Hz), with methods of identifying sources of oscillations. Disturbances are captured and characterised using real-time and post-event measures.

A new approach to wide area control is demonstrated, addressing the need for fast frequency control with reduced inertia in the grid. This approach accelerates response and prioritises action close to the source of the disturbance in order to improve stability rather than degrade it, controlling various non-conventional resources to deliver a fast, proportionate and predictable response.

KEYWORDS
Disturbances, electromechanical oscillations, frequency response, inertia, sub-synchronous oscillations, synchrophasors, WAMPAC, WAMS.

1. INTRODUCTION

Recent rapid growth in the penetration of renewable energy resources and power electronic connections leads to changes in the dynamic behaviour of the power system:

- **Reduced inertia** results in faster changes in frequency in response to disturbances and greater divergence of frequency during the disturbance. Regional variation of inertia is also an issue, and large synchronous generation retiring in Scotland influences stability limits.
- **Angular stability** between regions of the grid changes, related to the inertia issue. One particular example of this is the influence of retiring large synchronous generation in Scotland on the stability of the Scotland-England "B6" transmission boundary.
- **Frequency stability** is more challenging with the inertia reduction, as Rate of Change of Frequency (RoCoF) is projected to increase from 0.125Hz to 0.3Hz/s, possibly as early as 2021, with further increase anticipated [1]. Without mitigation, this leads to load shedding in 2.7s, which is short in comparison with the conventional 2-10s primary response service. In a low inertia scenario, frequency and angles diverge more rapidly during a disturbance. Faster frequency control actions will influence first-swing response and contribute (positively or negatively) to the angular stability of the network.
- **Load-flow patterns** change as renewable generation sources tend to be in different locations from conventional generation. There is also larger, more rapid variation in system states. In the GB case, there are plentiful renewable energy resources in Scotland, leading to constraints in southward power flow.
- **Transmission technology** is changing, with series compensation being added to relieve stability constraints and an embedded HVDC link built to supplement the parallel AC corridor transmission capacity. These new transmission technologies extend network capability, but also introduce more complexity. Sub-synchronous oscillations and the potential for resonance are particular concerns.
- **Dynamic interactions** can become more complex, and ensuring the stability of oscillations is increasingly challenging. The range of oscillation frequencies is wider, from very low frequency oscillations related to governor/frequency control (typically 0.05Hz) through to sub-synchronous oscillations and interactions between series compensated lines and conventional or renewable generation (up to 50Hz).
- **Disturbances** involving larger losses with new HVDC interconnections and large offshore generation give rise to larger frequency deviations.

With this background, it is very important that the dynamics of the system can be observed and interpreted. Since many of the changes in grid behaviour involve frequency and phase angle dynamics, Synchrophasor Measurement Technology (SMT) is an appropriate foundation for GB-wide monitoring infrastructure and enables a wide variety of Wide Area Monitoring, Protection and Control (WAMPAC) applications [2]. There are also extensions required to standard synchrophasor measurement to enable observation of higher frequency sub-synchronous oscillations that can approach the nominal system frequency.

This paper describes two initiatives in the GB transmission system. Firstly, the VISOR project [3] is a joint innovation initiative led by SP Energy Networks, involving the transmission owners and system operator to put in place an integrated monitoring system with shared data across the GB network. It incorporates synchrophasor measurements at 50Hz as well as waveform measurements at 200Hz for detecting sub-synchronous oscillations. A suite of monitoring applications to manage oscillations and disturbances is being introduced with the target of providing better real-time and historic information on dynamic behaviour and risks.

Secondly, reduced system inertia is addressed by a new wide area control approach being demonstrated in the SMART Frequency Control project led by National Grid [4]. This aims to show that response to a disturbance can be deployed within a second in the areas of the grid closely linked to the source of a disturbance, and that a timely, proportionate and predictable overall response is obtained. The demonstration is expected to lead to a future rollout where various diverse frequency response resource providers can participate in a new service market, where speed of response is rewarded.

2. POWER SYSTEM DYNAMICS MONITORING APPLICATIONS

Low Frequency Oscillations and Source Location, 0.002-4Hz

The GB system was the first to implement real-time oscillation monitoring in the 1990s, which was used with operational alarms and guidelines to manage a 0.5Hz oscillation between Scotland and England. While the damping of the 0.5Hz mode is now almost always sufficient, there are other modes that occur that are less well understood. Furthermore, the changes to the generation profile, inertia and transmission topology are expected to affect the frequencies and patterns of oscillation that occur. For these reasons, improved understanding and closer monitoring of these oscillations is very important as the GB system evolves.

To address oscillation damping problems, it is important to know where to take action. The new source location method provides this information. This supports both real-time measures and longer-term analysis and control tuning.

The wide-area oscillation analysis being demonstrated in GB incorporates novel features:

- **Extended lower frequency range**, from the present electromechanical range of 0.04-4Hz, down to 0.002Hz to cover slow governor/frequency control dynamics. Low frequency oscillations are increasingly important with lower inertia and fewer large thermal plants available to participate in frequency control.
- **Novel source location methods** to identify the closest measurement point to a source of poor damping, thus enabling interpretation and response to oscillation issues. This source location approach uses the relative phase of oscillations, made possible by the accurate synchronisation of PMU data. The source location method is further described in [6].

Although unstable oscillations are rare in the GB network, there has been a case observed where a mode at 0.54Hz was observed with 55MW swings in one (of four) lines in the Scotland-England corridor. Analysis of this event showed significant participation from Scotland to South West England.
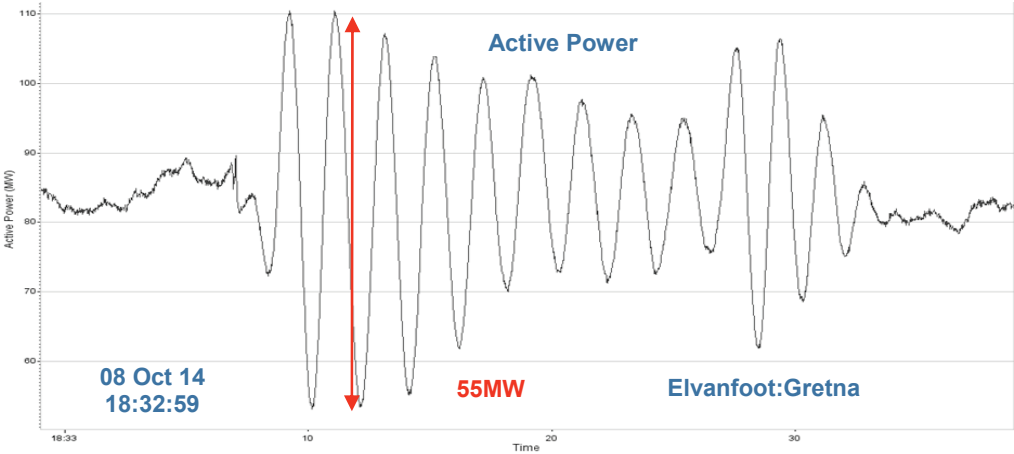

Figure 1 Large 0.54Hz oscillations following fault

In addition to this 0.5Hz mode, there has been a mode at 0.7-0.8Hz observed with incidences of poor damping over several years. Although this mode has not been known to grow in amplitude, it is seen over a wide area from Scotland to the south of England. Prior to the VISOR project, there was little information to identify where the main contributions were. The incidences of poor damping observed during this project have consistently indicated that the closest monitoring point to the source of oscillation was in the generation-rich Humber estuary region (Figure 2). Restoration of PMU visibility to two temporarily unmonitored regions – South-West England and Northern Scotland – will provide further detail of the contributions.
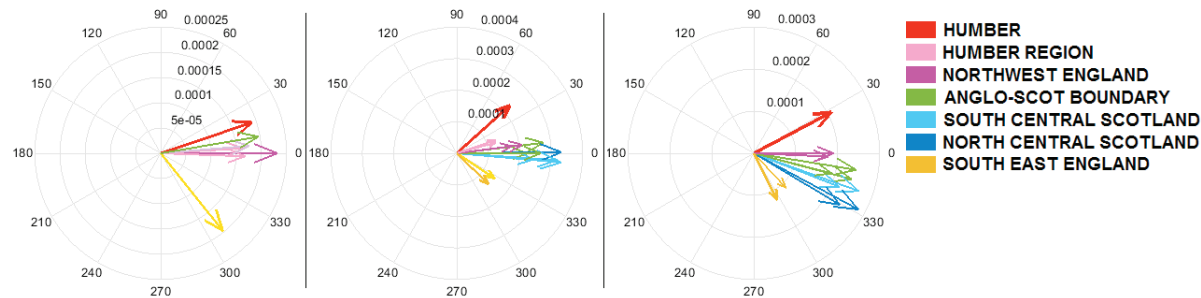

Figure 2 Mode shape of 0.79Hz oscillation across 3 separate events, showing Humber leading the group, indicating a significant source near the monitored point

There have been some historic occurrences of large amplitude, very low frequency oscillations in the GB network around 0.04Hz, related to governor frequency dynamics. However, there have been no major recurrences in the course of the project so far. Oscillations have been observed in all frequency measurement points with almost exactly the same amplitude and phase throughout the system, however these have been small in amplitude during the course of the monitoring period. Problems with large oscillations at low frequency tend to occur in systems that are already low inertia [7], [8], or have a large proportion of hydro generation providing frequency control [11]. Although there is not a current problem in GB relating to very low frequency oscillations, it is important to monitor this frequency range as the inertia reduces and new forms of frequency response services are commissioned.

In addition to the issues described in this paper, a wide range of other modes of oscillation have been observed at different frequencies and locations in the grid. These tend to be small, but can be poorly damped. Not all are electromechanical modes, and some oscillations vary in frequency, or appear as non-sinusoidal periodic forcing (potentially power electronic controls). Some issues appear to be related to dynamics of windfarms. Oscillation performance data are reviewed and documented, and issues of particular concern are highlighted. In [9], [10] a nonlinear parameter estimator is presented and applied for monitoring inter-area oscillations in GB network, confirming results of the above mentioned studies.

Sub-Synchronous Oscillations, 4-46Hz (SSO)

In order to relieve the stability constraint on southwards power flow across the Scotland-England boundary, series compensation has been added to the transmission circuits in this boundary. Also, a subsea HVDC link is being commissioned in parallel with the AC corridor. The potential for sub-synchronous resonance between series compensation and torsional modes in long-shaft generators is well known, and is an identified risk in this case as there are nuclear and thermal power stations in the area. This has been mitigated by extensive study, series compensation design, and protection installation conducted prior to the commissioning of the new series compensation. However, there are less defined risks relating to other interactions between any elements of windfarms, HVDC controls, series compensation and long-shaft generator torsional oscillations, which can occur in unusual network topology.

Since these higher frequency oscillations and interactions can occur at any frequency up to the nominal synchronous frequency, the process of acquiring the data is different from standard synchrophasor measurements. Synchronised phasor measurements are typically derived using a data window with duration of a few cycles of the nominal frequency. Even if performed at a high update rate, this measurement process filters out higher frequency components and synchrophasor measurements, even if produced at a high data rate, will tend not to accurately reproduce dynamics above about 10Hz.

The approach taken in the GB system is for a new measurement function to produce filtered and downsampled voltage, or current waveforms, as well as analogue (rotor speed) measurements at a 200Hz update rate. By design, this process retains an accurate frequency bandwidth up to about 80Hz. The 200Hz data (i.e. samples of original voltages and currents) is streamed as "analogue" type measurements using the same communication protocol as synchrophasor data (the IEEE C37.118 standard). The 200Hz update rate used is faster than typical IEEE C37.118 data streams, but is fully in line with the standard.

The SSO data is integrated into the existing wide area monitoring system, and is analysed, presented and alarmed at a central WAMS server. A new software module enables system-wide comparisons across voltage, current and generator rotor speed measurements, where available. The application allows for direct comparison between oscillation frequencies observed in the mechanical domain, and the complement of the mode frequency (50-f_i) which is seen in the electrical measurements.

The results from the monitoring period so far show that expected generator torsional modes are observable in the network voltage and current signals, as well as showing other high frequency oscillations (see Figure 3). The monitoring system has already been extensively used in the course of commissioning series compensation, in the initial live system tests, and in subsequent network operations and tests. The oscillations observed in this frequency range have been small, and no significant problem has emerged. The observations to date have enabled alarm thresholds to be configured around a baseline of normal behaviour, so that any excursions of behaviour with raised amplitude and poor damping can be flagged in real-time and for post-event analysis.

One observation of interest is a mode around 10-15Hz seen across South/Central Scotland and North England, that appears strongest in the west of Scotland (Figure 3, leftmost peak). This mode is not a generator torsional oscillation, and is present independently of the status of the series compensation. The mode varies in frequency and amplitude, with larger amplitude tending to occur at the lower end of its frequency range, which is relatively close to a generator torsional mode. The variations in amplitude may indicate some degree of interaction between them, although it is noted that the amplitudes are small throughout the period of monitoring.
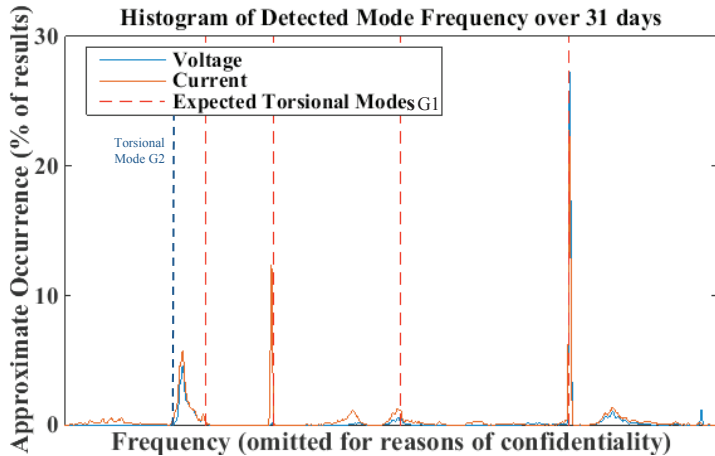

Figure 3 SSO frequencies observed at one location in the GB system. Expected torsional modes of generators are shown as dashed lines

System Disturbance and Islanding Monitoring

Accurately synchronised measurements of voltage phasors and frequency can be used to identify the location and impact of disturbances in the system. It is useful from both operational and post-event analysis perspectives to have a rapid view of a disturbance that captures the geographic area where the event was triggered, and presents the disturbance as a single system event. By contrast, a SCADA/EMS view is generally related to the individual components, and a single disturbance will appear as a number of events and violations that are not normally synchronised. A large event can produce a flood of alarms that can be difficult to assimilate quickly. Furthermore, a phasor-based view can provide a summary picture of a disturbance throughout the system with sparse measurements. In particular, a limited non-confidential set of voltage phasors from external networks can provide a high level perspective which the SCADA/EMS system does not cover, thus providing a wider context of system condition to guide restorative action.

A view of network disturbances is extracted from the fast, synchronised phasor information of the system's response to the disturbance. Sudden loss of generation or load will lead to a rapid change in voltage phase angle close to the loss. This angle shift will take time to propagate through the network due to the effect of inertial generation and loads, and therefore the measurement point closest to the trigger will show the earliest movement. The extent of angle and frequency movement is an indication of the impact of the event on the system, and will also show cases where multiple events occur. This information on disturbances is useful both in real-time operations and in review and analysis of disturbance events and system performance.

If a disturbance progresses to an out-of-step condition or islanding, this is clearly seen in a fast-update geographic view of the system. This approach has several benefits over conventional EMS-based islanding tools, including:
1. Independence from SCADA-based topology
2. Identifies out-of-step conditions that are not identifiable by topology
3. Displays rapid state changes induced, for example, by auto-reclosing lines
4. Displays whether the resulting islands are stable
5. Supervision of restoration, with diagnostics for failure of breakers to close or remain closed

Islanding has not been observed in the GB system over the project period, however islanding occurs more commonly in low inertia systems and may become a higher priority issue. The same application is also useful in the black start process, and may be trialled as part of GB black start capability testing. The experience gained in monitoring the dynamic performance of the grid during disturbances provides valuable input and learning for the automatically controlled disturbance response approach described later in this paper.

Area Angle Differences and Stability Constraints

The stability limit across a transmission boundary is directly related to the angle separation between the areas that are linked by the transmission corridor. In the GB system, the transmission boundary between Scotland and England is stability limited, restricted by the power transfer that the corridor can deliver without risking separation between Scotland and England in the event of a fault. The actual transfer limit varies with operational factors such as the geographic distribution of power in the centres of inertia north and south of the boundary, and the infeed of renewable generation across the corridor. In general, an increment of power infeed in the far north of Scotland has a greater effect on the angle separation (and therefore the stability limit) than the same increment close to the boundary. The angle separation is a closer representation of the physical limit than the standard practice of defining the constraint as the sum of power flow across a cut-set of lines. It is expected, therefore, that a constraint incorporating angle as a metric would result in a less conservative limit, maximising capacity [12].

Determining this angle separation metric between Scotland and England involves creating a representative "centre of angle" from a number of phasor measurements in each centre of inertia, north and south of the boundary. The operating point is expressed as power across the boundary and angle difference between these two centres of angle. Limit values can be defined through off-line contingency analysis, similar to existing practices. The margin to an insecure operating point can be read in terms of the distance from the power and/or angle boundary, and in the case of angles, an indication is given that relates the angle margin to capacity for generation increase in various geographic zones.
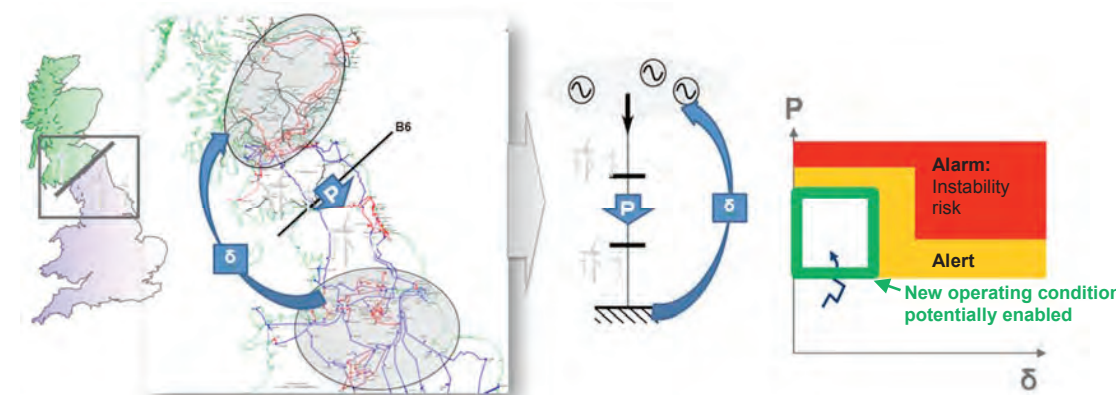

Figure 4 Power-angle representation of Scotland-England boundary stability constraint

The concept of creating an equivalent angle and frequency representing the behaviour of an area of the network is introduced in the representation of the stability limit. In the case of the Scotland-England boundary, there are two areas of inertia at each end of a constrained corridor. The approach is taken further in the following section in a control application, where the power system is represented by aggregated angle and frequency signals, each representing an area of the grid. Within the areas, it is assumed that the network is sufficiently meshed that angle differences will be relatively small and out of step operation unlikely, while there is greater angle difference between these clusters of inertia. A disturbance can be observed and identified to a particular area through the relative movements of the equivalent angle and frequency of these areas. The equivalent angle and frequency measures are created by a weighted average of measurements within the area.

3. FAST WIDE AREA FREQUENCY RESPONSE

Frequency Response and Angle Stability

In the conventional approach to system stability, the timeframes for frequency stability and angle stability have allowed the problems to be dealt with separately. Frequency stability following a loss of generation or load involved the response of governors of large central plants with high inertia. The frequency response capability was fully deployed within 10 seconds of the disturbance, which was sufficiently fast to halt a frequency decline before load shedding occurred. Angle stability is a faster phenomenon, typically involving the electromechanical first-swing response after a network fault and loss of a transmission line, for which the first second is particularly important and conventional governor/frequency response is too slow to participate. In the GB system, the key limiting first-swing stability issue is between Scotland and England, where a fault and line loss in the transmission corridor at the maximum transfer for stability results in loss of synchronism in around 1.3 seconds, as shown in the simulations from a simplified GB network model in Figure 5.

Studies carried out by National Grid indicated that the total time window available from the triggering disturbance to load shedding could reach around 2.7 seconds as early as 2021 (see Table 1). In order to ensure that resources are brought on in time for the resources to ramp to their targets and halt the frequency decline, the first actions should be initiated well before 2.7 seconds, and a response within the first half-second is targeted. This fast response should be sufficient to halt the frequency decline, or

at least to reduce the system average RoCoF such that slower more conventional resources can be effective. Increasingly, it will be important that the timescale for fast frequency response is as short as possible, with the effect that fast frequency response will interact with transient angular stability.

During the first second following a disturbance, the frequency measured at various points across the grid diverges significantly. This is illustrated in **Figure 6** for a recent frequency disturbance in the GB system, recorded by the WAMS system. This divergence of frequency is directly related to the divergence of voltage phase angles across the system, with angles close to a generation loss lagging those further away from the loss. Within this first second, it is particularly important that fast frequency response is prioritised close to the source of the frequency disturbance, otherwise the frequency response may cause the angular separation in the grid to increase further, and increase the risk of system separation [13]. If, for example, a large source of offshore generation tripped in Scotland, and was compensated in less than a second by a large infeed from an interconnector in England, it is clear that the angle separation across the transmission boundary between Scotland and England could rapidly become large and the system could separate . By contrast, if fast frequency response is targeted in Scotland near the loss of the generation, the angle movement would be reduced and stability across the boundary improved.
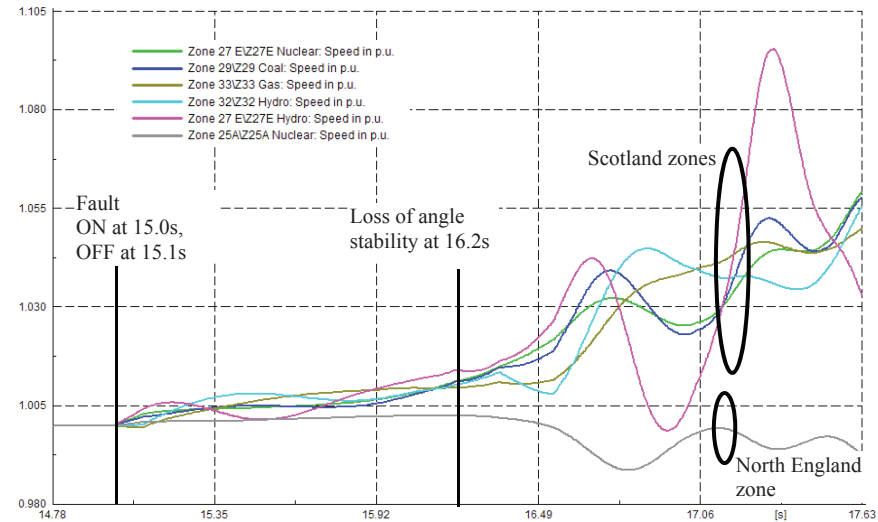

Figure 5 Simulated Example of Loss of Angle Stability across Scotland-England Corridor

Maximum RoCoF (Hz/s)	Slow Progression	Gone Green	Time (s) from disturbance to reach load-shed at 49.2Hz
0.125	2013/14	2013/14	6.4
0.2	2019/20	2018/19	4.0
0.22	2022/23	2019/20	3.6
0.25	2023/24	2020/21	3.2
0.3	2024/25	2021/22	2.7

Table 1 Increasing RoCoF and reducing time available for frequency response for different future energy scenarios [14]

The frequency excursion shown in **Figure 6Error! Reference source not found.** also illustrates the challenge of identifying that a real frequency disturbance event has occurred. From local signals only, it would not be possible to differentiate a frequency disturbance from a transient line fault within the first second, and neither local RoCoF nor local frequency is a good indicator of the size of the disturbance until much later in the event progression. Using wide area signals, it is possible to discriminate between a network event which has no net gain or loss of power, and a frequency disturbance where a response is justified. The wide area frequency signals can also be used to derive an equivalent system frequency, removing local effects, and a "system RoCoF" can be derived that is related to the size of the disturbance. Thus, wide area signals can be used to accelerate the frequency

response, target the response to a particular area, and to create a response that is proportionate to the size of the disturbance.
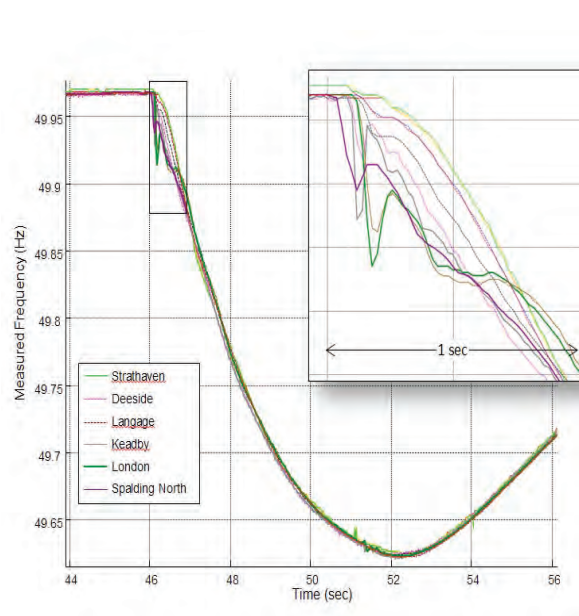

Figure 6 Frequency differences during a GB system disturbance event

Figure 7 Regional RoCoF and angle deviation in response to a disturbance

The locational emphasis of the fast frequency response is derived from the voltage phase angles and their movement during the disturbance. The angle behaviour following a disturbance based on **Error! Reference source not found.Figure 6** is illustrated in **Error! Reference source not found.Figure 7**. In **Figure 6Error! Reference source not found.**, the measurement at Spalding North showed the largest frequency decline at the start of the event. This would be observed through the angle behaviour in **Error! Reference source not found.Figure 7** with the voltage phasor angle at Spalding North lagging the most relative to the pre-event angle pattern. The overall differences in angle across the system increase, thus increasing the risk of loss of synchronism. These relative angle movements can be used to target a response close to the disturbance and inhibit response in regions which could contribute to a loss of synchronism.

Wide Area Control System for Fast Frequency Response

The wide area control scheme is implemented with synchrophasor measurements. The control scheme accelerates response in the areas close to the source of the disturbance in the system, through the use of angle behaviour across the system. It is anticipated that there are a wide range of technologies providing the service, with different unit sizes and response time characteristics, compiled to form a fast and sustained response, proportionate to the disturbance.

The structure of the control scheme is illustrated in Figure 8, and comprises the following elements:

Regional Aggregator	Aggregates multiple PMU frequency and angle signals weighted according to distribution of inertia, to produce equivalent angle and frequency signals for the centre of inertia of the region it is representing. This aggregation is robust against loss of individual PMU signals supplying it.
	Aggregated signals are supplied to all controllers participating in the wide area control mechanism.
Controllers	Control is implemented by control units that are associated with each controllable

resource. The controllers observe the wide area response of the system, detect the occurrence of a frequency disturbance event (distinguished from other network faults), identify the required response related to the overall system RoCoF, and deploy the controlled resource according to the response volume required and the influence of the disturbance. The influence relates not only to the electrical distance to the disturbance source, but also to the inertia of the surrounding area, and areas with low inertia can show significant angle movement over a large area. Resources in the regions most affected will act first, followed by those in the less affected regions.

There is an option for local controllers to act autonomously, without the wide-area input, for smaller resources where the cost of communication would not be justified. Local control acts at a later stage than wide area control.

Central Supervisor	Co-ordinates and arms the controllers that will participate in the frequency response. The Central Supervisor tracks the resource capability available in each area, and the time-response profile offered by each. It will arm the local controllers so that sufficient response will be available, and also distribute the selection across the regions. It can also change the sensitivity of the Local Controllers to events.
	The Central Supervisor is not used during the fast-response action to the disturbance. Its role is in pre-event co-ordination of the controllers, rather than real-time response.
Resources	The resources are the plants that participate in providing the response. Each will declare a capability in terms of MW capacity and time characteristic, and the availability will be tracked as the plants energy use or output changes.

Event Detection, Location and Resources Deployed

The response triggering is determined in controllers associated with the devices providing the response. These controllers are distributed around the system, and receive a number of signals broadcast from the regional aggregators corresponding to the angle and frequencies of the regions of the network. The controllers are armed using the central supervisor which co-ordinates the resources to ensure that the volume of any response will be relative to the size of the disturbance. Each controller will trigger a fast response if it is within a region highly affected by the disturbance (i.e. if the angle within its region responds faster than the system average). This difference in angle can be caused by proximity to the disturbance, or the effects of the regional inertia where lower inertia regions further from a disturbance may be more affected than higher inertia regions closer to the disturbance. This means that the fast response acts to reduce angle deviation during the first-swing response, improving the stability of the network and reducing the possible of out-of-step operation.

If a fast response is not triggered during an event, the resource may still be useful later in the progression of the event, after the fast stability response has been initiated. In this case, the response is triggered depending on the aggregated system RoCoF, and this second-stage response is not targeted to location. This second stage is designed to avoid an over-response, to correct any under-response, and to extend the response in complex disturbances with multiple events, with the target for the system frequency to reach a zero gradient.

There is also scope to incorporate local response without receiving synchronised wide area measurements. This is required both as a graceful degradation in conditions where some or all of the wide area signals are not received, or where a fast communications link is not justified.

The event detection is carried out first by combining the regional aggregator signals into a system equivalent frequency without local and regional effects, and identifying movement that shows that an event has occurred. The scheme's ability to take the local and regional effects into account is critical to

avoid incorrect control operation in response to oscillations and network fault responses. A purely local approach requires a much longer window to avoid false detection or incorrect determination of the disturbance characteristics. The mechanism uses an initial RoCoF detection with a growing window as the event proceeds, until a confident event detection can be made, differentiating from effects such as governor-frequency control oscillations. This mechanism minimises detection delay and provides faster detection for larger events compared with fixed window approaches, allowing for earlier response.

The system is designed to bring on the controlled response in proportion to the event, and to sustain the response either limited by the resource's capability, or until it is restored to normal service in a controlled way. By contrast, a local control approach that is directly proportionate to frequency and/or RoCoF would result in the response not being sustained, more spurious operations, and may introduce negative damping of oscillations.

Fast Frequency Response as a Service

In the demonstration project, the fast response resource technologies used are representative of a variety of responses to system disturbances, including:
- Solar
- Battery storage
- Conventional thermal generation that is capable of providing faster response than the present primary response requirements
- Controlled wind power response
- Controlled demand side response
- Physical inertial response

The focus of this paper is on the wide area control of resources that can be triggered, however it is recognised that there is a value to natural response such as physical inertia.

The prospective future market for fast frequency response should reflect the value of the service provided to the grid, irrespective of the specific technology. The basic principle of the future market could include a time and geographic element. The faster the response can be initiated in the vicinity of the initial disturbance, the less the overall impact of the event. The service provided should therefore be valued in inverse proportion to the time to deploy, and the proximity to the disturbance (i.e. a stability service). Both a capacity payment and deployment payment are likely to be part of the prospective market. The lessons learnt in this demonstration project will feed into the design of these future markets.
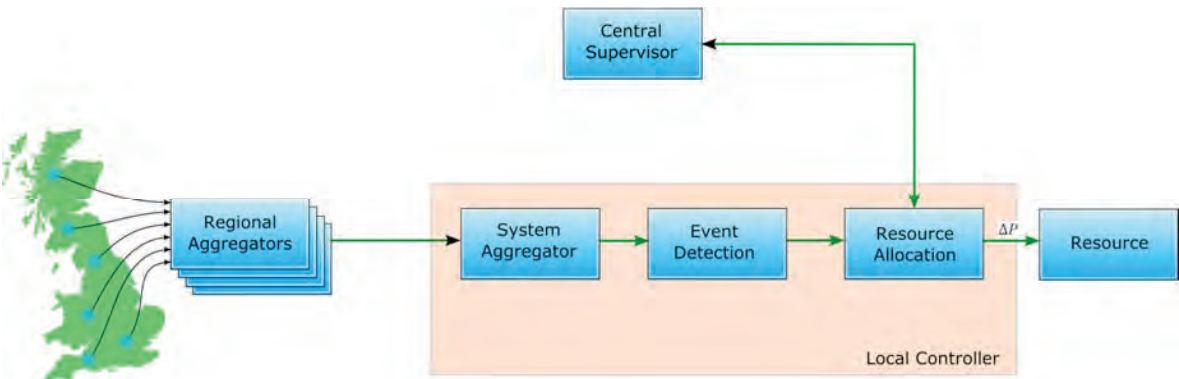

Figure 8 Structure of fast frequency response control

6. **WAMS INFRASTRUCTURE FOR MONITORING AND CONTROL**

Prior to the WAMS projects, synchrophasor measurements had been deployed by enabling a PMU function on disturbance recorders. While this is an efficient way to obtain measurements without the delays for outages to install devices, some issues were experienced with the performance of legacy equipment where synchrophasors were not an original design feature or primary requirement. Practical lessons learnt include:

- Compliance to the IEEE C37.118 (2014) standard for synchrophasor measurements is a necessary baseline for static and dynamic performance requirements
- Continuity of data with minimal gaps is important, including continuity from the PMU through the communications network to the PDC, and through different layers of PDC hierarchy. Minimising data losses improves the integrity of the dependant applications, however applications must also be robust against some inevitable loss or degradation of data.
- Options contained within the IEEE C37.118 standard must be selected for the needs of the user. For example, frequency data should be available in floating point format in the GB system rather than lower resolution integer format, otherwise the smaller oscillation information useful for locating sources may be lost. By contrast, integer phasors (rather than floating point) can be used to reduce bandwidth and storage without significant loss of information, provided polar format and suitable full-scale values are used.
- There is metadata on the signal validity, including GPS lock, defined by the IEEE C37.118 standard and communicated by PMUs. It is important that this metadata is correctly and consistently reported according to the standard, to avoid misinterpreting the data.

The requirements for use in wide area control go beyond the monitoring system requirements, and include:

- Latency requirements incorporating the time budgets for PMU calculation and data packet export, communications latency and PDC latency
- Key nodes (such as the Regional Aggregators) may require a more secure communication infrastructure than other PMU connections.
- In the frequency control application described, data from the Regional Aggregators is shared with all participating controllers, and therefore a multicast or broadcast approach is more appropriate than a point-to-point hierarchy typically used in monitoring systems.
- Cyber security is of greater importance in automated control, and IEC 61850-90-5 has improvements over IEEE C37.118 in the area of cyber security
- Handling measurement quality issues is critical to ensure continuous, reliable operation of the overall scheme with tolerance to data loss or degradation. Defining and using data quality metadata throughout the system is important.

Further technical demonstration work is planned to demonstrate that standard synchrophasor data and 200Hz data can be derived from IEC 61850-9-2 process bus data. Also, the infrastructure for flexible wide area control will be demonstrated in an IEC 61850 substation environment.

7. CONCLUSION

There is a clear need in the GB power system to make more extensive use of synchrophasor monitoring to manage the changing performance of the grid as inertia reduces and the generation profile changes. Significant progress has been made in deploying the technology and using it in off-line review and analysis, with a view to introducing it for real-time applications. Through the results so far, new insights in system performance have been gained, and the value of the technology has been demonstrated. Deployment challenges have been encountered, and lessons learnt for future development of the infrastructure.

In terms of system monitoring, it is recognised that the applications available to the users must provide the necessary guidance to define a course of action, whether in real-time or in longer-term control improvements. For this reason, there has been an emphasis on identifying sources of oscillations and

disturbances, and a geographic view of the impact, that leads to a directed response rather than a general identification of issues.

The synchrophasor view of disturbances has been valuable in designing a control approach for fast frequency response. The deviations of frequency and angle throughout the system, particularly during the first second following the disturbance, are of interest for defining the mechanism for fast frequency response, and justify the need for wide area control. The wide area frequency control demonstration is intended to prove that wide area control is justified and necessary in order to respond to disturbances in the timeframe required in the low inertia future, and that it is feasible using infrastructure and technology available now or in the near future.

BIBLIOGRAPHY

[1]   National Grid "System Operability Framework 2015", http://www2.nationalgrid.com/UK/ Industry-information/Future-of-Energy/System-Operability-Framework/

[2]   D.Cai, P.Wall, M.Osborne, V.Terzija, "A Roadmap for the Deployment of WAMPAC in the Future GB Power System", IET Generation, Transmission & Distribution; early access paper, IEEEXplore.

[3]   VISualisation Of Real-time dynamics (VISOR), http://visor-project.org.uk/

[4]   SMART Frequency Control (SFC, previously EFCC), http://www.nationalgridconnecting.com/The_balance_of_power/

[5]   V.Terzija, G.Valverde, D.Cai, P.Regulski, V.Madani, J.Fitch, S.Skok, M.Begovic, A.Phadke, "Wide Area Monitoring, Protection and Control of Future Electric Power Networks", Proceedings of IEEE, Volume: 99, Issue: 1, pp 80-93, 2011.

[6]   N. Al-Ashwal, D. Wilson, and M. Parashar, "Identifying sources of oscillations using wide area measurements" (Grid of the Future Symposium, CIGRE US National Committee, 2014)

[7]   Ciarán Geaney "How measured data is being used to help Operate the transmission network" (CIGRÉ Training Day, Dublin, 2nd December 2015, pages 13-14)

[8]   Nils Gústavsson "Using PMUs in Iceland" (NASPI Work Group Meeting, Bellvue, Washington, June 2008)

[9]   D.Cai, P.Regulski, M.Osborne, V.Terzija, "Wide Area Inter-area Oscillation Monitoring Using Fast Nonlinear Estimation Algorithm", IEEE Trans. on Smart Grid, Volume: 4, Issue: 3, 2013, pp. 1721-1731

[10] V.Terzija, D.Cai, V.Stanojevic, G.Strbac, "Frequency and Power Components Estimation from Instantaneous Power Signal", IEEE Transaction on Instrumentation and Measurement, Volume: 60, Issue: 11, pp 3640-3649, 2010

[11] O. J. Arango, H. M. Sanchez, D.H. Wilson "Low Frequency Oscillations in the Colombian Power System – Identification and Remedial Actions", CIGRE Session, Paris, August 2010

[12] D. Wang, D. H. Wilson and S. Clark: "Defining Constraint Thresholds by Angles in a Stability Constrained Corridor with High Wind", IEEE T&D, Chicago, April 2014

[13] V.V. Terzija, "Adaptive Underfrequency Load Shedding Based on the Magnitude of the Disturbance Estimation", IEEE Transactions on Power Systems, Vol. 21, No. 3, August 2006, Page(s): 1260- 1266.

[14] National Grid UK "Enhanced Frequency Control Capability (EFCC)" Electricity Network Innovation Competition Full Submission, October 2014, http://www.smarternetworks.org/

Novel Sub-Synchronous Oscillation Early Warning System for the GB Grid

S. L. Zimath	D. Wilson	M. Agostini	R. Giovanini	S. Clark
Alstom	**Alstom**	**Alstom**	**Alstom**	**Alstom**
Brazil	**UK**	**Brazil**	**UK**	**UK**

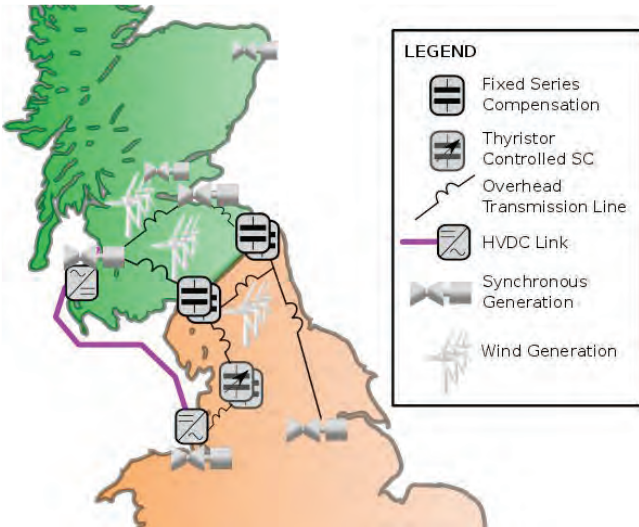**sergio.zimath@alstom.com**

Summary

Figure 1: Series Compensation, Generation and Power Electronic Converters around the Scotland-England Transmission Boundary

Renewable energy supply is rapidly increasing in the Great Britain (GB) power system, leading to greater power transfer from high wind resource areas in Scotland to the load centres in the south. To relieve constraints to this southwards flow, series compensation is being installed in the transmission path, and a subsea High Voltage Direct Current (HVDC) link is being installed. This increases the boundary capability substantially, but introduces the risk of sub-synchronous resonances of various forms that need to be managed.

Series compensation introduces new natural frequencies of oscillation that can in certain circumstances interact with thermal generation, HVDC links and renewable generation. In addition, there is potential for interaction of HVDC link & wind farm converter control systems with thermal generation. While studies, planning and design, filters and protection systems reduce the risk of occurrence and damage from this resonance effect, monitoring will also form a key element in overall risk mitigation strategy. A novel monitoring approach is taken to improve understanding of interactions that do not immediately lead to protection action or large-scale disturbances, and that enables a new risk management approach.

This paper describes a system commissioned in 2015, under a partnership led by Scottish Power [1], the transmission owner in Central and Southern Scotland, for the detection and monitoring of sub-synchronous oscillations. The system will provide early warning of oscillations in real-time operational timescales, and facilitate off-line analysis of system behaviour related to interaction between the series compensation, HVDC systems and nearby generation units. The commissioning of this system coincides with the installation of series compensation at six locations on the Scotland-England transmission boundary, as well as the new, parallel, Western HVDC link from Scotland to North Wales.

The sub-synchronous oscillation detection system is composed of data acquisition devices at several locations, and a central server that receives, collates, stores and processes the measurement data in real-time. This central server performs the sub-synchronous oscillation analysis, detects abnormal behaviour such as raised amplitude or poor damping of an SSO mode at one or more monitored locations, and raises alarms to the Grid Control Room. Operational actions can then be taken, such as bypassing of the series capacitors.

A challenge in this project was the need for a standard data acquisition approach, with sufficient bandwidth to capture oscillations of up to 46Hz. Existing wide-area monitoring systems using Phasor Measurement Units (PMUs) reporting via the IEEE C37.118 protocol at 50 or 60 samples/second do not achieve this bandwidth, and it is not possible to achieve fast enough response with synchrophasors without degrading the accuracy. The solution uses a traditional PMU hardware, adapted to transmit a supplementary data stream of direct voltage & current waveform samples at 200 fps via the IEEE C37.118 protocol. The device has been termed a Waveform Measurement Unit (WMU). In addition, the system has the capability to record rotor speed signals synchronously with waveform data, in order to observe torsional oscillations together with network oscillations. This solution, using a measurement rate of 4 samples per cycle, provides sufficient bandwidth to capture SSO phenomena, whilst using a standard and widely-adopted transmission protocol. The approach could also be upgraded to higher sampling rates if needed.

Keywords

Sub-Synchronous Resonance, Sub-Synchronous Oscillations, Torsional Interaction, Control Interaction, Series Compensation, HVDC, Waveform Measurement Unit, WMU, Oscillation monitoring, VISOR Project

1. Introduction

The use of technologies such as High-Voltage Direct Current (HVDC) links and series compensation of transmission lines presents an attractive alternative to the construction of additional overhead transmission lines – which is made increasingly difficult by public opposition and civic planning approval processes. This approach does however raise new challenges. These are not only in protection when considering fault scenarios, but also in steady state and post-fault operation – with the potential for Sub-Synchronous Oscillations (SSO) [4-5]. These oscillations fall into three main categories [6]:

- **Sub-Synchronous Resonance** (SSR)**:** probably the most well-documented form, this involves interaction between generator shaft torsional modes and electrical resonances created by series capacitors and network impedance.

- **Sub-Synchronous Control Interaction** (SSCI)**:** interaction of power electronic converters, such as HVDC links and doubly-fed wind turbines, with electrical resonances created by series capacitors and network impedance.

- **Sub-Synchronous Torsional Interaction** (SSTI)**:** interaction of power electronic converters with generator shaft torsional modes.

With the installation of series compensation and power electronic converters, several measures are taken including studies, planning and design, and implementation of filters and protection systems to reduce the risk of occurrence and damage from these oscillations. However, a key requirement remains for a monitoring approach that will:

- Characterise power system behaviour pre- and post-commissioning, serving to validate study conclusions and planning & design models

- Aid in the commissioning of protective plant

- Provide early warning of oscillations in operational timescales, prior to the triggering of protection equipment.

- Highlight underlying low-level oscillations that do not trigger protective action but may cause undue plant wear, or may escalate to more serious levels following a system event.

By improving knowledge of SSO behaviour and providing Control Room situational awareness of SSO, operation action can be taken to address interaction before plants are at risk of damage. Since the power plants most exposed to SSO are large nuclear and thermal units, the potential benefit is significant.

2. Challenges Associated with SSO Monitoring

Traditional Phasor Measurement Unit (PMU) based Wide Area Monitoring Systems (WAMS) utilise synchronised phasor measurements transmitted via the IEEE C37.118 protocol at up to 50 / 60 samples per second – once per cycle. The bandwidth defined by the C37.118 standard in its 2014 revision is defined as $F_s/5$, typically 10Hz for a 50Hz system – this is influenced by:

- The need to ensure adequate attenuation of aliased components means that filter roll-off must begin lower than the theoretical 25/30 Hz Nyquist limit.

- The window length employed in the phasor calculation process – a typical window spans multiple 50/60 Hz cycles to achieve greater phasor accuracy at the cost of attenuating higher frequencies. Reducing the calculation window increases bandwidth but reduces accuracy. Thus, reducing the window for synchrophasor calculation introduces spurious errors and noise.

These factors lead to a practical observable range of up to about 10 Hz, which is sufficient to capture governor-mode and electromechanical oscillations along with some voltage control modes. With the proliferation of PMUs, wide-area monitoring of such oscillations has been implemented in many utilities across the world [7].

A further challenge emerged from the need to differentiate generator shaft torsional oscillations, which appear in grid electrical measurements as sidebands at $f_{grid} \pm f_{mechanical}$, from electrical-only oscillations such as voltage control modes.

In order to extend this visibility up to the 4-46 Hz range required for observability of sub-synchronous oscillations in the GB use case, an approach utilising direct waveform measurements at 200 samples/cycle was taken. This approach served to provide a true representation of oscillatory components in the 4-46 Hz range, whilst providing visibility of the 54-96 Hz range so as to differentiate generator torsional oscillations from electrical resonances.

3. Waveform Measurement Unit (WMU)

In this work it was developed a new data acquisition approach based on a traditional PMU. It was implemented a special algorithm in a commercial PMU device, that can send the waveform

samples using the analog values of the IEEE C37.118.2-2011 protocol. The device has been termed a Waveform Measurement Unit, or WMU. The WMU architecture is shown in Figure 2.
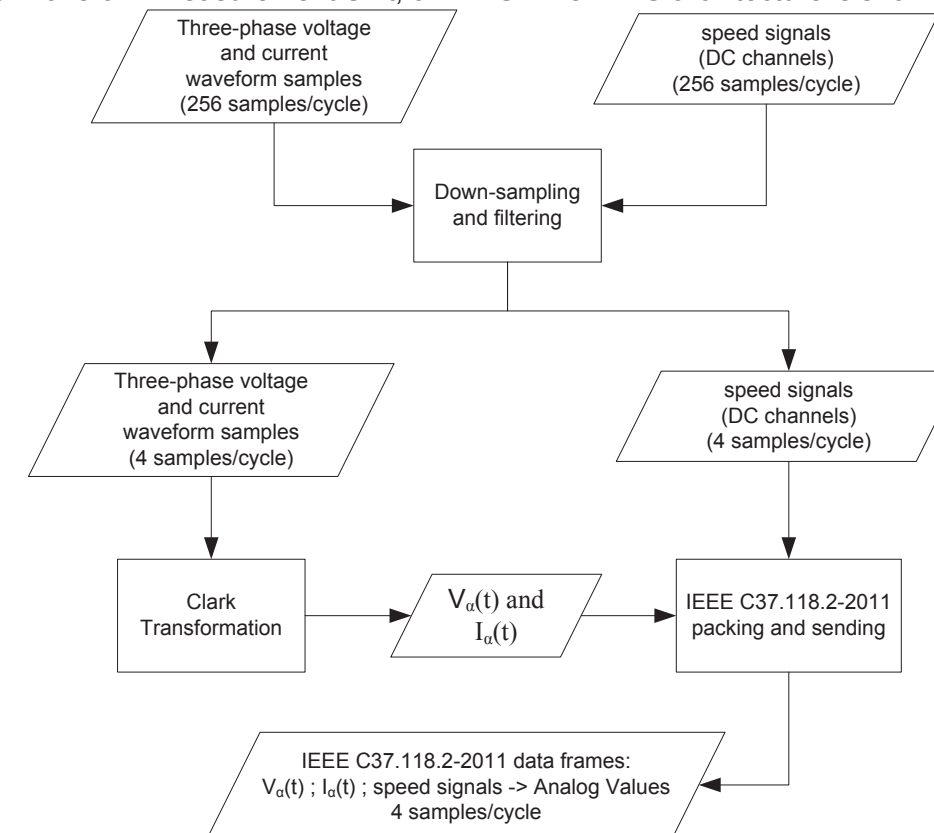

Figure 2 – WMU Architecture

The WMU measures three-phase voltage & current signals, as well as generator speed measurements. These speed measurements can be derived from shaft-mounted toothed wheel or encoded tape transducers feeding an external pulse train counter, with the output acquired at 0-20 mA / 10 V DC transducer inputs.

The primary data acquisition rate of the device is 256 samples per cycle. All signals (voltage, current & speed) are then filtered and down-sampled to 4 samples per cycle, equivalent to 200 fps in a 50 Hz electrical system. The filter used is an 8th order Butterworth low pass filter, with cut-off at 80 Hz. This ensures sufficient attenuation of aliased components above 100 Hz, and attenuation of 3rd Harmonic and above greater than 43 dB.

For each three-phase set of downsampled voltage / current waveform signals, a single phase equivalent value is then derived from the individual phase measurements that are valid and available. A Clarke (or α-β-0) Transformation is used, described in (01) below. This is a space vector transformation of time-domain signals (e.g. voltage, current, etc.) from a natural three-phase coordinate system (a-b-c) into a stationary two-phase reference frame (α-β-0).

$$\begin{bmatrix} X_\alpha \\ X_\beta \\ X_0 \end{bmatrix} = \frac{1}{3}\begin{bmatrix} 2 & -1 & -1 \\ 0 & \sqrt{3} & -\sqrt{3} \\ 1 & 1 & 1 \end{bmatrix} \cdot \begin{bmatrix} X_a \\ X_b \\ X_c \end{bmatrix} \tag{01}$$

where:
X_a ; X_b ; X_c → threee-phase components (voltages or currents, real or complex numbers)
X_α ; X_β ; X_0 → α-β-0 components (voltages or currents, real or complex numbers)

In this way, within the WMU algorithm time-domain voltage and current waveform samples (real numbers) are used to calculate single values $v_{\alpha\beta0}(t)$ and $i_{\alpha\beta0}(t)$.

All the signals (voltage and current waveforms, and speed signals) are then encapsulated in a 200 fps standard IEEE C37.118 data stream as "analog" type values, in floating-point format. Synchrophasors are not included in the WMU stream. The STAT bits and Time Quality flags in the FRACSEC value are used to properly reflect the status of the device, in the same way as they do for the traditional PMU function.

The data frames are sent to the PDC (with the SSO detection algorithm) at a rate of 4 frames per cycle (200 Hz at a 50 Hz electrical system), over the UDP protocol. It should be noted that this use of a higher sample rate of 200 fps is fully compliant with the C37.118 standard, and is in fact encouraged [3]

The WMU new function has been implemented in the device without effects on the traditional PMU function. The device can send both IEEE C37.118 data streams at the same time, with different rates.

4. Central Wide-Area Monitoring System (WAMS) Server

The incoming data streams from multiple sites, containing 200 fps voltage, current & speed waveform samples, are collated, processed and stored on a central WAMS server. Here, the 200 fps waveforms are analysed, with the amplitude, frequency & damping of sub-synchronous oscillatory modes in the 4-46 Hz range extracted. This information is then presented to users in a wide-area view, with analysis results stored for historical review and wider analysis (such as model validation studies). Visibility of the 54-96 Hz range is also provided to enable users to differentiate between mechanical and electrical modes.

Normally, the real-time view will show non-resonant oscillations, such as the electrical resonant frequencies from series capacitor and line inductance, generator torsional modes, and independent control modes. This expected behaviour is useful for longer term analysis of the variability of these effects and for model validation.

If however there is interaction between natural frequencies involving different plants across the network, this is an early warning that implies a risk of escalation in the present event, or an indication that a future event may be more serious. This represents a departure from previous approaches, where only severe resonance effects are captured and analysed. In this development, the users can learn from experience of events that do not create a major disturbance. Also, resonance is quite likely to occur first as a smaller scale event and grow as system conditions vary, thus providing an opportunity to respond in real-time to avoid tripping events.

5. Conclusions

The proposed solution to measure voltage and current to SSO monitoring is based on a standardized wide-area monitoring approach, employing the existing IEEE C37.118 protocol which is already deployed across many utilities worldwide. It extends existing practices of wide-area oscillatory stability monitoring to the sub-synchronous oscillation range, providing valuable validation and risk mitigation around the issues associated with increasing use of Flexible AC Transmission plant, power electronics technologies and non-synchronous generation.

Bibliography

[1] VISOR Project (www.visor-project.org.uk)

[2] IEC/IEEE 60255-118-1 Ed. 1 MEASURING RELAYS AND PROTECTION EQUIPMENT Part 118-1: Synchrophasor for power systems – Measurements – Draft

[3] IEEE C37.118.1-2011 - IEEE Standard for Synchrophasor Measurements for Power Systems

[4] A. Mulawarman; P. Mysore "Detection of Undamped Sub-Synchronous Oscillations of Wind Generators with Series Compensated Lines" (Minnesota Power Systems Conference, 2011)

[5] North American Electric Reliability Council "Lesson Learned - Sub-Synchronous Interaction between Series-Compensated Transmission Lines and Generation" (2011)

[6] T. Ackerman, R Kuwahata "Lessons Learned from International Wind Integration Studies" (AEMO Wind Integration WP4(A), 2011)

[7] "Identification of Electromechanical Modes in Power Systems" (IEEE Task Force Report, Special Publication TP462, IEEE Power and Energy Society, 2012)

GE
Grid Solutions

VISOR Project

Justification of 200fps Waveforms for Visibility of SSO

12/04/2016

GE-VISOR-R20160406-Justification of 200fps Waveforms for Visibility of SSO-v1.docx

Authors: Dr Natheer Al-Ashwal, Dr Douglas Wilson, Stuart Clark

GE
Grid Solutions

Summary

Prior to the VISOR Project, research was carried out by GE's Grid Solutions on the best approach to determine a measurement quantity suitable for wide-area observability and co-ordinated analysis of Sub-Synchronous Oscillations (SSO), that:

- Would accurately represent Sub-Synchronous Oscillation (SSO) content in its original quantity (e.g. a voltage waveform on the transmission network), and

- Could be communicated in a practical manner and in real time between an acquisition unit (e.g. PMU) and a central Wide-Area Monitoring System (WAMS) server, given that bandwidth may be restricted.

The research investigated what form of data was best suited, comparing downsampled waveform data with true RMS and fundamental RMS. The research suggested that downsampled waveform data best replicated the signal characteristics of interest and avoided potential signal processing problems.

Background

Sub-Synchronous Oscillations

The purpose of the SSO monitoring is to observe the natural frequencies of oscillation and interactions between devices connected in the network, as illustrated in Figure 1. The measurement process is intended to capture behaviour that allows interpretation of the issues observed. The following categories of behaviour can be observed in the grid:

1. **Frequency modulation**
   The grid fundamental frequency near 50/60Hz is modulated at an SSO frequency. A **generator shaft torsional oscillation** will appear as frequency modulation.

2. **Amplitude modulation**
   The magnitude of the 50/60Hz grid fundamental waveform is modulated, while the frequency remains steady. Fast acting **power electronic control** can modulate the magnitude of voltage.

3. **Added oscillation**
   An independent frequency component can be observed, summed with the fundamental component. A **network inductor-capacitor (LC) oscillation** is an added oscillation.

It is critical that the phenomena of interest are captured by the measurement process, and that the most appropriate signal choice and signal processing are used to capture interactions between the network and connected plant. It is also useful to preserve key characteristics of the SSO phenomena in order to interpret them correctly.
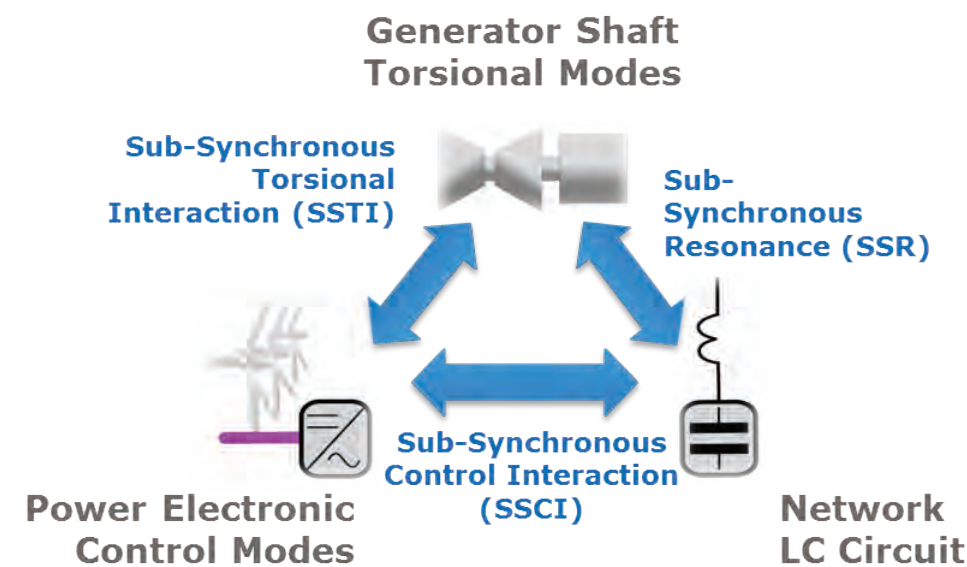
Figure 1 Sub-Synchronous Oscillation Interactions

Sub-synchronous oscillations in generator torque and speed are seen in voltage and current waveforms as modulation in amplitude and frequency. Thus, a speed oscillation with a frequency F_O is seen in electrical waveforms as two frequency components at 50-F_O and 50+F_O.

Other sub-synchronous oscillations may present as added oscillations – for example electrical modes due to LC circuits, which involve one added frequency component at $\frac{1}{2\pi\sqrt{LC}}$.

Whilst the focus of real-time oscillation monitoring will be on sub-synchronous components (4-46Hz), visibility of super-synchronous components (54-96Hz) is of diagnostic value during manual analysis, providing the ability to distinguish added oscillations from modulations.

RMS & Phasor Calculation

The process of deriving phasor measurements or RMS values demodulates the waveform, and therefore gives the frequency of any amplitude oscillations. However, the results may be misleading if the oscillations present are not amplitude modulations but include added components.

Furthermore, RMS and phasor values are by necessity derived over a time window, which can range from a half-cycle (10/8ms) to multiple cycles. The choice of window length will have an effect on accuracy and on the degree to which higher frequencies, which may include the SSO range, are attenuated. In addition, the calculation of phasor amplitude and fundamental RMS are designed to focus on the fundamental 50Hz component of a waveform and thus will attenuate both higher and lower added frequencies.

GE
Grid Solutions

Investigation

Some examples are given below comparing waveform and RMS data, both at 200 Hz. The RMS data is taken from half a cycle and updated every quarter of a cycle.

Example 1: Amplitude Modulation

Figure 2 shows Fast Fourier Transform (FFT) analysis of a waveform with an amplitude modulation at 20 Hz. The waveform analysis gives two frequency components at 30 and 70 Hz, while the RMS has two components at 20 and 80 Hz. The waveform analysis can easily be interpreted as a modulation at 30Hz, while the RMS results could be interpreted as an addition of 30Hz which is demodulated by calculating RMS, or a modulation at 30Hz. Thus, the analyst would not be able to distinguish whether the mode was a torsional oscillation or other control-related modulation, or a network LC oscillation (addition).
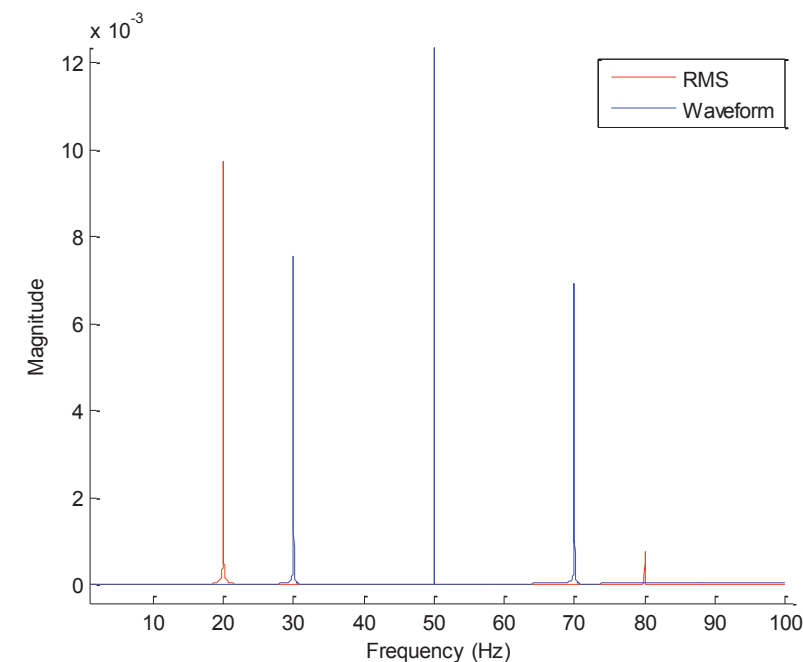

Figure 2 FFT analysis of RMS and waveform signals for an Amplitude Modulation

Example 2: Added Sub-synchronous Oscillation

Figure 3 shows FFT analysis of a waveform with an added 30 Hz component. The RMS FFT analysis is similar to the previous case with 20 Hz and 80 Hz components, while the waveform only contains a 30 Hz component. The waveform contains information that clearly shows that the mode is an addition, rather than a modulation.
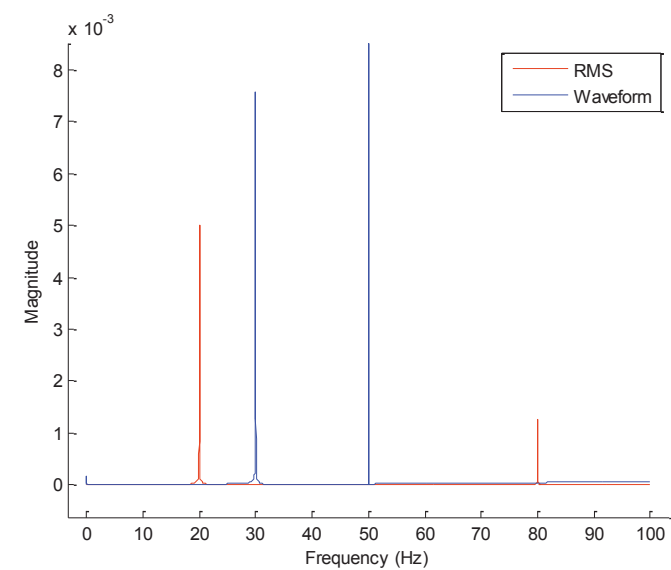
GE
Grid Solutions

Figure 3 FFT analysis of RMS and waveform signals with an added sub-synchronous oscillation

Example 3: Added Super-synchronous Oscillation

Figure 4 shows FFT analysis with a 70 Hz component in the waveform, while the RMS component has two components at 20 Hz and 80 Hz.
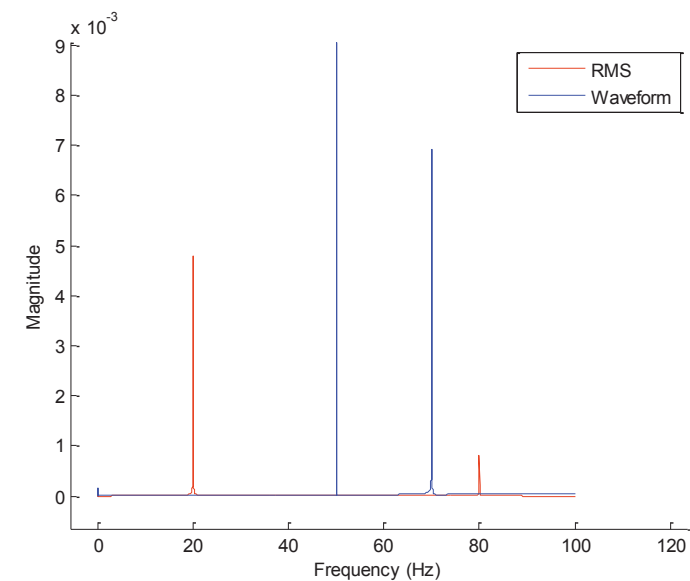

Figure 4 FFT analysis of RMS and waveform signals with an added super-synchronous oscillation

Analysis of Examples 1-3

The frequency content of the RMS signal is very similar for the first three scenarios presented – a modulation, an added sub-synchronous component and an added super-synchronous

GE
Grid Solutions

component. The waveform signal on the other hand enables the three cases to be distinguished from one another.

To avoid cases where a super-synchronous oscillation is reported as a sub-synchronous oscillation, a low-pass filter could be applied before the RMS process to remove content >55Hz. However, this could result in attenuation of frequency components in the 4-45 Hz band and of the 50 Hz component. In the case of waveform signals, the low pass filter can have a corner frequency of 80-90 Hz, avoiding attenuation of the frequency band of interest.

Example 4: Frequency Modulation

In the case of a frequency modulation rather than an amplitude modulation, the oscillation may not be observable from the RMS value which only represents the amplitude of the waveform. Figure 5 shows FFT analysis of a signal with frequency modulation at 10 Hz. The waveform signal has two components at 40 and 60 Hz, while the RMS signal has much smaller components at 10 and 90 Hz. This is expected as the amplitude is not varying and the RMS would ideally be constant. To detect such oscillations, it would be required to measure the angle in addition to the magnitude. This means doubling the amount of communication, storage and computation to take into account the magnitude and angle of each signal.
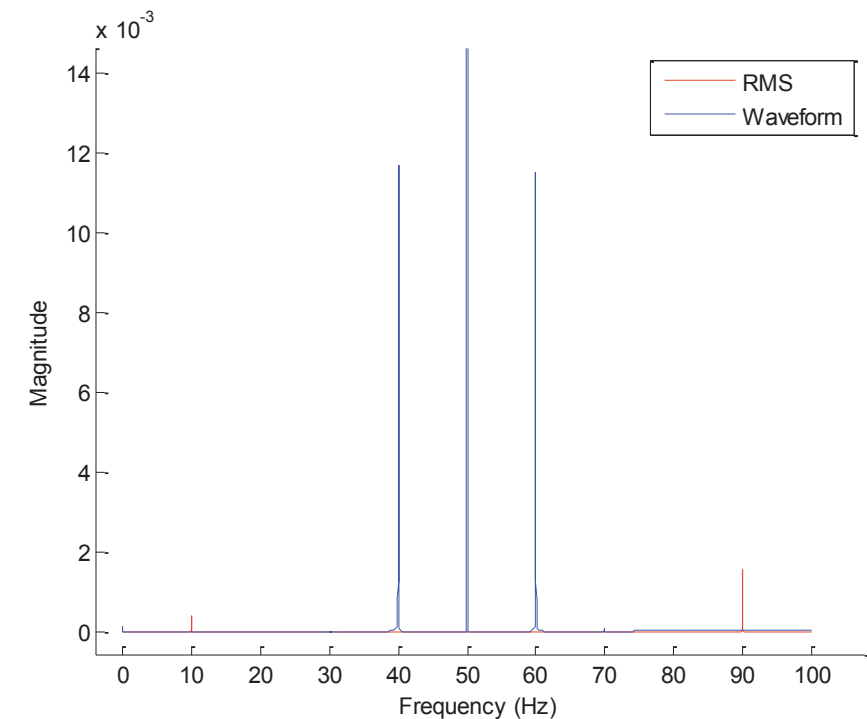

Figure 5 FFT analysis of RMS and waveform signals with Frequency Modulation

GE
Grid Solutions

Conclusions

Taking the RMS of voltage and current waveforms leads to loss of information about the frequency content. In comparison, the waveform signal provides more information for the same transmission bandwidth and storage requirements:

- Distinguishing between different cases of added and amplitude modulating oscillations where RMS measurement does not.

- Providing visibility of frequency modulating oscillations where RMS measurement does not.

It may be noted that generator shaft torsional oscillations are predominantly seen in the electrical network as frequency modulation, and may not always be seen as RMS amplitude modulation. Therefore, situations may arise where a generator shaft torsional oscillation may be propagating into the electrical system, but would not be observable in RMS values.

The derivation of 200fps waveform data is relatively straightforward, involving application of anti-aliasing filtering followed by downsampling to a 200fps sample rate. This simplicity lends itself to achieving a consistent performance across multiple device vendors and models. By contrast, derivation of RMS or phasor information involves the additional steps of spectral analysis and/or RMS calculation, and factors such as choice of calculation window length will produce variations in performance across different devices.

The simplicity of the 200fps measurement process means that the acquisition process is easily specified for implementation in hardware, and a standard filter design can be applied. Thus, the core measurement process is easily standardised. Defining and achieving a standard dynamic response using RMS or fast-phasor measurement would be much more challenging.

Therefore, while RMS or phasor measurements can be adapted to show SSO phenomena, the investigation carried out suggests that 200fps waveforms are a more practical and effective choice, with greater consistency between measurement sources, retaining key information for interpretation of the SSO issues.

Monitoring Subsynchronous Oscillations in Power Systems using Synchronised Measurement Technology

P. WALL, P. DATTARAY, A. NECHIFOR and V. TERZIJA
The University of Manchester
United Kingdom
peter.wall@manchester.ac.uk

Summary

This paper studies the performance of several commercial PMUs and a fault recorder when used to monitor Subsynchronous Oscillations (SSO) in a laboratory. An Omicron CMC256 is used to inject signals into these devices, the outputs are captured using a data concentrator and analysed in Matlab. The study uses constructed signals (Matlab) to understand the behaviour of each device for specific conditions. The ability of each device to accurately monitor SSO and the extent to which out of band SSO will degrade the performance of a PMU is studied.

The monitoring of SSO is relevant because Series Compensation (SC) is a cost effective tool for increasing the capacity of existing transmission networks but introduces the risk of Subsynchronous Resonance (SSR) that can cause significant damage to generating plant. Whilst Thyristor Controlled Series Compensation (TCSC) has been shown to be SSR neutral, the increasing levels of power electronics (PE) in power systems increases the risk of Subsynchronous Interactions (SSI). These interactions may require a redefinition of SSR, as PE lacks the distinguishable torsional modes that exist for turbine-generator shafts. Therefore, using traditional, electromagnetic offline studies to address these new forms of SSR may prove challenging and time consuming, in the absence of the well-established benchmark models, theory and experience that exists for classical SSR.

Using Wide Area Monitoring Systems (WAMS), based on Synchronized Measurement Technology (e.g. PMUs), for the online monitoring of SSO could create a valuable tool for the real time detection of dangerous oscillations that does not require extensive offline studies, new models or system/device data. However, developing such a tool would require a full understanding of the response of sensors in the presence of SSO and prior to its practical deployment the vulnerabilities of a measurement based solution would need to be considered, e.g. guaranteeing sufficient observability.

Phasor Measurement Units (PMUs) form the basis of WAMS and typically have a maximum reporting rate of once per cycle (50/60 Hz), so the theoretical limit on the highest frequency SSO they can accurately report is 25/30 Hz. Whilst this limits the ability of a PMU to report the full range of SSO, a more critical issue is that the accuracy of the PMU could be compromised if it fails to reject out-of-band signals. This may pose a challenge for modern power systems, as many utilities are increasingly using WAMS based solutions to improve system operation. Whilst the C37.118.1a-2014 standard does provide requirements for the rejection of SSO, WAMS installation is a long term process; so, many PMUs may not comply with the most recent standards. Devices with a higher reporting rate can be used to capture the full range of SSO. This study includes a synchronised fault recorder that reports waveform samples at a rate of 200 Hz.

Keywords

Fault Recorder, Phasor Measurement Units, Subsynchronous Oscillations, Subsynchronous Resonance, Synchronised Measurement Technology, WAMPAC, Wide Area Monitoring

1. Introduction

Synchronised Measurement Technology (SMT) uses high accuracy time stamps from Global Navigational Satellite Systems (GNSS) and/or local clocks to produce accurate measurements of power system signals (including direct measurement of phase angles) that can, with suitable communication and computing resources, be collected from across a wide area power system and synchronised into a single record [1]. These time stamped records are created by a Wide Area Monitoring System (WAMS) and can be used to create a range of powerful new tools for improving the efficiency and security of power system operation [2]. These tools may include visualisations that provide operators with an accurate, real-time view of how close the system is to its stability limits or, more ambitiously, could include closed loop control or even protection as part of Wide Area Monitoring, Protection and Control (WAMPAC) [3].

Phasor Measurement Units (PMUs) are presently the most widespread synchronised measurement device and produce estimates of voltage and current phasors, frequency and rate of change of frequency (RoCoF), usually at 25 or 50 Hz in a 50 Hz system. The measurement performance of these devices is standardised in IEEE C37.118.1a-2014. However, the sheer size of a WAMS for a bulk transmission system poses a number of financial and logistical challenges that make a staged deployment necessary, which means that many of the devices installed may not conform to the most recent measurement performance standards. Given this drawback of staged deployment, the inevitable variation of device performance within the standardised limits and the key role that WAMPAC may come to play in system operation, it is of paramount importance to critically assess the performance of SMT devices to identify their relative merits and limitations.

One of the operational problems that SMT can be used to address is the threat posed by Subsynchronous oscillations (SSO), which have been reported in the following ranges:

- torsional modes from rotating machines (5 – 120 Hz);
- control modes, e.g. from AVRs, governors and HVDC controllers (0.1 – 0.5 Hz);
- local interactions between a single generator and the system (0.8 – 2.5 Hz);
- inter area interactions between groups generators (0.1 – 0.8 Hz); and
- SSR interactions between series capacitors and generators (4 Hz and 47 Hz).

SSO may be defined as an electrical condition where the power system is disturbed from it equilibrium by small disturbances (e.g. load changes) and then experiences an oscillation about its stable operating point. In classical systems with significant amounts of synchronous generation, these oscillations are usually small and well damped. However, with increased penetrations of distributed generation and power electronics (PE), the effective damping provided by the system has become more variable and difficult to ascertain. Subsynchronous Resonance (SSR) is a special case of SSO that occurs in the presence of series compensation and entails the exchange of considerable energy between the electrical system and the mechanical system (generator shafts) when one of their respective modes coincide at a frequency below nominal [3].

Therefore, the assessment of the small signal stability of these more variable networks will call for detailed dynamic models of new technologies and extensive planning studies, which is not always feasible in the absence of a clear definition of the modes of PE interfaced DGs or their specific control algorithms. In this context, a measurement based approach to SSO mitigation offers an attractive alternative that could provide operators with greater confidence in dealing with SSO based threats in real-time without having to resort to planning based solutions or the crude application of increased operating margins

However, whilst PMUs are already viewed as a vital tool for monitoring low frequency oscillations in a power system [4], they will not be able to provide monitoring of the full frequency range of SSO, due to the Nyquist limit (25 Hz for a 50 Hz reporting rate), so new devices will be needed to provide monitoring of the full range. Furthermore, in the presence of increased and more variable SSO the measurement performance of PMUs may be compromised. Therefore, the contribution of PMUs to the monitoring of SSO and the robustness of their measurements in its presence must be assessed. To this end, this paper presents an initial laboratory based study of the performance of four commercial 50 Hz PMUs that report phasors and a 200 Hz fault recorder with dedicated SSO monitoring

functionality, which reports waveform samples. In contrast to previous work on PMU testing, e.g. [5], this paper focuses on the ability of these devices to monitor SSO and its impact on the measurement performance of the PMUs.

2. Testing Methodology

The objective of the tests presented here is an initial study of the response of several PMUs and a Fault Recorder (FR) when exposed to simulated power system signals with subsynchronous components. The test signals consist of an oscillation, $v_f(t)$, at fundamental frequency, f_f, with fixed magnitude, V_f. A subsynchronous oscillation is included in the form of an additive oscillation, $v_a(t)$, of single frequency, f_a, and fixed magnitude, V_a.

$$v(t) = v_f(t) + v_a(t) = V_f \sin(2\pi f_f t) + V_a \sin(2\pi f_a t) \qquad (1)$$

The laboratory setup that is used for this study is depicted in Figure 1. An Omicron CMC 256 is used to amplify the simulated test waveforms and the phasor/waveform data produced by the devices is captured using the Java application presented in [6]. The Java application extends OpenPDC to allow identification of bad samples and to perform data aggregation with time alignment on the measurements reported by the PMUs and the fault recorder. The Java application finds the relevant historian ids in the OpenPDC archiving system for the timestamps that correspond to the duration of the test and any missing measurements or bad timestamps are automatically reported and are not included in the final extraction file. Any tests for which the application identified that the quality of the GPS signal had been discontinued or data packets had been discarded were repeated.
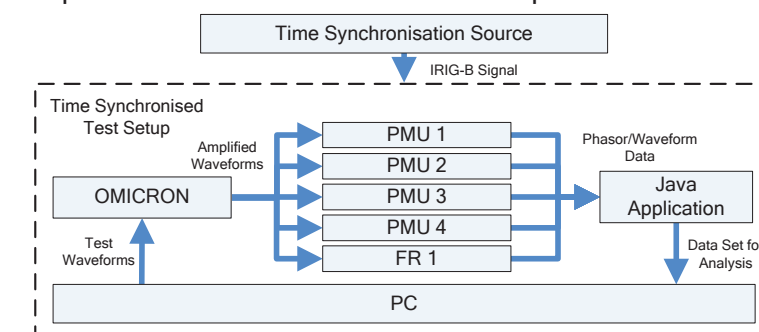

Figure 1 : Time synchronised test setup

3. Test Results and Discussion

The tests presented here used the set up shown in Figure 1 to inject a sinusoidal voltage, as defined in (1), that consisted of a 50 Hz fundamental of 1 p.u. magnitude with six separate additive injections with frequencies of 1, 5, 10, 20, 30 and 35 Hz. Each additive oscillation was sustained for 25 seconds with a 5 second gap between them to allow any transients to end before the next additive frequency was introduced. This test was repeated with additive magnitudes, V_a, of 0.1 p.u. and 0.05 p.u.. Note, these magnitudes and frequencies were not selected to represent any specific power system conditions; rather they were selected to provide a broad range over which to observe the response of the devices under test. The measurement response of the four PMUs is presented in Figure 2 for an additive amplitude of 0.1 p.u.. After the output of the devices under test was captured, the voltage magnitude was processed to identify the dominant frequency components. This entailed applying a notch filter to remove the DC component and a hanning window to reduce leakage before performing a 3 cycle discrete fourier transform. The mean of several fourier transforms over the duration of the additive signals was used to improve the accuracy of the results. A selection of these results have been presented in Figures 3 – 6 to illustrate key points.
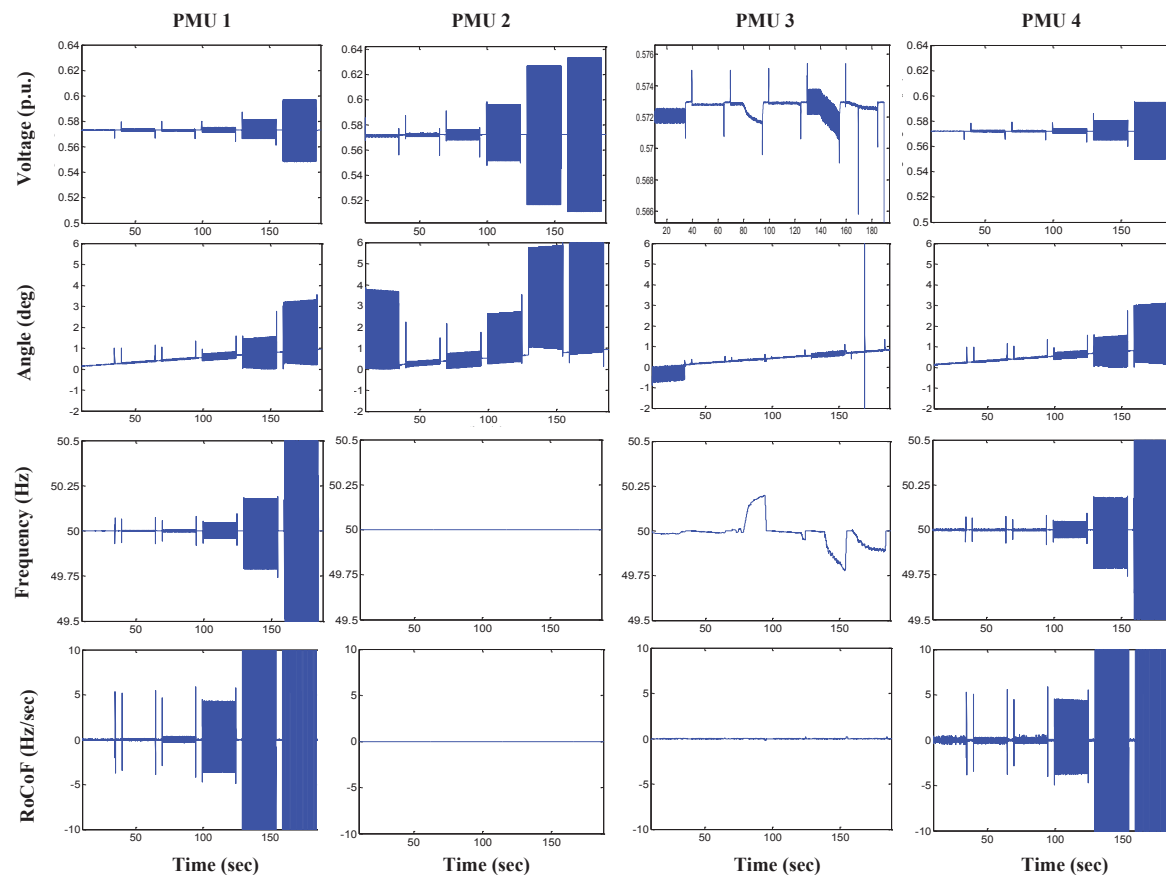
Figure 2 : Comparison of the measurement output of the 4 PMUs for V_a =0.1 p.u. The y axis of the magnitude figure for PMU3 is due to its greater attenuation of SSO and for the RoCoF it conceals that for PMU1 and 4 values of +/- 20 and 40 Hz/s are reached for the 30 and 35 Hz injections.

Figure 2 compares the estimated voltage magnitude, angle, frequency and rate of change of frequency of the four different PMUs for an additive amplitude of 0.1 p.u. This is used to understand any particular influence that this range of injected frequencies may have on the ability of these PMUs to perform their core functionality. One of the most noticeable features is that the small signal oscillations are misinterpreted as massive variations in angle, frequency and RoCoF for PMUs 1 and 4, which may cause false alarms for any frequency based protection schemes that would regard such large RoCoFs as potential fault conditions.

Figure 2 also reveals that PMUs 1, 2 and 4 have a tendency to attenuate the lower frequency components more than the higher frequency components, whilst PMU3 seems to attenuate the components equally. Moreover, it is of particular interest to note that PMU3 does not experience the same degree of oscillation in its angle, frequency and RoCoF estimates as PMUs 1 and 4. However, it does experience a drift in its frequency output that appears to be correlated to its eventual misreporting of a decline in magnitude during a sustained oscillation. A noticeable drift in the angle estimates can be seen for all PMUs. The angle estimates of PMU2 experience a far larger oscillatory error than is observed for the other PMUs, but much smaller errors in frequency and RoCoF. This would suggest that the impact of SSO on PMU performance will manifest itself quite differently for different PMUS algorithms, which may pose a challenge when performing a more detailed assessment. Furthermore, PMUs 2 and 3 particularly struggle with their angle estimates for the lower frequency injections, which is further confirmed by their FFT outputs in Figure 5, where PMU2 and PMU3 have wrongly reported a 1.5 Hz oscillation for a 0.75 Hz injection (This 0.75 Hz injection test was included in addition to the other tests to demonstrate the issue for the lower frequency range). In contrast, the FFT output for PMU1 and 4 shows that, although the 0.75 Hz component is seen to have a distinctive spike, another low frequency in the form of 2.4 Hz also appears with similar amplitude, making the detection of the 0.75Hz component rather imprecise, and PMU1 has similar amplitudes at 10 and 20 Hz.
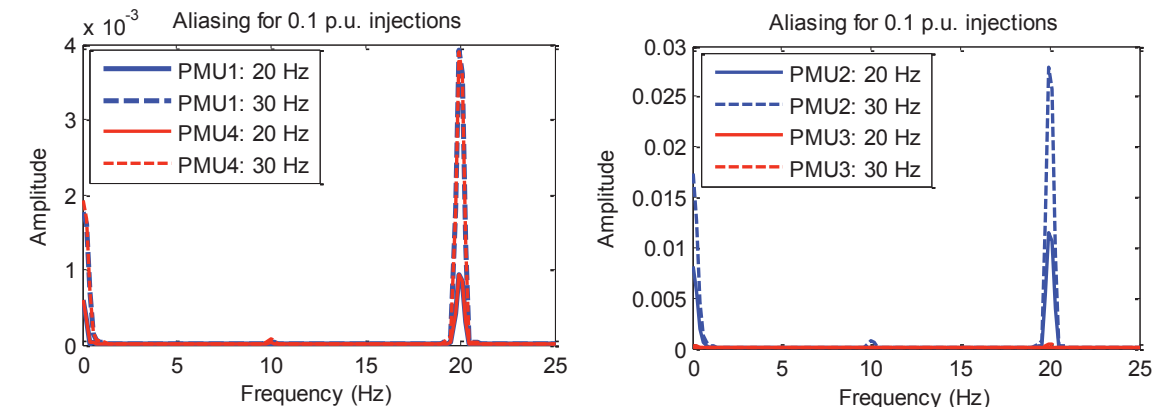
Figure 3 : Aliasing in the output of the four 50 Hz PMUs for injection magnitude of 0.1 p.u.
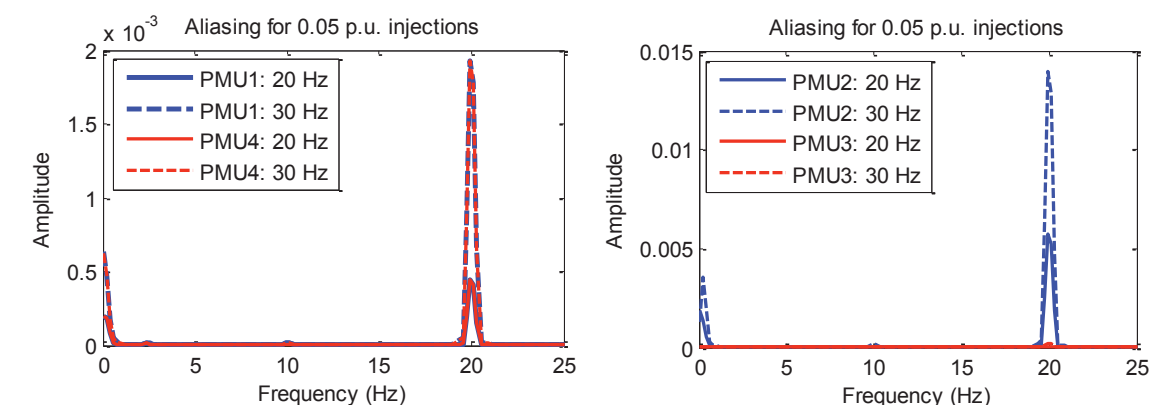

Figure 4 : Aliasing in the output of the four 50 Hz PMUs for injection magnitude of 0.05 p.u.

Figures 3 and 4 present the impact of the additive magnitude on the reporting of the subsynchronous frequencies. It can be seen that the magnitude of the oscillatory components directly influences the amplitude of the FFT output for the 20 Hz injection; in fact the attenuation is so great for PMU3 that it reports no significant frequency content. The larger amplitude component seen at 20Hz is an alias of the 30Hz injection and this occurs due to the reduced attenuation of this oscillation (Figure 2). However, the spike is still sharp for both 0.1 p.u. and 0.05 p.u. oscillation strengths, making the frequency detection more or less independent of magnitude. It is worth mentioning that any higher frequency components that might be present alongside the low frequency components in a signal will appear as aliased components and this may pose a major challenge in the proper detection of frequency components, which may undermine WAMS based protection schemes. Figure 6 shows that the Fault Recorder helps eliminate this problem with its 200Hz sampling rate and correctly identifies frequency components in the entire range of 4-40Hz.
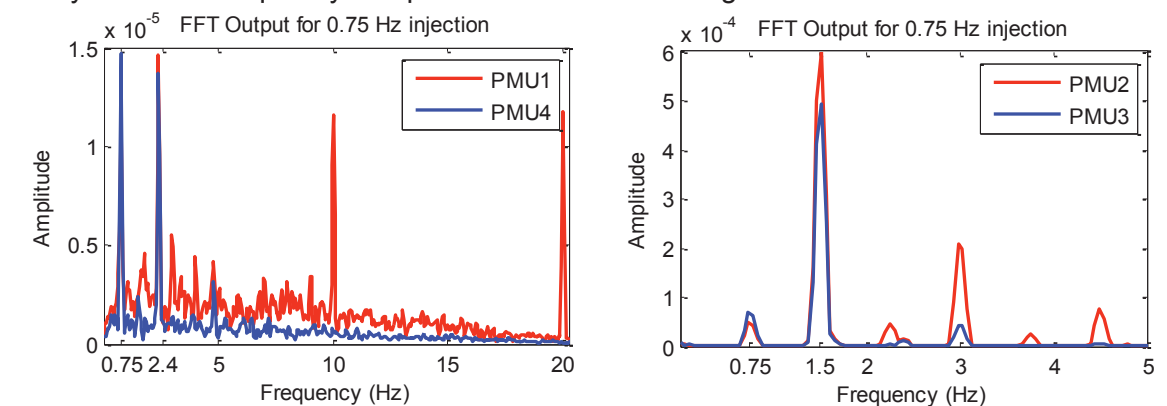

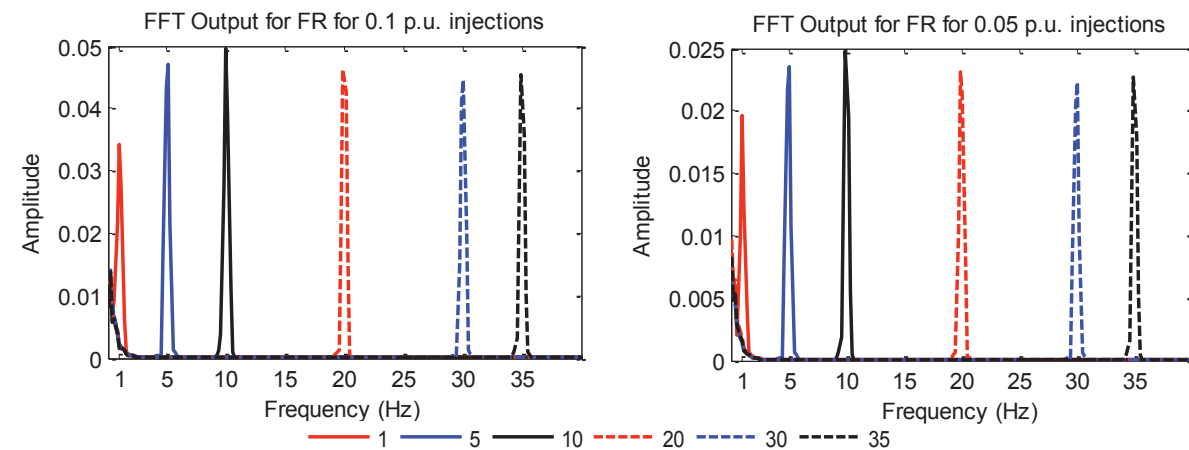Figure 5 : Output of 200 Hz FR for the range of test frequencies

Figure 6 : Output of 200 Hz FR for the range of test frequencies

4. Conclusions

This paper presents an initial study of the applicability of 50 Hz PMUs for monitoring SSO in the range of 1 Hz to 40 Hz, alongside a 200 Hz fault recorder with new, dedicated SSO monitoring capabilities. Laboratory tests were performed for four PMUs and the fault recorder by subjecting them to a range of additive SSO and then using the discrete fourier transform to analyse the device outputs. It has been observed that PMUs attenuate lower frequency components more than the higher frequencies. This may limit their ability to monitor lower frequency components and makes them particularly vulnerable to misreporting SSO due to aliased components from above their nyquist frequency, as these aliased components appear larger than an actual oscillation at the corresponding frequency. Furthermore, for some PMUs, significant cross talk in the angle, frequency and RoCoF is observed during the magnitude oscillations. The magnitude of this increases with the frequency of the injection and, particularly in the case of the RoCoF, this could cause false alarms. The 200 Hz fault recorder is more than capable of reporting the full range of SSO and future studies should include amplitude modulation to investigate the benefits of using waveform samples instead of phasors for distinguishing between additive and modulating oscillations.

Acknowledgements

Bibliography

[1] Phadke, A. G. and Thorp, J. S. Synchronized phasor measurements and their applications. New York; London: Springer, 2008.

[2] Chakrabarti, S.; Kyriakides, E.; Tianshu Bi; Deyu Cai; Terzija, V., Measurements get together," *Power and Energy Magazine, IEEE* , vol.7, no.1, pp.41,49, January-February 2009P

[3] Terzija, V.; et. al., "Wide-Area Monitoring, Protection, and Control of Future Electric Power Networks," *Proceedings of the IEEE* , vol.99, no.1, pp.80,93, Jan. 2 011 Reader's guide to Subsynchronous Resonance, IEEE committee Report, ' Transactions on Power Systems', Vol. 7, N0. 1, February 1992.

[4] Cai, D; Regulski, P.; Osborne, M.; Terzija, V., "Wide Area Inter-Area Oscillation Monitoring Using Fast Nonlinear Estimation Algorithm," *Smart Grid, IEEE Transactions on* , vol.4, no.3, pp.1721,1731, Sept. 201304275765AN test setup

[5] Moraes, R.M.; Yi Hu; Stenbakken, G.; Martin, K.; Alves, J.E.R.; Phadke, A.G.; Volskis, H.A.R.; Centeno, V., "PMU Interoperability, Steady-State and Dynamic Performance Tests," *Smart Grid, IEEE Transactions on* , vol.3, no.4, pp.1660,1669, Dec. 2012

[6] Nechifor, A; Albu, M; Hair, R; Terzija, V. "A flexible platform for synchronised measurements, data aggregations and information retrieval". Electric Power Systems Research, Vol. 120, March 2015, Pages 20 -31.

Impact of Load Dynamics on Torsional Interactions

Papiya Dattaray, Peter Wall, V Terzija
The University of Manchester
Manchester, United Kingdom

Diptargha Chakravorty
Electrical Engineering Department
Imperial College London,
London, United Kingdom

Priyanka Mohapatra,
James Yu
S.P. Energy Networks
Blantyre, United Kingdom

Abstract— This paper evaluates the impact of load dynamics on torsional interactions by considering a mix of static and dynamic loads aggregated at the bulk transmission level. This is essential to investigate the importance of detailed load modelling for subsynchronous resonance (SSR) studies to accurately assess damping contribution and capture system dynamics. SSR interaction with dynamic loads is investigated for both direct on line and drive connected motor loads. Damping contribution from dynamic loads is also assessed based on their location and size. The interaction of dynamic loads with classical SSR phenomenon is observed and introduced as the new concept of (Subsynchronous Resonance Load Interactions (SSR-LI)) . SSR-LI assumes critical importance for scenarios where the load and generation centers are in close electrical proximity and impact of loads on torsional damping is significant. Finally, the scope for using existing converter interfaced motors for torsional mode damping has been discussed.

Index Terms— Dynamic load, induction motor, static load, subsynchronous resonance (SSR), variable frequency drive

I. INTRODUCTION

Subsynchronous resonance (SSR) is a major concern for the integrity and operation of turbine-generators connected to a transmission system employing series capacitors. For analysis of SSR, computer models of the power system in electromagnetic transient simulations (EMTs) generally focus on the turbines, generators, speed governors and excitation systems. The network is modeled in detail using algebraic and ordinary differential equations; however, the effect of load models is either neglected (IEEE First and Second Benchmark models) or constant impedance models are used [1]. This paper demonstrates the importance of load modelling for SSR studies by simulating the impact of different load models on the torsional interactions, using EMT program. Static load models, like constant impedance type, are found to be fairly inadequate for capturing load and/or system dynamics/transients (suitable only for instantaneous responses) [2, 3]. Dynamic load models, on the other hand, being described by differential equations exhibit time-dependent responses that can capture dynamic responses pertaining to exchange of energy between the system and load (e.g. during SSR). For systems having high percentage of induction motor type loads, detailed dynamic load modelling is of utmost importance [4]. The impact of loads on system dynamics has been widely investigated for the classical stability studies [5] but not for torsional dynamics. [6-8]

discuss the effect of different load characteristics on transient stability while [9].deals with dynamic stability, considering mostly a mix of static and composite load models.

Load modelling for assessment of SSR risk becomes critically important when the load center is in close electrical proximity to a generation center [5]. It is worthwhile to analyze if approximate load representations can influence the behavior of RLC resonant circuits. The impact of various load models on the damping characteristics of torsional modes has been observed in [10] for the IEEE First Benchmark Model with linearized models for static and dynamic loads. The linearized analysis neglects generator stator transients and holds valid only for small disturbances (with the assumption of a balanced system model). Transient torque type of SSR interactions however are sparked by large transient system disturbances (e.g. short-circuit faults) that can be studied using EMTs only with detailed non-linear system modelling. Moreover, the linearized analysis fails to capture any non-linear dynamic interactions that might exist between dynamic motor loads and generators under instances of SSR (interactions between motor and generator rotors).

Transient interactions may cause both voltage and a frequency oscillation to appear at the terminals, so modelling of frequency characteristics of loads close to generators is of critical importance. With advanced computational capabilities, there is little reason to represent overall system load equivalents with static models.

The paper looks at several combinations of static and dynamic load models aggregated at the transmission level, shown in Fig. 1, using a kVA weighted averaging technique [4] and demonstrates how their modelling influences the damping of torsional oscillations for a classical case of SSR. Dynamic interaction of the motor loads (both direct on-line and variable frequency drive) has been discussed in particular detail in order to demonstrate how sub-synchronous oscillations propagate through power electronic drive interfaces and affect motor operation. Furthermore, damping contribution from dynamic loads has been evaluated based on motor size and location. The study reveals the impact of load types and their locations on torsional mode damping and illustrates the need for accurate load modelling for precise assessment of SSR risks. The paper also highlights the scope for use of variable frequency drive (VFD) motor loads as

auxiliary torsional oscillation damper with subtle modifications to the existing drive controls.
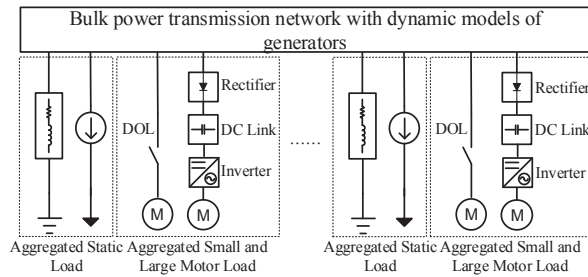

Fig. 1. Aggregation of loads at the transmission level

II. LOAD MODELLING

Load modelling is a well-established aspect of power system research. However, much of this research has focused on the modelling of loads for RMS system studies (not EMT) [11] and the model parameter estimation for these well-established RMS models [12]. This section outlines the modelling required to represent static and dynamic loads in EMT simulations for the study of SSR.

A. Definition of a Load Model

Load model approximates the effects of sub-transmission and distribution system lines, cables, reactive power compensation, on load tap changing transformers (OLTC), distribution voltage regulators, and even relatively small synchronous or induction generators [2]. Static load models express the active and reactive powers at any particular instant of time as functions of the bus voltage magnitude and frequency at the same instant. It is used primarily for modelling of static load components (e.g. heating loads, lighting loads, approximation of motor loads etc.). Dynamic load models however express the active and reactive powers at any instant of time as functions of the voltage magnitude and frequency at the past instants using difference or differential equations [2]. SSR studies, as pointed out previously, have always assumed the system load as static (constant impedance type) while assessing risks or studying interactions through EMTs. Following section discusses the different load models used in the current research to study their impact on torsional oscillation damping.

B. Modelling Of Considered Load Types

In the absence of accurate load data, international industry practice shows loads are represented by exponential static models for dynamic studies. The aggregated load is usually represented by constant current type for active power and constant impedance type for reactive power [13]. It is very difficult to correctly assess the exact composition of static and dynamic loads in a network as it may vary with time of the day or changing seasons. About 70% of the system operators around the world use static load models for power system stability studies while the rest use induction motors to represent dynamic loads [13]. The different types of load models used for this study are discussed in detail in this section.

a) *Constant impedance load:* For EMT simulations, DigSILENT models lumped loads as passive elements (RLC) either in the form of purely inductive or a mixed inductive-capacitive load. The admittance values are calculated based on the load flow solution. This type of load model represents the constant impedance part of static component of the aggregated power system load at transmission level.

b) *Constant current load:* In the absence of exponential or polynomial load models available for EMT simulation, the static load model for constant current type was realized using static generator with a built-in current controller. The controlled current source model of the static generator is modeled in DigSILENT using a voltage source with current control.

c) *Direct on-line (DOL) Motor load:* The majority of dynamic loads in the industrial and commercial sector comprises of induction motor type. These loads can be further classified based on their areas of application e.g. space heating, cooling/ventilation, industrial motors, compressed air and refrigeration. Industrial motor has the largest share among motor type loads [14] having motors ranging from 5 HP to 200 HP and above. In absence of further classification this category is considered to be equally divided into large and small industrial motors.

For EMT simulation of aggregated three phase induction motor loads, models with a single rotor circuit in each axis is generally held sufficient (third order model with slip and d, q axis internal voltage or flux as state variables) for large scale simulations [5].The DigSILENT model for asynchronous machine (double-cage preferred for starting or other kind of transient study) is of sixth order and fits the requirements of our study appropriately.

The generalized model recommended for mechanical load speed-torque characteristic is given in [15]. This torque model, as in (1) and (2), is suitable for a wide range of motor types including large and small industrial motors.

$$\frac{T_m}{T_{m0}} = A\left(\frac{w_m}{w_{m0}}\right)^2 + B\left(\frac{w_m}{w_{m0}}\right) + C + D\left(\frac{w_m}{w_{m0}}\right)^{am} \quad (1)$$

$$C = 1 - (A + B + D) \quad (2)$$

The corresponding values for the coefficients are also available in [15] which essentially suggests that bulk of the industrial motor loads are centrifugal type i.e. with a quadratic speed-torque characteristic.

d) *Variable Frequency Drive (VFD) motor load:* Some of the industrial motor loads are equipped with adjustable speed drives for better performance and improved effeciency. The percentage of drive based motor loads may be less compared to the share of direct online motors in the current scenario but is expected to hold a significant share in the near future. VFD motors provide the distinctive advantage of being able to operate over a wider range of speed whilst maintaining a constant maximum torque, given by (3).

$$T_{max} = \frac{K\left(\frac{V}{f}\right)^2}{\frac{R_s}{f} \pm \sqrt{\left[\left(\frac{R_s}{f}\right)^2 + 4\pi^2(L_s + L_r')^2\right]}} \quad (3)$$

In (3), V is the applied voltage, f is the supply frequency, L_s and L_r are stator and stator referred inductances, R_s is the stator resistance and K is a constant. In cases where f is not too low, $R_s/f << 2\pi(L_s + L_r)$ and the equation reduces to (4).

$$T_{max} = \pm \frac{K\left(\frac{V}{f}\right)^2}{2\pi(L_s + L_r')} \quad (4)$$

It can be seen from (4) that maintaining a constant V/f ratio helps the rotor to develop a constant maximum torque which allows for a constant torque mode of operation (except at low speeds). The impact of R_s/f cannot be neglected at low frequencies which are bound to affect the motor maximum torque which is of particular interest for the sub-synchronous range of frequencies that may appear at the motor terminals in case of SSR phenomenon. It is noted that in order to achieve high torque at low speeds or during motor starting, a relatively high V/f ratio needs to be maintained.

Variable voltage and frequency for motor drive control has been realized through Voltage Source Inverter (3-phase, 6-pulse VSI) using SPWM (Sinusoidal Pulse Width Modulation) switching. SPWM technique is widely used for generating sinusoidal inverter output voltage without lower-order harmonics. Higher order harmonics that may be introduced have been eliminated using filters.

Two common VFD control designs e.g. open loop and closed loop have been investigated for torsional interactions during SSR phenomenon. It is relevant to point out that the drives have been considered to have passive front ends (diode bridges) as active front ends (GTOs/ IGBTs) are rare due to their high overall cost.

a) *Open loop control:*The control strategy implemented compares the motor terminal frequency (f_s) with a reference set point (f_{setp}) and passes the corresponding frequency error (f_{error}) through a PI controller, as shown in Fig. 2.

Open loop motor drive control
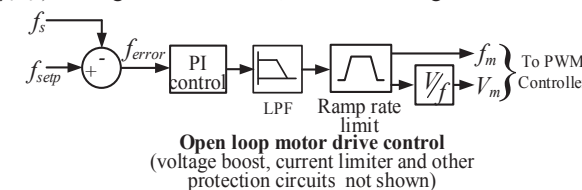(voltage boost, current limiter and other protection circuits not shown)
Fig. 2. Open loop motor drive control

The output of the PI block is passed through a low pass filter (to remove any unwanted noise) and then through a ramp rate limiter to restrict the rate of change of motor speed.

This is particularly important for passive front end drives as they do not support slip power recovery.causing any power fed back to the drive to only get wasted in a dump load. The output of the rate limiter is passed through a V/f block to vary the inverter ouput frequency and voltage simultaneously while keeping the ratio constant such that maximum electromagnetic torque can be achieved throughout the speed range.

b) *Closed loop control:* Closed loop VFD control strategy implemented for the study explicitly keeps track of the motor speed by measuring it at the shaft (w_r) and comparing it to a reference setpoint (w_{rsetp}) to get the motor speed error (w_{error}), as shown in Fig. 3. An additional slip speed (w_{slip}) control loop is introduced to maintain the motor slip within a specified value (e.g. 2%). Whenever the motor speed exceeds this value the motor speed error is updated to a new value (w_{error}^*) which is then passed through the PI controller to get the inverter set points for switching pulses while keeping the V/f ratio constant [16]. Closed loop VFD control is used for process control applications requiring precise motor speed control.

Closed loop motor drive control
(voltage boost, current limiter and other protection circuits not shown)
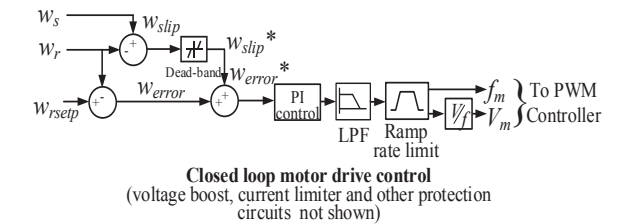Fig. 3. Closed loop motor drive control

c) *Performance Comparison of Open and Closed loop drive controls:* As discussed already, both type of motor controls maintain a fixed V/f ratio. However, this is maintained only till the nominal operating point of the motor. Above this point V/f ratio is no longer maintained as the motor terminal voltage is restricted to its nominal value in order to avoid insulation damage.

Operation of the VFD motor controls is shown in Fig. 4 by simulating a step disturbance in the load torque (Fig. 4 (a)). As open loop control has no speed feedback, the motor slows down slightly (Fig. 4 (d)) to cater to the increased torque demand by increasing its slip (Fig. 4 (c)) and thereby drawing more power (Fig. 4 (b)). Closed loop control, on the other hand, is seen to have successfully maintained the motor speed (and slip) by changing the supply frequency at the motor terminals in order to cater to the new load power requirement.
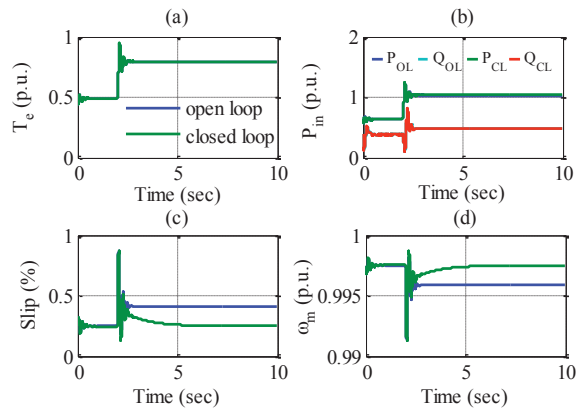
Fig. 4. Open and closed loop VFD motor control

C. Method adopted for Aggregation of Motor Load at the Bulk Transmission Level

Induction machines constitute a major portion of the overall power system load, making their accurate representation in simulation studies very important for realistic reproduction of system dynamic response. Motor loads connected at a particular bus will practically include different types of induction machines (e.g. small, large industrial motors), each having a different dynamic characteristic. It is thus appropriate to model this diverse group of machines by an aggregated equivalent motor, as given in [4]. Aggregation method B has been adopted for this work which calculates the equivalent motor inertia as the weighted average of the parameters of the individual motors in the group.

The motor types considered here is restricted to only small and large industrial motors having equal proportions in terms of KVA. The weighting co-efficient is defined as the relative KVA rating of the individual motors with respect to the KVA rating of the aggregate motor , as in (5).

$$\sigma_j = \frac{KVA_j}{\sum_{j=1}^{n} KVA_j} = \frac{KVA_j}{KVA_{agg}} \quad (5)$$

The electrical parameters of the aggregate motor have been calculated using weighted average of branch admittances i.e. stator, rotor and magnetizing branches, as in (6). This is equivalent to having multiple motors connected in parallel.

$$\frac{1}{Z_{agg}} = \sum_{j=1}^{n} \frac{\sigma_j}{Z_j} \quad (6)$$

Also, the critical slip (slip at which the motor torque-speed characteristic is the maximum) of the equivalent motor is obtained by calculating the weighted average of the individual motor slips. This ensures that the operating region of the aggregate motor lies between the regions of the individual motor characteristics.

III. CASE STUDIES

A. Study Network

The network under study is based on the IEEE First Benchmark model. A schematic diagram of the network is presented in Fig. 5. It consists of a single machine connected radially to a series capacitor. Rest of the network is represented by a voltage source. A load center is considered to be in close electrical proximity and represented by an aggregate load bus. Four different types of loads are considered: a) constant impedance; b) constant current; c) direct on-line motor and d) drive based motor loads. Constant impedance and current type loads comprise the aggregated static load while DOL and VFD motors represent the aggregated dynamic load. The VFD motors have been aggregated at 11 kV as majority of the large drive based industrial loads are connected at this voltage level. Rest of the loads are aggregated at the 500 kV level. The VFD motor drive has been modelled in detail with the dc bus reactor and capacitive filter tuned appropriately for continuous conduction of current. The system dynamic response is naturally unstable with 60% series compensation due to SSR phenomenon, without consideration of any load. All the case studies have been carried out at this compensation level.
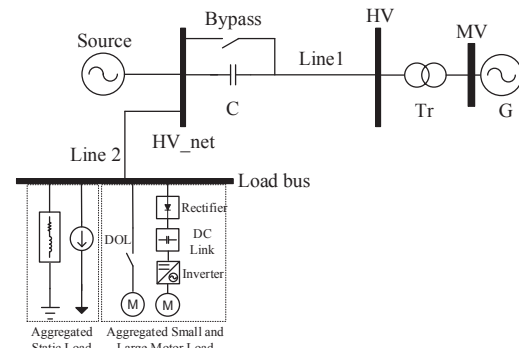

Fig. 5. Schematic of network under study

B. Impact Of Load Modelling On Damping Of Torsional Oscillations

In this study, SSR oscillations are monitored at the turbine output power for different load compositions at the load bus in order to investigate how realistic the classical assumption of either neglecting the loads completely (e.g. in IEEE 1st and 2nd Benchmark models for SSR studies) or considering them as constant impedance type is. Results as presented in Fig. 6 clearly indicate that inclusion of load dynamics may actually modify the effective damping for torsional interactions to an extent where the response may actually change from being unstable for Type 1 and 2, to being stable for Types 3, 4, 5 and 6. Such conservative results obtained with the classical load models may have significant impact while taking decisions both at the planning stage (regarding location and/or degree of compensation) or during operation (setting wrong thresholds for online alarms against dangerous interactions).

Table I describes the different load types that have been considered for the study. These load compositions are not

necessarily realistic but have been used in order to provide a basis for emphasizing the importance of dynamic load modelling in SSR studies.

Table I
List of load types considered

Load Type	Description
Type 1	Loads neglected
Type 2	100% Const. Impedance
Type 3	50% DOL and 50% VFD based Motor loads
Type 4	100% DOL connected Motor load
Type 5	30% Const. Impedance 30% Const. Current 40% DOL connected Motor load
Type 6	50% Constant Impedance 50% DOL connected

Fig.6 shows that the nature and composition of loads produce markedly different damping responses. While representing downstream loads as constant impedance type may result in slightly improved damping response compared to when loads are completely neglected, it is still a conservative assumption to capture the true nature of damping provided for torsional oscillations in SSR studies. Type 5 and type 6 represent the more realistic grid condition (at present scenario) and are found to provide the best damping among the six different load types that have been considered.
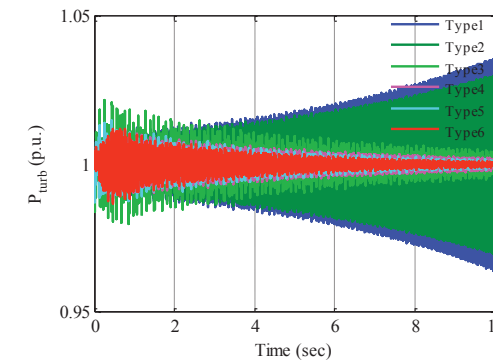

Fig. 6. Damping comparison of different load model

This case study clearly reveals the importance of accurate load representation for the reliable assessment of system dynamic performance and precise assessment of SSR risks especially when the load center is close to generation.

C. Impact Of Motor Size And Location On Damping Of Torsional Oscillations

Section B briefly explored how different load types when modelled into the simulation provide variable damping for torsional oscillations in an SSR condition, out of which motor type load is found to have the most significant impact. Further studies investigate how location, inertia (i.e. motor size in terms of rotational mass or moment of inertia, J in kgm^2) and varying percentage shares of motor loads impact the effective damping.

Fig. 7 (a) shows the generator turbine power output (P_{turb}) and power flow through series capacitor (P_{cap}) for two different locations (load bus and HV bus) of DOL type motor load during SSR. It can be seen that aggregated motor load at the HV bus provides much better damping than the load bus.

This can be justified by monitoring the power flow through the series capacitor. From the network diagram in Fig. 5 it can be seen that when loads are connected at the load bus, the power from the generator (G) has to flow through the series capacitor (C). As the generator is feeding into the SSR oscillations and the capacitor is exchanging energy with it during the period, higher power flow through the capacitor negatively affects the damping contribution from loads.

It is however interesting to observe the further impact of motor inertia at any given location and how location can effectively modify its damping contribution. Fig. 7 (b) illustrates the impact of location for aggregate motor (having same KVA_{agg}) with reduced inertia. For the same location (load bus), P_{turb} is heavily damped in case of low inertia motor in Fig. 7 (b) from being poorly damped in case of high inertia motor in Fig. 7 (a). Damping contribution from a given motor load is thus seen to vary with its size for different locations.

Low inertia motor provides positive damping at both the locations. However, at HV bus it causes high oscillations in the turbine output power as well the power flow through the capacitor. The initial power flow through the capacitor remaining the same, these oscillations are due to the proximity of the load to the source of disturbance (G) which is particularly aggravated for a small motor. The number of testing locations is limited for this simple radial network. Results presented here are to emphasize the importance of load location and size in determining effective damping contribution. However, this needs further investigation in a more complex network.
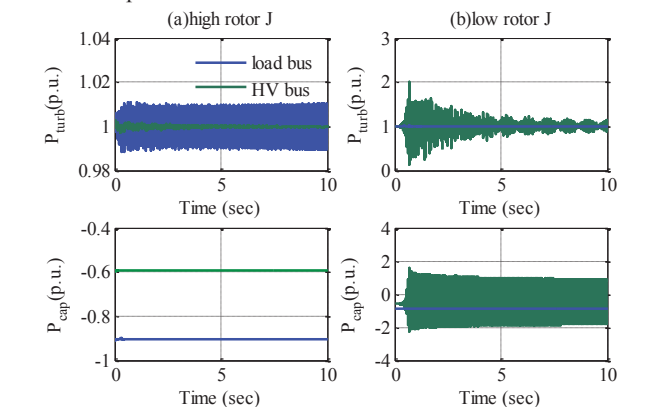

Fig. 7. Impact of motor shaft inertia and motor location on SSR damping

In the study network load bus is a more realistic load location. It is considered for further study to explain why motor with lower inertia can provide better damping than an equivalent motor with higher inertia. Fig. 8 shows that the lower inertia motor is more responsive and the rotor speed oscillations closely follow the variations in system frequency. For maximum damping the change in speed (and hence active power consumption) of the motor should be in phase with the change in system frequency. However, as already pointed out, the location of the load is an important factor, as proximity to generation may cause higher oscillations and poorer damping from the same motor.
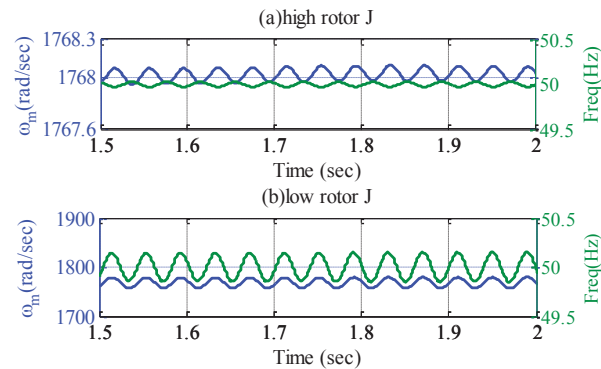
Fig. 8. Motor speed-bus frequency phase relation when load connected at the load bus

D. DOL Type Motor Interaction With SSR

Three-phase induction motors are the most common industrial machines in operation. They can have different types of motor starting and interface techniques like Direct-On-Line (DOL), star-delta transformer, autotransformer or variable speed drives. Based on the information availabe from the vendors of motor drives in Great Britain almost 80% of the total industrial and service sector motor loads are DOL type. For a DOL start motor, the stator being connected directly to the supply, makes them naturally vulnerable to any voltage and/or frequency changes appearing at its terminals.

During SSR phenomenon, subsynchronous frequency current components flow into the network. These subynchronous components give rise to a stator flux rotating at less than the synchronous speed on top of the nominal synchronous field. The overall stator flux magnitude is thus determined by the superposition of the fundamental (ψ_s) and the low frequency (ψ_f) component. As the magnetic field oscillates between $\psi_s + \psi_f$ and $\psi_s - \psi_f$, induction machine torque (hence speed) starts to oscillate. The turbine power output (P_{turb}) and the induction motor electrical (T_e) and mechanical (T_m) torque oscillations along with respective FFT results are shown in Fig. 9. A single cycle three phase short circuit fault is considered in this case study to magnify the impact of generator shaft torsional oscillations on T_e. The induction motor is considered to be connected at the load bus.
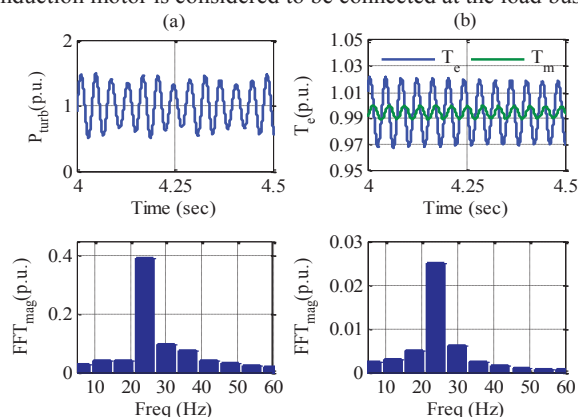

Fig. 9. DOL type induction motor interaction with SSR

Fig. 9 (b) clearly shows the same frequency component appearing in both T_e and P_{turb} oscillations (fixed mechanical torsional frequency of 25Hz). As electrical proximity between the generation and load centre increases, these interactions become particularly important. This phenomenon can be termed as Subsynchronous Resonance Load Interactions (SSR-LI), seperate from the three already reported interactions, namely SSR, SSTI (Subsynchronous torsional interaction) and SSCI (Subsynchronous Control Interaction). SSR-LI involves interaction of generator shaft, network LC mode and dynamic load.Oscillations appearing in the electrical torque causes a change in the operating point of the motor every subsynchronous cycle, leading to significant stress on the motor shaft. Oscillations can also be seen in armature current which may cause over-heating/ over-fluxing problems for the motor. This type of interaction may prove to be particularly detrimental for constant torque type loads (e.g. conveyers, positive displacement pumps, hoists etc.)[17]. It can thus be inferred that SSR can not only interact with generators but also with motor shafts and normal motor operation.

E. VFD Based Motor Interaction with SSR

The main objective of this case study is to investigate how the SSR oscillations propagate through power electronic intefaces to finally interact with the motor shaft. Fig. 10 (a) presents speed oscillations at different points of generator-turbine shaft e.g. exciter (speede), high pressure turbine (speedh), intermediate pressure turbine (speedi), low pressure turbine (speedla,speedlb) along with corresponding fft results. Fig. 10 (b) presents the oscillation in turbine power output (P_{turb}) and its correponding fft plot. Fig. 10 (c) presents the dc link capacitor voltage (V_{DC}) of the VFD and its fft which indicates that the torsional oscillations translate through the diode bridge to appear on the dc side which may then propagate to the motor side through the inverter. Fig. 10 (d) shows that this oscillation gets propagated to the machine electrical torque (T_e) which starts oscillating across the mechanical load torque (T_m) of the motor. It is interesting to see a 25 Hz frequency component appear at the motor terminal apart from the 5th and 7th harmonics which are characteristic of the 6-pulse inverter. The values at the motor drive end have been presented in absolute terms as their magnitude is significantly lower than the generator shaft oscillations. The magnitude of oscillations in T_e depend on the dc link capacitor (filtering). However, as the capacitor is tuned to smoothen out dc voltage ripples it may not be able to effectively filter out subsynchronous frequecies. Sustained oscillation of T_e may result in rotor shaft damage.

The results clearly indicate that SSR can translate through passive front-end VFD drives, for both type of controls. The results presented here are for closed loop control only.
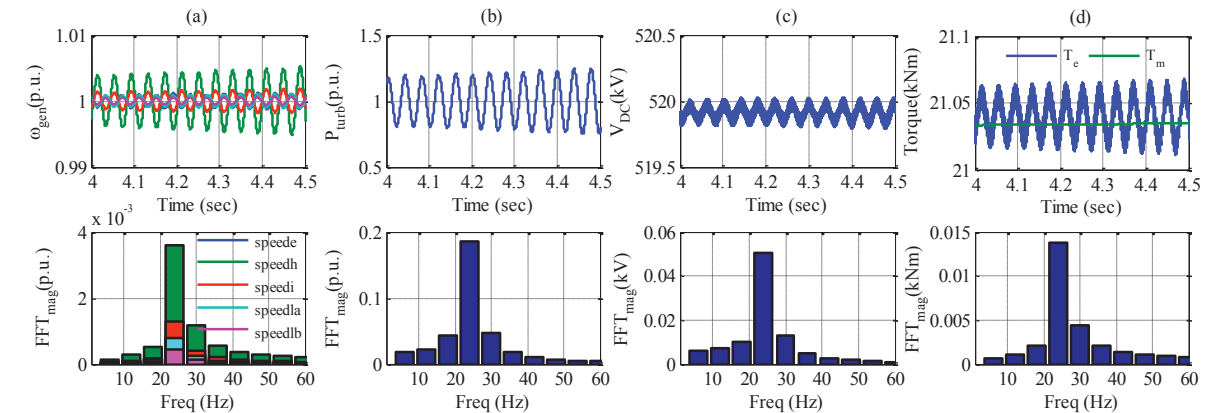

Fig. 10. (a) Generator-turbine shaft speed, (b) Turbine output power, (c) VFD dc link capacitor voltage and (d) Motor torque

IV. FUTURE WORK- AUXILIARY DAMPING CONTROL

A large number of SSR mitigation techniques have been known to be in use within the industry like the Static Blocking Filter (BF), Supplementary Excitation Damping Control (SEDC), Damping Rotor Resistor, TCSC, HVDC control or other FACTS devices [18]. However, each one of these solutions suffer from certain shortcomings, e.g. BFs being passive filters suffer from inherent errors of manufacture, once tuned are hard to operate optimally in real-time and are not the most recommended as they incur massive investments. Damping resistance in the rotor winding increases the complexity of rotor construction and needs to be considered at the manufacturing stage. TCSC or HVDC controls are promising but quite expensive. Based on the results that induction motor loads can positively contribute towards torsional damping, it is proposed that a certain amount of DOL start induction motor loads may be paid to be in service at specific locations (e.g. as ancillary service or demand side management for torsional damping) alongside VFD motor loads equipped with auxiliary damping controllers. Efficient and robust auxiliary damping controller may be designed by making subtle modifications in the existing VFD control loop. This can provide additional damping at very minimal cost. Auxiliary power plant loads like Forced Draft (FD), Induced Draft (ID) fans present a lucrative option as they are electrically close to generators and are 11kV VFD based large induction motor loads. Smaller motor loads that run downstream can be included to extract damping in large interconnected networks. Future work involves design of an auxiliary damping controller using existing VFD motor loads and demonstrate effectiveness of proposed demand side solution (large power plant loads and small downstream motor loads) in SSR oscillation damping for a meshed power system network.

V. CONCLUSION

This paper investigates the impact of dynamic load modelling in EMT studies for SSR phenomenon. Loads are classically either neglected or modelled as constant impedance type for SSR studies. The objective of this work is to investigate this classical assumption by modelling different types of loads and their compositions (aggregated at the bulk transmission level) to highlight their relative impact on damping of torsional oscillations. Analysis shows that static load model produces conservative results and modelling of dynamic loads is of critical importance in order to capture system dynamics or transient behavior for SSR studies. Modelling details for the EMT simulation of loads in DigSILENT for both static and dynamic load types have been provided. Dynamic loads have been modelled as induction motors (DOL and drive based). Both open and closed loop VFD motor controls have been investigated. Case studies highlighting the impact of size and location of motor type loads in providing damping for torsional oscillations have been presented in detail. Results revealed that low inertia motors have the capability to provide better damping than large inertia motors because their speed oscillations closely follow subsynchronous frequency oscillations. It has however been pointed out that load location plays an important role in the damping contribution especially, how it affects the power flow through the series capacitor. Phenomenon of Subsynchronous Resonance Load Interaction (SSR-LI) for conditions where the load centers are electrically close to the generation centers has been introduced and discussed for both DOL and VFD based dynamic motor loads. Results have been presented to show the propagation of torsional oscillations across passive front end VFD motor loads. Impact of subsynchronous components appearing at the motor terminals has been discussed in terms of motor operation. Finally, the scope for using VFD motor loads (especially power plant auxiliary loads) for SSR mitigation using supplementary damping control has been proposed and left open for future work.

VI. REFERENCE

[1]. J. Milanovic, A. Adrees, "Identifying Generators at Risk of SSR in Meshed Compensated AC/DC Power Networks", *IEEE Transactions on Power Systems*, Vol. 28, No. 4, May 2013.

[2]. IEEE Task force for Load Representation for Dynamic Performance, "Load Representation for Dynamic Performance Analysis", *IEEE Transactions on Power Systems*, Vol.8, No. 2, May 1993

[3]. O.H. Abdallah, M.E. Bahgat, A.M. Serag, M.A. El-Sharkawi, "Dynamic Load Modelling and Aggregation in Power system Simulation studies", *Power systems conference*, Middle-East, MEPCON, 2008

[4]. Farhad Nozari, M. David Kankam & William W. Price, "Aggregation of Induction Motors for Transient Stability Load Modeling," *IEEE Trans on Power Systems*, Vol. PRWS-2, No. 4, 1987.

[5]. B.L. Agarwal, J.A. Demcko, R.G. Farmer and D.A. Selin, "Apparent Impedance Measuring System (AIMS)," *IEEE Transactions on Power Systems*, Vol. 4, No. 2, May 1989

[6]. Dong Han, Guoqiang Zhang, Tao Lin and Hui Ding, "The effect of load models on electromagnetic transient stability in AC/DC power systems", *Electricity Distribution (CICED), 2012 China International Conference*, pp. 1-4, 2012

[7]. E. Sorrentino, O Salazar and D. Chavez, "Effect of generator models and load models on the results of the transient stability analysis of a power system", in *Universities Power Engineering Conference (UPEC)*, pp. 1-5, Proceedings of the 44th International, 2009

[8]. E. Santos, T.I. Asiain, D. Ruiz and D. Olguin, "The effect of load chracteristics on the transient stability studies of a laboratory electric

power system including induction generators", *International Conference on Electric Power Engineering, PowerTech Budapest 99*, pp. -81, 1999

[9]. W. Mauricio and A. Semlyen, "Effect of Load characteristic on the Dynamic Stability of Power Systems", IEEE Transactions on Power Apparatus and Systems, Vol. PAS-91, Issue no. 6, pp. 2295-2304, 1972

[10]. Chen, W.H.; Bi, T.S.; Fang, J.Y.; Yang, Q.X., "Interaction of torsional dynamics and loads," in *Advances in Power System Control, Operation and Management (APSCOM 2009), 8th International Conference.*, pp.1-5, 8-11 Nov. 2009

[11]. P. Kundur, *Power System Stability and Control*. New York: Mc-Graw-Hill, 1994.

[12]. Regulski, P.; Vilchis-Rodriguez, D.S.; Djurovic, S.; Terzija, V., "Estimation of Composite Load Model Parameters Using an Improved Particle Swarm Optimization Method," in Power Delivery, IEEE Transactions on , vol.30, no.2, pp.553-560, April 2015

[13]. J.V. Milanovic, K. Yamashita, S.M. Villanueva, S.Z. Djokic, "International Industry Practice on Power System Load Modeling,"

IEEE Transactions on Power Systems, vol. 28, pp. 3038-3046, Dec. 2012.

[14]. Department of Energy and Climate Change (2014). Energy Consumption in the UK Service sector data tables 2014 update. [Online]. Available: https://www.gov.uk/government/statistics/energy-consumption-in-the-uk

[15]. IEEE Task Force on Load Representation for Dynamic Performance, 'Standard load models for power flow and dynamic performance simulation,' *IEEE Trans on Power Systems*, Vol. 10, No. 3, 1995, pp. 1302-1313.

[16]. A. Hughes and B. Drury, Electric Motors and Drives, 4th ed. Elsevier Ltd., 2013.

[17]. Schneider S.A. (1995, May). Adjustable Frequency Controllers. [Online].Available:http://www2.schneider-electric.com/resources /sites/ SCHNEIDER_ELECTRIC/content/live/FAQS/105000/FA105387/en_ US/SC100.pdf

[18]. Padiyar, K. R. *Analysis of subsynchronous resonance in power systems*. Springer Science & Business Media, 2012.

Inertia Estimation using PMUs in a Laboratory

P. Wall, P. Regulski, Z. Rusidovic and V. Terzija*, Senior Member, IEEE*

School of Electrical and Electronic Engineering
University of Manchester
Manchester, UK
Peter.Wall@manchester.ac.uk

Abstract— This paper presents a comparison of the performance of an online inertia estimation method for three different C37.118 compliant PMUs in a laboratory. Inertia is a critical part of ensuring stable system frequency and improving operator awareness of inertia will help preserve high quality frequency control in power systems with high levels of wind generation and converter interfaced generation. This study is necessary as inertia estimation is based on active power and rate of change of frequency measurements recorded immediately after a disturbance. Therefore, the transition time and inherent difficulty of estimating derivatives may mean that not all PMUs can support inertia estimation. Indeed, the results presented show that not all PMUs are capable of supporting inertia estimation. Therefore, it must be acknowledged that the installation of a PMU at a bus does not necessarily imply that it will be possible to perform inertia estimation at that bus.

Index Terms— Inertia, Inertia Estimation, Laboratory Testing, Phasor Measurement Units, WAMS.

I. INTRODUCTION

The advent of Synchronized Measurement Technology (SMT) in power systems, the leading example of which is the Phasor Measurement Unit (PMU) [1], has led to the rapid development of a broad range of Wide Area Monitoring Protection and Control (WAMPAC) applications [2][3].

One of these applications is the estimation of power system inertia, commonly defined using the inertia constant *H*. The inertia of a power system describes the amount of energy stored in the rotating masses connected to the system, e.g. synchronous generator shafts and induction motors. This inertia is a key factor in determining the initial frequency response of a power system to an imbalance between generation and load; specifically, as system inertia is reduced the system will experience a faster and deeper fall in frequency for the same generation loss. Therefore, inertia is critical to ensuring the frequency security of a power system.

However, many of the coming changes in power systems, e.g. the increasing penetration of wind generation and the connection of generation over converters, will cause the power system inertia to become much smaller and far more variable than in the past. In smaller, isolated power systems, like the GB National Grid, this will pose a threat to the

provision of suitable frequency control in an economically viable way [4].

This threat can, in part, be countered by developing inertia estimation methods that allow operators improved awareness of the system inertia. Inertia estimation based on the swing equation was first proposed in [5] and [6] for offline use without PMUs. The swing equation was then proposed for online inertia estimation based on PMU measurements of active power and rate of change of frequency in [7] and [8]. In [9] and [10] the swing equation was used for offline estimation of inertia based on a known disturbance size and an estimate of the rate of change of frequency from PMU measurements of frequency.

However, the performance of WAMPAC applications is dependent on the data they receive from PMUs. This may prove a particular issue for online inertia estimation, as it is dependent on measurements of the rate of change of frequency (ROCOF) and active power that are made soon after a disturbance that will have caused a simultaneous step change in voltage and current as well as a ramp in frequency.

The IEEE C37.118 standard exists to ensure interoperability between PMUs from different vendors. However, no robust measurement device can respond instantaneously to a step change and this is accommodated for in the standard by a relaxation of the accuracy requirements during the transition between the two levels of the step. This could mean that the ROCOF and active power data required by inertia estimation may not be accurately recorded by all PMUs. Therefore, this paper presents a comparison of the performance of inertia estimation method for three different C37.118 [11] compliant PMUs.

The paper is structured as follows: Section II provides a brief overview of the window based inertia estimation method that is used here. Section III describes the laboratory setup that is used to perform the testing and Section IV presents the results of this testing. Section V summarizes the results presented and discusses future developments.

II.   INERTIA ESTIMATION

This section provides a brief theoretical background to inertia and the swing equation as well as the window based inertia estimation method that is used for the tests presented

here. More details on these subjects can be found in [12], [13] and [14] and [7] and [8], respectively.

A. The Inertia Constant (H)

Power system inertia is a measure of the stored energy in the rotating masses of the system [13]. The inertia of a rotating mass is commonly defined using its inertia constant H, which is calculated as follows [12]:

$$H = J\omega_n^2 / 2S_B \qquad (1)$$

where H is the inertia constant in seconds, J is the moment of inertia of the shaft in kgm^2, S_B is the base power in MVA and ω_n is the nominal speed in rad/s.

B. The Swing Equation

The inertia governs the initial frequency response of the power system to a change in the active power according to the swing equation [12] [13] [14]:

$$2H \Delta df(t)/dt = p_m(t) - p_e(t) \qquad (2)$$

where, p_m is the mechanical power driving the rotor in p.u., p_e is the power across the air gap of the machine in p.u. and df/dt is the ROCOF in p.u./s. The swing equation (2) can be modified to only contain variables measured on the electrical side of the system by exploiting the slow changing nature of mechanical power relative to electrical power. This involves substituting the mechanical power term in (2) with the previous measured value of electrical power.

$$2H\big(df(t)/dt - df(t-\Delta t)/dt\big) = p_e(t-\Delta t) - p_e(t) \qquad (3)$$

where Δt is the interval between measurements and p_e is now the active power at the location at which the ROCOF is measured. The validity of this approximation in the context of inertia estimation is demonstrated in [8]. This approximated form of the swing equation is only valid immediately after a disturbance, i.e. when the assumption that the mechanical power is approximately equal to the previous measurement of electrical power holds true.

C. Window Based Estimation of Inertia

A Window based method for estimating inertia is presented in [8]. This method is also used here and can be summarized as follows. The algorithm uses four smoothing filters, two for the active power and two for the rate of change of frequency (ROCOF), these are labeled P_1, P_2, R_1 and R_2, where P denotes active power and R denotes the ROCOF. The windows are placed either side of the time of disturbance (t_d), which is assumed to be known, and the subscript 1 denotes the window prior to the disturbance and 2 denotes the window after the disturbance, see Fig. 1.

Each window has a width of A data points, and therefore a width of $(A-1)\Delta t$ seconds, and the separation between each pair of windows is determined by the width of any pre-filtering applied to the data, $W\Delta t$ seconds.

For the case where a straight mean of the data points is taken the output of the windows can be defined as follows:

$$P_1 = \frac{1}{A}\sum_{t=t_1}^{t_d} P(t) \quad (4) \qquad P_2 = \frac{1}{A}\sum_{t=t_2}^{t_e} P(t) \quad (5)$$

$$R_1 = \frac{1}{A}\sum_{t=t_1}^{t_d} \dot{f}(t) \quad (6) \qquad R_2 = \frac{1}{A}\sum_{t=t_2}^{t_e} \dot{f}(t) \quad (7)$$

Each of the windows provides one of the variables in swing equation (3). This can be represented by adjusting the notation of the swing equation (3) to correspond to the window definitions as follows:

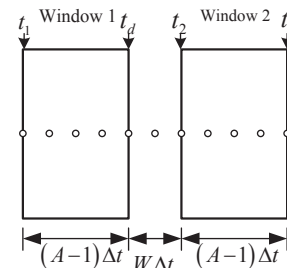$$H = 0.5(P_1 - P_2)/(R_2 - R_1) \qquad (8)$$

Figure 1: A pair of windows are used to estimate the pre and post disturbance active power and ROCOF, in this example the black circles are data points so the window width is A=5 and the width of pre-filtering is W=2. t_d denotes the time of disturbance (end of window 1), t_e is the end of window 2 and t_1 and t_2 are the start time of the windows 1 and 2, respectively.

In [7] and [8] generator inertia was estimated by taking Active Power and ROCOF measurements from the terminal bus of a generator. This approach is also adopted here, as it offers the benefit of allowing the use of the generator inertia as a true value when assessing the error in the inertia estimate. This paper focuses on the impact of the different performance of different PMUs on the output of this window process, so the time of disturbance estimation element of [7], which is based on the sliding implementation of the windows, is not considered here and it is assumed that the time of disturbance (t_d) is known. The time of disturbance can also be estimated by detecting a step change in the active power or ROCOF [5]. It has been shown in [8] that any error in this time of disturbance will be translated in to an error in the inertia estimate.

III. LABORATORY SETUP

This section presents the laboratory setup and procedure that is used to perform the inertia estimation tests.

A. Test Setup

The laboratory test setup is depicted in Fig. 2. It includes the following elements: An Omicron CMC 256, PMU 1, PMU 2, PMU 3, a Phasor Data Concentrator (PDC), and a PC running Omicron Test Universe, Mathworks Matlab, DIgSILENT PowerFactory, and the SyncroWave PDC.

B. Experimental Procedure

The procedure followed when using the PMUs to estimate system inertia was as follows:

1. Prepare instantaneous voltage and current signals with a sampling rate of 5 kHz in COMTRADE or comma separated values (CSV) file format for a dynamic simulation performed in DIgSILENT PowerFactory.
2. Play the simulation using the Omicron CMC 256. The signals (voltage and current) generated at the Omicron's outputs are measured by all three PMUs at the same time.
3. The PMU data is then collected and time-aligned within the PDC, from which it can be exported to Matlab in a CSV file to perform the inertia estimation
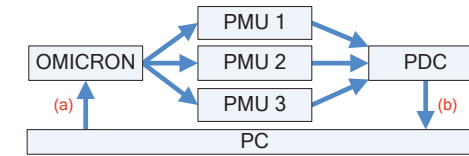

Figure 2: Laboratory test setup, all three PMUs measure the same voltage and current generated by the OMICRON. (a) is the communication of Comtrade or comma separated values (CSV) files to the Omicron and (b) is the transfer of CSV files for processing in Matlab.

IV. RESULTS OF INERTIA ESTIMATION BASED ON PHASORS ESTIMATED BY PMUs

This section describes the results of using the laboratory set up described in Section III to test the performance of the inertia estimation method described in Section II for three C37.118 compliant PMUs.

A. Generaton of Testing Signals

The signals used to perform the tests are created using the 9 bus system depicted in Fig. 3, the parameters of which are given in [13]. The inertia constant of each generator is given in Fig. 3 on a 100 MVA base, as are all per unit power values in the paper. The generators in this system all have quite different inertia constants. This is beneficial as it will allow the influence of the inertia itself on the estimation process to be studied. A load increase of 0.5 p.u. at bus 5 was simulated to generate the testing signals for the PMUs for all three generators, as described in Section III. Each set of signals created in this way for each generator forms a separate test. The rms active power, frequency and rate of change of frequency (ROCOF) at the terminals of each generator are presented in Fig. 4, Fig. 5 and Fig. 6, respectively.

A load change is used here to create a step change in active power A load change does not cause a change in system inertia, like a generation loss would, but this is not an issue as the windowing process estimates the post-disturbance inertia and does not observe the pre-disturbance inertia. The application of the window based inertia estimation method for a generation loss is described in [7]. A benefit of this approach is that it allows an inertia estimate to be made for all three generators when they are connected to the system. If a generator is disconnected then a PMU can only estimate its inertia if it is on the generator side of the breaker. If the PMU is on the system side of the open breaker then it will return an estimate of the 'local' inertia of that part of the system.

It can be seen in Fig. 4 that the load on each generator steps up after the load increase and then oscillates toward a new steady state. Gen 3 has the largest step change due to its higher inertia, but this high inertia also means that Gen 3 has the smallest step change in ROCOF. The curves in Fig. 5 are not as smooth as those in Fig. 4. This is because the high sampling frequency that the data is generated at (5 kHz)

causes small fluctuations in the ROCOF. These small fluctuations appeared to have no significant influence on the signals generated for the testing procedure.
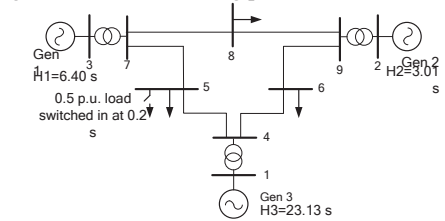

Figure 3: The 9 Bus Power System used to create the test signals. A 0.5 p.u. load is switched in at 0.2 seconds, each generator provides one test signal
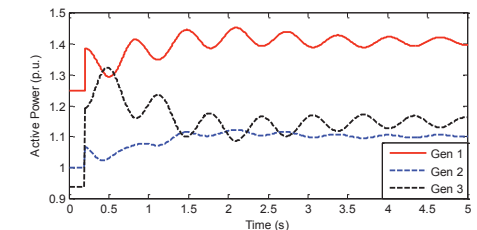

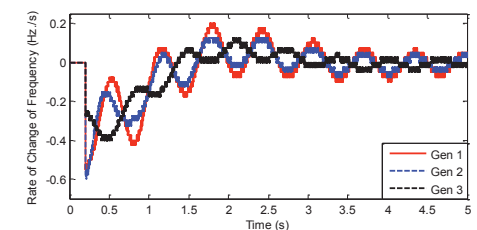Figure 4: Response of active power load at terminals of each generator.

Figure 5: Response of ROCOF at terminals of each generator.

B. Comparison Active Powerand Rate of Change of Frequency Measured by the PMUs

The measurements made by the PMUs for each of the generators are compared in this section through a visual comparison of the signals estimated by each PMU and a comparison of the normalized absolute error in the estimations made by each PMU.

1) Comparison of estimated and true signals

The first comparison is of the estimated active power and ROCOF with the true signals to visually study the quality of the estimation by each PMU, Fig. 6. It should be noted that the use of smoothing filters means that the PMUs appear to respond to the disturbance before it occurs, as the time stamp represents the center of the filter window.

It can be seen that the estimates made by all three PMUs reconstruct the steady state and post-step change oscillation of the active power signal in a satisfactory way. PMU 2 has a small offset from the true signal for all three generator tests, fortunately this should not be an issue in this case as the inertia estimation process considers the change in active power and not its absolute value (8).

The transition of each PMU after the step change reveals that PMU 1 has the shortest filter width and responds the fastest to the step change. PMU 2 has a similar filter width to PMU 1, although slightly longer, and PMU 3 has a much

longer filter width. The length of the filter used by PMU 3 means that it filters out the step change in active power.

Now let us consider the ROCOF measurements, as before it can be seen that PMU 1 has the shortest filter width and PMU 3 the longest. However, in the case of the ROCOF it is apparent that, in contrast to the active power measurements, PMU 3 is not capable of accurately measuring the oscillations after the step change. This renders PMU 3 unsuitable for supporting inertia estimation.

The shorter filter width allows PMU 1 to respond more quickly to the step change than PMU 2; an advantage, as it preserves the step change. However, it can be seen that this comes at the cost of noise in the ROCOF measurement; a disadvantage, as it will introduce errors into the estimation.

2) Comparison of Acitve Power and Rate of Change of Frequency Errors for each Generator case

Presented in Fig. 7 are the absolute errors in the estimation of active power and ROCOF for each PMU and for all three generators. These errors have been normalized using the size of the step change in the active power and ROCOF. This allows them to be compared in terms of their relative impact on the estimation process. It should be noted that this normalization makes the approximately fixed error in the active power estimate of PMU 2 appear to vary in Fig. 7.

The active power errors are characterized by a small error in the pre step change steady state and post step change oscillations but have a significant increase during the transition for the step change. It is important to recognize that this is tolerated in the C37.118 standard and in no way indicates a failure on the part of the PMU. However, the data recorded immediately after a disturbance (the step change) is the most useful for inertia estimation. The duration of this increase in the error is a function of the width of the PMU filter. However, the maximum error in this period is linked to the relative position of the step change in the filter window of the PMU and will be more variable for shorter filter widths.

This transition period is accommodated by the inertia estimation method by separating the two windows by W data points, see Fig. 1, where W is the width of the filtering.

The ROCOF errors for PMU 2 follow a similar trend as the active power errors. In contrast the short filter width of PMU 1 means that it is has larger errors during the pre and post step change signals and PMU 3 has very large errors after the step change as it fails to accurately measure the dynamic rate of change of frequency.

C. Comparison of the Inertia Estimates for the PMUs

This section presents the results of applying the inertia estimation method described in Section II to PMU measurements for each of the three testing signals. The results for PMU 3 are not included here as the poor estimation of the ROCOF by this PMU meant that it is not worthwhile analyzing them. Tables I, II and III present the errors for PMU 1 and PMU 2 for the simulated test signals for each generator after a 0.5 p.u. load increase and for five different estimation window lengths (A).

It was remarked on in Section IV B that PMU 1 has a shorter filter width than PMU 2, see Figure 6. This is

beneficial in terms of reducing the number of measurements of both active power and ROCOF that are lost to the transition after the disturbance. However, a longer filter window can aid in limiting corruption of the measurement by noise, see the errors for PMU 1 in Fig. 7. The discussion of these results is mostly focused on the impact of the ROCOF errors, as they are larger than the active power errors relative to the size of the step change.

TABLE I.   RELATIVE INERTIA ESTIMATE ERRORS (%) FOR GEN 1

A	1	2	5	10	20
PMU 1	10.69	5.78	5.03	5.68	18.97
PMU 2	-2.49	-1.12	3.93	10.88	26.65

TABLE II.   RELATIVE INERTIA ESTIMATE ERRORS (%) FOR GEN 2

A	1	2	5	10	20
PMU 1	6.02	-1.12	-3.73	-1.54	13.94
PMU 2	0.51	-4.18	-0.50	2.36	20.44

TABLE III.   RELATIVE INERTIA ESTIMATE ERRORS (%) FOR GEN 3

A	1	2	5	10	20
PMU 1	-31.26	-11.29	2.47	3.94	5.55
PMU 2	9.16	1.91	1.24	2.78	7.07

It can be seen for all three generators that the window length of 1 fails to reliably produce accurate results, due to their greater vulnerability to errors in a single measurement. This proves a particular issue for the inertia estimates made based on the measurements from PMU 1 due to the greater errors in its ROCOF measurements. Furthermore, it can be seen in Table II that for PMU 2 the performance for an A value of 2 is worse than it is for A=1. This is in contrast to the other cases and occurs due to a large error in the second measurement, which highlights the risk of using a small number of data points for the estimation of inertia.

The issue of noise in the ROCOF measurements of PMU 1 means that, in general, PMU 2 offers more accurate inertia estimates for the estimation window widths (A values) of 1, 2 and 5. In contrast, for the A values 10 and 20 the estimates of inertia using PMU 1 are generally more accurate. This is likely because of the nature of the errors in the ROCOF measurements of each PMU, see Fig. 7. PMU 1 has larger errors that are seemingly randomly distributed between being positive and negative. In contrast, the errors for PMU 2 tend to be underestimates of the true ROCOF. This may mean that as the window is extended the calculation of the mean for PMU 1 causes the errors to be balanced out, improving the inertia estimation, whilst for PMU 2 this does not occur.

Furthermore, the accuracy of both PMUs initially improves when A is increased, as the increased quantity of data makes the estimation more robust against noise. However, the estimation accuracy then begins to fall when A is further increased. This occurs because the validity of the equation used to estimate the inertia (3) decays for larger A values, as it is assumed that post-disturbance mechanical power is equal to the pre-disturbance electrical power.

However, certain results do not follow these trends (e.g. G2-PMU2- A2 and G3-PMU2- A10). This would suggest that the estimation process is vulnerable to anomalies in the raw data that have more influence than the general trends. This vulnerability could be overcome by replacing the existing windows with more sophisticated low pass filters.
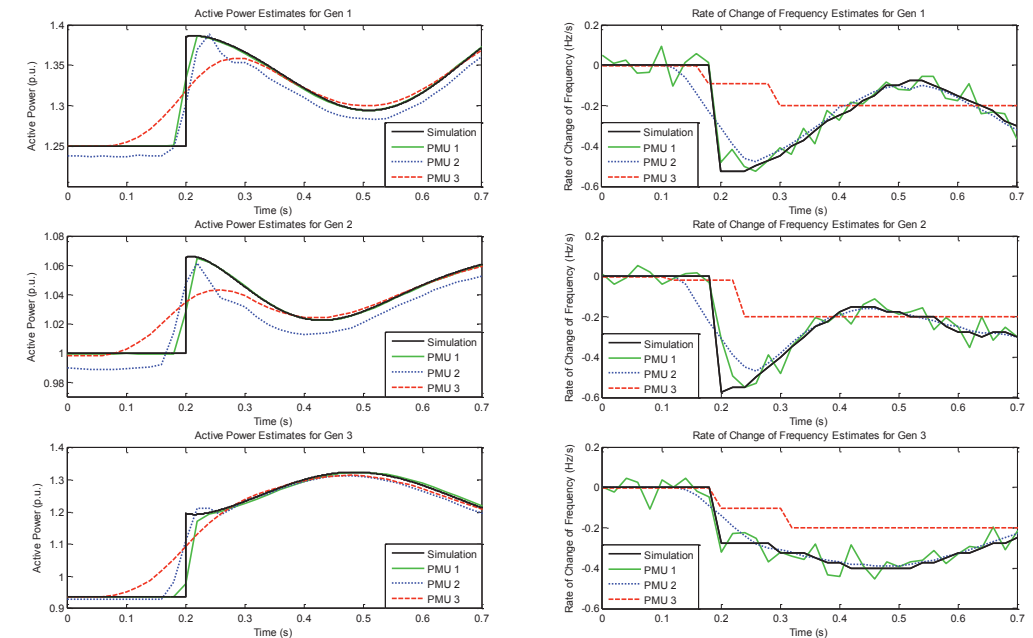

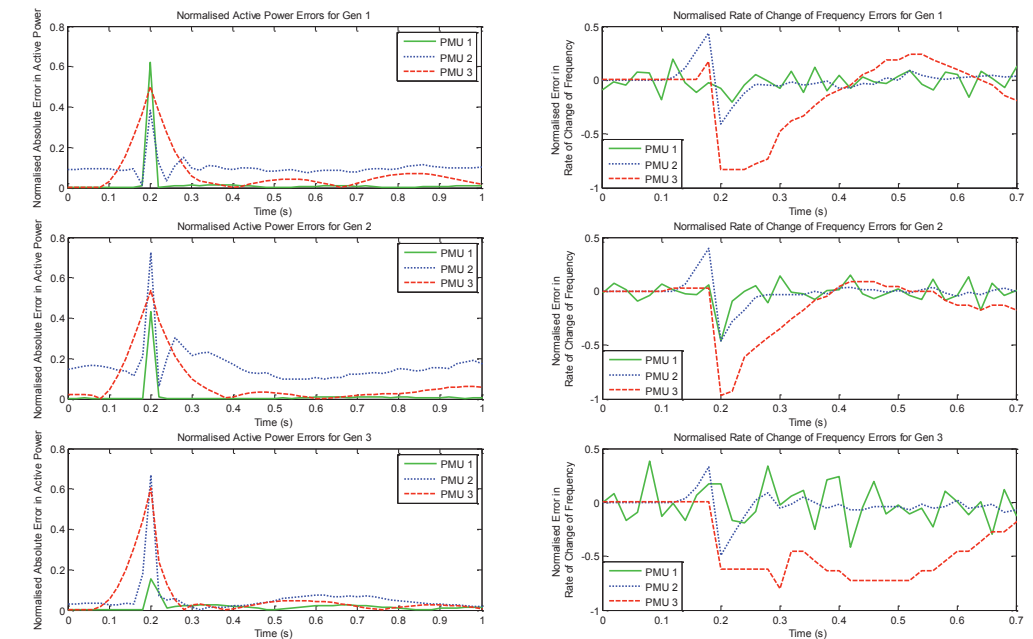Figure 6: The Active Power and Rate of Change of Frequency measured by each PMU for each Generator

Figure 7: The Normalized errors in Active Power and Rate of Change of Frequency measured by each PMU for each Generator

The inertia of Gen 3 (H=23.13 s) is far higher than the inertia of Gen 1 (H=6.4 s) and Gen 2 (H=3.01 s). This means that, in general, the estimation process is less accurate for Gen 3. This is because the step change in ROCOF will be smaller for Gen 3 for the same disturbance in active power, so the errors in the PMU measurements are more significant. This is particularly evident for the smaller A values. However, the accuracy of the estimation of inertia for Gen 3 decays more slowly when A is increased. This is because the

larger inertia of Gen 3 means that the oscillations in the response of the generator to the disturbance are smaller. This serves to limit the decrease in accuracy of the estimation process for larger A values because the measured active power and ROCOF are more consistent after the disturbance, which allows the mean of these values to be a more accurate representation of the behavior of the generator immediately after the disturbance. This suggests that a relationship exists between the accuracy for a given window width and the true

magnitude of the inertia, which is undesirable. Specifically, a larger window width should be used for higher inertia, as the smaller variations in the ROCOF makes the process more vulnerable to noise. In contrast, a shorter window width should be used for lower inertia, as the assumption of constant mechanical power decays more quickly.

D. Execution Time of the Method

The time necessary to execute the estimation process is an important practical consideration. This execution time is dictated by several factors. These include in order of significance: the window width (A), the delay from the time of disturbance estimation method, the filter delay of the PMU, the communication delay and the computation time. Therefore, the delay in receiving an inertia estimate after a disturbance is likely to be on the order of half a second.

V. CONCLUSION

This paper presented a laboratory study of the suitability of three C37.118 compliant PMUs for online inertia estimation based on the swing equation and measurements of active power and rate of change of frequency (ROCOF).

The results presented have shown that certain PMUs should be capable of supporting online inertia estimation. However, these results make it apparent that not all PMUs are capable of this; PMU 3 was unable to provide accurate measurements of the ROCOF. Therefore, it must be acknowledged that the installation of a PMU at a bus does not guarantee accurate and reliable inertia estimation at that bus.

These results indicate that the most important factors to consider when selecting a PMU for inertia estimation will be accurate measurement of ROCOF and the speed of response to a step change. Based on these criteria, PMU 2 is the most suitable PMU, as it has a reduced level of random noise in its output and sufficient speed of response to accurately observe the step change. This allows it to perform well for smaller A values; which is attractive, as A is one of the most significant components of the execution time of inertia estimation.

The results also indicate that the errors in the PMU measurement of the ROCOF will be the most significant barrier to online inertia estimation. Therefore, the performance of the estimation method will be highly dependent on the PMU available, which is undesirable. This may be a particular issue due to the widely varying nature of PMU algorithms and the inherent challenges related to the accurate estimation of ROCOF.

Finally, the transition time of the PMUs tested here did not prevent the estimation algorithm from having access to data that is suitable for supporting online inertia estimation.

Future developments of this laboratory work would likely need to include a study of the range of possible disturbances that will allow accurate estimation of the inertia. This study would need to consider the definition of a suitable disturbance, both in terms of size (smallest disturbance that returns an accurate estimate) and type (ramps and sequential steps). Furthermore, the sensitivity of inertia estimation to harmonics and the other forms of signal corruption present in power system measurements will need to be assessed.

Understanding the sensitivity of inertia estimation to different PMUs is a necessary step in developing practical methods for the online monitoring of inertia. However, many other steps are also necessary. The most important of these will be developing a methodology for determining where best to monitor the inertia of the system. This is necessary as it will not be practical to monitor the inertia at every bus and monitoring the inertia of a generator, whilst useful for verifying the accuracy of the estimation of known generator inertia, provides no insight into the spatial variation of system inertia and the contribution of loads.

REFERENCES

[1] A. G. Phadke and J. S. Thorp, Synchronized phasor measurements and their applications. New York; London: Springer, 2008.
[2] V. Terzija, G. Valverde, D. Cai; P. Regulski, V. Madani, J. Fitch, S. Skok, M. M. Begovic, A. Phadke, "Wide-Area Monitoring, Protection, and Control of Future Electric Power Networks," *Proceedings of the IEEE* , vol.99, no.1, pp.80,93, Jan. 2011
[3] S. Chakrabarti, E. Kyriakides, B. Tianshu, C. Deyu and V. Terzija, "Measurements get together", IEEE Power and Energy Magazine, vol. 7, no. 1, pp. 41-49, January-February 2009
[4] National Grid, "Electricity Ten Year Statement", Nov. 2012 [Online],Available: https://www.nationalgrid.com/uk/Electricity/ten-year-statement/ [Accessed: May 16, 2014]
[5] T. Inoue, H. Taniguchi, Y. Ikeguchi, and K. Yoshida, "Estimation of power system inertia constant and capacity of spinning-reserve support generators using measured frequency transients," Power Systems, IEEE Transactions on, vol. 12, pp. 136-143, 1997.
[6] D. P. Chassin, Z. Huang, M. K. Donnelly, C. Hassler, E. Ramirez, and C. Ray, "Estimation of WECC system inertia using observed frequency transients," Power Systems, IEEE Transactions on, vol. 20, pp. 1190-1192, 2005.
[7] P. Wall and V. Terzija, "Simultaneous Estimation of the Time of Disturbance and Inertia in Power Systems," *Power Delivery, IEEE Transactions on* , vol.PP, no.99, pp.1-14
[8] P. Wall, F. González-Longatt, V. Terzija, "Estimation of Generator Inertia available during a disturbance", in *Power and Energy Society General Meeting, 2012 IEEE.*
[9] P.M Ashton, G.A. Taylor, A.M. Carter, M.E. Bradley, W. Hung, "Application of phasor measurement units to estimate power system inertial frequency response," *Power and Energy Society General Meeting (PES), 2013 IEEE* , vol., no., pp.1,5, 21-25 July 2013
[10] P.M Ashton, C.S. Saunders, G.A. Taylor, A.M. Carter, M.E. Bradley, "Inertia Estimation of the GB Power System Using Synchrophasor Measurements," *Power Systems, IEEE Transactions on* , vol.PP, no.99, pp.1,9
[11] IEEE Standard for Synchrophasor Measurements for Power Systems," *IEEE Std C37.118.1-2011 (Revision of IEEE Std C37.118-2005)* , vol., no., pp.1,61, Dec. 28 2011
[12] P. Kundur, N. J. Balu, and M. G. Lauby, Power system stability and control. New York; London: McGraw-Hill, Inc., 1994.
[13] P.M. Anderson and A.A. Fouad, *Power System Control and Stability*, 2nd ed. New York: IEEE Press, 2003.
[14] J. Machowski, J.W. Bialek, and J.R. Bumby, Power System Dynamics—Stability and Control2nd ed,Wiley, 2008.

BIOGRAPHIES

Peter Wall is a post-doctoral research associate at the School of Electric and Electronic Engineering, University of Manchester.
Pawel Regulski is a post-doctoral research associate at the School of Electric and Electronic Engineering, University of Manchester.
Zina Rusidovic is currently working towards her MPhil degree at the School of Electric and Electronic Engineering, University of Manchester.
Vladimir Terzija (SM'00) is the EPSRC Chair Professor in Power System Engineering, School of Electrical and Electronic Engineering, The University of Manchester, Manchester, U.K.

Identifying Sources of Oscillations Using Wide Area Measurements

Natheer Al-Ashwal, Douglas Wilson
Alstom Grid (Psymetrix), UK

Manu Parashar
Alstom Grid, USA

SUMMARY

Synchrophasor measurement and dynamics analysis applications exposes stability issues that were previously unseen. This provides valuable information and warnings, but it can be challenging to translate a warning on oscillatory stability to a specific, targeted action. Oscillations often involve many generators in a power system, and sometimes the entire system is affected. To achieve a targeted action plan for use in operations and planning, it is necessary to locate the most significant contributions to the mode that are degrading stability. This paper presents a novel approach to locate the area of the grid where the stability of the mode is degraded, using a practical set of synchrophasor data achievable with presently installed measurements, and not relying on a model. The approach is equally applicable in small power systems or large interconnections where a high-level identification is needed on whether there is a contribution within the system operator or co-ordinator's area of responsibility. With this information, the stability issues and warnings identified can be addressed practically and the risks reduced.

This paper describes the oscillation source location method using wide area measurements without reference to a dynamic model, and illustrates its use in a number of practical examples. By identifying which measurements are closest to the source of stability degradation, the problem is focused on a small area of the grid. The method is suitable for application in real-time monitoring and operational procedures, as well as post event analysis and control system tuning.

Generators that provide less damping have a leading phase of oscillations compared to generators providing more damping. The source of the oscillation can be identified by comparing the phase of oscillations from different parts of the system, and the changes in mode phase as the damping degrades. A small number of voltage phasor measurements covering the whole system is sufficient to identify the region containing the source. An example of the approach is given, from a real event observed in ISO New England's area of supervision. In this case, the location identified using phase analysis is consistent with the onset of large oscillations compared to the rest of the system.

KEYWORDS
Power Systems, Oscillations, Source Location, Damping, PMU, WAMS.

1. INTRODUCTION

Power system oscillations are a complex phenomenon involving many interacting plant. In many cases simulation results can be different from real system behaviour. A well-known example is the unstable oscillations which lead to the WECC 1996 blackout, that were not reflected in the dynamic model at that time. Significant effort was expended to modify the model, in order to reproduce the unstable oscillations leading to the blackout [1]. However, some of the challenges in managing stability are inherently very difficult to address analytically, for example, representing control system malfunction or misconfiguration, and the dynamic behaviour of loads.

Measurement based oscillation monitoring using Wide Area Monitoring Systems (WAMS) has been used to complement dynamic modelling [2]. This has proved to be a valuable application of WAMS, which has been used in operational control rooms. In cases where there are well-known modes of oscillation with behaviour and sensitivities that are understood, the system operator can design rules to mitigate the risk of degraded damping progressing to instability. However, the widespread deployment of WAMS and dynamics monitoring applications has exposed several stability issues that were not expected. In such cases, it can be very challenging to identify the source of a change in behaviour of a mode, and link the warning to an effective action. Not only is it difficult to design an operational rule for such cases, it is also difficult to identify the generator(s) where investigation and control tuning are most appropriate.

A method to identify the source of an oscillation is therefore very valuable to determine a course of action to resolve an observed degradation of stability. If the source can be identified using measurements, this enables a real-time dispatch response to move the generator away from the active/reactive power setpoint in which the damping problem occurs. Furthermore, it focuses the analysis and design effort towards a particular generator, avoiding the need for widespread field testing and model validation.

Previous work has been done on oscillation source location. Energy based oscillation source location methods require power measurements on branches in order to trace the flow of energy to the source [3, 4]. This approach requires the condition of constant undamped oscillations, and therefore is limited in its effectiveness for identifying stable but poorly damped oscillations. The approach also relies on power measurements, and few (if any) power systems have sufficient PMU measurements for a consistent implementation of the method. Other work has focused on statistical sensitivities between SCADA measurements of the system state and the stability measures [5]. This approach resolves the observability issues as most transmission systems are fully observable by SCADA, however there are disadvantages relating to spurious correlations in a large search area, and identification in cases where there are not repeated incidences of the condition.

The method is based on detecting differences in the damping contribution from different generators. These differences can be seen from the phase of oscillation at different parts of the system. Generators with a leading phase provide less damping to the mode, while generators with lagging phase provide more damping. When there is a change in the damping of a mode, the coincident change of phase of the oscillations at participating generators indicates where the degradation in damping has occurred. The approach can be applied using the damping and phase of oscillations derived either from ambient noise or ring-down data obtained from PMUs, and can be applied in real-time or post-event.

The method presented here relies on a much smaller number of voltage phasor measurements. It is therefore more practical to deploy because it does not require current measurements, and can yield useful results without a high density of measurements. It can be applied to damped and undamped oscillations. It is also applicable to large interconnections, where detailed SCADA data sharing is impractical and only high-level voltage phasors and frequency can be shared. The results of a single excursion of damping can be interpreted, without the repetition that a statistical method requires. The approach is therefore a significant step forward in addressing the problem of managing the stability of oscillations in power systems.

2. DETAILED DESCRIPTION

The damping ratio of a mode can be seen as a result of damping contributions from different generators in the system. Some generators provide more damping than others and this can be seen from the phase of the oscillations. The objective is to identify the generators with the smallest damping contribution, as being the source of the oscillation.

2.1 Phase of Angle, Speed and Power Oscillations

First we look at the phase relationships within one generator. The swing equation that can be used to describe a generator as a second order system is shown below

$$\ddot{\delta} = \frac{1}{2H}(P_m - P_e) \qquad (1)$$

Where H is the inertia constant and P_m is the mechanical power and P_e is the electrical power.

For a mode with eigenvalue λ, the derivative leads the state by the angle of the eigenvalue. The angle of λ is given as a function of the damping ratio ζ, as follows

$$angle(\lambda) = cos^{-1}(\zeta) \qquad (2)$$

Speed leads angle by $cos^{-1}(-\zeta)$, and acceleration leads angle by $2cos^{-1}(-\zeta)$. For oscillations with constant mechanical power, the electrical power will be out of phase with the acceleration. As a result, electrical power leads the angle by $180° + 2cos^{-1}(-\zeta)$. The oscillatory modes of interest have a damping ratio less than 20%. In the case of 20% damping, speed leads angle and power by $90±12°$.

Figure 1 shows a phasor representation of power, angle and speed oscillations, for undamped, positively damped, and negatively damped modes.

Power can be broken into two components, one in phase with angle and one in phase with speed. A positive component in phase with speed causes damping, while a negative component causes negative damping. This can be seen from the equation of a damped second order system where the damping term is in phase with the first derivative.

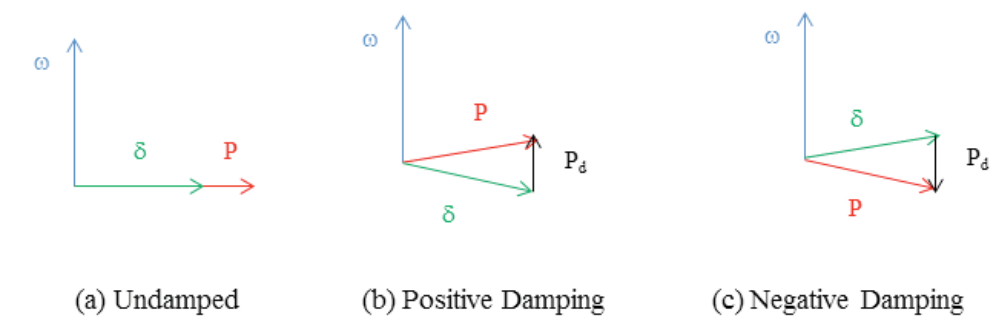$$\ddot{x} + 2\zeta\omega_n\dot{x} + \omega_n^2 x = 0 \qquad (3)$$

(a) Undamped	(b) Positive Damping	(c) Negative Damping

Figure 1 Speed, power and angle phase relations

2.2 Interaction between two generators

Power flow between two generators is proportional to the angle difference. A movement of angle at one generator will cause power flow changes at all generators. This can be expressed in equation (4) below.

$$c_{ij} = \frac{\partial P_j}{\partial \delta_i} \qquad (4)$$

where c_{ij} is the partial derivative of the power output of generator j with reference to the angle of generator i.

An angle increase at generator i will cause a power increase at generator i and a power reduction at all other generators. Therefore, c_{ij} is negative for $i{\neq}j$, and positive for $i{=}j$. The power change at generator j due to an angle oscillation at generator i, results in a power component which could cause positive or negative damping depending on whether it is in phase or out of phase with the speed at generator j.

First, consider two identical machines with opposing oscillations. The phase difference between the oscillations at the two machines is exactly 180° as shown in Figure 2 (a). Power flow due to angle difference is in phase with the generator angles. A similar relationship can be obtained for two generators oscillating in phase, where all phase differences are zero.

For two generators with different damping contributions, the phase relations between power, angle, and speed at each generator are determined by the damping ratio of the mode and are the same. However, the phase shift between the two generators can be different.

Figure 2 (b) shows the phase relationships when generator 1 is providing positive damping, and generator 2 is not providing any damping, i.e., $P_{d1}{>}0$ and $P_{d2}{=}0$. In this case, the electrical power due to the angle difference (δ_1-δ_2) has a component which is not in phase with the angles. The angle oscillations at δ_1 result in a power component at generator 2 which is in phase with the speed (a damping power), while the angle oscillation δ_2 causes a power component at generator 1 which is out of phase with speed (negative damping).

The damping could be considered as two parts, an internal part provided by the generator itself P_d, and another part due to angle oscillations at other generators. In this case generator 2 gets damping power from the network, due to angle oscillations at generator1, while generator 1 gets negative damping power due to oscillations at generator 2.

The damping power in generator 2 as a result of generator 1 angle oscillations is proportional to $Sin(\theta_2\text{-}\theta_1)$; where θ_i is the angle of oscillations at generator i. The same relationship applies for generators oscillating in the same direction as shown in Figure 2 (c). It can be concluded that the generator with the least damping contribution is therefore the generator which is leading by an angle of less than 180°.
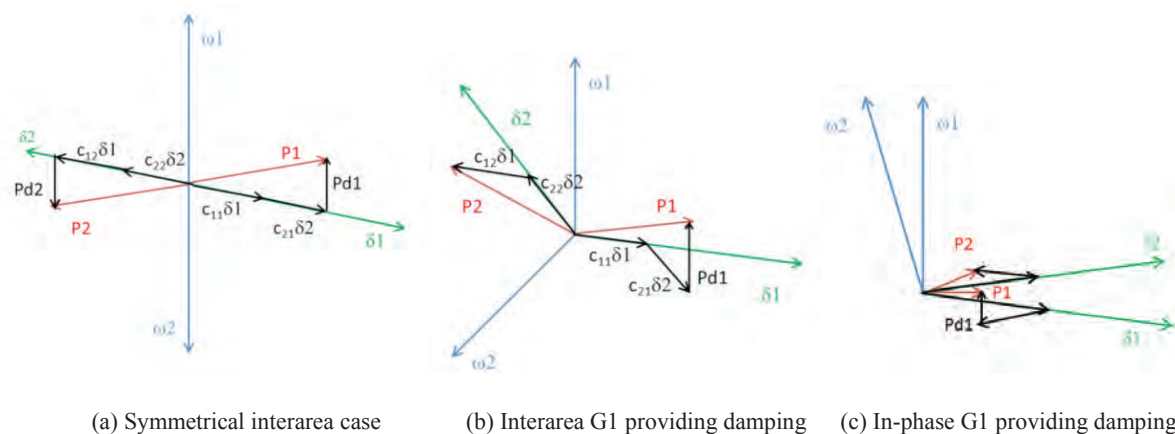

<center>(a) Symmetrical interarea case   (b) Interarea G1 providing damping   (c) In-phase G1 providing damping</center>

Figure 2 Phase of oscillation for two generators

2.3 Generalization for more Generators
This can be generalized for any number of generators. The Damping Contribution of generator i is defined as the sum of damping powers at all generators due to angle oscillations at generator i and is given in equation (5) below.

$$D_i = \sum_{j=1}^{n} c_{ij} * a_i * Sin(\theta_i - \theta_j) \qquad (5)$$

When all generators are providing identical damping, all D_i values are equal to zero, as phase differences are either 0 or 180°. This is considered the reference case. A positive D_i indicates that a generator i is providing more damping than in the reference case. A negative D_i means that generator i is providing less damping than the reference case. The generator with the smallest D_i is the generator providing the least internal damping (possibly negative), and is considered the source of the poor damping.

2.4 Simplifying Assumptions
The calculation of damping contributions requires knowledge of power angle sensitivities, which can be obtained from the system model. In order to eliminate model dependency, we can make some simplifying assumptions.

For opposing oscillations such as inter-area modes, generators can be divided into two opposing groups. The distances within each group are considered very small compared to the distance between the two groups. Therefore, the damping contribution of a generator is only considered to affect generators in the same group. For the interaction between groups, we treat each group as one equivalent generator and find phase difference between the two equivalent generators. Finding the source of oscillations is done in two steps.

First Step
Divide measurements between the two opposing directions of oscillation. After that, find an average phase for each group. This becomes equivalent to the two generator case. The group which is leading by less than 180° is identified as the group containing the source.

Second Step
If one of the two groups has a leading phase, we find the most leading location within this group. If the phase difference is approximately 180° and there is no clear leading group, we find the most leading location in each group. This would produce two locations of interest.

For modes without opposing oscillations step one is skipped and step 2 can be applied directly with all measurements considered in one group. This is the case with local electromechanical modes, and with most governor-frequency control modes.

3. TEST CASE

An example from ISO-NE is given here to demonstrate how the source of oscillations can be found from PMU measurements. In this example, sustained 0.9 Hz oscillations were observed for several minutes. Measurements from 39 PMUs covering the entire ISONE system were analysed.

Figure 3 shows the oscillations from four of the PMUs. It can be seen that PMU31 has significantly large amplitude of oscillation compared to the other PMUs. It can also be seen that PMU30 leads PMU19, and PMU34 is out of phase from the other locations.
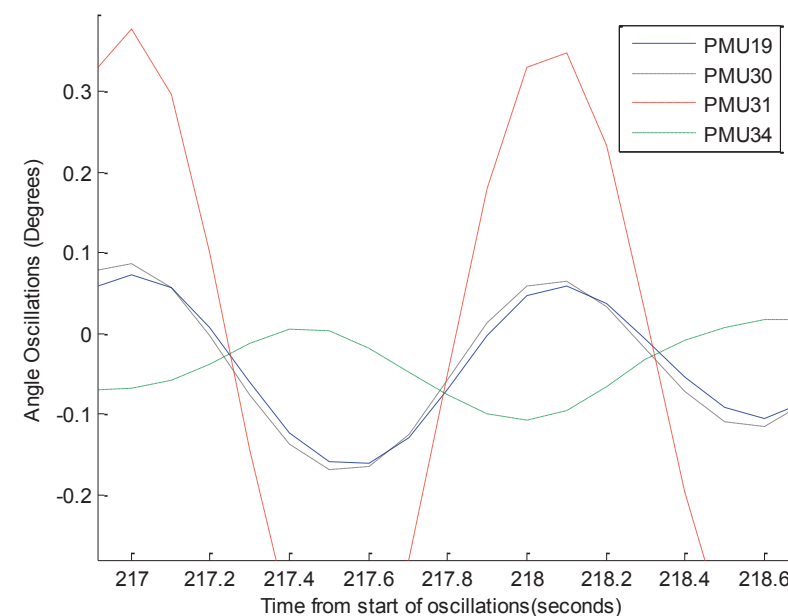
Figure 3 Time domain plot of voltage angle oscillations

The phase of the 0.9 Hz oscillations was extracted from the voltage angle measurements, and shown in compass plots. In Figure 4 (a) all arrows are of equal length and only the angle of oscillations is considered. In Figure 4 (b) the arrow lengths represent the normalised amplitude, with the largest amplitude at PMU31 equal to 1.

The measurements were divided into two opposing groups as shown in the compass plots. Group 1 is leading by approximately 150°. Within Group1, the most leading location is also the largest amplitude, which is PMU31.

This could be an obvious conclusion due to large amplitude at PMU31, which is more than three times the amplitude observed in the other measurements. However, the same location could have been identified without having PMU31. The second most leading is PMU30 which is located in the same substation at a higher voltage level. There are also cases where such amplitude differences are not observed, particularly for inter-area modes and low frequency common modes.
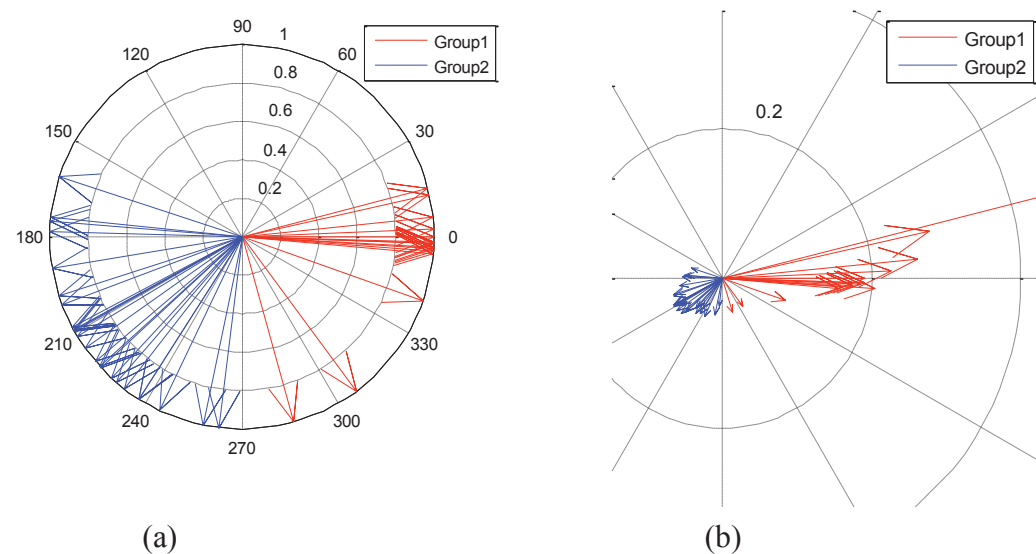
(a)

(b)

Figure 4 Compass Plots

In order to demonstrate suitability for real-time applications, the analysis was carried out on 3 minute windows updated every 5 seconds. The first results are obtained after 10 seconds from the disturbance. The results are initially biased due to the large transient at the start of the event, but they become more consistent after 10 seconds. Figure 5 shows the group phase difference. During the whole period, Group1 is leading by less than 180° indicating that the source is within Group 1. The gaps in the figure are periods of time where the group phase difference could not be obtained due to the small amplitude in Group 2.

> Group 1 leading by 130-150° (ie leading by <180°), indicating that less damping provided by Group 1 than Group 2.
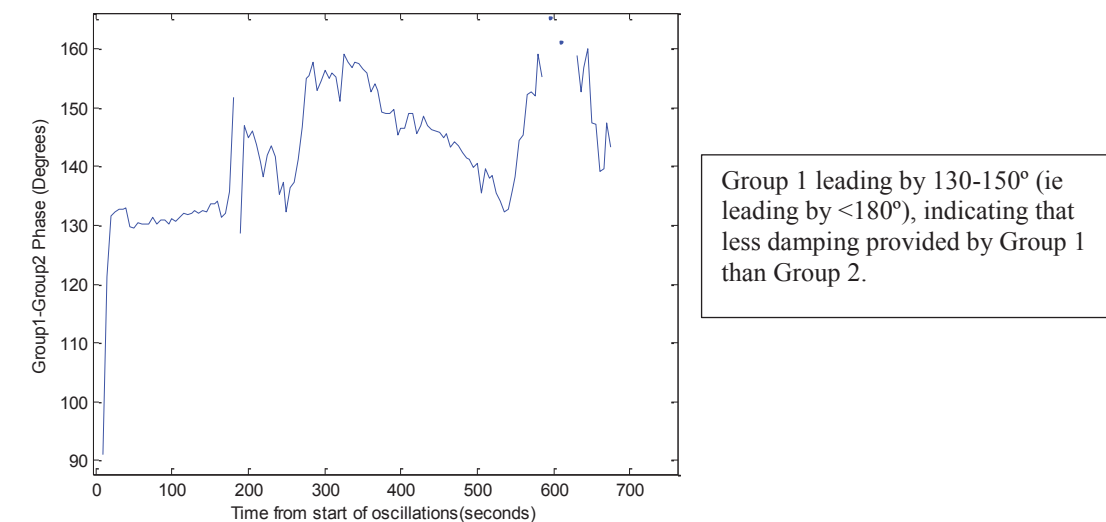
Figure 5 Phase Difference between Groups 1 and 2

Figure 6 shows the phase results for the most leading 4 locations within Group 1. These 4 locations are in the same geographic region, and were the most leading in Group 1 during the whole period of the event. It can also be seen that the order from most leading to least leading for these 4 locations is consistent through the whole period of analysis.

> Within Group 1, PMU31 is consistently leading, indicating that less damping is provided (or negative damping) by generation near PMU31.
>
> If PMU31 was not available, PMU30 would be indicated, which is located close to PMU31, but showing much lower mode amplitude. A correct conclusion would be reached without PMU31.
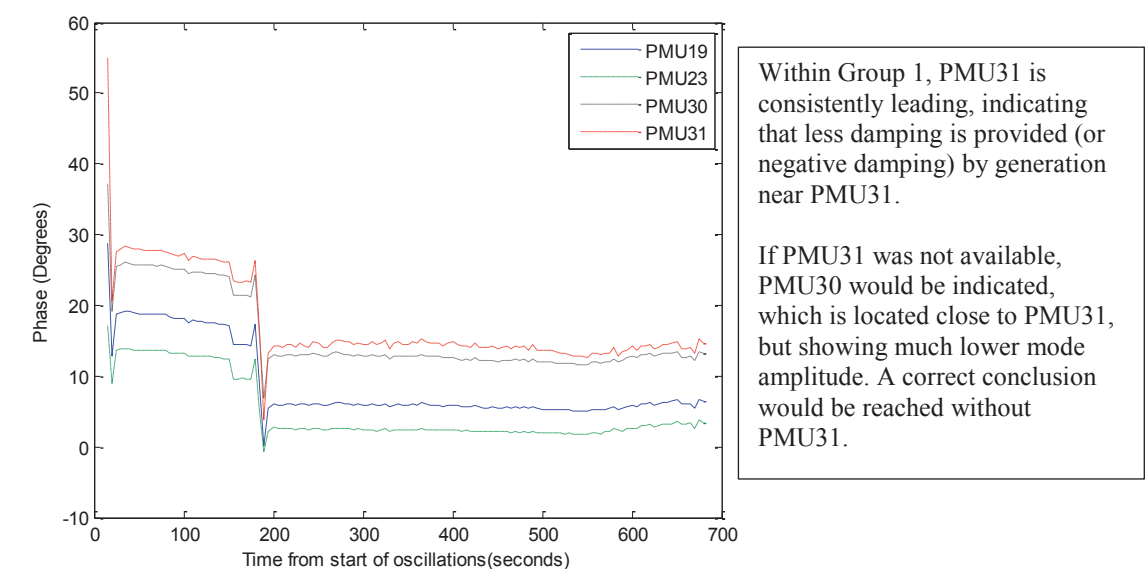
Figure 6 Phase Difference for the most leading four locations

These results show that useful information can be obtained within a short period of time allowing for real-time applications.

4. APPLICATION TO LARGE INTERCONNECTION

In a large interconnection, there may be several system operators and security co-ordinators responsible for the operation of the system, as is the case in the North American Eastern Interconnection and the European ENTSOE (continental) system. There can be several modes of oscillation over a wide area, crossing the boundaries of responsibility. In this situation, a system operator or co-ordinator has an interest in knowing whether there is a significant contribution within the area of responsibility. If there is a contribution in the region, then more detail is required to diagnose the problem, while if the contribution is outside, then it is sufficient to know that the problem is best addressed by another grid stakeholder.

The source location approach described in this paper could be applied to a large interconnection by sharing a high-level set of voltage phasor measurements. This sharing is already feasible, and would require much fewer phasor measurements than those already installed in Europe and North America. Also, the data shared is not commercially sensitive, as it does not contain power information that would reveal generation market participation. The operator can combine a high-level interconnection-wide observation of oscillations with a detailed identification of sources arising within its own region. Thus, the previously challenging issue of addressing poorly damped modes involving several operators can be resolved with this approach.

5. CONCLUSIONS

A measurement based oscillation source location method has been described that identifies the relative influences of damping between generators oscillating in the same coherent group, or in opposing phase. The method is based on analysing differences in damping contributions at different locations. The phase of oscillation is used to identify which locations contribute less damping and are identified as the source. The phase of oscillations can be extracted from PMU voltage measurements.

The method was applied to an example from ISO-NE. The phase results indicate that the source is the location with the largest oscillations. In this case, the selected location was an obvious suspect due to the significant amplitude near the source. However, it was shown that a correct conclusion would be reached even if the largest amplitude measurement was not part of the measurement set. The approach applies to both damped and undamped oscillations, and in cases where amplitude would not lead to the correct conclusion.

BIBLIOGRAPHY

[1]   DN Kosterev, CW Taylor, W.A. Mittelstadt "Model validation for the August 10, 1996 WSCC system outage" IEEE Transactions on Power Systems, Vol.14, Issue 3, 1999, Pages 967-979)

[2]   IEEE Task Force Report TP462, "Identification of Electromechanical Modes in Power Systems" (June 2012)

[3]   Lei Chen, Yong Min, Wei Hu "An energy-based method for location of power system oscillation source", IEEE Transactions on Power Systems, Volume:28, Issue:2 Pages: 828- 836

[4]   Yiping Yu, Yong Min, Lei Chen, Ping Ju "The disturbance source identification of forced power oscillation caused by continuous cyclical load" (4th International Conference on Electric Utility Deregulation and Restructuring and Power Technologies, 6-9 July 2011, Pages: 308 – 313)

[5]   P. McNabb, D. Wilson, J. Bialek: "Classification of Mode Damping and Amplitude in Power Systems using Synchrophasor Measurements and Classification Trees", IEEE Transactions on Power Systems, Volume:28, Issue:2 Pages: 1988 - 1996

Development of a WAMS laboratory for assessing PDC compliance with the IEEE C37.244 Standard

A. Nechifor, M. Albu, *Senior Member, IEEE*, R. Hair,
P. Dattaray, P. Wall, and V. Terzija, *Senior Member, IEEE*

Abstract--**The paper proposes a WAMS laboratory infrastructure for Phasor Data Concentrator (PDC) testing according to the IEEE C37.244 Standard. The architecture makes use of an underlying communication infrastructure to forward packets from the PMUs to the PDC through multiple communication nodes. The IEEE C37.118 frames received are aggregated into a PDC stream and forwarded, while the PDC processing times are qualitatively and quantitatively assessed. Correlations between communication delays within the network and PDC processing delays are investigated. Tests on the platform have encompassed five different PMU models from four different vendors and have been performed for both the TCP and the UDP protocols.**

Index Terms--**communication delays, C37.244, PDC, WAMS**

I. INTRODUCTION

THIS paper analyses the delays introduced by Phasor Data Concentrators (PDC) within the WAMS processing chain. PDC functions like data aggregation (with or without time alignment) and data forwarding can have a significant impact on the delay with which the synchronized measurements reach the final processing algorithm [1-2]. Evaluating an accurate estimate of the PDC latency and comparing it with other delays within the WAMS measurement data flow (communication delays, detection algorithm running times, etc.) can help identifying and improving the latency bottle-neck within the WAMS architecture.

In order to test the PDC according to the performance guidelines defined in the C37.244 Standard [3], both qualitative and quantitative testing approaches have been employed. For the qualitative tests, the PDC functionality, inter-operability and security are assessed. For the quantitative tests, measurements of time delays are conducted on the PDC processed data from five different PMU models stemming from four different manufacturers.

For each type of PMU, the paper analyses the delays introduced by the forwarding function of the PDC, as well as data aggregation delays when merging multiple PMUs streams into a single concentrator stream. Cumulative distribution functions of the results are built in order to investigate correlations between the PDC processing delays and communication delays.

The voltage and current signals measured by the PMUs are generated using an Omicron CMC-256 amplifier according to COMTRADE Standard compatible files generated in Matlab and PSCAD, respectively. The signals for the virtual PMUs are generated in real time within the Real Time Digital Simulator (RTDS) RSCAD simulation environment.

The internal processor clock of the server running the Phasor Data Concentrator has been synchronized with an external UTC time source. The procedure to attain precise time delay measurements involves the use of Shared Hardware Memory between the server and the external oscillator and an automatic low level parser for TCP and UDP protocol frames. The resulting uncertainty of the PDC latency measurements is lower than 1 ms.

In order to assess the impact of cyber security measures on the PDC operation, the communication link between the laboratory where the PMUs, WMU and RTDS reside and the server room where the measurements get concentrated has been secured using an IPsec approach.

The resulting platform offers an automatic and reliable framework for assessing the performance of Phasor Data Concentrators according and not limited to the guidelines to be found in the IEEE C37.244 standard.

II. WAMS LABORATORY ARCHITECTURE

There have been several criteria set in place when designing the WAMS architecture:

A. Scalability

The communication architecture employed needed to be applicable to a real case scenario. Therefore, a similar concept to the one presented in [4] has been employed: the functionality of the communication infrastructure is encapsulated in a server and several routers that run a Linux based operating system. The scalability of this setup and its applicability when working with real substation measurements has already been proved in [4] using 3G as the main

Alexandru Nechifor, Papiya Dattaray, Peter Wall and Vladimir Terzija are affiliated with University of Manchester, Oxford Rd, Manchester M13 9PL
Mihaela Albu is affiliated with Politehnica University of Bucharest, Splaiul Independenței 313, Bucharest 060042
Richard Hair is affiliated with E.ON, Nottingham NG11 0EE

communication medium. In the laboratory developed for this paper, all links are based on a wired Ethernet connection. Therefore, the communication delays reported are lower, as expected.

B. Complexity

Delays introduced by the Phasor Data Concentrator (PDC) under test could have been assessed by connecting all devices via an Ethernet switch to the machine where the PDC resided. However, this would have been grossly unrealistic for a Wide Area Measurement System scenario, where usually several communication nodes (hops) are interposed between the sensors and the Phasor Data Concentrator where the data is analysed, aiming to reach the optimal control decision. Therefore, several communication nodes have been included within the WAMS laboratory design, as depicted in Fig. 1.
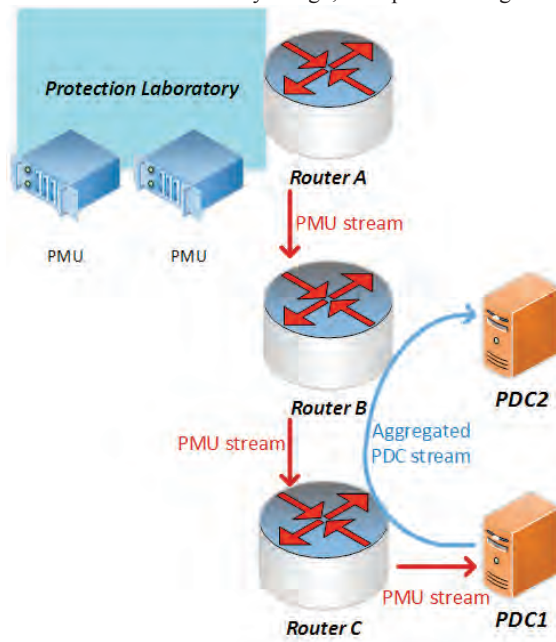

Fig. 1. WAMS Architecture for PDC performance testing

The three routers in Fig. 1 store relevant certificates and encryption keys for securing the communication within the network. Particular attention needs to be paid to the firewall and routing tables, in order to attain the desired data flow and isolate the traffic from external intrusion. The security overhead contributes to the overall complexity of the network.

Although all tests in this paper are applicable to any type of PDC, it should be mentioned, for the sake of completeness, that both PDC1 and PDC2 are OpenPDC instances [5]. PDC1, the unit under test, runs on a Windows virtual machine installed on a High Performance Server: Dual Eight Core Intel Xeon E5-2667v3 3.2GHz, 20MB Cache and 64GB DDR4-2133 RAM. PDC2 is used only as a destination for the forwarded packets from PDC1, therefore the configuration of the machine running PDC2 is not critical: Intel Core i7-3632QM 2.20GHz and 8GB RAM.

C. Sensor Diversity

The robustness of the Phasor Data Concentrator has been tested against five different models/makes of Phasor Measurement Units and one Waveform Monitoring Unit, the latter characterized by its 200 Hz reporting rate. The technical details of each type of sensor are given within this subsection, but throughout the rest of the paper they will be referred to using the codifications defined below:

A1 type PMU is represented by Arbiter 1133A Power Sentinel [6]. Although not yet compliant with the newest version of the C37.118 standard [7], the functionality of the A1 type sensor can be categorized as that of an M-class device. The A1 type PMU focuses on higher accuracy of the phasor estimate, rather than on fast response time. This behaviour has also been confirmed by the results of the tests performed in section IV. All other PMUs included in the tests can be categorized as P-class devices. The A1 PMU is configured for TCP communication.

S1 type PMU is represented by SEL487E [8]. The S1 type PMU comes with an interesting security feature that blocks communication to a client (PDC) outside the Local Area Network (LAN) where the S1 PMU resides. This issue has been circumvented using a forwarding technique similar to the one described in [4]. The S1 type PMU listens for TCP connections on port 8812.

S2 type PMU is represented by SEL451 [9]. The S2 type PMU is actually used on a regular basis for frequency monitoring purposes. It measures the socket voltage though a 230V/110V transformer. The S2 type PMU uses the same communication protocol (TCP) as S1.

R1 and R2 type sensors represent different instances of the same prototype RPV311 device [10] from Alstom. The physical device monitors voltage and current on six synchronized channels. The R1 instance is a PMU and estimates phasors, frequency and rate of change of frequency at a reporting rate of 50Hz. The R2 instance is a Waveform Monitoring Unit, reporting instantaneous voltage and current samples at 200 Hz. Both R1 and R2 type sensors communicate via UDP.

T1, T2, T3, etc. represent virtual Phasor Measurement Units created within a Real Time Digital Simulator [11]. They output C37.118 streams from within an RTDS GTNET card and make use of the RTDS GTSYNC card for GPS synchronization. As expected and as confirmed by the test results in section IV, they have the fastest communication response. The virtual T type PMUs have been configured for TCP based communication.

III. PDC Testing Methodology

There is a multitude of tests that can be performed to produce an extremely detailed assessment of the Phasor Data Concentrator robustness and performance. Categories of such tests, as also given in [3], can range from vendor defined design tests to interoperability and cyber security tests. Analysing every aspect of the Phasor Data Concentrator

mentioned in the IEEE C37.244-2013 Standard would have been an impossible task to achieve within the scope of the paper. Therefore, testing procedures have been focused on the most critical aspects of the C37.244 Standard, as listed in [4] and further detailed within this section.

The PDC should be TCP and UDP capable, as listed in section 5.3.3.1 of the C37.244 Standard. The communication platform setup for this paper is based Linux based routers similar to the ones described in [4]. Therefore, switching between TCP and UDP is only a matter of straightforward configuration. Four of the five PMUs communicate via TCP, while the latter via UDP.

COMTRADE and CSV are listed as the two data logs options within section 4.2.3 of the C37.244 Standard. Through a Java EE7 application built on top of PDC1, there is is a multitude of machine readable formats (JSON, XML, etc.) available, additional to the ones mentioned in the standard. A detailed assessment of the Java application is performed in [4].

The C37.244 Standard proposes a detailed assessment of security within section 5.17. Security is ensured within the WAMS laboratory on three levels: availability, authenticity and confidentiality. Availability represents resilience versus denial of service attacks. This is enabled through a TLS authentication [12] key loaded within routers at both the PMU and the PDC side. Authenticity is ensured through issuing certificates for each communication node (router), probing the router's identity within the network. Confidentiality is attained using a similar methodology to the AES256-CBC encryption procedure [13].

The most strenuous tests for the PDC performance are defined in sections 5.1 and 5.2 of the C37.244 standard and they refer to data aggregation and data forwarding tests. A very detailed emphasis will be put on these types of tests within the next section. The methodology for conducting such tests is inspired from section 7.3 of the C37.244 standard and uses a packet sniffer (Wireshark [14]) to intercept network traffic on the network interface of PDC1. In order to assess PDC data forwarding delays, the timestamp difference between the packet arrival into PDC1 and the packet departure from PDC1 is evaluated (see Fig. 1). For communication delays, the computational goal is the difference between the C37.118 timestamp set by the PMU for a particular data frame and the arrival of that data frame into PDC1.

The above methodology requires a reliable timestamp on the PDC side, as the PMUs are already synchronized to a common UTC time source. Consequently, GPS synchronization has been put in place for PMU1. The chosen solution is similar with the setup described in [4] and relies on an external GPS synchronized time source: LC2750 GPS [15]. The actual synchronization between the CPU clock and the internal oscillator within LC2750 has been attained through the use of a Shared Hardware Memory mode. The uncertainty of the resulting CPU timestamp is continuously maintained under a 1ms threshold. The synchronisation setup is depicted in Fig. 2.
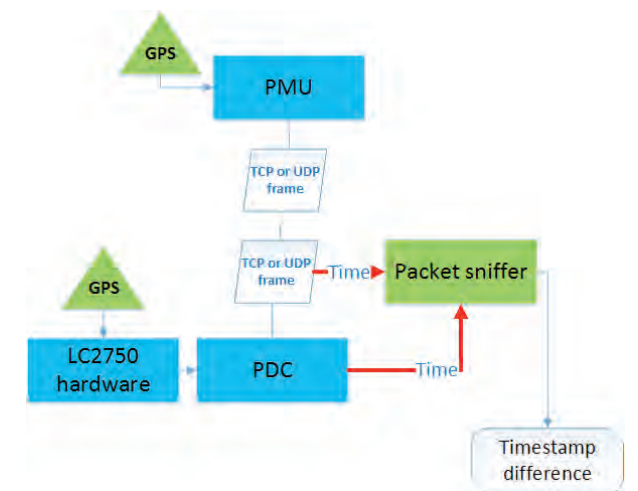

Fig. 2. PDC synchronization setup

IV. Data Aggregation and Forwarding Tests

As already announced in the previous section, the most important category of tests that have been performed is data aggregation and forwarding tests. The Cumulative Distribution Functions of the PDC forwarding delays within one data aggregation test are depicted in Fig. 3, while their means and standard deviations are summarized in Table I.
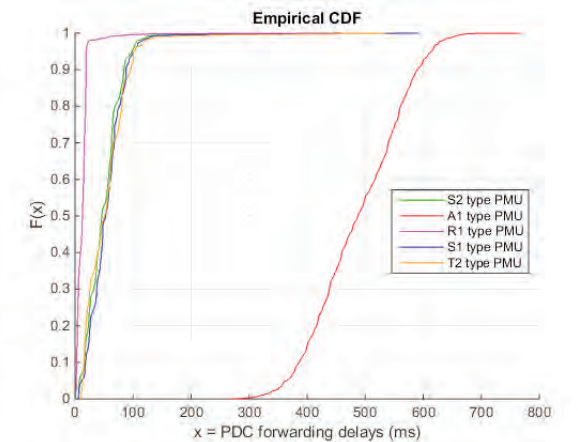

Fig. 3. PDC forwarding delays

TABLE I
PDC FORWARDING DELAYS – MEANS AND STANDARD DEVIATIONS

DELAYS	MEAN (MS)	STANDARD DEVIATION (MS)
S2 TYPE PMU	50	35
A1 TYPE PMU	488	79
R1 TYPE PMU	13	17
S1 TYPE PMU	55	35
T2 TYPE PMU	53	40

As one can see from Fig. 3, the R1 type packets are processed the fastest, while the A1 type packets take the most amount of time to process. Before jumping to quick conclusions solely from this plot, one needs to revisit the methodology for computing PDC forwarding delays. One

packet from a PMU (let us name it X) arrives into PDC1 at time t1 and PDC1 sends it towards PDC2 at time t2. The time difference Δt = t2 - t1 represents the processing delay of PDC1. Within the time interval between t1 and t2, PDC1 performs aggregation on samples that have arrived from 5 PMUs and tries to forward packages of 5 different samples at a time as part of the concentrator stream to PDC2. Therefore, Δt for PMU X depends not only the arrival time of the data frame from PMU X, but also on the arrival times of data frames from other PMUs. This behaviour is best depicted with a simple experiment: disconnecting from its power supply one PMU (let us name it Y), member of the PDC stream. Data frames from the disconnected PMU will never reach PDC1. PDC1 will keep waiting for PMU Y packets to include them into the PDC stream until an internal time-out occurs. This experiment has been performed by shutting down the T2 type PMU. As expected, the PDC processing delays have spiked for all other PMUs from the PDC stream. The forwarding delays for the A1 type PMU when the T2 type PMU is disconnected are depicted in Fig. 4, as a relevant example.

Fig. 5. Communication delays

TABLE II
COMMUNICATION DELAYS – MEANS AND STANDARD DEVIATIONS

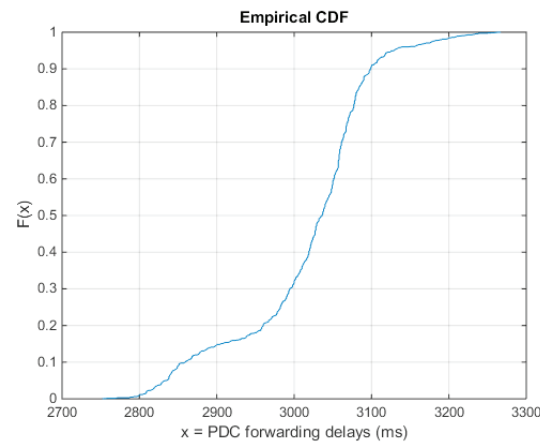| DELAYS	MEAN (MS)	STANDARD DEVIATION (MS)
S2 TYPE PMU	56	15
A1 TYPE PMU	157	32
R1 TYPE PMU	104	15
S1 TYPE PMU	50	14
T2 TYPE PMU	36	12

Fig. 4. A1 type PMU forwarding delays, in case of T2 PMU disconnected

According to Fig. 4, communication delays of other PMUs within the PDC stream can have an impact on the PDC processing delays for one particular PMU. Therefore, before drawing conclusions from Fig. 3, the communication delays for all PMUs involved in the communication chain need to be analysed. Consequently, the Cumulative Distribution Functions of the communication delays are depicted in Fig. 5, while their means and standard deviations are recorded in Table II.

When comparing Fig. 3 and Fig. 5, the correlation between communication delays and PDC processing delays becomes apparent. The CDF functions for T2, S1 and S2 have a similar trajectory for both communication and PDC processing delays. This is to be expected, because they all are categorized as P-class devices and they communicate using the same protocol (TCP). The R1 type PMU is slower in transmitting the data than the TCP P-class devices (see Fig. 5), but PDC1 seems to spend the least amount of time processing its data frames.
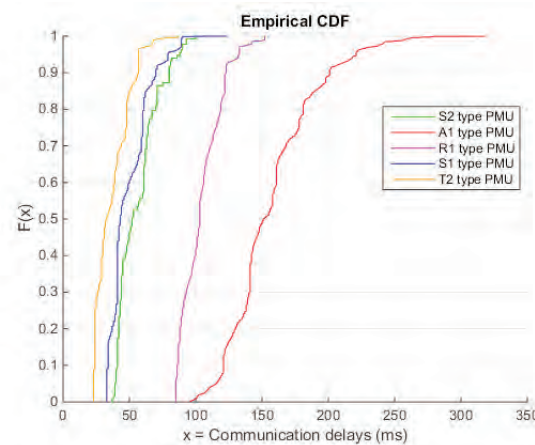
This can be easily explained, taking a simpler example: let X and Y be the only PMUs defined in PDC1 and PMU X have a lower latency than PMU Y. At t1, a packet from PMU X arrives into PDC1. PDC1 does not send out the packet yet, because PMU X is part of a concentrator stream to be forwarded. At t¬2>t1 a packet from the slower PMU Y arrives into PDC1. Now PDC1 has enough data to forward at t3>t2>t1 a concentrator stream packet, containing both frames received from PMU X and Y respectively. Consequently, (t3-t2) < (t3-t1), therefore the packets from the slower PMUs (up to a point) spend less time into the PDC. Applying the same logic, the slowest PMU from Fig. 5, i.e. A1 type PMU, should have the lowest PDC processing time. However, this is not the case, because A1, which is more similar to an M-class device, tends to queue several C37.118 data frames together in the same TCP frame, consequently changing the way it interacts with the concentrator completely. Lumps of A1 data frames arrive at once; therefore, PDC1 almost always has a buffer from which to add A1 data frames to a PDC concentrator stream data packet. Hence, although sequences of A1 frames arrive at the same time, some of them only get used "much" later, after several PDC stream packets had been sent out. Such interaction would also explain why the A1 type PMU has the highest standard deviation for concentrator processing delays (see Table I).

V. CONCLUSION

The most important conclusion to be drawn from the work presented in this paper is the causality between communication delays and PDC aggregation delays, with the former having a significant impact on the latter. When forwarding multiple

PMU streams, bundled into a PDC stream, the delays and the order in which the packets arrive influence the data aggregation and forwarding processes within the PDC. As it could also be seen from the behaviour of the A1 type sensor, the software implementation of the TCP/IP stack of each PMU also represents a strong factor influencing these delays. Several C37.118 data frames sent together in a TCP frame can obscure any intuitive attempt of understanding the mechanisms according to which the data aggregation is performed within the Phasor Data Concentrator.

VI. REFERENCES

[1] Kun Zhu; Nordstrom, L.; Al-Hammouri, A.T., "Examination of data delay and packet loss for wide-area monitoring and control systems" in Proc. of IEEE International Energy Conference and Exhibition (ENERGYCON), Sept. 2012

[2] Babazadeh, D.; Chenine, M.; Kun Zhu; Nordstrom, L.; Al-Hammouri, A., "A platform for wide area monitoring and control system ICT analysis and development" in Proc. of IEEE PowerTech Grenoble, 2013

[3] IEEE Guide for Phasor Data Concentrator Requirements for Power System Protection, Control, and Monitoring, 2013, IEEE Std C37.244™-2013

[4] Nechifor, A.; Albu, M.; Hair, R.; Terzija, V., "A flexible platform for synchronized measurements, data aggregation and information retrieval", in Elsevier Electric Power System Research, vol. 120, pp. 20, 31, Mar. 2015

[5] OpenPDC Phasor Data Concentrator, Documentation, available at "http://openpdc.codeplex.com/documentation", as of July 2015

[6] Arbiter Systems, Inc., Arbiter1133a Data Sheet, available at "www.arbiter.com/files/product-attachments/1133a.pdf", as of July 2015

[7] IEEE Standard for Synchrophasor Measurements for Power Systems -- Amendment 1: Modification of Selected Performance Requirements, IEEE Std C37.118.1a-2014 (Amendment to IEEE Std C37.118.1-2011), Apr. 2014

[8] Schweitzer Engineering Laboratories, Inc. (SEL), SEL-487E Data Sheet, available at "https://www.selinc.com/SEL-487E/", as of July 2015

[9] Schweitzer Engineering Laboratories, Inc. (SEL), SEL-451 Data Sheet, available at "https://www.selinc.com/SEL-451/", as of July 2015

[10] Alstom Reason RPV311, Digital Fault Recorder Documentation, available at "http://www.alstom.com/grid/products-and-services/Substation-automation-system/measurement-merging-gps/RPV311-Digital-Fault-Recorder-with-PMU-and-TWFL/" as of July 2015

[11] RTDS Technologies, Pmu Applications Documentation, available at "https://www.rtds.com/applications/pmu-studies/", as of July 2015

[12] Krawczyk, H.; Bellare, M.; Canetti, R., "HMAC: Keyed-Hashing for Message Authentication", Internet Engineering Task Force (IETF), Request for Comments (RFC) 2104, February 1997, available at: "https://www.ietf.org/rfc/rfc2104.txt", as of July 2015

[13] Yenuguvanilanka, J.; Elkeelany, O., "Performance evaluation of hardware models of Advanced Encryption Standard (AES) algorithm," in Proc. of the IEEE Southeastcon 2008

[14] Wireshark network protocol analyser, Documentation, available at "https://www.wireshark.org/docs/", as of July 2015

[15] Timetools, Limited, LC2750 GPS Time Server Data Sheet, available at "http://www.timetools.co.uk/solutions/gps-time-server/", as of July 2015

Defining Constraint Thresholds by Angles in a Stability Constrained Corridor with High Wind

D. Wang, D. H. Wilson and S. Clark

Abstract—Conventionally, transient stability limits are defined in terms of the active power transfer through a cut-set of the transmission lines connecting the participating centres of inertia. However, the industry is experiencing two changes that suggest a change of practice in defining the limits. Firstly, increasing penetration of renewable and distributed generation, often connecting at nodes between the centres of inertia, increases the volatility of power transfers. This generation does not contribute to inertia, and breaks the direct relationship between power and angle that underlies the conventional expression of a transient limit in MW. The definition in MW is often very conservative. Secondly, the ability to measure angle differences is a relatively recent capability, and affords the opportunity to include angle difference in the definition of power system limits.

This paper describes studies to investigate the potential benefit of defining a stability limit in terms of angle difference. The study is motivated by the British grid, where there is a transient stability limit in the corridor between Scotland and England, with 1.5GW of wind generation connected between the centres of inertia. The studies indicate that a definition of the limit by angle difference can enable 10-12% uplift in the corridor transfer during high wind conditions when the capacity is most valuable.

Index Terms—Transient stability, phasor measurement, transfer constraints, angle difference

I. INTRODUCTION

IN the power system in Great Britain, the transfer limit in the corridor between Scotland and England is normally transient stability limited, in the region of 3.5GW. Between the centres of inertia of synchronous generation in central Scotland and northern England, there is about 1.5GW of wind connected. At present, the transfer is defined in terms of MW according to the usual practice worldwide, taking the sum of power through a cut-set in the transmission corridor. However, it is noted that the volatility introduced by wind generation in the corridor affects the transient stability limits significantly. A stability threshold applies for a period which can be a few hours if limits are identified off-line, or typically 15-30 minutes for online limit calculation. During this time, system conditions (and wind) can vary significantly. Operationally, the most conservative limit for the full period must be applied.

To explore the potential benefit of the use of angle measurement, an experimental model was created that represented the key physical phenomena related to transient stability with wind injection. This study is intended to be illustrative of the angle constraint concept, rather than accurately representative of the British grid.

The use of angle difference as a constraint variable has been addressed in literature. Ochoa et al describe an angle difference approach to constraining generation through an active generator control mechanism [1]. In the Ochoa paper, the limits are related to constraints in the distribution grid, and the angle difference is used as a proxy to simplify the definition of the control variables. The concept was further described by Wang and Murphy, relating to a pilot implementation in the Scottish Power Manweb 33kV system [2]. Other work related to angle as a constraint was carried out by Dobson et al, describing an approach to derive a representative angle difference that defines the stress in a corridor [3].

This paper contributes an assessment of the potential benefit in transfer constraint relief by angle limit definition. It also contributes a study of angle difference relating to transient stability issues that have not been addressed before. It also incorporates the influence of wind power and volatility in the constraint definition.
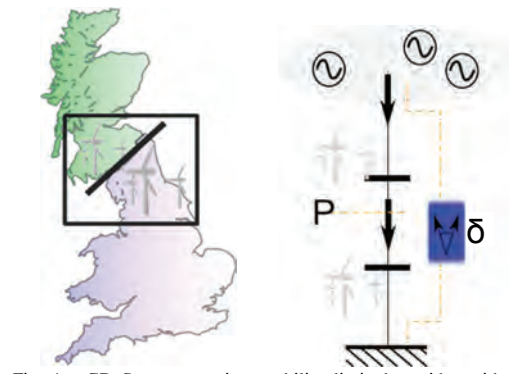
Fig. 1. GB System transient stability limited corridor with 1.5GW wind injection and simplified conceptual representation by power (P) and angle difference (δ)

II. TRANSIENT STABILITY AND ANGLE MEASUREMENTS

Transient stability is essentially the ability of the system to return to a stable operating point after a fault has caused acceleration in the generation region, and therefore an advance in the angle relative to the rest of the system. The transient stability of the system is closely related to the angular separation between the accelerating region and the bulk power system.

The principle behind the angle constraint concept is illustrated in Fig. 2. Power (P) is considered to be the power crossing the cut-set illustrated in Fig. 1, and the angle (δ) represents the angle difference between the centres of inertia. The no-wind (and negligible load) scenario will appear as a simple corridor and a classical power-angle relationship.

$$P = \frac{V_1 V_2}{X} \sin(\delta) \tag{1}$$

Increasing wind within the corridor will change both P at the cut-set, and the angle across the corridor, however the angle is derived over a proportion of the impedance, and not the whole corridor. In other words, 1MW transferred across the entire corridor will have a greater effect on the angle than 1MW transferred across a shorter distance. Wind within the corridor changes the vertical position of the power-angle (P-δ) curve. If wind is injected in north of the cut-set (see Fig. 1), P-δ is raised, but if the injection is in the south, it moves down.

The angle swing during the fault is directly related to the energy input of the prime mover, the inertia of the generator, and the nature of the fault, and not dependent on the generator-to-system P-δ. The worst-case angle advance for the dimensioning fault is therefore predictable. Subsequent to the fault, the ability to resynchronize depends primarily on the pre-fault angle and the angular advance during the fault.

It should be noted that transient stability is related to synchronous generation and its inertial response in the grid. Because of the nature of connection of wind generation to the grid, it contributes very little to the inertial response of the system, but it does change the loadflow and angles.
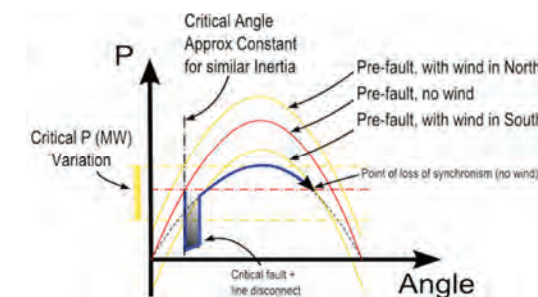

Fig. 2. Effect of Wind Injection on Power Angle Curves, and Implications for Constraints

III. EXPERIMENTAL DYNAMIC MODEL

The model used to investigate the limiting angles is shown in Fig. 3. In this model, there are four synchronous generators. TSO-1 represents the "stiff" end of the interconnection while TSO-2 is the exporting region. The two regions are separated by a corridor with relatively high impedance. The angle difference is measured between the central buses in each region. The level of power export from TSO-2 to TSO-1 is limited due to the potential for transient instability. To find the stability limit, the demand at bus 6 is gradually increased and met by the increased generation in TSO-2 until the system cannot recover from a disturbance.

To compare with the conventional approach to a MW limit threshold, a boundary is defined as a cut-set between buses 7 and 8. There is an injection of wind around the middle of the corridor at bus 8. The dimensioning fault is at bus 10, which causes acceleration of both synchronous generators in TSO-2. The fault is sustained for 100ms and followed by loss of a line between buses 9 and 10, which weakens the connection between the areas.

The wind injection at bus 8 is modeled as negative load, and the experiments involve assuming certain values for the wind injection in different loading scenarios, and exploring the transfer limit in MW and angle difference through different network loading scenarios.
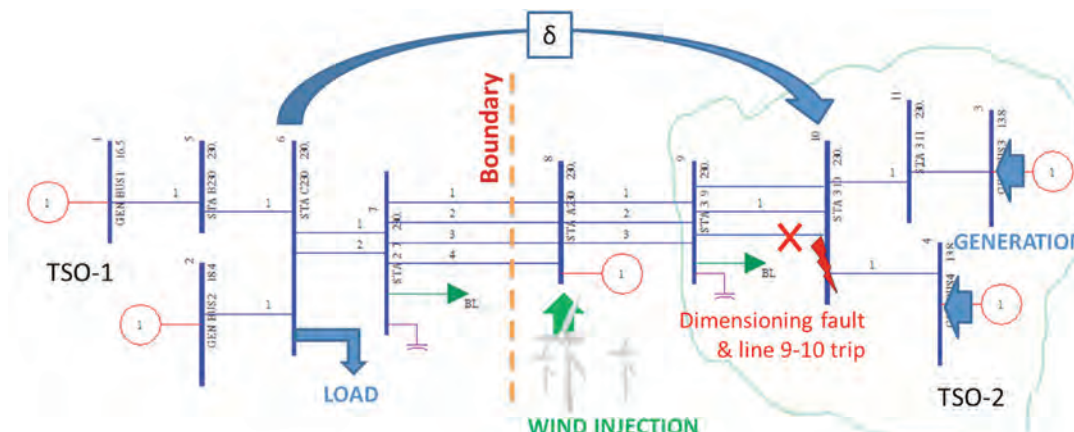

Fig. 3. Dynamic model including synchronous generation, a transiently constrained corridor, and wind generation injection.

IV. TEST SCENARIOS AND RESULTS

Three base case scenarios were studied to compare the power and angle definition of the transient stability limit:

1. Intact network
2. One of 8-9 lines is out of service
3. Intact network, but lower TSO-2 generation inertia.

In each scenario, wind injection in the corridor is varied and the effect on the limit observed. The transient stability limit is taken to be the lowest of the critical values for the different wind injection scenarios, shown in bold in the results tables. This assumes that the wind power can vary between 0 and 700 MW without a new limit being defined. For the angle difference limits, the value of MW transfer corresponding to the flow at the critical angle shows how much power could be transferred if angle difference was used as the limit value. Furthermore, in each scenario, two different generation dispatch patterns of the synchronous machines were applied, in order to balance the increase of the wind generation while keeping the initial demand the same:

- *Dispatch Pattern A*: the increasing wind generation is balanced by a decrease in generation in TSO-1.
- *Dispatch Pattern B:* the increasing wind generation is balanced by a decrease in generation in TSO-2.

It is envisaged that, given the same demand and level of the wind generation, the system would be less stressed with dispatch pattern *B* than *A*, as larger proportion of the demand in TSO-1 is supported by the local generation rather than from remote. In practice, the proportion of generation balancing in the exporting and importing areas will vary with generator droop settings, AGC and economic dispatch, thus the patterns *A* and *B* represent the two extremes.

A. Scenario 1: Intact Network

The MW and angle difference limits at different wind generation levels are indicated in TABLE II. If the MW limit is adopted, then the limit is equal to 3223.5 MW obtained from the case with 0 MW wind generation. If the angle limit is applied, the limit is equal to 21.2° and 21.3° with the dispatch pattern *A* and *B* respectively. With dispatch pattern *A* the angle limit is obtained with 700 MW wind generation, while with dispatch pattern *B* it is from the case with no wind generation.

TABLE II
MW and angle limits in the scenario with intact network

Wind Injection (MW)	Power Transfer Limit (MW)		Angle Difference Limit (deg)	
	A	B	A	B
0	**3223.5**	**3223.5**	21.3	**21.3**
300	3383.8	3539.2	21.5	22.8
500	3481.4	3737.4	21.5	23.6
700	3540.9	3931.7	**21.2**	24.5

Fig. 4 shows the additional power transfer through the corridors if the angle difference limit is used compared to the MW limit. The results show that, in general, applying angle difference limit allows more power to be transferred though the corridors than applying the MW limit. The benefit increases with increasing wind generation.

With dispatch pattern *A*, applying the angle limit would in

fact yields a slightly more conservative power flow constraint in the case with no wind generation. However, in the other three cases with the wind generation increases to 300 MW, 500 MW and 700 MW, adopting the angle limit allows 123MW, 220 MW and 317 MW more power transfer respectively than applying the MW limit.

With dispatch pattern *B*, adopting the angle limit always results in equal or more power transfer than adopting the MW limit. The benefit yielded with dispatch pattern *B* is slightly greater than with dispatch pattern *A*, with 146 MW, 241 MW and 341 MW more power transfer than adopting the MW limit in the case with 300 MW, 500 MW and 700 MW wind generation respectively.
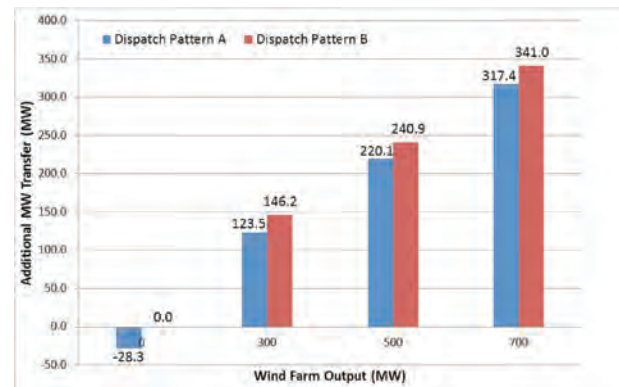

Fig. 4. Additional power trasnfer allowed by adopting angle difference limit compared to MW limit in the scenario with intact network

B. Scenario 2: One line out of service between buses 8-9

In this scenario, the power transfer limits are defined where the network is weakened by a line out of service. This can be planned, in which case limits can be prepared ahead of time, or it can be unplanned, in which case the immediate result of the line outage is an insecure state where a new transfer limit needs to be defined.

TABLE III
MW and angle limits in the scenario with N-1 network condition

Wind Injection (MW)	Power Transfer Limit (MW)		Angle Difference Limit (deg)	
	A	B	A	B
0	**3081.8**	**3081.8**	23.3	**23.3**
300	3250.9	3390.7	23.3	24.7
500	3341.7	3592.9	23.3	25.6
700	3430.7	3791	**23**	26.5

TABLE III indicates the MW and angle difference limits found at different wind generation levels. If a MW limit is applied, the limit is equal to 3081.8 MW that is found in the case with no wind generation. If angle limit is applied, the limit is equal to 23.0° and 23.3° with the dispatch pattern *A* and *B* respectively. The angle limit found with dispatch pattern *A* is from the case with 700 MW wind generation, while with dispatch pattern *B* the angle limit is obtained from case with no wind generation.

As showing in Fig. 5, in general, applying angle difference limit allows more power transfer than applying the MW limit. The benefit increases with increasing wind generation. In a planned outage such as in this scenario, there is up to 349 MW

and 383 MW more power transferable in the high wind case with dispatch pattern *A* and *B* respectively by using the angle limit. The additional amount in this scenario is slightly greater than in the previous scenario of the intact network. The effective network impedance (*X* in Eq. 1) in this scenario is greater than in the previous scenario. As a result, in this scenario a smaller change in real power transfer produces a given angle change.

If the outage is unplanned, then the Scenario 1 (Intact Network) angle difference limit is conservative if applied to the Scenario 2 situation. This is reasonable, since weakening the network will tend to open the angles, but the angle limit value will stay approximately the same, or rise slightly because the synchronous generator output will be reduced to respect the limit, and the accelerating energy is reduced.

There is a security benefit in the use of angle difference as the constraint variable. If the system is operated to a limit of 21° as per Scenario 1, and a line is lost, then the operator can continue to use the same angle limit, which will be conservative, until the limit values can be revised. By contrast, if the limit is defined as 3223MW and a line is lost, the secure limit is in fact 3082MW, but until the limit is revised, the system will be insecure or a heuristic rule will be required.
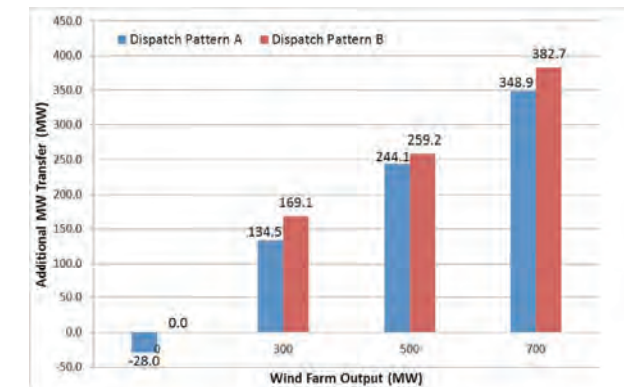

Fig. 5. Additional power trasnfer allowed by adopting angle difference limit compared to MW limit in the scenario with N-1 network condition

C. Case 3: Intact Network, but Reduced TSO-2 Inertia

In systems such as the GB grid where wind penetration is high, the inertia can be reduced in periods of high wind and low load. This is particularly significant at the Scottish end of the stability constrained boundary, as a large proportion of wind generation connects in Scotland.

In this scenario the inertia constants of the generators in TSO-2 are reduced by one third of those in previous scenarios. This is a simplified representation of inertia changes in a real network due to the choice of units running at a given time. The MW and angle limits at different wind generation levels are indicated in TABLE IV. If the MW limit is applied, the limit is 2677.7 MW obtained from the case with no wind generation. If angle limit is adopted, the limit is equal to 16.8° for both dispatch patterns.

With lower inertia, the acceleration of the generators will be greater, and therefore the pre-fault critical angles are smaller than those found in the previous scenarios.

TABLE IV
MW and angle limits in the scenario with lower generation inertia in TSO-2 with different wind generation levels

Wind Injection (MW)	Power Transfer Limit (MW)		Angle Difference Limit (deg)	
	A	B	A	B
0	**2677.7**	**2677.7**	16.8	16.8
300	2876.7	2987.9	17.3	18.2
500	2992.6	3174.5	17.4	18.9
700	3082.8	3363.7	17.4	19.7

According to Fig. 6, it is also clear in this scenario that the angle limit enables greater transfer than the MW limit. In the case with the highest wind generation, the benefit is up to 346MW (dispatch pattern *A*) and 365 MW (dispatch pattern *B*), which is approximately 13% and 13.6% more than the power transfer if MW limit is applied.

If the inertia in the model is lower than the actual value, both the MW and angle difference limits are conservative, and the system would be over-constrained. If either the 16.8° or 2678MW limit was used when the inertia was actually as Scenario 1, the limit is conservative. Inertia has an important effect, however the limit is defined.
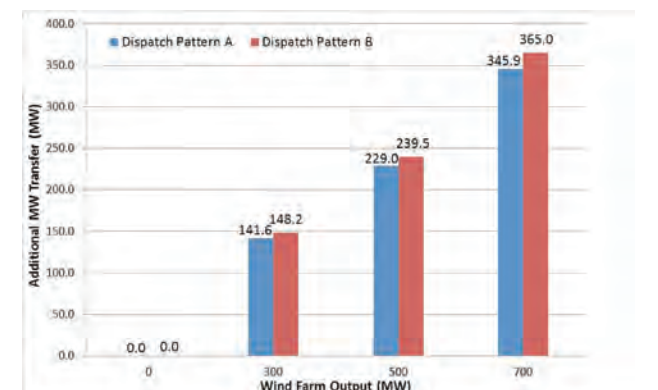

Fig. 6. Additional power trasnfer allowed by adopting angle difference limit compared to MW limit in the scenario with lower generation inertia in TSO-2

It should be noted that the acceleration during the fault is a function of the individual synchronous generation units, while the effective inertia of the area (TSO-2) is important following fault clearing. Further work should examine whether it is sufficient to use the known operating schedules of the synchronous generators to define which limit sets to use, or whether a more detailed representation of the inertia of the area, including load, affects the limit thresholds significantly.

V. DISCUSSION

The results showed that, in the scenarios considered, expressing the transient stability limit as an angle difference could allow more power to be transferred through interconnectors than adopting MW as the measure of transient stability limit. The benefit is mainly due to the vertical shift of the P-δ curve with the increase of the wind generation, resulting in relatively small change in the angle difference compared to the change in MW flow though the cut-set.

While the cases generally show less conservative limits

using angles, there are conditions where a MW limit is preferable, and a practical operating guidance would require respecting either the angle or the MW limit. One example is if the MW limit is measured at the cut-set between bus 8 and 9, instead of between bus 7 and 8. With dispatch pattern A, using the angle difference limit would still yield more benefit than using the MW limit. However, with dispatch pattern B, using the MW limit would be the better choice. This is because despite of the increasing wind generation, the least stable network conditions with different wind injection levels have very similar MW flow through the cut-set between bus 8 and 9, while there is a noticeable angle advance between each case. Applying the angle difference limit thus results in a more restrictive MW flow through the cut-set than the MW limit. Both the MW and angle difference limits can be used and combined in a logical way in order to maximize the benefit.

With the increasing wind generation, the angle limit varies very little with dispatch pattern *A*, while with dispatch pattern *B* the angle limit advances noticeably. The advance of the angle limit with dispatch pattern *B* is due to the extra power flowing through the corridors from bus 8 to 7 that is generated by the wind farm. However, with dispatch pattern *A*, the increase of voltage angle difference between bus 7 and 8 due to the increasing wind output is in fact countered by the decrease in the voltage angle difference between bus 8 and 9 due to the decrease in generation in TSO-2. In other words, with dispatch pattern *A* the increasing wind generation output leads to a more stressed network, and the total amount of generation from TSO-2 before the system becomes unstable is lower than in dispatch pattern *B*.

Generally, similar thresholds are obtained in the cases of dispatch patterns *A* and *B*. The more conservative values would be used as the actual constraint, but it is shown that this is not significantly over-constraining. The feature that the limit is insensitive to the way in which the system is re-dispatched to balance the wind is very positive for the use of the approach.

Regardless of which limit is used, reducing uncertainty through shorter-term or more accurate forecasting improves definition of the constraint. Using angle reduces the sensitivity of the limit. There is an advantage to base the limit calculation on a forecast as close as reasonably practical to the real-time condition, but the use of angles reduces the sensitivity to wind volatility and accommodates longer cycles between limit calculations without over-constraining the system.

The angle limit adopted in this paper refers to the voltage angle difference between bus 6 and 10, which are the central buses of the generators in TSO-1 and TSO-2 respectively. A practical improvement would be to use the difference between the centers of angles in TSO-1 and TSO-2 instead, such as the approach described in [3-5]. This center of angle would represent an aggregate angle derived from measurements close to the higher inertia synchronous machines.

While the simplified network model and the simulations done in this paper tried to capture the real network operation conditions of the GB system, further work should be done to apply the concept to a detailed network model, applying

similar threshold definition processes used for operational planning of the real system. Also, further work would be of value to investigate the effect of wind injection outside of the corridor in question at various points in the network.

VI. CONCLUSION

This paper contributes an assessment of the potential benefit in transfer constraint relief by angle limit definition. The results showed that that if the boundary constraint is expressed as an angle difference instead of the sum of power, more power can be transferred through the corridors, which enables the system to be operated closer to the real stability limit and deferring expensive network reinforcements. Modifications to current study and operational practices that apply to the MW limit are modest. The same simulation procedures are required to define the constraints, except that angle differences are recorded as well as MW values. Most transient stability simulation tools record voltage angle results as well as the power flow results in the least transient stable network condition found. The approach provides particular benefits in situation where there is a high level of volatility in the loading within the corridor, which is the case with high wind penetration.

VII. REFERENCES

[1] L. F. Ochoa, D. H Wilson. "Angle Constrained Active Management of Distribution Networks with Wind Power" in IEEE PES ISGT Conference, Gothenburg, Sweden, Oct 2010

[2] D. Wang, D. H. Wilson, S. Venkata, G. Murphy. "PMU-Based Angle Constraint Active Management on 33kV Distribution Network" CIRED Session, Stockholm, 2013.

[3] Dobson I. Parashar M. "A cutset area concept for phasor monitoring" in IEEE PES General Meeting, Minneapolis, USA, July 2010.

[4] G. Li, M. Rovnyak. "Integral Square Generator Angle Index for Stability Ranking and Control" in IEEE Trans. on Power Systems, Vol. 20, No. 2, 2005.

[5] M. Sherwood, M. Venkatasubramanian. "Real-Time Detection of Angle Instability using Synchrophasors and Action Principle" in IREP Symposium – Bulk Power Dynamics and Control, Aug 19-24, 2007.

VIII. BIOGRAPHIES

David Wang is a Power Systems Engineer with Psymetrix, an Alstom owned company specializing in WAMS, smart grid applications and dynamics. He graduated with B.Eng (Hons) in Electrical Engineering from the University of Auckland NZ in 2005, and MSc (2006) and Ph.D (2010) in Renewable Energy from the University of Edinburgh. He has published over 12 technical papers. His research interests include renewable generation integration, active distribution network management and planning optimization.

Douglas Wilson is Chief Technical Officer of Psymetrix Ltd, where he has worked since 1998. He leads the Power Systems Team and is responsible for research and design of software applications. He is also involved with utilities in real-time monitoring and control functions, and power system analysis and consulting. He graduated with B.Eng (Hons) and PhD from the University of Edinburgh, and MSc in Power Systems from the University of Manchester.

Stuart Clark received his MEng degree from the University of Bristol in 2012. He is currently a Power Systems Engineer with Psymetrix, involved in WAMS deployment & testing, utility collaborative R&D and consulting. Previously he worked at Scottish Power in the application, implementation & management of monitoring systems including fault recording, WAMS and transformer DGA, and in protection and event investigations. Stuart has been responsible for WAMS deployments in South Africa, Europe and the UK.

VISOR

Visualisation of Real-Time System Dynamics using Enhanced Monitoring

Our electricity networks are evolving to meet the needs of the changing energy landscape, and so must the technologies and practices we use to monitor and control them.

The £7.4m project brings together the National Electricity Transmission System Operator and the three GB mainland Transmission Owners to collectively establish the next generation in system monitoring and analytical tools to enhance our ability to manage and protect the network.

The VISOR WAMS

About the Project

1st unified GB Wide Area Monitoring System

Trialling new 200Hz point-on-wave Waveform Measurement Units (WMUs)

Combined use of existing 50Hz Phasor Measurement Units (PMUs)

**Phasor Data collectors and Analysis in each Network Licensee region**

Centralised Data Hub at National System Operator with full national view

New sophisticated analysis platform and applications, providing new insight into the dynamic system behaviour

New ability to detect and locate more Sub-synchronous (<50Hz) power oscillations

WAMS demonstration and proof of concept facility in SPEN Control Centre
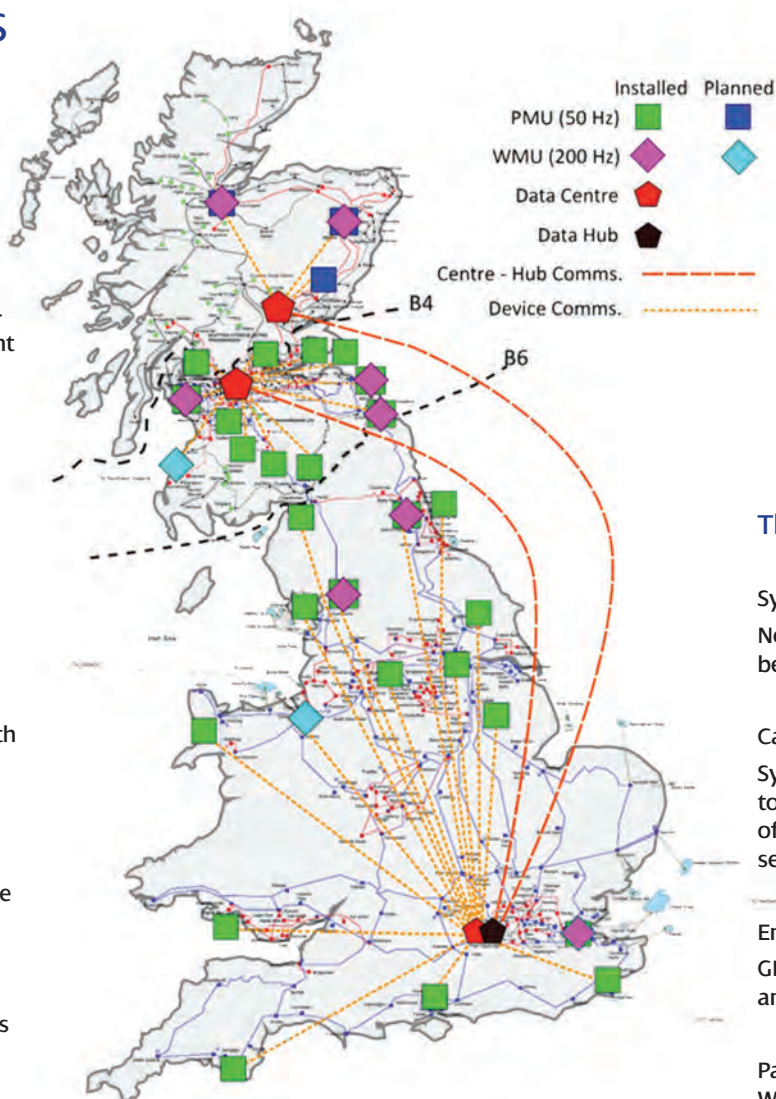
The Benefits

System Reliability:
New visibility of oscillations between 4Hz-46Hz

Capacity Release:
Synchronised measurement to better understanding of system dynamics and security limits

Enhance modelling:
GB System Model validation and improved accuracy

Paving the way for new WAMS-based technology and applications, such as wide-area control and oscillation source location